

Innovative Interlocking Connection System For Medium-rise Timber Modular Structures

by

Zhengyao Li

Submitted in accordance with the requirements for the degree of
Doctor of Philosophy

Supervisors: Prof.Konstantinos Daniel Tsavdaridis (External, City, University of London)
Assoc. Prof David Richardson (University of Leeds)
Dr. Ioannis Mitseas (University of Leeds)

The University of Leeds

School of Civil Engineering
April 2024

The candidate confirms that the work submitted is her own and that appropriate credit has been given where reference has been made to the work of others.

This copy has been supplied on the understanding that it is copyright material and that no quotation from the thesis may be published without proper acknowledgement

The right of Zhengyao Li to be identified as Author of this work has been asserted by her in accordance with the Copyright, Designs and Patents Act 1988.

The candidate confirms that the work submitted is her own, and the contribution of the candidate and the other authors to this work has been explicitly indicated below. The candidate confirms that appropriate credit has been given within the thesis where reference has been made to the work of others.

The work in Chapter 1 and 2 of the thesis has appeared in the following publication:

Li, Z., & Tsavdaridis, K. D. (2023). Design for seismic resilient cross laminated timber (CLT) structures: A review of research, novel connections, challenges and opportunities. *Buildings*, 13, 505.

Li, Z., Tsavdaridis, K. D., & Gardner, L. (2021). A review of optimised additively manufactured steel connections for modular building systems. In M. Meboldt & C. Klahn (Eds.), *Industrializing Additive Manufacturing - Proceedings of AMPA 2020*.

The work in Chapter 3 and 4 of the thesis has appeared in the following publications:

Li, Z., & Tsavdaridis, K. D. (2023). Limited-damage 3D-printed interlocking connection for timber volumetric structures: Experimental validation and computational modelling. *Journal of Building Engineering*, 63, 105373-.

Li, Z., & Tsavdaridis, K. D. (2023). A novel limited-damage 3D-printed interlocking inter-module connection system for cross laminated timber (CLT) volumetric structure. In *World Conference on Timber Engineering 2023 (WCTE2023)*.

Li, Z., Tsavdaridis, K. D., & Gardner, L. (2021). A review of optimised additively manufactured steel connections for modular building systems. In M. Meboldt & C. Klahn (Eds.), *Industrializing Additive Manufacturing – Proceedings of AMPA 2020*.

All aspects of the publications above were undertaken by the candidate. As the first author of all the published papers, the candidate's contributions spanned the full scope of the research projects, including: Idea and Conceptualisation, Literature Review, Methodology Design, Data Collection and Analysis, Writing. However, the candidate benefited from the guidance and suggestions from the named corresponding author who played the usual role of supervisor. The contributions of the other authors were reviewing and editing.

This copy has been supplied on the understanding that it is copyright material and that no quotation from the thesis may be published without proper acknowledgement. The right of Zhengyao Li to be identified as Author of this work has been asserted by her in accordance with the Copyright, Designs and Patents Act 1988.

Abstract

Cross Laminated Timber Modular Construction (CLTMC) represents a cutting-edge advancement in the construction industry, merging the ecological benefits of timber with the streamlined processes of modular construction. This innovative approach offers a sustainable alternative to conventional construction methods, promising significant reductions in environmental impact and improvements in building efficiency. Despite these advantages, recent research has identified critical inefficiencies within existing CLTMC connection systems, particularly concerning their mechanical performance, installation complexity, and overall sustainability. These inefficiencies pose significant challenges to the broader adoption and development of CLTMC technology.

This thesis addresses these challenges by introducing an innovative sliding and stacking installation method for CLT modules. Central to this method is a novel, damage-controlled, continuous interlocking connection system designed to enhance the efficiency of module assembly while reducing onsite labour demands. The proposed connection system was rigorously evaluated through a combination of experimental and numerical analyses. This comprehensive evaluation included local-scale testing to assess immediate translational mechanical properties, parametric studies with validated numerical models to explore the influence of various design parameters, and macro-scale shear wall simulations to evaluate performance under realistic loading conditions.

The results of these analyses demonstrate that the proposed connections offer satisfactory stiffness, strength, and deformation control effect. These connections effectively mitigate damage to both timber and fasteners, thereby enhancing the overall durability of the construction. Additionally, the research presents a robust design framework for CLTMC connections, providing detailed guidelines for implementation in real-world projects. This framework emphasises not only the technical performance but also the practical aspects of construction, such as ease of assembly and potential for material reuse.

The innovative connection design introduced in this thesis represents a significant advancement in the field of modular construction. By facilitating more efficient and flexible assembly processes, the design has the potential to transform how CLT modules are utilised in construction projects. Furthermore, the damage-controlled nature of the connections suggests a substantial reduction in the permanent damage to structural materials throughout

the service life of a building, thereby extending the usable lifespan of these materials. Along with the incorporated design strategies for deconstruction and reuse, this system is expected to contribute to greater overall sustainability.

In summary, this research provides a comprehensive review to existing challenges in CLTMC, offering a novel approach to the identified challenges, which improves construction efficiency, enhances flexibility, and promotes the sustainable use of materials. The findings underscore the potential of the proposed connection system to revolutionise modular construction practices and contribute to the sustainable development of the built environment.

Keywords: CLT modular construction, Connection design framework, Interlocking connection, Damaged controlled connection, 3D printing, Quasi static testing, Numerical analysis, Parametric study, Circularity

Acknowledgement

In this acknowledgment, I wish to express my profound gratitude to those who have accompanied me on this challenging but fulfilling journey. Firstly, my heartfelt appreciation goes to my supervisor, Prof. Konstantinos Daniel Tsavdaridis from City, University of London. This PhD journey would not have been possible without his support, invaluable expertise and guidance. Konstantinos's insights in modular construction have been inspiring, and his rigorous scientific approach and attention to details have built me a much-improved scientist. I am also indebted to Mr. Marco Pagliarin, the Technical Project Manager Timber at Hilti, for his mentorship, supervision, and sharing of crucial industry insights from the outset of my PhD. His efforts to align my research with industry needs and his facilitation of key industry connections have been invaluable. My gratitude extends to my collaborators over the last four years, whose insights and suggestions have been pivotal in the development of connections and the publication of our findings.

The support from the George Earle Laboratory team, especially technician Marvin Wilman, with whom I've worked closely for three years, has been crucial. His assistance in experimental design, specimen fabrication, and testing has been invaluable.

I must also acknowledge my family and friends, both in China and the UK, whose support, particularly during the isolating initial years of quarantine, has been a cornerstone of my journey. I am profoundly grateful to my parents for their unwavering love, support, and belief in me, which have been my guiding light throughout this journey. Being the delightful distractions, my friends, with their companionship and shared moments in badminton, travel, and social gatherings, have been a significant source of joy and strength. It is these people that have made it a pleasure to live in Leeds everyday. Special appreciation goes to Liji for driving me around in the weekends, and to Shiwen, for being a steadfast companion ready to share a drink whenever and wherever needed. I would like to extend special thanks to my friend Biyan, an architectural PhD student, for being a big critic to the quality of my drawings in all my papers.

I cherish every moment of guidance and support shared along this journey, and it is with a heart full of gratitude that I look back on these invaluable contributions to my personal and academic growth.

List of Content

CHAPTER 1 INTRODUCTION	23
1.1 Mass Timber Construction with Sustainable Engineered Wood Products (EWPs)	23
1.2 Modern Mass Timber Modular Construction	24
1.3 CLT Modular Construction	25
1.4 Research Questions	29
1.5 Aim	30
1.6 Objectives	30
1.7 Research Methodology	31
1.8 Contribution to Knowledge	33
1.9 Chapter References	33
CHAPTER 2 LITERATURE REVIEW	35
2.1 Overview of CLT and CLT Modular Structures	35
2.2 Lateral Performance of CLT Modular Structures	40
2.3 The Design of Multi-Storey Ductile CLT Structures	47
2.4 Conventional CLT Connections and Existing Challenges	49
2.5 Novel Connection Systems for CLT Modular Buildings	56
2.6 Connection Performance Evaluations: Connectivity, Manufacturability, Constructability	72
2.7 Demolition of Timber Structure and The Reuse of Wasted Timber	78
2.8 Novel Timber Connection Design Framework	83

2.9 Literature Review Findings	84
2.10 Conclusions	85
2.11 Chapter References	84
CHAPTER 3 CONCEPTUAL DESIGN OF THE INTERLOCKING CONNECTION SYSTEM FOR CLT MODULAR STRUCTURES	95
3.1 Overview of Interlocking Techniques in Construction	95
3.2 Novel Interlocking Connection System for CLT Modular Construction	96
3.3 Components Design of The Interlocking Connection System	104
3.4 Conclusions	116
3.5 Chapter References	95
CHAPTER 4 LABORATORY TESTS	120
4.1 Testing Configurations and Loading Process	120
4.2 Testing Material Preparation	124
4.3 3D Printed Steel Material Property Characterisation - Coupon Test	131
4.4 Outline of Screw Testing	133
4.5 Chapter References	120
CHAPTER 5 NUMERICAL SIMULATIONS AND ANALYTICAL STUDIES	148
5.1 Validation of Numerical Connection Model	148
5.2 Translational Behaviours of the Interlocking Connections with S235	158
5.3 Parametric Study	163
5.4 Analytical Work	175

5.5 Conclusion	187
5.6 Chapter References	148
CHAPTER 6 PUSH OVER ANALYSIS – CLT SHEAR WALL BEHAVIOURS COMPARATIVE STUDY	190
6.1 CLT Shear Wall Modelling and Validation	190
6.2 Set-Up of Shear Wall Comparative Study	197
6.3 Results of CLT Shear Wall Comparative Study	203
6.4 Conclusions	214
6.5 Chapter References	190
CHAPTER 7 CONCLUSION	218
7.1 Limitations in Existing CLT Connections	218
7.2 Novel Interlocking Connection Development	218
7.3 Feasibility Evaluation of The Novel Connection	219
CHAPTER 8 LIMITATIONS AND RECOMMENDATIONS	220
APPENDIX A NUMERICAL AND ANALYTICAL RESULTS OF PARAMETRIC STUDY	222
APPENDIX B PLANNED PUBLICATIONS	227

List of Figure

Figure 1.1. Configurations of different engineered wood products (EWPs)	24
Figure 1.2. Different structural systems in timber modular construction	24
Figure 1.3. Full building gwp comparison of different structural systems	26
Figure 1.4. CLT volumetric project woodie student accommodation, a 6-storey timber modular structure.	27
Figure 1.5. Illustrations of hold-downs and brackets in typical CLT modular structures	28
Figure 1.6. Problematic construction process in TMC	29
Figure 1.7. Methodology flow chart of the connection design program	33
Figure 2.1. Configuration of CLT	36
Figure 2.2. Natural defects within timber	36
Figure 2.3. Platform-type and balloon-type CLT panelised buildings	37
Figure 2.4. Structure of typical clt module	38
Figure 2.5. Illustration of conventional inter-module connections	39
Figure 2.6. The tallest volumetric buildings to date	40
Figure 2.7. Shake table test in Sofie project	41
Figure 2.8. Failure modes observed in Sofie project	42
Figure 2.9. Timber panels damage observed in the quasi-static test of CLT buildings	42

Figure 2.10. Global load-displacement curve of a single timber framed module (left) and the detected displacement vectors	44
Figure 2.11. Deformability modes of a single-panel system (top) and a multi-panel system under lateral load (bottom)	45
Figure 2.12. Lateral deformation pattern detected in CLT structures with large panels (left) and coupled small panels (right) under the same loading condition	46
Figure 2.13. Commonly used connections in CLT structures	49
Figure 2.14. Hysteresis loops and monotonic curve for (a) a 2-storey full-scale CLT building and the (b) angle brackets and (c) hold-downs that used in the building	51
Figure 2.15. The failure modes of (a) timber-to-timber connections, and (b) steel-to-timber connections that are considered in european yield models (EYMs)	52
Figure 2.16. Concept of over-strength method: the resistance of connection should be smaller than the resistance of brittle members with sufficient ratio	54
Figure 2.17. Different kinds of failure modes in timber plate connections	56
Figure 2.18. Pinching behaviour in conventional hold-downs (top) and innovative connections (bottom) with ‘strong fasteners-weak metal connector’ behaviours	74
Figure 2.19. Panel lifting	76
Figure 2.20. Waste hierarchy proposed by the EU waste framework directive	78
Figure 2.21. Design flowchart of novel CLT modular connections	84
Figure 3.1. Interlocking connection system used in (a) Yingxian wooden tower in 1056 ad [3.1] and (b) modern construction (lock connector from rothoblaas ltd.)	96

Figure 3.2. 3D renders of continuous connectors attached on the CLT panels using fasteners	97
Figure 3.3. Application overviews of the novel interlocking connection system for different clt modular structures and the close-up of construction details	99
Figure 3.4. End-locking devices for (a) shear connection and (b) tensile connection.	100
Figure 3.5. The illustrations of the interlocking connection working mechanism in single module and the sectional elevation of the structure showing the overall constraints: (a) CLT volumetric structures; (b) CLT platform structure; (c) CLT balloon structure.	102
Figure 3.6. Comparison in potential building life cycles between clt buildings using conventional connections (top) and interlocking connections (bottom).	103
Figure 3.7. Evaluations of connection design.	104
Figure 3.8. Capacity design strategies of conventional connection (left) and interlocking connection with damage-controlled capacity (right)	106
Figure 3.9. Capacity design flow chart of (a) conventional plate connections and (b) novel interlocking connection	108
Figure 3.10. Conventional mortise-tenon connections	109
Figure 3.11. Schematisation the basic units of interlocking connection (in mm)-version 1	110
Figure 3.12. Schematisation the basic units of interlocking connection (in mm)-version 2	112
Figure 3.13. Sectional views of connection within (a) CLT volumetric structure; (b) CLT panelised platform-type structure; (c) CLT panelised balloon-type structure.	114
Figure 3.14. The joining details of (a) conventional CLT volumetric structures and (b) CLT volumetric structures with interlocking connections	115

Figure 3.15. Illustrations of model installation and details of interlocking connections on timber modules.	116
Figure 3.16. Interlocking connection-reinforced timber modules under (a) lateral and (b) vertical load.	116
Figure 4.1. Experimental set-ups for (a)&(c) interlocking shear connection and (b)&(d) tensile connection	122
Figure 4.2. Loading profiles employed in (a) monotonic test and (b) cyclic test	124
Figure 4.3. Conditioning of CLT panels before testing	125
Figure 4.4. Marked position for connection and predrilling on panels	126
Figure 4.5. Dimensions of screws	127
Figure 4.6. Locations of shear connectors (left) and tensile connector (right) on CLT panels.	127
Figure 4.7. 3d printed connection specimens	130
Figure 4.8. Unpolished and polished (a) shear connector and (b) tensile connector	131
Figure 4.9. Coupon dimensions determined by EN ISO 6892-1	131
Figure 4.10. coupon test of SS420/BR (a) testing set-up for coupon test (b) coupons specimens machined from the bottom plate of the tested connectors (c) tested specimens	132
Figure 4.11. Experimental data of coupon test and the mean material properties used as input data in simulation	133
Figure 4.12. Geometry, cross-section, and details of in push-out test on HBSP12120	135
Figure 4.13. Geometry, cross-section, and details of pull-out test on LBS7100	135

Figure 4.14. Typical connection behaviours when applying EN 26891	136
Figure 4.15. Force-displacement (left) and deformation response (right) of the new and the used hbsp12120	137
Figure 4.16. Force-displacement (left) and deformation response (right) of the new and the used LBS7100	138
Figure 4.17. The hysteresis loops (a) and (b) the primary deformation modes in shear connection specimens	140
Figure 4.18. Deformation of shear connection specimens	141
Figure 4.19. The hysteresis loops (a) and (b) the primary deformation modes in tensile connection specimens	142
Figure 4.20. Deformation of shear connection specimens in (a) cyclic testing and (b) monotonic testing	142
Figure 4.21. Comparison of screw deformation in interlocking connection and STC connection	144
Figure 5.1. The outline and boundary conditions of fe model of the shear connection	149
Figure 5.2. Non-linear contact relationship employed in shear screws-timber contact modelling	151
Figure 5.3. Four buckling modes extracted by ‘block lanczos’ method	152
Figure 5.4.the outline of boundary conditions of fe tensile connection model	152
Figure 5.5. Simplified FE model for screws in tension	153
Figure 5.6. Mesh size considered in the mesh sensitivity study of (a) shear male connector (b) tensile male connector	155

Figure 5.7. Force-displacement response obtained from different mesh size in (a) shear male connector model and (b) tensile male connector model	155
Figure 5.8. Comparisons between experimental results and FEA output in (a) hysteresis loops and (b) the deformation modes in shear connection specimens (in mm)	156
Figure 5.9. Comparisons between experimental result and FEA in (a) hysteresis loops and (b) the deformation modes in tensile connection specimens (in mm)	157
Figure 5.10. Force and displacement curve of interlocking shear connection	159
Figure 5.11. Shear connection buckling behaviours analysis on primary working direction	160
Figure 5.12. Stress distribution on shear connections and screws under the displacement of 30 mm in (a) the primary direction and (b) the secondary direction	160
Figure 5.13. Force and displacement curve of interlocking tensile connection	162
Figure 5.14. Von mises stress contour in the interlocking tensile connections under the displacement of 15 mm in (a) the primary direction and (b) the secondary direction	162
Figure 5.15. Linearisation of tensile connection response.	166
Figure 5.16. Initial parametric study on tensile connections for parameter T1-T5	168
Figure 5.17. Deformed shapes of tensile connection at 25 mm vertical displacement with the minimum and maximum values in parameter (a) T1, (b) T2, (c) T3, (d) T4, (e) T5	170
Figure 5.18. Output of detailed parametric on tensile connection	170
Figure 5.19. The changes in connection stiffness at different stages with the changes in parameters T1 and T4	171
Figure 5.20. Initial parametric study on shear connections for parameter S1-S6	173

Figure 5.21. The buckled shape of shear connection at the first buckling point with the minimum and maximum values in parameter (a) S1, (b) S2, (c) S3, (d) S4, (e) S5, (f) S6	174
Figure 5.22. Output of detailed parametric on shear connection	175
Figure 5.23. Different deformation modes considered in the interlocking tensile connector	176
Figure 5.24. Force analysis of tensile connection under tension for deformation 1	177
Figure 5.25. Force analysis of vertical connection under tension for deformation 2	179
Figure 5.27. Force analysis of vertical connection under tension for deformation 3	181
Figure 5.28. Comparison between analytical and fem results of parameters T1 (top) and T4 (bottom)	182
Figure 5.29. Comparison of FE and analytical connection detailed key parameter for the tensile connection	183
Figure 5.30. Force analysis of shear connection under lateral load	184
Figure 5.31. Comparison between analytical results and FEM in (a) parameter s3 and (b) parameter s6	185
Figure 5.32. Performance of the analytical methods in predicting the yield strength of shear connection	186
Figure 6.1. Validation model (a) experimental set-up (b) FE model	192
Figure 6.2. Load-displacement relationship for fasteners in (a) transverse direction and (b) axial direction	194
Figure 6.3. CLT shear wall modelling validation (a) overview of FE model of CLT shear wall (b) FEM results (c) experimental results	196

Figure 6.4. Force-displacement curves of experiment and fem of conventionally reinforced CLT shear walls.	197
Figure 6.5. Geometries and connection arrangements of the investigated walls	198
Figure 6.6. Model of continuous tensile connection with simplified screws elements	199
Figure 6.7. The strength comparison between the detailed and the simplified tensile model	202
Figure 6.8. Deformation in wall-P-1 at 80 mm displacement	204
Figure 6.9. Deformation in wall-P-2 at 80 mm displacement	205
Figure 6.10. Deformation in wall-I-1 at 65 mm displacement	207
Figure 6.11. Deformation in wall-I-2 at 65 mm displacement	208
Figure 6.12. Deformation in wall-I-3 at 65 mm displacement	209
Figure 6.13. Deformation in wall-I-4 at 65 mm displacement	210
Figure 6.14. Push-over results summary	212
Figure 6.15. Calculation of sliding and rocking contribution	213
Figure 6.16. Sliding and rocking drift in shear walls with different connection configurations	214
Figure 6.17. Deformation mechanisms of CLT shear wall with (a) conventional connections and (b) interlocking connections	215

List of Table

Table 2.1 List of novel connections and reinforcing systems for CLT modular construction	57
Table 2.2 Comparison of the experimental results for the novel connections	64
Table 2.3. DfR connection design criteria and weightings	81
Table 3.1. Summary of design specifications of the interlocking connections	117
Table 3.2. DfR performance assessment of the interlocking connections	118
Table 4.1. Material properties for CLT panels (spruce)	125
Table 4.2. Dimensions of screws used in experiment (in mm)	127
Table 4.3. Material properties of SS420 3D printed coupons	133
Table 4.4. Key test results (mean values) obtained for both shear and tensile testing (EN26891)	138
Table 4.5. Key test results (mean values) obtained for both interlocking shear and tensile connection testing (EN26891)	143
Table 5.1. Geometries and material parameters of tensile connection models in the parametric study	164
Table 5.2. Geometries and material parameters of shear connection models in the parametric study	165
Table 6.1. Material parameters for CLT panels	193
Table 6.2. The screw properties calculated from ec5 and adopted in the models	194
Table 6.3. Comparison of overstrength factors for different connection systems	201

List of Abbreviations

Abbreviation	Meaning
3D	Three-dimensional
AEC	Architectural, engineering and construction
AM	Additive manufacturing
BCA	Building and Construction Authority
C&D	Construction and demolition
CLTPS	CLT panelised structures
CLTVS	CLT volumetric structures
DfD	Design of deconstruction
DfDR	Design for deconstruction and reuse
DfR	Design for reuse
DMLS	Direct Metal Laser Sintering
EWPs	Engineered Wood Products
EYMs	European Yield Models
EYMs	European Yield Models
FE	Finite Element
GWP	Global Warming Potential
JMA	Japan Meteorological Agency
KPIs	Key Performance Indicators
LCA	Life Cycle Assessment
LVDTs	Linear Variable Differential
LVL	Laminated Veneer Lumber
MMC	Modern method of construction
NBCC	National Building Code of Canada
PGA	peak ground acceleration
SLS	Serviceability limit state
STC	Steel-timber composite
TMC	Timber modular construction
ULS	Ultimate limit state
WAAM	Arc Additive Manufacturing
WRA	Wood Recy-cler Association

Terms and definitions

Steel-to-Timber composite connection	An engineered joint connecting steel and timber to enhance structural performance.
Cyclic test	Repetitive loading and unloading of a structure to evaluate durability and seismic resilience.
Monotonic test	A continuous load application to a structure until failure to determine its maximum capacity.

Chapter 1 Introduction

In recent years, the architectural, engineering, and construction (AEC) industry has increasingly recognized the need to prioritise sustainability. The construction industry must balance the imperative to protect natural resources with the demand for development and urbanization to accommodate a growing population. Therefore, a profound rethinking of traditional housing construction practices is necessary. This necessitates the consideration of carbon-neutral or carbon-negative construction materials while mitigating the extensive use of highly energy-intensive and high carbon-emitting materials like steel and concrete. In this context, sustainable practices are increasingly adopted, with a growing interest in mass timber construction, which offers significant benefits in terms of efficiency and environmental impact. Among these innovations, Cross-Laminated Timber (CLT) modular construction has gained attention for its potential to revolutionise low to mid-rise building designs. This chapter begins with an overview of mass timber construction and the advantages of using engineered wood products (EWPs). It then delves into modern mass timber modular construction techniques, highlighting the unique aspects of CLT modular construction. Following this, the research questions that drive this study are presented, alongside the aim and objectives. The chapter also outlines the research methodology and discusses the anticipated contributions to knowledge.

1.1 Mass Timber Construction with Sustainable Engineered Wood Products (EWPs)

Timber is one of the oldest construction materials, now resurges as an environmentally friendly alternative in the modern construction market. With the fast-developing manufacturing methods such as veneering, fastening, gluing and lamination being applied in timber material production, the limitations of natural timber (size and natural defects) can be overcome. This leads to significantly enhanced material properties and better size flexibility, and the resulting timber products are known as Engineered Wood Products (EWPs).

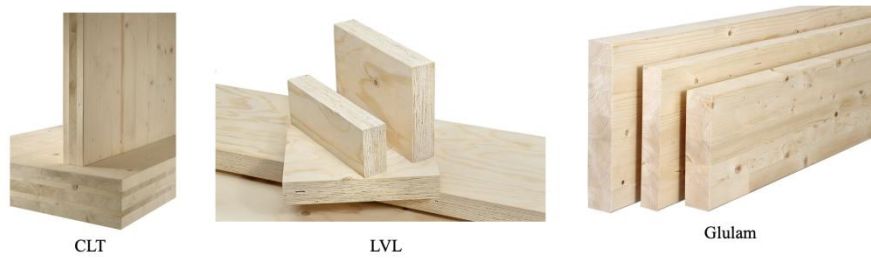


Figure 1.1. Configurations of different Engineered Wood Products (EWPs) [1.1]

Modern mass timber construction adopts EWPs that can be used as structural material, such as Glulam, Laminated Veneer Lumber (LVL) and Cross-Laminated Timber (CLT) [1.2] (Figure 1.1). When being used as structural material, timber is easily machinable with good accuracy, light in weight, and comparable in strength to concrete and steel, enabling greater design flexibility and easier handling with reduced workforce. In terms of structural performance, engineered timber has a strength-to-weight ratio more than 5 times higher than concrete and around 20% higher than steel [1.3 and 1.4], making it possible to build a timber structure with comparable stiffness and as little as one-fifth the self-weight of their counterparts, thus reducing the requirements on foundation and soil conditions. As timber is the only renewable load-bearing construction material currently available [1.5], another major benefit of using EWPs comes to the direct sustainability. Timber can be sourced from managed sustainable forests with planned cultivation and consumption; the carbon absorbed by timber during its growth can contribute to significantly reduced embodied energy. Moreover, timber can help improve the operational energy performance of buildings with its inherent relatively low thermal conductivity [1.6 and 1.7].

1.2 Modern Mass Timber Modular Construction

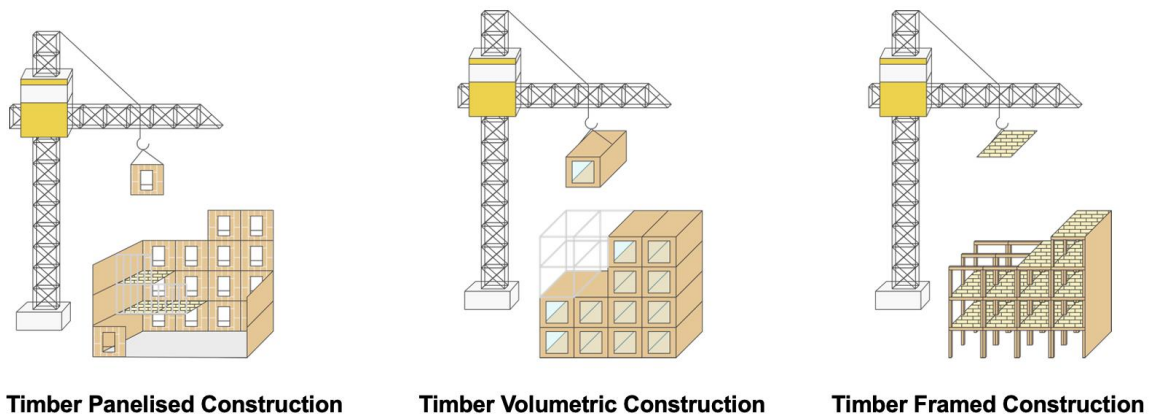


Figure 1.2. Different structural systems in timber modular construction

Modular construction is a modern method of construction (MMC) that involves high degree of prefabrication. Its application with concrete and steel is now rapidly growing in densely populated regions due to their great efficiency and reduced disruption to construction site, while the potential of EWPs in modular construction is also being explored for its additional material sustainability [1.8]. Timber modular construction (TMC) (Figure 1.2) is benefited from both the efficiency of modularity and the sustainability of timber materials. In this construction method, timber structural elements, such as post, beams, panels and room modules are manufactured and sized in the factories and then transported to the construction sites for being assembled into the complete buildings. During off-site manufacturing, enhanced quality control and project efficiency are ensured, leading to a reduction in waste and noise production on-site. This approach also minimises deviations in the construction sequence, while offering significant potential for dismantlement and reuse. [1.9].

Most of the published Life Cycle Assessment (LCA) case studies show that timber structures demonstrate better environmental performance than reinforced concrete structures [1.10]. In a comparative study by Aye et al [1.11], the greenhouse gas emission of timber modular construction is similar to the conventional concrete construction but is around 9% less than the steel modular construction, even when excluding the carbon sequestration of timber in the plantation phase. Further reduction in embodied energy can be achieved by considering the carbon sequestration of timber material (component, member and systems) reusability of modular buildings.

After realising the efficiency and sustainability of timber construction, increasing government policies are in place to promote the adoption of timber structural material, to be used solely or in combination with steel, also known as hybrid steel-timber. For instance, Singapore's Building and Construction Authority (BCA) has published rules requiring at least 30% certified timber from sustainably managed forests in all new public buildings. In addition, countries like Finland are providing incentives for developers who commit to using certified timber products by offering discounts on taxes related to development projects [1.12].

1.3 CLT Modular Construction

Cross Laminated Timber (CLT) is one of the most used EWPs and is experiencing rapid development. Being made from layers of timber planks that are glued perpendicularly [1.13], CLT breaks the size limitation of original timber material and achieves better strength

uniformity and dimensional stability [1.14, 1.15]. Due to its superior sustainability, higher degree of prefabrication and strength-to-weight ratio than conventional construction materials [1.7, 1.16], CLT is increasingly popular in the application of prefabricated low-rise (3-4 stories) and mid-rise panelised and volumetric structures (5-8 stories) [1.8]. According to a comprehensive comparative study by Jensen, et al. [1.17], although multi-storey CLT shear wall systems deploy more material than other timber structural systems, it is benefited significantly from being self-sustainable without concrete core, which is the primary source of Global Warming Potential (GWP) reductions. CLT shear wall and floor system has the lowest GWP among all studied structural systems, and is 52% less than the conventional concrete and steel structures (Figure 1.3). Therefore, CLT modular construction is potentially a powerful tool for the construction industry to combat climate changes.



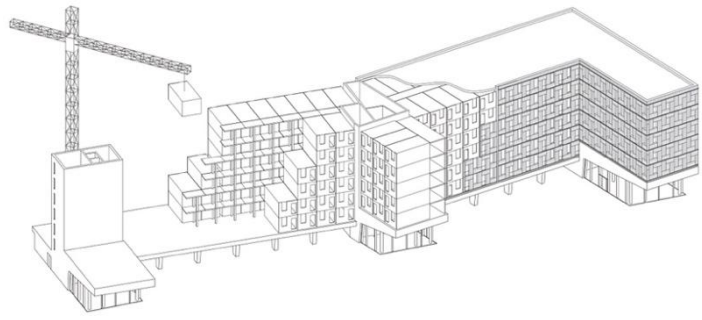
GLOBAL WARMING POTENTIAL & MATERIAL MASS
per building assembly

The total global warming potential (GWP) of each option is shown with a breakdown by building assembly. The Ref 1 and Ref 2 options have the highest GWP, with the bulk impact embedded in the floor slabs. Timber 9 offers a slight reduction in GWP, with the savings realized in the floor slabs. Timber 5, a post beam and plate option, offers a relatively typical approach to building with timber, showing savings in floor slabs, beams and columns. Since Timber 8 and 7 are cellular approaches with load-bearing walls, these options included steel podiums to accommodate the ground floor program. Timber 8 shows how a hybrid approach with light gauge metal yields GWP savings in floor slabs, structural walls and exterior walls, despite the addition of the podium. Lastly, Timber 7 emphasizes how a completely cellular CLT timber approach yields impressive reductions in nearly every category.

Figure 1.3. Full building GWP Comparison of different structural systems [1.17]



(a)



(b)

Figure 1.4. CLT volumetric project Woodie student accommodation, a 6-storey timber modular structure. (a) Lifting of timber module [1.18]; (b) Construction diagram [1.19]

To further develop the timber construction market, many studies are focusing on the development and sustainability of high-rise timber buildings for high-density urban areas, where almost all new buildings are high-rise towers built to accommodate the large population over the competitive use of limited land space. Emerging architectural designs for high-rise CLT buildings, even skyscrapers (Tree Tower Toronto [1.9], 191-199 College Street [1.10]), bring great emphasis on the engineering challenges that need to be overcome [1.11], such as the performance of CLT structural systems under environmental forces. The light-weight nature of timber contributes to lower seismic forces, while it also reduces buildings' overturning resistance to lateral load [1.12], which necessitates the development of high-performing connectors for the CLT shear wall panels or volumetrics. Due to the discrete nature of connectivity in modular structures [1.20], connections are the critical components for structural performance, robustness, and integrity. Due to the relatively recent development of this construction technology, research on its connection systems is still in its early stages [1.3].

Current timber modular structures are relatively vulnerable under environmental forces such as wind loads and seismic actions due to the absence of high-performing and specially designed timber connections [1.21]. The existing timber connections products (angle brackets and hold-downs) have their own limitations and limited applicability to timber modular structures. Insufficient capacities, unpredictable behaviours and the risks of brittle failure in metal connectors are apparent. These limitations hinder the realisation of large timber modular structures.

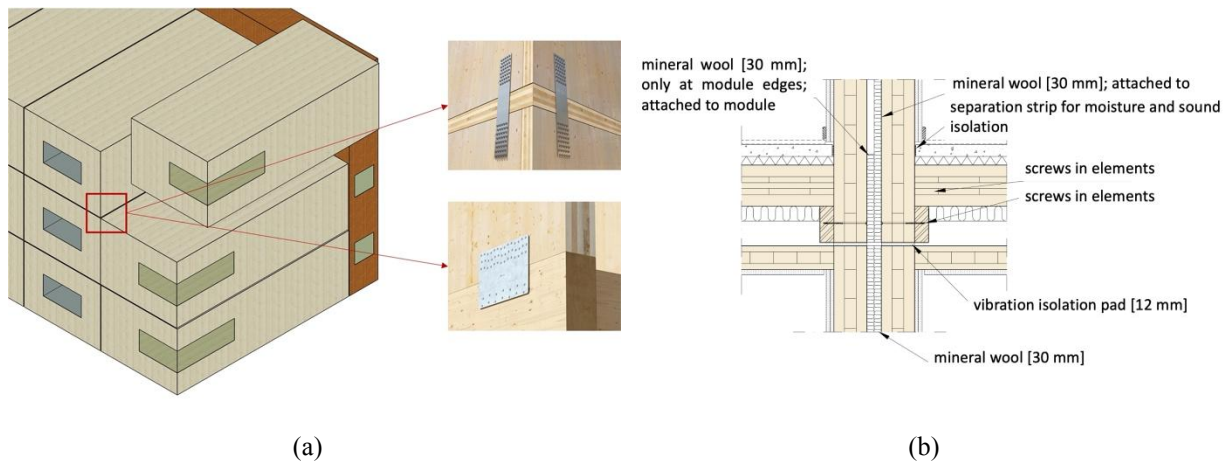


Figure 1.5. Illustrations of hold-downs and brackets in typical CLT modular structures (a) and the joint between modules with no inter-module connection (b) [22]

In addition to the structural performance, the construction/installation process of timber modular structures is also problematic. Due to the brittleness of timber material, large number of fasteners such as nails and screws are used in timber connections to achieve desired ductility, which however, introduces difficulty in the manual installation of connections on-site. In multi-storey timber modular structures, particularly those utilising large areas of timber panels like CLT modular structures, the available space for accessing connections can be constrained (Figure 1.5). On-site operations with inherent risks, such as working at height for connection installation, are sometimes necessary. Therefore, the installation of connections may require experienced technicians and involve risky external access using a mobile platform (Figure 1.6.a). In the case of CLT volumetric structures, drilling on panels is essential to access points for connection installation due to the enclosed space between room modules (Figure 1.6.b), which limits the time and cost efficiency of timber modular construction and as well as damage the structural integrity.



(a)



(b)

Figure 1.6. Problematic construction process in TMC: (a) Manual connections installation at height; (b) Access inter-module connections via a hole on the gable wall

With a shared objective of reducing environmental impact and its tremendous potential in transitioning to construction 5.0, CLT modular construction is a powerful tool to pave the way for a zero-carbon future, which has received increasing interest in the market. Therefore, CLT construction is expecting to experience continuous growth. However, CLT modular construction still faces challenges as a relatively new technology, with issues encompassing unclear structural performance, limited understanding of financial and environmental benefits, lack of suitable connection devices, and excessive material usage due to insufficient investigation. Therefore, CLT modular construction has not reach its full sustainable and construction potential. New connection devices designed specifically for CLT modular construction to achieve enhanced structural performance with better efficiency is urgent needed to meet the challenges associated with fast-developing CLT construction.

1.4 Research Questions

In this section, the below central questions are presented to guide the investigations in CLT modular connection development in this research:

1. What are the immediate challenges in constructing CLT modular buildings that are related to conventional connection systems, considering factors such as construction time, ductility requirements, and damage mitigation?
2. What factors were considered in the design of previous novel CLT modular connections and what kind of novel design strategies were adopted in these connection designs to address the identified challenges?
3. What is the construction strategy of the proposed connection system and how is the construction efficiency of it compared to conventional connections?
4. What are the mechanical properties and behaviours of the proposed interlocking connection under working conditions, and how do these properties compare to traditional connection methods used in CLT construction?
5. How can advanced simulation techniques, such as finite element analysis and computational modelling, be employed to predict the response of medium-rise CLT modular buildings equipped with the novel interlocking connection?

1.5 Aim

The aim of this project is to explore novel connection solutions for medium rise CLT modular buildings, with particular focus on the ease of assembly and the enhanced lateral resistance under environmental forces, meanwhile to bridge the research gaps in CLT modular connections by contributing on the design, performance evaluation and optimisation practice of innovative timber connections.

1.6 Objectives

The project has a number of objectives:

1. Gain a general understanding of the design, construction and performance of CLT modular structures and conventional timber connections via literature review, then identify the existing challenges in realising medium-rise CLT modular structures that are related to existing connection systems.
2. Talk with the industry to understand the latest demands in CLT modular construction and determine the design directions of the new connection system as well as the assembly and

disassembly requirements.

3. Propose an innovative connection system for medium rise CLT modular structures to address challenges identified in the literature review and through the industrial meetings; liaise with engineers about the connection design to ensure the innovation and practicability.
4. Employ FE (Finite Element) analysis to study the behaviours of the preliminary connection design, then improve the design details and plan experimental works accordingly based on Eurocode 5.
5. Test the proposed connection system in the steel-to-timber connection assembly with testing apparatuses that simulate realistic working conditions to understand the mechanical performance and deformations, as well as the load transfer mechanism between CLT, the proposed steel connectors and fasteners.
6. Validate the numerical models using experimental outputs and conduct parametric studies to assess the influence and sensitivity of different geometrical parameters to the stress and strain distribution, initial stiffness, ductility and failure modes of connection.
7. Construct a FE macro-model of the CLT structure with the proposed connections to study load transfer between structural elements under lateral force; make a comparative study between conventional connections and the new connections in the same numerical structure to evaluate the impact of the proposed connections subject to lateral behaviours.
8. Develop a design process implementing analytical models that couple geometrical parameters with mechanical properties of the proposed connections for future standardisation, design and application.

1.7 Research Methodology

1.7.1 Concept development of the new connection system

A comprehensive review of existing connection methods and their limitations within the context of timber and CLT modular construction was first conducted. This review serves as the theoretical foundation for identifying key challenges and opportunities for improvement. Based on the outcomes of literature review, connection design was conducted to realise the

novel functionalities (damage control, interlocking technique, continuous reinforcement) that address the identified challenges. These developed connection concepts were evaluated against the criteria such as structural performance, ease of installation, manufacturability, and compatibility with modular construction principles. The evaluation allowed for the refinement and optimisation of the proposed concepts, ensuring they align with the desired objectives and overcome the identified challenges.

1.7.2 Experimental works

Quasi-static monotonic and cyclic testing prescribed in Eurocode 5 were carried out on the connection prototypes in the format of steel-to-timber assembly to evaluate their stiffness, strength, ductility and failure modes. Conventional steel-to-timber composite connections using the same plate thickness and screw diameter as the new connections, were also tested under the same boundary conditions to compare the behaviour differences between the conventional connections and the novel connections.

1.7.3 Numerical simulations

Numerical analysis using commercial FE software ABAQUS was adopted to examine the mechanical behaviours of the proposed connection. Prior to the experiments, three-dimensional FE models were first developed for the preliminary connection design, adopting validated modelling methods in published studies of steel-timber composite connection to explore the load-slip behaviours, the load transfer and interaction between connection components, and the failure modes in several loading cases. Following the FE validation with the experiments conducted as part of this thesis, parametric studies were carried out using the numerical connection models by varying geometric parameters in a given range. After calibrating the spring elements using connection and fastener properties, FE macro-models for full-scale panellised modular structures with both conventional plate connections and new connections were developed to assess the impact of the new system on the lateral behaviours timber modular structures.

1.7.4 Analytical methods

Theoretical analysis based on code provisions or the literature were carried out to verify the numerical and experimental analyses and to derive formulae for calculating the load-bearing capacity of the proposed connection for application and standardisation.

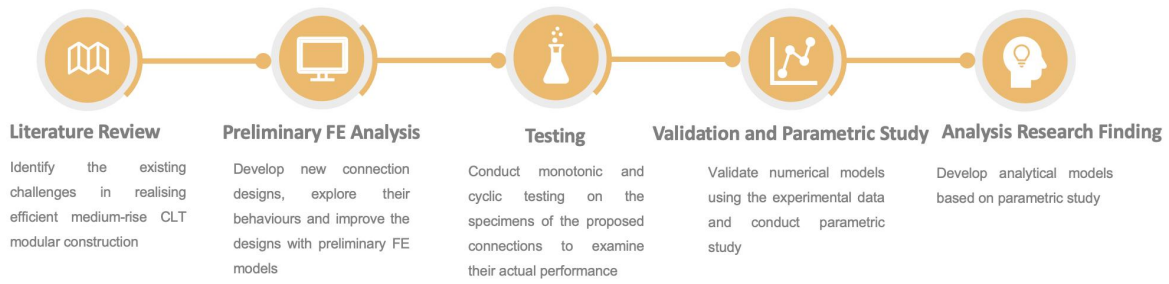


Figure 1.7. Methodology flow chart of the connection design program

1.8 Contribution to Knowledge

This research summarised and discussed the state-of-art timber connections, and proposed a new evaluating framework to holistically consider the mechanical, manufacturing and constructing performance of connection, which can serve as a valuable reference to guide the development of future timber connection. An innovative connection system was proposed for under this framework for medium-rise CLT modular buildings in this research for simplifying the assembly process and improving the structural integrity. It showcases a new strategy of connecting structural elements to the timber construction industry, which allows effortless assembly as well as potential disassembly and reusability. The numerical analysis conducted at a macro-scale during the latter stages of the research enhanced the limited understanding of the lateral performance of timber modular structures with continuous interlocking connections.

1.9 Chapter References

- [1.1] puuinfo. *WHY WOOD? | ENGINEERED WOOD PRODUCTS*. 2020. Available from: <https://puuinfo.fi/puutieto/engineered-wood-products/?lang=en>.
- [1.2] Timber Trade Federation. *Engineered Wood Product*. n.d. Available from: <https://ttf.co.uk/timber-trade-topics/engineered-wood-products/>.
- [1.3] Wood Solution. *Strength Performance*. n.d. Available from: <https://www.woodsolutions.com.au/articles/strength-performance>.
- [1.4] Davies, A., *Modern Methods of Construction: A forward-thinking solution to the housing crisis?* 2018, Royal Institution of Chartered Surveyors.
- [1.5] Ramage, M.H., Burrige, H., Busse-Wicher, M., Fereday, G., Reynolds, T., Shah, D.U., Wu, G., Yu, L., Fleming, P., Densley-Tingley, D., Allwood, J., Dupree, P., Linden, P.F. and Scherman, O. *The wood from the trees: The use of timber in construction*. Renewable and sustainable energy reviews, 2017. **68**: p. 333-359.
- [1.6] Structural Timber Association. *Cross-laminated timber construction - an introduction*. Available from: <http://www.structuraltimber.co.uk/assets/InformationCentre/eb11.pdf>.
- [1.7] Liu, Y., Guo, H., Sun, C., Chang, W.S, *Assessing cross laminated timber (CLT) as an alternative material for mid-rise residential buildings in cold regions in china—a life-*

- cycle assessment approach*. Sustainability (Basel, Switzerland), 2016. **8**(10): p. 1047-1047.
- [1.8] Svatoš-Ražnjević, H., L. Orozco, and Menges, A., *Advanced timber construction industry: a review of 350 multi-storey timber projects from 2000–2021*. Buildings (Basel), 2022. **12**(4): p. 404.
- [1.9] Koppelhuber, J., Hintersteiner, K., and Heck, D., *Industrialized timber construction – construction management aspects and influences in modular timber building systems*, in *Interaction between Theory and Practice in Civil Engineering and Construction*. 2016. p. 399-404.
- [1.10] Cadorel, X. and Crawford, R. *Life cycle analysis of cross laminated timber in buildings: a review*, in *Engaging Architectural Science: Meeting the Challenges of Higher Density: 52nd International Conference of the Architectural Science Association*. 2018, The Architectural Science Association and RMIT University. p. 107-114.
- [1.11] Aye, L., Ngo, T., Crawford, R.H., Gammampila, R. And Mendis, P., *Life cycle greenhouse gas emissions and energy analysis of prefabricated reusable building modules*. Energy and buildings, 2012. **47**: p. 159-168.
- [1.12] PBCtoday. *How can sustainable structural timber help achieve net zero?* 2023; Available from: <https://www.pbctoday.co.uk/news/mmc-news/how-can-sustainable-structural-timber-help-achieve-net-zero/122865/>.
- [1.13] Karacabeyli, E. and Gagnon, S., *Canadian CLT Handbook*. 1 ed. Vol. 1. 2019: FPInnovations.
- [1.14] Hassanieh, A., Valipour, H.R. and Bradford, M.A., *Composite connections between CLT slab and steel beam: Experiments and empirical models*. Journal of constructional steel research, 2017. **138**: p. 823-836.
- [1.15] Kurzinski, S., Crovella, P. and Kremer, P., *Overview of Cross-Laminated Timber (CLT) and timber structure standards across the world*. 2022. **5**: p. 1-13.
- [1.16] Guo, H., Liu, Y., Meng, Y., Huang, H., Sun, C., Shao, Y., *A comparison of the energy saving and carbon reduction performance between reinforced concrete and cross-laminated timber structures in residential buildings in the severe cold region of china*. Sustainability, 2017. **9**(8).
- [1.17] Jensen, A., Sehovic, Z., St. Clair Knobloch, N., Klein, J., Richardson, P., Janiski, J. *Mass Timber Solutions for Eight Story Mixed-Use Buildings: A Comparative Study of GHG emissions*. in *the 35th PLEA Conference on Passive and Low Energy Architecture*. 2020. A Coruña: University of A Coruña and Assoc.
- [1.18] Wrage, G., *Student Residence UDQ, Hamburg*. n.d; Available from: <https://www.getzner.com/en/case-studies/student-residence-udq-hamburg>.
- [1.19] Sauerbruch, H. *Universal Design Quarter, Hamburg*. n.d. Available from: <http://www.sauerbruchhutton.de/en/project/udq>.
- [1.20] Corfar, D.-A. and Tsavdaridis, K.D. *A comprehensive review and classification of inter-module connections for hot-rolled steel modular building systems*. Journal of Building Engineering, 2022. **50**: p. 104006.
- [1.21] Ormarsson, S., Vessby, J., Johansson, M. and Kua, L. *Numerical and experimental study on modular-based timber structures*. Modular and offsite construction (MOC) Summit Proceedings, 2019: p. 471-478.
- [1.22] Stora Enso. *3–8 Storey Modular Element Buildings*. n.d.; Available from: <https://www.storaenso.com/-/media/documents/download-center/documents/product-brochures/wood-products/design-manual-a4-modular-element-buildings20161227finalversion-40en.pdf>.

Chapter 2 Literature Review

To identify knowledge gaps in the field of CLT modular construction (CLTMC) and to understand the appropriate connection design strategies, this chapter presents a literature review covering the materials, structural, and connection systems currently utilized in this modern method of construction. The chapter thoroughly reviews current research practices, including experimental and numerical studies, to gain insights into the structural behaviours of CLT buildings. Following this, the discussion focuses on the challenges encountered in the construction of medium-rise CLT modular structures, particularly regarding existing timber connections, as revealed in published findings.

2.1 Overview of CLT and CLT Modular Structures

2.1.1 Cross Laminated Timber (CLT)

CLT is one kind of EWPs that typically composed of 3, 5 and 7 layers of timber boards that are stacked and glued perpendicularly (Figure 2.1), to form panels with a thickness between 60 mm and 500mm. The common width of CLT panels is about 3.5m, and the length can reach up to 16m, while it is theoretically unlimited. The cross-lamination process in the manufacture of CLT reduces the impact of the orthotropy of each timber layer, and limits the affected areas of the inherent defects (knots, shakes, checks, splits, etc) in natural timber [2.1] (Figure 2.2). This manufacturing process results in enhanced and more uniform properties, and allowing for the use of smaller, lower quality and under-utilised timber. It also exhibits better stiffness on the orthogonal direction than other EWPs, in which the lumbers and veneers are stacked in the same direction (parallel to grain) [2.2]. In structural design, the axial compressive resistance of structural CLT panels is determined by the thickness of the timber boards considering only the layers orienting parallel to the loading direction. The enhanced stiffness of CLT panels ensures increased in-plane stability of CLT structural components, such as walls and floors. Therefore, CLT panelised and volumetric structures can be applied in mid-rise or even high-rise structures, while timber framed structures are normally used in low-rise structures [2.3].



Figure 2.1. Configuration of CLT [2.4]

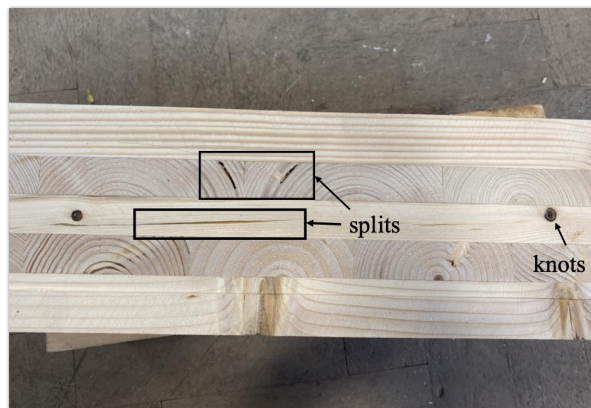


Figure 2.2. Natural defects within timber

2.1.2 CLT modular structures

CLT panels in modular structures can be used as both vertical shear walls and horizontal floors. Depending on the panel arrangements, CLT modular structures can be divided into CLT panelised structures (CLTPS) and CLT volumetric structures (CLTVS).

CLT panelised structures (CLTPS)

Two construction techniques can be found in CLTPS: platform-type construction and balloon-type construction (Figure 2.3). In platform-type construction, each floor serves as a platform for the structure above, where the walls on each floor function as an independent rocking system that is connected to the floor below. The wall assembly is composed of individual panels that are connected vertically through joints. The drawback of platform-type construction is that it entails a large number of panels to be handled on-site, as well as numerous connections between panels and floors. This results in the accumulation of connection deformations at each level and perpendicular-to-grain compressive stresses on the floor panels. In contrast, the balloon-type system utilises continuous panels on both sides,

spanning multiple floors, so it is exceptionally effective in terms of resisting lateral load [2.5]. The intermediate floors are framed into the face of the wall panels, eliminating the perpendicular to grain bearing between floors. This approach allows for the construction of walls with slender panel aspect ratios and reduces the number of connections compared to platform-type structures.

Platform-type construction is currently the most widely adopted technique in CLT construction, with all design provisions tailored specifically to this approach [2.5]. In contrast, the concept of balloon-type construction has been relatively recently proposed, so currently there is limited research and a few practical applications for it, such as the two-story Begbie Elementary School in Vancouver, Canada [2.5-6]. Increasing research [2.5-10] are performed recently to better study the performance of this construction method to support design code proposal.

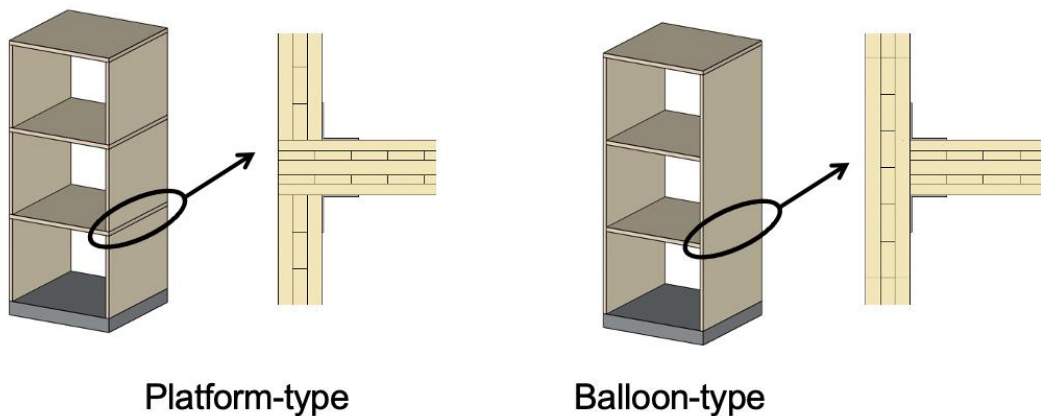


Figure 2.3. Platform-type and balloon-type CLT panelised buildings

CLT Volumetric structures (CLTVS)

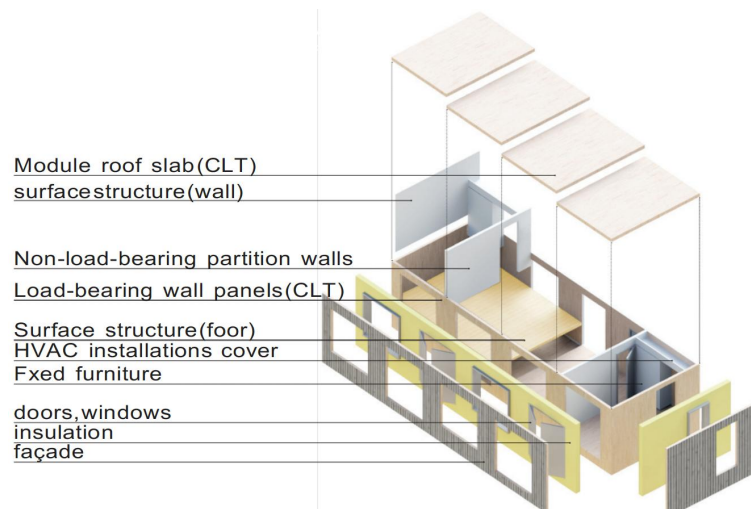


Figure 2.4. Structure of typical CLT module [2.11]

In CLTVS, CLT flat modules are prefabricated with preassembled building accessories such as cladding, internal finishes and MEP services (Figure 2.4). This increases its efficiency compared to volumetric construction methods using other materials, as the modules in which have to be left unfinished (without drywalls, plaster joint and paint) upon delivery for the required space for accessing connections. The structure of most CLT modules is similar to the platform type of CLT panelised structure, where the wall panels are placed between floor and ceiling panels to form the typically rectangular flat modules. Thus, the gravity load is transferred via the bearing between vertical and horizontal timber panels [2.12]. The high level of prefabrication of this construction method can help reduce waste production, workspace requirements and reliance for on-site manual work.

Once placed onsite, CLT modules are horizontally and vertically linked to each other by inter-module connections in a multi-step process, forming a continuous load path from the roof to the foundation. However, the installation of inter-module connections is a time-consuming operation; workers need to access various connection locations to fix screws and bolts to build the connectivity between modules after the placement of the upper modules on top of the lower modules. Additionally, due to the closure feature of CLT modules, inter-module connections can only be discretely installed on the outer surface of modules, when the internal surface is normally left disconnected, relying only on joint connections and friction between modules for lateral resistance [2.13-14], compromising the overall reinforcing impact (Figure 2.5). When necessary, gable wall may need to be drilled to access

inter-module connections (Figure 1.6 (b)), which could potentially damage the structure of modules and cause delay in the construction schedule. Therefore, the inter-module connections in CLTVS strongly impact not only the overall structural performance, but also the construction efficiency.

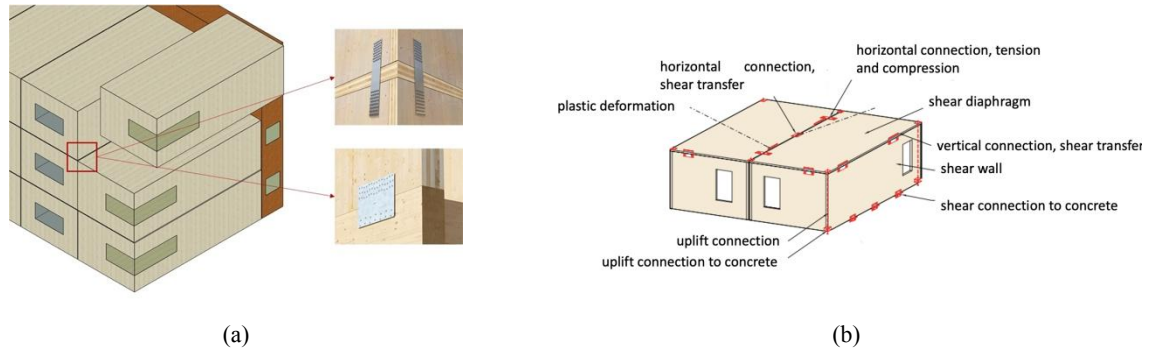


Figure 2.5. Illustration of conventional inter-module connections: (a) the conventional hold-down (top) and bracket (bottom) and (b) their locations in CLT volumetric structures [2.11]

2.1.3 Challenges in the realisation of multi-storey CLT modular buildings

When the tallest steel volumetric building to date, 101 George Street in London, reached a height of 135m [2.15], timber modular structures were limited to 14 storeys (Figure 2.6). The tallest timber modular building to date is ‘Treet’ in Norway, completed in 2015, standing at a height of 52.8m. It utilises stacked modules as the secondary structural system to support gravity loads and a thick Glulam frame as the primary lateral system [2.14]. Due to the discrete nature of modular construction, the brittleness of timber and the sensitivity of timber structures to the lateral load, design guidebooks [2.11, 2.16] require timber modular structure that exceeds 5 stories to be reinforced by additional Lateral load Resisting System (LLRS) such as moment-resisting frames, timber cores, concrete cores, or interior demising walls. These reinforcements lead to increased material usage and higher costs [2.17], thereby limiting the overall sustainability of timber buildings. To achieve medium-rise CLT modular buildings without or with reduced use of additional reinforcing systems, it is important to further investigate the structural behaviours of CLT modular structures under lateral loads and all the dominant design factors to their lateral performance.



(a)



(b)

Figure 2.6. The tallest volumetric buildings to date: (a) 101 George Street [2.18] (b) and 'Treet' [2.14]

2.2 Lateral Performance of CLT Modular Structures

2.2.1 Full-scale CLTPS

One of the most comprehensive research projects of CLTPS to date is the project 'Sistema Costruttivo Fiemme (SOFIE)', which dynamically tested 3-storey and 7-storey full-scale CLT buildings using shake table experiments [2.19-21] (Figure 2.7), and both of which were built with platform-type construction.



(a)



(b)

Figure 2.7. Shake table test in SOFIE project: (a) the 3-storey [2.20] and (b) the 7-storey CLT buildings [2.19]

The full-scale tests applied three different earthquakes: El Centro, Japan Meteorological Agency (JMA) Kobe and the Italian earthquake of Nocera Umbra. These tests demonstrated the feasibility of multi-storey CLT construction in seismic regions, as both tested buildings exhibited structural integrity and minimal permanent deformation despite being subjected to the complete range of seismic activity, including near-collapse conditions. In the tests with low peak ground acceleration (PGA), the buildings only experienced minimal damage, evidenced by the reduced natural frequencies measured after each test. When higher PGA was applied, localised damage started to be recorded in the wall-to-floor connections as shown in Figure 2.8. The damage led to reduced structural stiffness, which cannot be fully restored despite implementing repair interventions such as connector replacements and fastener tightening after each test [2.19].

The damage in dynamic testing was consistently observed in the one and two storeys CLT buildings being tested under quasi-static monotonic and cyclic loading [2.22-24]. Additionally, damages also developed in the CLT panels when the building being tested statically in the lateral directions (Figure 2.9) at the later loading stage under large displacements. These damages include the embedment of wall panels due to the panel rocking and cracking in the corners of large door and windows openings due to the in-plane

panel deformation [2.22-24]. It can therefore be concluded that, the potential deformation modes of CLT buildings under lateral load include in-plane deformations (shear, bending, axial) in wall panels, rigid rotation of wall panels, and deformations in wall-to-wall and wall-to-foundation connections [2.25].

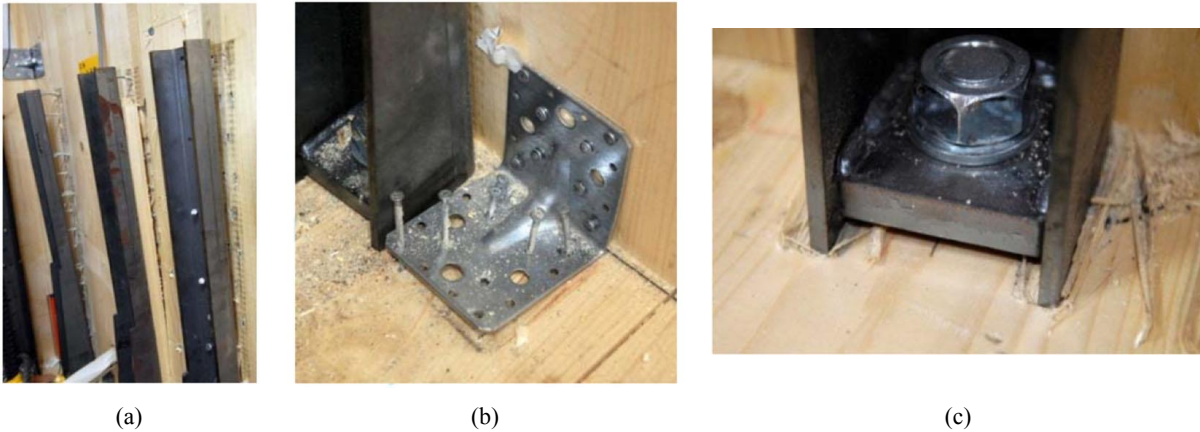


Figure 2.8. Failure modes observed in SOFIE project: (a) out-of-plane bending (b) pulling-out of nails (c) connector embedment [2.19]



Figure 2.9. Timber panels damage observed in the quasi-static test of CLT buildings: (a) embedment of wall panels into floor panels (b) cracking in the corner of large opening [2.22]

The actual impact of wind on tall timber structures remains unclear due to insufficient data. Recent research [2.17, 2.26-29] and numerical analysis [2.30, 2.31] indicate that, although high-rise timber structures can withstand strong wind and earthquake vibrations without collapsing, the inter-storey drifts are much higher than the conventional concrete structures with half of the mass, which exceeds the service limits given in building codes and is the controlling criteria in timber structural design. Bezabeh et al. [2.27, 2.32] numerically analysed the dynamic response of buildings using a combination of CLT core shear walls and RC spandrel beams at the edges as LLRS under wind-induced vibration. The results showed that the 20-story hybrid mass-timber building generally met the requirements of The National

Building Code of Canada [2.33] in most cases, while the taller options (40 and 30 stories) only satisfied the requirements under specific exposure conditions and with certain damping levels. Reynolds et al. [2.28] analysed a hypothetical tall timber building using the Eurocode 1 method, highlighting the potential unacceptable dynamic response due to the lightweight nature of timber structures. These findings indicated the acceleration impact on timber buildings due to the light-weight nature and the insufficient structural stiffness. Most of the existing full-scale testing were performed on platform-type CLT panelised buildings, while limited research has been done on full-scale balloon panelised CLT buildings due to its novelty. In 9th May 2023, a 10-story mass timber tower with balloon-type structure was tested on an earthquake shaking table in UC San Diego Englekirk Structural Engineering Centre, aiming to explore the possibility of building high-rise timber building with this new structure system.

2.2.2 Full-scale CLTVS

Different from CLT panelised structures, limited research has been conducted on CLT volumetric structures, hence there is still lack of understanding regarding their performance. A timber-framed module was tested under static displacement-controlled load by Ormarsson, Vessby [2.34] to study its lateral behaviour. As shown in Figure 2.10, the module experienced a combination of horizontal and vertical movement in the experiment. The loading point, located at the top left corner of module, experienced the largest lateral displacement, while the corner below the loading point observed the biggest vertical movement. The majority of deformation occurred in the hold-downs and angle brackets between the tested module and the steel foundation, while the module itself exhibited a relatively high level of stiffness. This experiment highlighted the significant influence of both the horizontal and vertical inter-module connections on the overall performance of timber volumetric structures, aligning with previous research conducted on high-rise steel modular buildings [2.35-36].

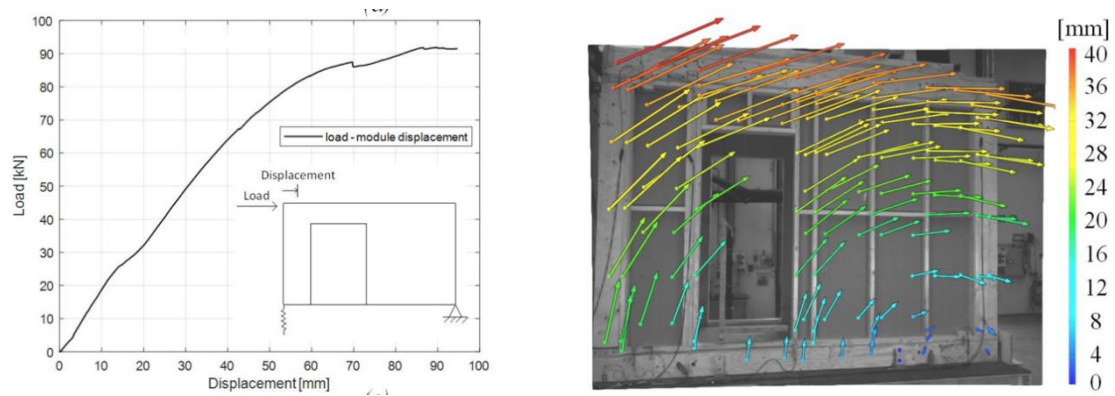


Figure 2.10. Global load-displacement curve of a single timber framed module under horizontal loading (left) and the detected displacement vectors [2.34]

2.2.3 CLT shear walls

To gain further insights into the components interactions within CLT modular structures, and how different shear wall configurations can impact the structural performance, a series of experimental and numerical studies has been conducted on macro-scale CLT shear wall systems. In addition to the impact on overall structural deformability, connectors have also been proven to have significant influence in the kinematic behaviours of CLT shear walls. Based on the vertical and horizontal movements of panels measured in quasi-static tests, four essential deformation components can be identified: rocking, sliding, shear and bending (Figure 2.11). The proportions of these components vary depending on the arrangement and properties of the connectors [2.22, 2.37]. It was reported that, when panel rocking dominates the kinematic behaviour, the panels have the capability to revert to their original position upon unloading, facilitated by gravitational forces, thus achieving better ductility, energy dissipation and ultimate displacement. This behaviour is considered to be superior to sliding, which results in significant residual lateral displacement [2.38-39].

Deng et al. [2.40] conducted parametric studies on a single CLT shear wall system to investigate how different parameters (connector boundary conditions, aspect ratio and gravity load) can affect the deformation behaviours of the system. The studies demonstrated that the strength of the vertical and shear connectors has the most significant impact, whereas the contribution from friction and gravity load are minimal. Therefore, when aiming to achieve energy-dissipative kinematic behaviour in CLT shear wall systems, the design must carefully consider the connections as essential factors.

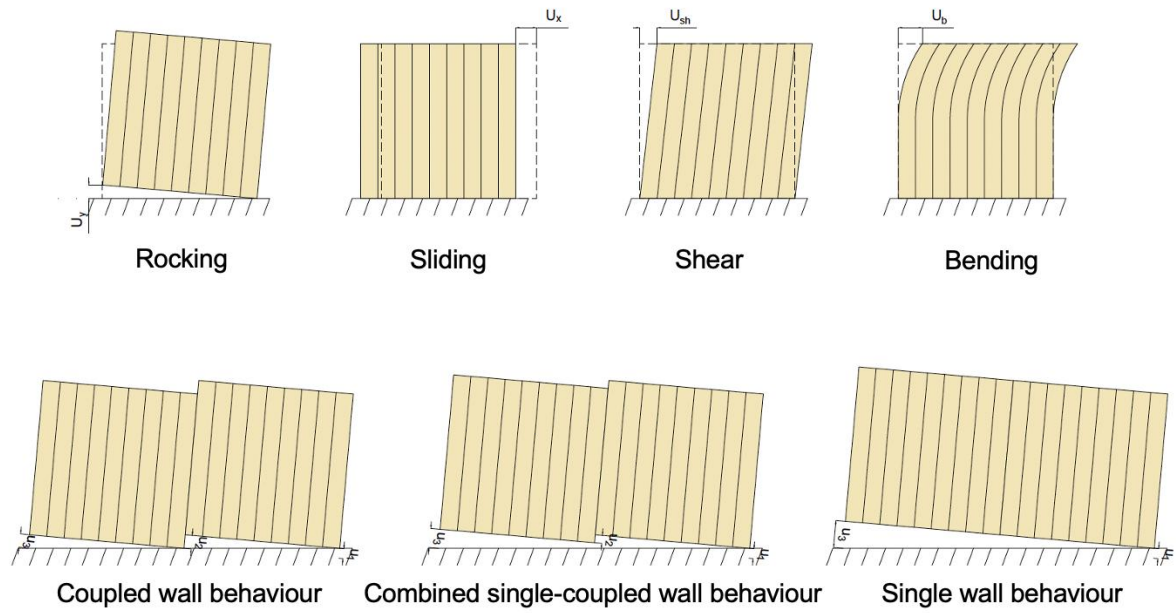


Figure 2.11. Deformability modes of a single-panel system (top) and a multi-panel system under lateral load (bottom)

For multi-panel structures, the coupling effect of CLT panels can be classified into three categories (Figure 2.11): coupled, combined single-coupled, and single wall behaviours, depending on the relative displacement between panels. The coupling effect can be quantified using the coupled wall behaviour parameter κ :

$$\kappa = \frac{u_2}{u_1 + u_3} \tag{Equation 2.1}$$

where u_1 , u_2 , and u_3 respectively represent the uplift of first wall panel, the relative vertical displacement between two wall panels, and the vertical displacement of the rotation centre in the second panels (Figure 2.11). When the panels behave as a single wall, indicating insignificant relative movement, both u_2 and κ approach 0. Conversely, when the wall behaves as a coupled wall, κ approaches 1.

The dominant deformation mode of a multi-panel shear wall system is determined by the stiffness of panel-to-panel connections. Panel-to-panel connections with high stiffness restrict the relative displacement between panels, enabling panels to act as a whole to resist lateral load (single-wall behaviour). Yasumura et al. [2.23] conducted an experiment comparing the behaviours of a CLT structure using large panels and discrete small CLT panels (Figure 2.12). The structure using large panels exhibited twice the stiffness compared to its counterpart, resulting in significantly smaller inter-story drift. These finding highlight that the attainment of single wall behaviours can enhance structural integrity and lateral stability of panelised

structures. However, despite the higher stiffness, the deformation mode in structure using large panel is normally the combinations of panel slips and connection deformation, while the deformation modes of the small panel structure are mainly connection deformation along with panel rotations, demonstrating better energy dissipating capacity via higher average equivalent viscous damping.

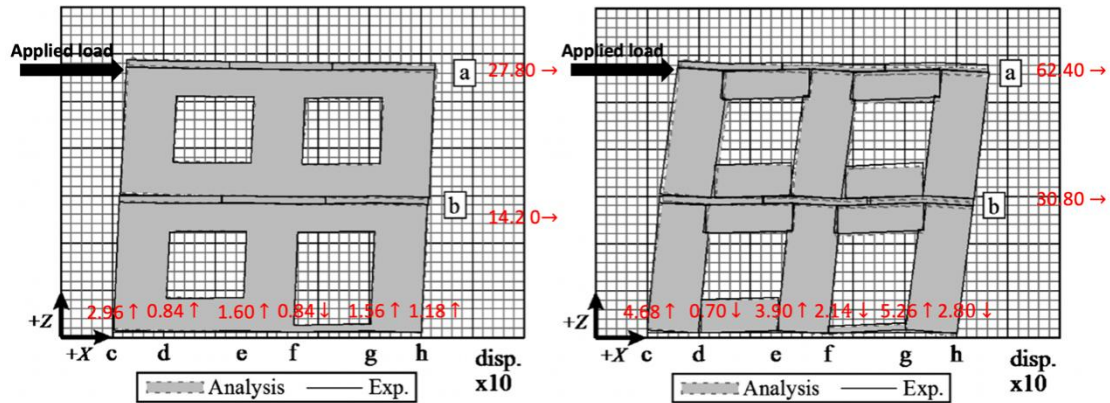


Figure 2.12. Lateral deformation pattern detected in CLT structures with large panels (left) and coupled small panels (right) under the same loading condition [2.23]

However, a different trend was observed in a comparative study between scale-down platform-type and balloon-type structures, which have different panel integrity in vertical direction [2.7]. Although similar ultimate load-resisting capacities were achieved in both construction methods, the balloon-type shear wall, which used continuous vertical panels, exhibited greater energy dissipation compared to the platform-type shear wall, primarily due to the reduced slip between panels but larger deformations occurring in connections. This is attributed to the larger height-to-length ratio and in-plane stiffness of the larger vertical panels, where connection deformations at the bottom of panels contribute significantly to the dissipation of energy. Whereas, in addition to global rocking, in-plane deformation is also a major source of deformation in structure using discrete panels [2.7, 2.8]. Although the current recommended practice for achieving a ductile structure is to use small panels and increase the number of connections [2.23, 2.25], it remains challenging to determine the most suitable panel and connection configurations and arrangements for ductile CLT structures due to the limited studies at present. Therefore, the design of coupling wall behaviours should depend on structural requirements of different projects and further development of analytical tools and standardisations are needed.

2.3 The Design of Multi-Storey Ductile CLT Structures

Previous numerical and experimental studies have consistently emphasised the significance of attaining moderate ductility in CLT modular structures, given the inherent brittleness of this natural material. A ductile structure should be capable of dissipating energy during a seismic event through plastic deformation in specific regions, facilitating load redistribution, sustaining substantial deformation without collapsing (serving as a warning to occupants), being resilient to unforeseen events, and recovering of functionalities rapidly [2.41], while retaining its load-bearing capacity to a significant extent [2.42].

Despite the importance of ductility and robustness in CLT structures, specific design codes or guidance for CLT have not yet been developed in most regions [2.43]. In North America, mass timber structures have been incorporated into the 2020 National Building Code of Canada (NBCC) [2.33] as well as the 2021 International Building Code [2.33], for gravity-load systems in buildings up to 12 stories and 18 stories, respectively. In addition, the NBCC 2022 was the first structural code adopted CLT shear walls as seismic LFRS in the CLT building' seismic design, referring to Canadian Standard for Engineering Design in Wood (CSA O86) [2.44]. It detailed provisions to ensure rocking to be the energy dissipative kinematic mechanism. In Europe, the design of CLT structures currently follows the general rules for timber buildings in EC5 and EC8, as well as information from relevant literature, though they are not fully applicable. Ongoing research is focused on developing specific design rules for CLT buildings in the future versions of EC5 and EC8 [2.44]. The new generation of Eurocode 8 - timber part - will introduce an updated list of timber-based structural systems with clear definitions of dissipative and non-dissipative zones in structures, which are needed for the newly introduced capacity design rules and overstrength factors for each type of structural system. CLT shear wall systems that are not present in the current version, will be included as an independent timber structural system in the Standards [2.44]. Further, a new procedure for application of non-linear static (pushover) analysis will be provided [2.11]. In this context, rapid development of CLT panelised construction is foreseeable in the near future.

One essential issue in the ductile structure design is the identification of appropriate and ductile failure mechanism. In accordance with EC8 guidelines, the structural elements (timber) in timber buildings should remain elastic, with the dissipative zones positioned in the connections to resist seismic actions. The current version of EC8 classifies the ductility

behaviour of structures based on the achieved ductility ratio (the ratio between ultimate displacement and yielding displacement) in the dissipative zones, categorising them into Low Dissipative Capacity (DCL), Medium Dissipative Capacity (DCM), and High Dissipative Capacity (DCH). As prescribed in EC8 8.8.(3)P, the dissipative zones in CLT buildings should achieve a static ductility ratio of 4 for ductility class M and 6 for ductility class H. Alternatively, compliance with the provisions of 8.8.(3)P can be accomplished by limiting the fastener diameters to a maximum of 12mm, and ensuring a minimum timber thickness of 10 times the fastener diameter [2.45]. Therefore, the wall-to-floor and the wall-to-foundation connections are normally designed as energy dissipating devices in CLT structures. The wall-to-wall and floor-to-floor connections are normally over-designed as non-ductile connections to prevent plasticisation, which can result in torsional rotation of the building and impact the higher modes of vibration.

The SOFIE (Sistema Costruttivo Fiemme) project mentioned earlier, along with seismic testing on CLT modular structures, revealed that CLT panels behaved as rigid bodies under dynamic excitation, with the connections playing a significant role in the system's ductility [2.46, 47]. These experiments proved that timber modular structures dissipate energy via the elastic and plastic deformation in connections and the rocking of panels, which are recognised as the desirable kinematic mode to avoid brittle damage in timber during vibration. In addition, the discrete nature of modular buildings often results in larger inter-storey drift under lateral load, highlighting the crucial role of timber connections in achieving required serviceability performance [2.48, 2.49].

Furthermore, although the current low-rise CLT structures have demonstrated sufficient lateral resistance, the realisation of multi-storey CLT structures that are more lateral load-sensitive is still challenging. This limitation is primarily due to the inherent low density of timber and the current connection systems' lack of sufficient stiffness, which are critical factors in structures that are more sensitive to lateral loads. Therefore, the governing role of connections in defining the overall structural performance necessitates the development of high-performing connections. These connections should aim to minimise high accelerations in CLT buildings, enhance ductility, and enable rocking and recentering behaviours in shear wall systems, thereby achieving safe mid- to high-rise CLT modular structures [2.19].

2.4 Conventional CLT Connections and Existing Challenges

In an existing CLT structure, several kinds of connections are commonly used: spliced, nailed and screwed connections in wall-to-wall and floor-to-floor connections [2.50], and metal plate connectors (hold-downs and angle brackets) with dowel type fasteners in wall-to-floor and wall-to-foundation connections [2.51]. Screwed connections (Figure 2.13. (a)) are versatile for varied locations, including wall-to-wall, wall-to-floor and floor-to-floor connections. Brackets (Figure 2.13. (b)) and hold downs (Figure 2.13. (c)) are mainly used in joints that subjects to a combination of shear and tension, such as wall-to-floor and wall-to-foundation connections. Plate connections (Figure 2.13. (d)) are used to establish a continuous load path between external vertical wall panels to resist uplifting [2.52, 2.53]. Conventional connection systems are highly versatile and can be integrated into a wide arrange of timber structural systems due to their availability in a multitude of sizes and shapes, coupled with standardised mechanical properties. Their design allows for easy application at various positions within a timber structure, eliminating the necessity for any modifications or cuts to the timber components, thereby facilitating a smoother and more efficient construction process.



(a)



(b)



(c)



(d)

Figure 2.13. Commonly used connections in CLT structures: (a) screws (b) angle bracket (c) hold down (d) plate [2.52]

2.4.1 Experimental studies

The behaviours of the aforementioned connection systems have been comprehensively studied via experimental, numerical and analytical analysis. In common practice, yielding of metal fasteners in the wall-to-floor connections is viewed as a favourable ductile failure mode [2.54] in timber connections and the main sources of ductility in CLT structures [2.42, 2.55]. This typical behaviour of metal plate connectors is the “strong plate-weak fastener” behaviour [2.56], and one of their unique characteristics is the permanent damage fasteners introduced in timber. All other failure mechanisms, such as splitting in timber and buckling in steel plate, are considered as brittle, since timber is not a ductile material and prone to brittle tension, bending and shear failures [2.42]. The deformed fasteners crush timber and create permanent cavities around them, which can lead to degraded stiffness and strength at load reversals (known as the pinching effect), reduced resistance and delayed attainment of maximum strength during the cyclic process (Figure 2.14. (b)&(c)). These features make the conventional connectors unpredictable and unrepairable, reduce the structure’s capacity and energy dissipation during the seismic event, meanwhile leave great residual displacements that reduce the structure’s resistance to aftershocks [2.19, 2.50, 2.57, 2.58]. In addition, similar features can also be observed in the hysteresis loops of full-scale buildings and the used connectors (Figure 2.14. (a)), further illustrating the dominant influence of connection properties on the overall performance of buildings.

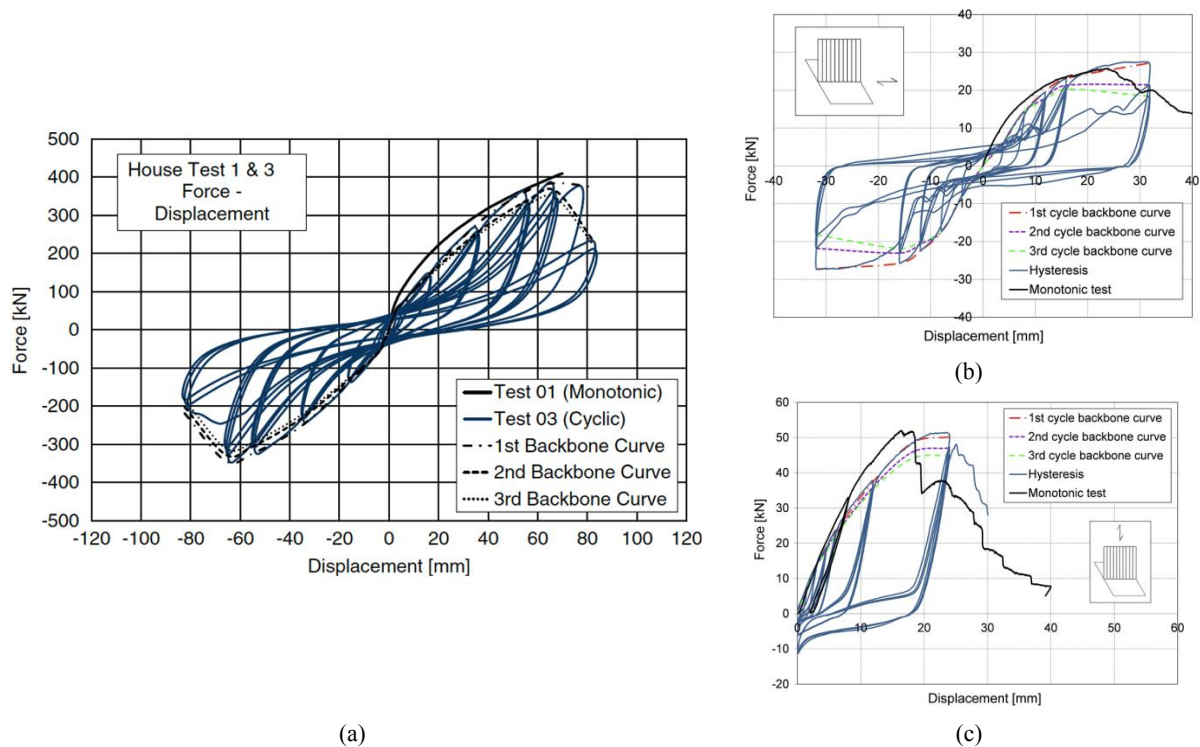


Figure 2.14. Hysteresis loops and monotonic curve for (a) a 2-storey full-scale CLT building [2.22] and the (b) angle brackets and (c) hold-downs that used in the building [2.39]

In addition to timber damage, both angle brackets and hold-downs are characterised by high stiffness but insufficient ductility in their primary directions [2.39, 2.59], falling into the Low ductility class ($2 < \mu < 4$) or M-medium ductility class ($4 < \mu < 6$) as prescribed in EC8 [2.45]. To achieve the required ductility class (M-medium or H-high ($6 < \mu$)), the recommended design methods for ductile timber structures with conventional connections involve increasing the number of connectors and utilising small-diameter fasteners [2.35, 2.36]. However, the significant quantity of connectors and fasteners can lead to time-consuming on-site fastening work with hard-to-verify assembly quality [2.60]. Moreover, it hinders the full potential of reusing timber components due to labour-intensive removal of nails and screws, which may cause additional damage to the structural material [2.61]. Additionally, small-diameter fasteners can induce high stress in timber and penetrate the fibres before the capacity of timber is fully developed, causing brittle failure with sudden reduction in connection strength and large residual displacement even after the removal of the external loading. This kind of brittle failure is highly unfavourable in structural design as it causes irreversible damage on the structural elements which results difficulties in structural maintenance.

2.4.2 Analytical models and design rules

Strength calculations

Based on the components on connection shear planes, connections are classified as timber-to-timber connection and steel-to-timber composite connection with varied kinds of fasteners (bolts, nails, screws) in EC5. The lateral capacity ($F_{lat,Rk}$) of these connections can be predicted associating with the European Yield Models (EYMs) proposed by Johansen and prescribed in EC5 [2.62] based on different failure modes (Figure 2.15) of laterally loaded screw fasteners. As shown in Figure 2.15, only the deformation of screws and the crushing of timber are considered in EYMs.

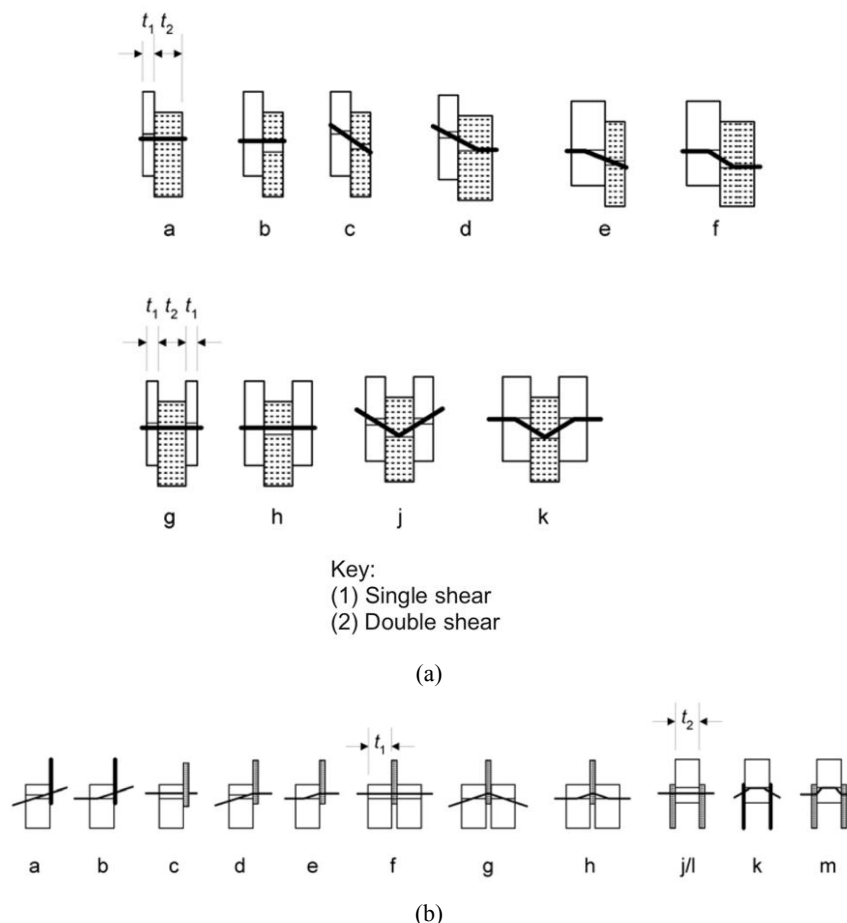


Figure 2.15. The failure modes of (a) timber-to-timber connections, and (b) steel-to-timber connections that are considered in European Yield Models (EYMs) [2.62]

However, previous comparative studies between EYMs and experiment results [2.39, 2.59, 2.63] revealed a conservative strength prediction (lower than 80% of the tested results) and a significant stiffness overestimation (up to 9 times higher) of this analytical model of timber

connections [2.39, 2.64]. The prediction errors can be attributed to several factors of timber connections. The bearing capacity of timber in conventional connections is defined by the combinations of the embedment strength $f_{h,k}$, the sensitivity to splitting, the connection configurations and variation of fastener types in connections [2.65]. Due to its heterogeneity, timber behaves differently in different directions and may have inherent defects such as large knots, resin pockets, bark inclusions [2.66], leading to the greater scattering of timber material properties than the steel material [2.67]. Therefore, relying the connection capacity on the timber with dispersive properties as a natural material [2.68] may lead to unpredictable connection behaviours and considerable variations between specimens, as well as accurate modelling methods [2.63], especially when the complex deformation and damage progression mechanism at the contact area between fasteners and timber connections are still unclear [2.69]. Numerous modelling methods were proposed to simulate this mechanism, such as the one proposed by Hong [2.70] that include all the dimensional details of the threaded part, which however can lead to overcomplicated numerical models with great computational efforts, making it unsuitable for practical application.

Previous experiment [2.71, 2.72] also identified the contribution of withdrawal capacity of screws when they are loaded in lateral direction (as known as ‘rope effect’). It was found that although the withdrawal capacity does not impact much screw behaviours at the quasi-elastic region, it shows pronounced influence on load-carrying capacity and the shape of the slip curve at larger displacements. The EYMs consider this factor by adding an approximate frictional force with a frictional coefficient 0.25 in to the calculation of shear resistance ($F_{v,RK} = F_{lat,RK} + 0.25 F_{withdrawl}$), for the failure modes that are governed by screws deformation (e.g. Figure 2.16(a) d, e, f, j, k & Figure 2.17(b) b, e, g, h, I, k, m), which however, was proved to be inaccurate and insufficient [2.72].

In addition, EC5 does not include any specific design provisions for CLT-screwed connections and conventional metallic connectors such as angle brackets and hold-downs. Therefore, the design of these connections should be assisted by research work conducted by Blaß and Uibel [2.73] on CLT connections, or ETAs for specific metal connections.

Capacity design

In timber structural design, the overstrength method developed by Jorissen and Fragiacommo (Equation 2.2) [2.42] is widely employed on both building and connection levels to ensure

the full activation of all ductile elements and prevent plasticisation in non-ductile zones [2.74], as required in EC8 [2.45]. To avoid premature brittle failure, timber panels need to be over-strengthened [2.42, 2.43] (Figure 2.18), allowing them to remain in the elastic phase when plastic deformation is only processed in connectors. At building level, all timber elements and connections in non-dissipative zones (e.g., wall-to-wall and floor-to-floor connections) are strengthened to avoid plasticisation. At connection level, timber elements are strengthened to ensure the development of localised yielding in fasteners [2.44]. In this method, the introduction of the overstrength factor γ_{Rd} in the design strength of brittle elements ($R_{d,brittle}$) is to mitigate the influence of factors that could result in higher-than-expected capacity in ductile elements ($R_{d,ductile}$). Initially, conventional connection overstrength was determined through cyclic tests [2.43], but Trutalli et al. [2.67] suggested using parameters from monotonic tests for a more conservative design due to lower connection strength in cyclic tests caused by the accumulated pinching effect.

$$\gamma_{Rd} R_{d,ductile} \leq R_{d,brittle} \quad \text{Equation 2.2}$$

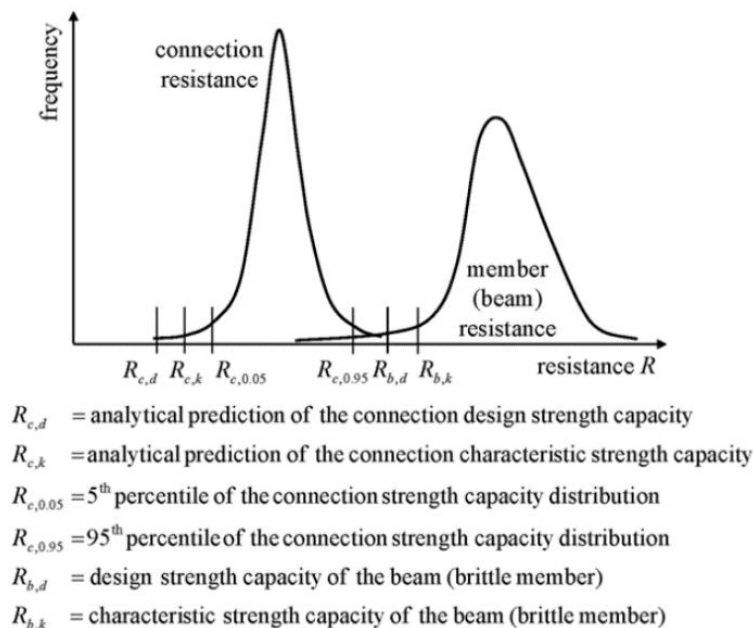


Figure 2.18. Concept of over-strength method: the resistance of connection should be smaller than the resistance of brittle members with sufficient ratio [2.42]

However, specific overstrength factors for different connections are not currently standardised [2.43]. The estimated overstrength factor could be insufficient and limit the attainment of the overstrength effect. Therefore, apart from employing the overstrength

method, common strategies recommended by EC5 to prevent brittle failure in timber connections involve implementing prescriptive safeguards in connection configuration design. These include minimum spacings, minimum number, slenderness ratios, edge distances and the effective number of fasteners [2.63]. Nevertheless, as documented in an experimental study [2.75], conventional steel connectors may still experience brittle failure despite the proper implementation of these safeguarding measures, due to the anisotropy and inherent defects of timber material.

Furthermore, the capacity of brittle elements (timber) and ductile elements (fasteners) are considered independently when applying overstrength method, which however is unrealistic due to the simultaneous deformation in timber, steel plate and fasteners in conventional plate connections in working conditions. Desirable fastener yielding (ductile behaviour) is typically accompanied by other failure modes, including timber crushing or splitting (brittle behaviour), steel plate fracture (brittle behaviour) or bending (ductile behaviour), as well as nail breakage and pulling-out (brittle behaviour) [2.51, 2.76-79] (Figure 2.19). The primary failure modes varied according to different connection factors, such as fastener types, arrangements and geometry, timber properties, loading directions, connection locations, as well as connector configurations. The interaction between these factors is still unknown, making it difficult to predict the primary failure mode of connections using existing analytical models, in which only timber crushing and fastener yielding are considered along with the assumption of rigid steel plates.

The ignorance of the composite effect and the rigid plate assumption could lead to significant estimation errors, especially for connections with small steel plate thicknesses, as they overlook the deformation contribution of steel elements [2.39, 2.59]. For example, it is suggested in EC5 that, the stiffness calculated for steel-to-timber connections should be doubled up to account for the strengthening of steel plate, which was proved to lead to greatly higher connections stiffness [2.64, 2.80]. The inaccurate representation of connection stiffness, which is especially crucial to the global stiffness of CLT shear wall system as discussed above, can lead to significant errors in the estimation of the principal elastic vibration period in seismic design, as proved in a numerical parametric study [2.81]. When having all brittle failure modes considered, some newly proposed analytical models with more complicated formulas [2.82-84] showed better agreement with the test results and

provided clearer identifications of the related failure modes [2.63, 2.85], indicating the need of further improving the design guideline of the conventional metal plate connections.

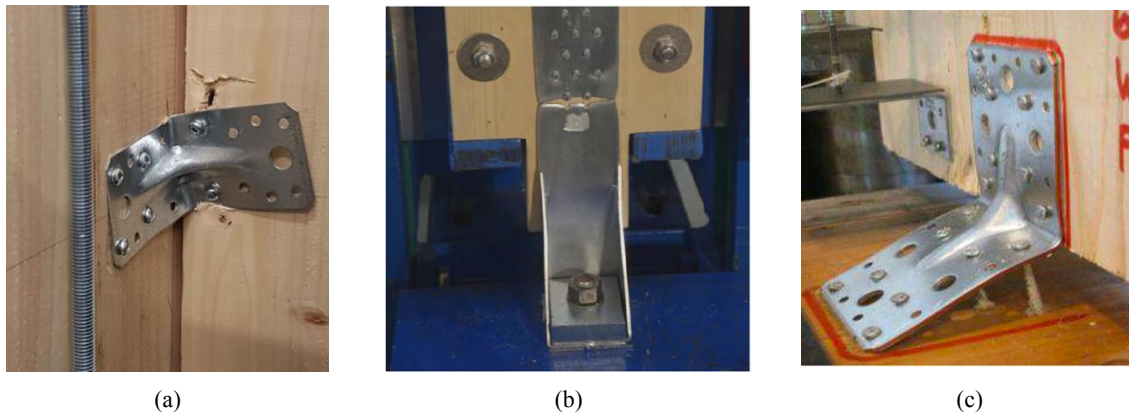


Figure 2.19. Different kinds of failure modes in timber plate connections: (a) cutting-through of fasteners in timber (b) breakage in metal connector (c) pulling-out of fasteners [2.59, 2.80]

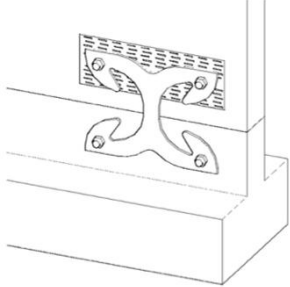

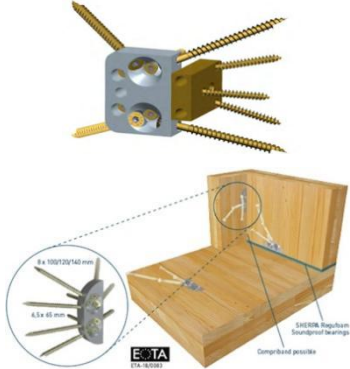
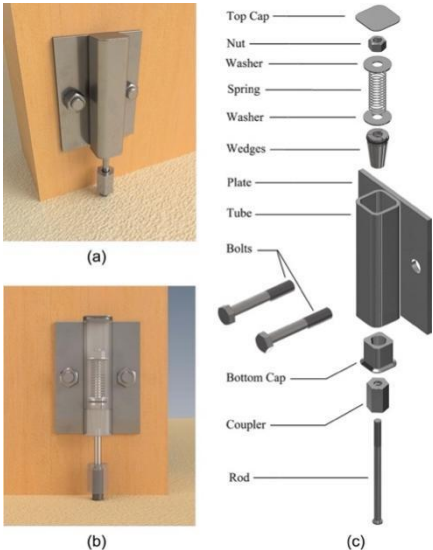
2.5 Novel Connection Systems for CLT Modular Buildings

Although CLT structures are widely applied and proven feasible for low-rise structures, the local- and macro-scale testing has revealed the insufficient mechanical performance, the risk of brittle failure and the performance instability of conventional timber connections to be applied in large CLT construction. The performance of timber connections is complex and not yet fully understood and standardised, which can lead to risks of unforeseeable connection behaviours and difficulties in structural design. Furthermore, the absence of design guidance, in particular for the identification of suitable, ductile failure mechanisms, further increases the difficulties of designing ductile timber connections for seismic resilient timber structures. This represents the primary barrier to the slow adoption of timber structures in the construction sector and the prevalent hesitation, despite the architects' and engineers' desire for wider utilisation of this sustainable material. In addition, due to the lack of standardisation among the existing connections, manufacturers must modify the production line according to connections used in different projects (metal plate, hole drillings), leading to additional cost and waste, and often hinder people's choices on this construction methods.

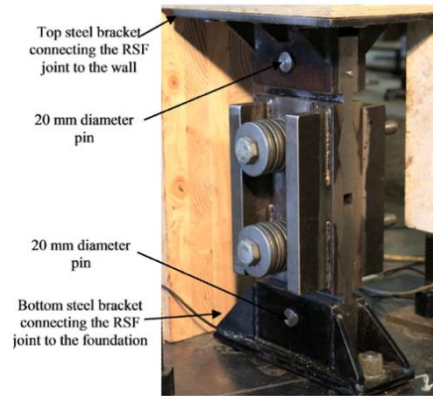
In addition to mechanical considerations, growing attention has been directed towards the feasibility of conventional screw-based connection systems, particularly within the context of large CLT structural systems. In CLT panelised and volumetric structures that utilise large areas of structural panels, the accessibility of connection becomes limited, posing a major challenge in connection installation for achieving necessary rigidity for CLT modular

structures. Additionally, issues like imprecise pre-drilling, potential timber damage around screw holes, and variations resulting from manual labour can introduce varying degrees of initial slippage in connections, thereby causing nonlinear contact effects between steel fasteners and timber even in the initial stages [2.14]. Such nonlinearity is highly undesirable in structural design, as it may culminate in inadvertent failure or undesired dynamic behaviours. To enhance both the structural performance and construction processes of CLT modular structures, various alternative connection systems have been proposed to address specific challenges inherent in timber construction (Table 2.1)

Table 2.1 List of novel connections and reinforcing systems for CLT modular construction

Index	Name	Connection Figure	Descriptions	Ref
Connectors for CLT panels (CLT-C)				
CLT-C1	X-bracket		The X-bracket is a novel steel bracket designed for providing CLT buildings with improved ductility and energy dissipative capacity in both shear and tensile direction, as well as for reducing permanent damage in timber, strength degradation and pinching effect.	[2.46, 2.50, 2.58]
CLT-C2	The X-RAD, Rothoblaas Ltd.		The X-RAD is a multi-directional point-to-point connection that links wall and floor CLT panels, which is easy to assemble and disassemble but requires precise profiling and fitting. With the inclined screws and the linking metal panels, this connector is characterised by high strength and stiffness with adequate ductility.	[2.37, 2.59, 2.60]
CLT-C3	SHERPA CLT Connector		The SHERPA-CLT-connector is a coupling element that can be used in the angle joint, t-joint and longitudinal joint of CLT panels. It is designed for safe and high-precision assembly without the need of any scaffolding, as the connectors are placed in the interior of buildings.	[2.61, 2.62]
CLT-C4	Pinch-free Connector (PFC)		The PFC is a novel tensile connector, which is designed to overcome the pinched effect in conventional timber connections with improved reload stiffness and better hysteresis performance. The equipped preloaded spring ensure the permanent contact between timber and connector, therefore eliminating the crushing-induced slack through a ratcheting mechanism.	[2.32]

CLT-C5 Slip-friction connector (Tectonus)



The Tectonus is a friction tensile connector, which allows rocking and fully self-centring behaviours in CLT shear walls. It can dissipate energy via friction and effectively eliminate the slip between the connected elements. This system is recently commercialised and applied in the newly built 'Fast+Epp' building in Vancouver [2.15].

[2.63-66]

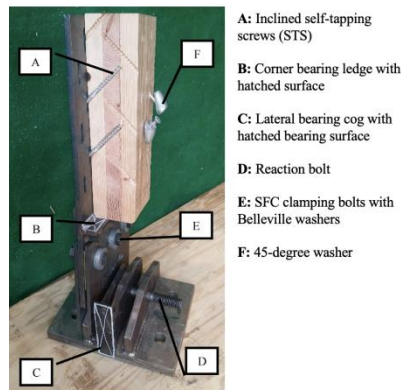
CLT-C6 Shear key with slots



This is a novel type of shear transferring device that designed along with CLT-C5 for the rocking shear wall behaviour. It behaves similarly to angle bracket connections when working in shear, while the slots with special shape allow for uplifting during the rocking of CLT panels.

[2.63-66]

CLT-C7 Slip-friction connector (Slotted-bolted connection)



This slip-friction connector (SFC) is a vertical connector that is made with steel plates clamping together with slotted bolt holes and fixed to timber with inclined self-tapping screws. Certain degree of linear movement is allowed in this connector to achieve satisfying energy dissipative performance with limited strength degradation.

[2.67, 2.68]

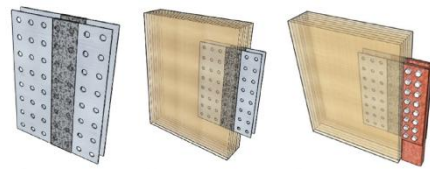
CLT-C8 XL-stubs



The XL-stubs are modified hold downs with hourglass steel plates to replace the original rectangular steel plates. The reduced area at the middle of the hourglass steel plate can help trigger deformation localisation during loading and reduce plastic deformation in timber, thus achieving improved energy dissipation capacity.

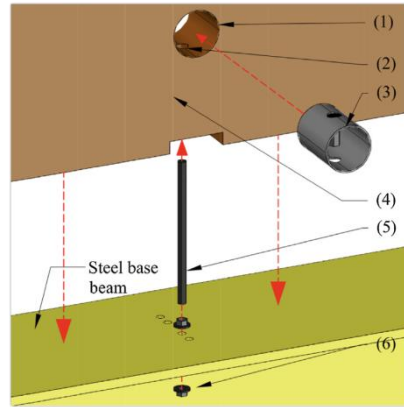
[2.31, 2.69]

CLT-C9 Holz-Stahl-Komposit (HSK) System



Holz-Stahl-Komposit (HSK) System is a shear connector formed by steel plates that are inserted into timber and bonded with chemical adhesive. Duct-tape is used with this connector to prevent the formation of adhesive bond in specific areas, creating a 'weak zone' that can act as a yielding fuse. [2.12, 2.70]

CLT-C10 Novel tube connector



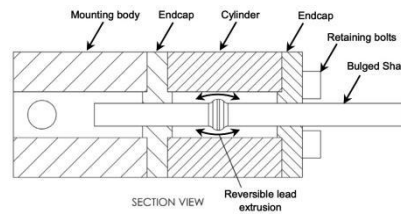
This tube connector is a hollow steel tube placed within the hole drilled on CLT panels, connecting panels to the foundation by a threaded rod that goes through the panels. Apart from the improved mechanical performance, this connector is also designed for limited timber damage, and easy installation and replacement. [2.71, 72]

CLT-C11 High-Force-to-Volume (HF2V) damping devices

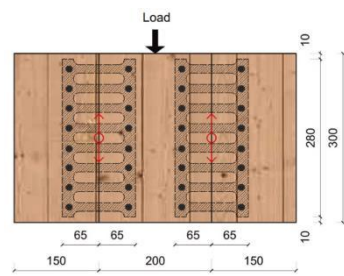


HF2V Device

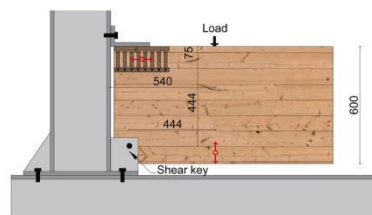
The HF2V damping device is a substitute to the conventional tensile connections with loading resistance and energy dissipation being provided by the reversible plastic extrusion of lead. It also enables self-centring of shear walls with insignificant damage in both device and timber, and can therefore be fully reused. [2.73-75]



CLT-C12 Internal-perforated-steel-plate (IPSP) connections with self-drilling dowels (SDD)

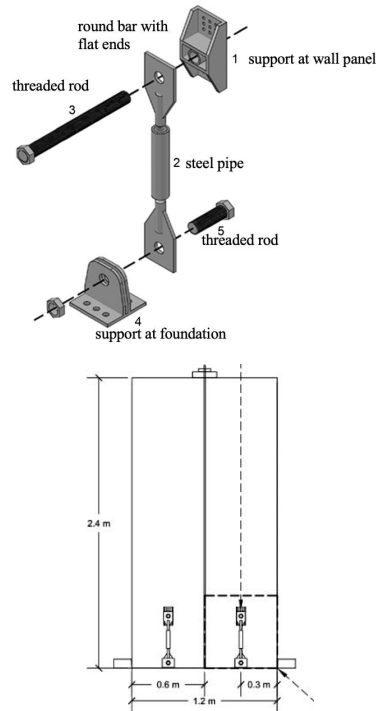


This is a modified IPSP connector that joints timber panels using SDD instead of adhesive. It can be transformed into hold-downs and panel-to-panel connectors. The reduced area of steel plate (steel bridge) is the designated weak area to deform first to prevent the bending of SDD and the crushing of timber. [2.76]



CLT-C13

Energy dissipators with steel buckling restrained steel braces (BRB) concept

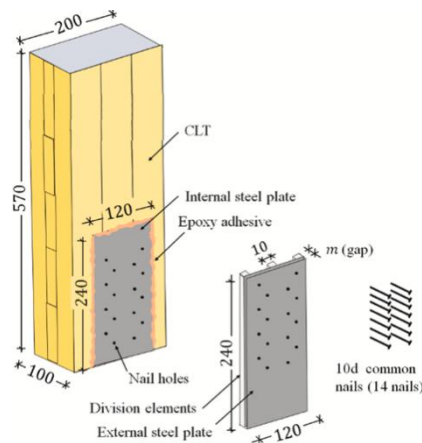


This connector is an energy dissipater for CLT panels that has a milled portion enclosed in a grouted steel pipe that is designed to yield first in connector. An end-pinned system is included in the connector to allow rotation at the ends of the energy dissipators and reduce internal moments.

[2.77]

CLT-C14

Gap Reinforced Fastened Connector (GRFC)

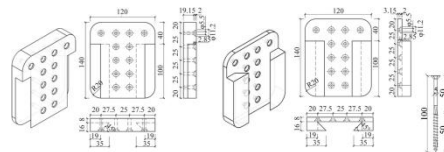


The GRFC is a modified hold-down incorporates a gap between two steel plates that are bonded by adhesive. The gap creates space for the yielding of fasteners, thus reducing the crushing on timber during deformation. The adhesive layer creates rigid interface between fasteners, reducing the connections space requirements in EC5.

[2.78]

CLT-C15

Prefabricated Metal Dovetail Connector



The prefabricated metal dovetail connector consists of a mortise part and a tenon part, which is designed for screw-free onsite installation of CLT panels.

[2.79]

CLT-C16

LOCK Connector from Rothoblaas Ltd.

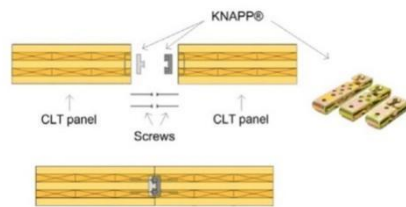


The LOCK connector system is a concealed connector for the easy and accurate joining of CLT panels to concrete foundation by sliding, which also provide convenient disassembly after the end-of-life of structures. By varying the length of connector, this system can be used on both CLT panels and beams.

[2.80]

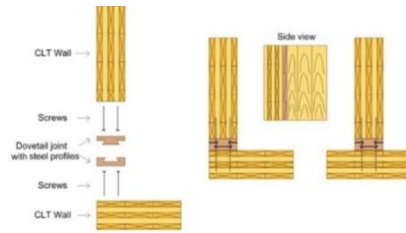


CLT-C17
The Knapp® connector



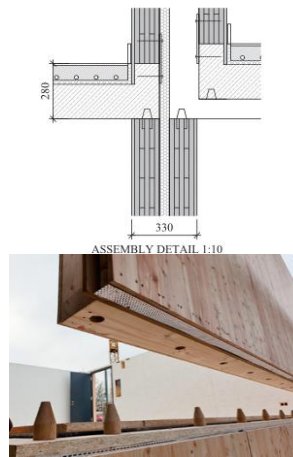
The Knapp connector is an interlocking panel-to-panel connections. It provides both the out-of-plane and in-plane resistance as well as the uplifting resistance. It is easy to assemble but difficult to install as it requires complex plan on the wall segments. [2.86]

CLT-C18
The Dovetail metal brackets



The Dovetail metal brackets are interlocking panel-to-panel connection that designed to simplify the on-site wall erection process. It also provides continuous reinforcement along the edge of panels. [2.87]

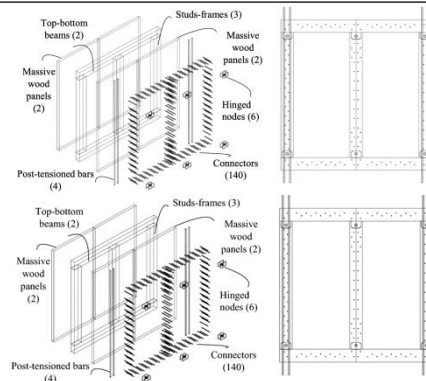
CLT-C19
Heidelberg Student Accommodation (Mobi-Space System)



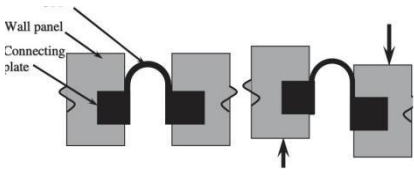
A bespoke interlocking inter-module connection for the easy installation of CLT flat modules. [2.88, 2.89]

CLT shear wall reinforcement systems (CLT-R)

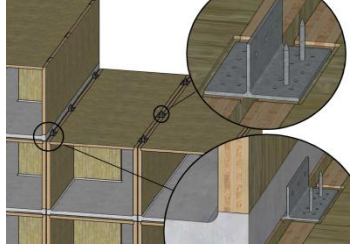
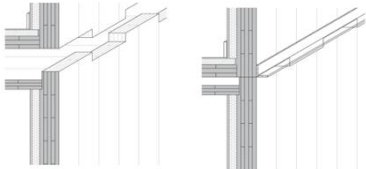
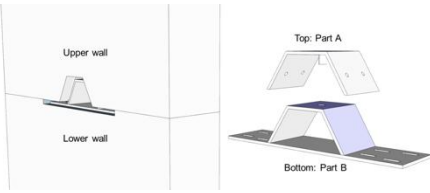
CLT-R1
Framing Panel Shear Walls (FPSW)



FPSW is a hybrid shear wall system formed by CLT panels, articulated hollow steel bracing and steel tendons. This system provides reduced overturning effect and improved structural performance than conventional CLT shear walls. The steel frame ensures structural integrity when the load-bearing CLT panels are damaged, thus allowing low-cost rehabilitation. [2.81]


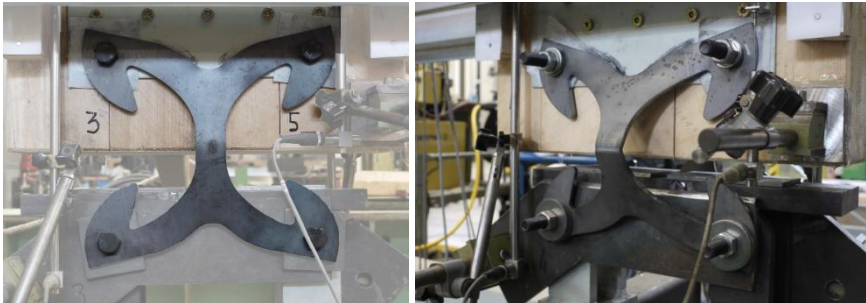
CLT-R2	Post tensioned hybrid shear wall with U-shaped flexural plates (UFPs)		This hybrid shear wall system is reinforced by prestressed tendons and energy dissipating devices (UFPs). Recentring and sufficient energy dissipation can be achieved in this system through metal yielding with little timber damage, which allows low-cost repair by replacing the sacrificial UFPs after seismic events.	[2.82, 2.83]
--------	---	---	--	--------------

Connector For CLT volumetrics (CLT-V)




CLT-V1	Jakarta Hotel		A steel T-shaped angle plate with pins for the accurate alignment and translational constraints of modules, which was designed specifically for the Jakarta Hotel project.	[2.90]
CLT-V2	Moxy Modular Hotels (Marriott)		A specially designed notched CLT panel used as the side wall of modules and the inter-module connection for the easy on-site modules' assembly, what was designed specifically for the Moxy Modular Hotels project.	[2.91]
CLT-V3	A novel inter-module horizontal connection proposed by the University of British Columbia		A replaceable inter-module connection to achieve good energy dissipation and limit plastic deformation in timber.	[2.92]

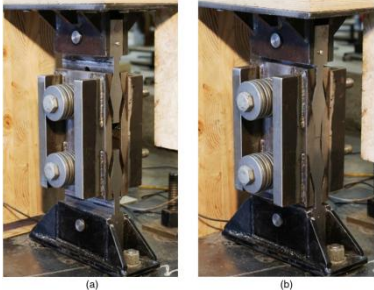


Complementary to the introduction of the innovative connectors, the experimental studies carried out to prove the mechanical performance of these CLT connectors are summarised in Table 2.2.

Table 2.2 Comparison of the experimental results for the novel connections

Index	Connection Type	Fasteners Type	Scale of Testing	Loading Protocol	Ductility Factor	Deformation and Failure Modes
CLT-C1	Angle bracket (Shear)	4* M16 bolts	Local/Macro	Cyclic	23.43	 <ul style="list-style-type: none"> • Out-of-plane buckling in the vertical web, which may cause embedment damage in timber.
	Hold-down (Tension)					 <ul style="list-style-type: none"> • Out-of-plane flexural buckling under compression and extension under tension in the vertical web. • Minor steel embedment and slight plastic deformations can be observed in M16 bolts

with no visible damage in timber after testing.

	Angle bracket (Shear)			Monotonic/Cyclic	2	 <ul style="list-style-type: none"> Block-tearing of the inclined metal fasteners along with the deformation at steel envelope.
CLT-C2		6*Ø11 × 300 mm Inclined screws and M12 bolts	Local/Macro			
	Hold-down (Tension)			Monotonic/Cyclic	6.3	 <ul style="list-style-type: none"> Bending of the inclined metal fasteners along with the deformation at steel envelope.
CLT-C4	Hold-down (Tension)	4*M10/ 2*M16 bolts	Local/Macro	Cyclic	10	 <ul style="list-style-type: none"> Embedment in wood and yielding in fasteners, depending on the diameters of fasteners used with the connector.

CLT-C5	Hold-down (Tension)	2*M20 bolts and 8* \varnothing 11 \times 550 mm screws	Local/Macro	Cyclic	N/A		<ul style="list-style-type: none"> • Movement of the centre plate within the grooved outer cap plates along with the compression of the Belleville springs.
CLT-C6	Angle bracket (Shear)	8*M20 bolts	Macro	Cyclic	N/A		<ul style="list-style-type: none"> • In the lateral direction, CLT-C6 has similar behaviours to conventional angle brackets. • In the vertical directions, bolts can slide within the slots along with the movement of panels.
CLT-C7	Hold-down (Tension)	27* \varnothing 10 \times 140 mm screws	Local/Macro	Cyclic	N/A		

- Slipping between cap plate and brass shim
- No damage to the self-tapping screws in connection was observed and no washers fell out of their slots.

CLT-C8

Hold-down
(Tension)

8*M12
bolts and
2*M18
bolts

Local

Monotonic/
Cyclic

52.2



- Bending or fracture in the middle point of the hourglass steel plate

CLT-C9

Hold-down
(Tension) & panel-
to-panel connection
(Shear)

Adhesive

Local/Macro

Monotonic/
Cyclic

31.8



- Deformation of steel around the holes that are covered by duct tape and not adhesively bond with timber.

CLT-C10

Hold-down
(Tension)

1* \varnothing 12.7
mm
threaded
rod and 2*
nuts rods

Local

Monotoni
c/Cyclic

4-8.7



- Deformation and buckling of the steel tube.

Panel-to-panel
connection (Shear)

16* \varnothing 7 \times
133 mm
screws

Local/Macro

Monotoni
c/Cyclic

14.5



- Bending or rupture at the steel bridge of the perforated steel plate.

CLT-C12

Hold-down
(Tension)

1* M28
bolt and
16* \varnothing 7 \times
133 mm
screws

Local/Macro

Monotoni
c/Cyclic

22.1



- Bending or rupture at the steel bridge of the perforated steel plate.
-

CLT-C13

Hold-down
(Tension)

9*
Ø6.35 ×
76.2 mm
screws, 1*
threaded
rod and 1*
Ø25.4 mm
bolt

Local

Monotoni
c/Cyclic

N/A



- lateral buckling at the milled section near the shoulder, which is caused by the rotation of steel pipe during the compression of cyclic loading.

CLT-C14

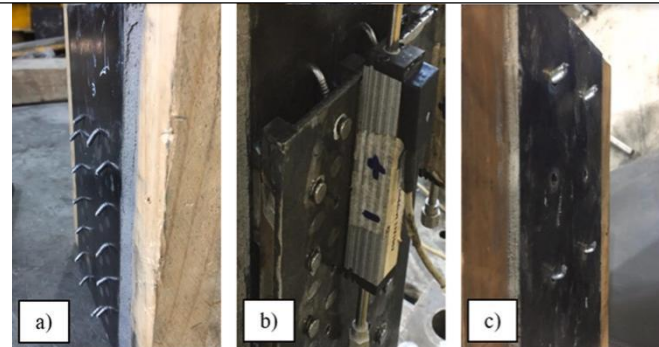
Hold-down
(Tension)

Adhesive
and 14
*Ø3.76 ×
76.2 mm
nails

Local

Monotoni
c/Cyclic

0.44-2.55

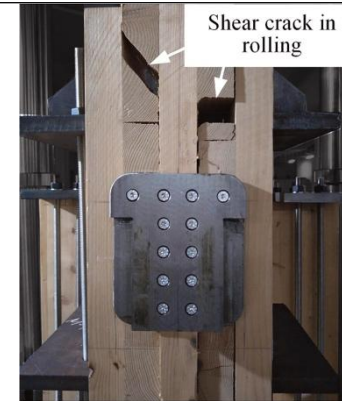


- Yielding of nails (b) inside the gap area and the shear-off of nails (a)&(c).

Hold-down
(Compression)

Monotoni
c/Cyclic

4.67



CLT-
C15

24* ϕ 5 ×
100 mm
screws

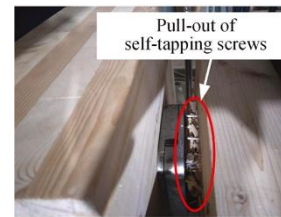
Local

- Pull-out of screws along with cracking in the middle layer of CLT panel.

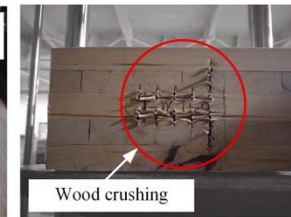
Angle bracket
(Shear)

Monotoni
c/Cyclic

1.67



(a)



(b)



(c)

- Screw yielding (a) accompanied by wood crushing (b) and screw fracture (c).

CLT-R1	Shear wall system	128 * Ø7 x 233 mm screws and 6*Ø38 mm bolts	Local/Macro	Cyclic	4.83	

- The loss of attachment between the CLT panels and the steel frame (a) due to the pulling-out of screws (b) and embedment failure in timber (d).

CLT-R2	Shear wall system	4*Ø12.7 mm tenons and self- drilling screws	Local/Macro	Cyclic	N/A	

- Bending of UFPs during shear wall rocking

Note: Detailed experimental records of CLT-C3, CLT-C11 and CLT-C16 are missing in the literature

2.6 Connection Performance Evaluations: Connectivity, Manufacturability, Constructability

2.6.1 Performance evaluation for novel CLT connectors

According to Figure 2.1, most new CLT connector designs incorporate additional two- or three-dimensional steel connectors as alternatives to conventional steel plates. In addition to enhanced mechanical performance, novel connectors possess unique features that specifically address the limitations of conventional connectors. It is therefore difficult to directly evaluate or compare the connectors' performance when their design philosophies are somewhat, and in certain cases completely, different.

In addition to fulfilling the structural requirements, the manufacturing and constructional performance of connectors define the efficiency and the overall cost of CLT construction, and therefore should also be well considered in the design of CLT connectors to promote practical applications. Previous studies by Srisangeerthan et al. [2.93], Corfar & Tsavdaridis [2.94] and Li & Tsavdaridis [2.95] introduced multi-attribute performance evaluation systems for steel modular connectors, encompassing comprehensive considerations and explanations of structural performance, manufacturability, and constructability. Some evaluating criteria are herein adopted and tailored to reflect the unique characteristics of CLT construction, thereby providing clearer insights and enhancing the discussions on the performance of such connections.

2.6.2 Structural performance

Translational properties

From the structural performance perspective, panelised structures like CLT shear wall systems require connectors to have adequate planar forces capacity, such as shear and tension. Although all new connectors as summarised in Table 2.2 can provide sufficient resistance in their primary working direction, certain connectors (CLT-C4-8, 11, 13, 16) are designed for unidirectional use and possess limited capacities in the secondary direction. By eliminating any coupling effects between shear and tension, this characteristic can contribute to a clearer understanding of the relationship between connection properties and shear wall performance. However, limited capacity and the occurrence of unfavourable failure modes in the secondary

working direction can result in unforeseen failures (e.g., buckling failure observed in CLT-C13 under compression), preventing the attainment of full capacity. Consequently, it would be preferable to have sufficient capacity in both working directions, with the strength in the secondary working direction serving as additional reinforcement for the structures.

Strong fasteners-weak metal connector behaviours

Contrary to the “strong plate-weak fasteners” concept for conventional connections, the majority of the new connectors (CLT-C1, 4-14) achieve ‘strong fasteners-weak metal connector’ behaviours along with the much-improved ductility (Class H). This is achieved by employing large-diameter fasteners that offer greater yielding strength in timber-fastener connections compared to metal connectors. As a result, the inelastic deformation mechanism shifts from fastener yielding and timber crushing, as observed in conventional connections, to the more ductile bending (CLT-C1, 8-10 and 12) or sliding (CLT-C4-7) of the steel connectors. Owing to the well-standardised homogeneous properties of steel material, the controlled deformation of metal elements can provide improved ductility and predictable mechanical performance, while mitigating the influence of inherent defects in the connected timber elements. Moreover, the minimised deformation in fasteners can prevent timber damage, avoid stiffness degradation in the load reversal, and mitigate the risk of brittle failure in structural elements. By comparing the hysteretic curves of conventional connection and a novel timber connection equipped with ‘strong fasteners-weak metal connector’ behaviours, it is showed that much plumper curve can be achieved in the new connector, indicating better energy dissipating capacity (Figure 2.20). The common application of the so-called ‘damage avoidance philosophy’ in the novel connector design reflects the widely recognised concerns toward timber damage with regards to conventional connections.

Also, the better ductility in those connectors (CLT-C4-8, 10, 11 and 13) that designed as the alternatives to conventional hold-downs connections, can facilitate rocking behaviour for enhanced energy dissipation in CLT shear wall systems. This feature also meets the growing requirements for uplift resistance and energy dissipation in large-scale timber construction. Furthermore, certain new connectors (CLT-C4, 5, 7, 11) incorporate special elements like springs and reversible plastic extrusion to enhance recentring capabilities during panel rocking. This design approach enables higher stiffness in the unloading process, resulting in a significantly larger hysteresis curve.

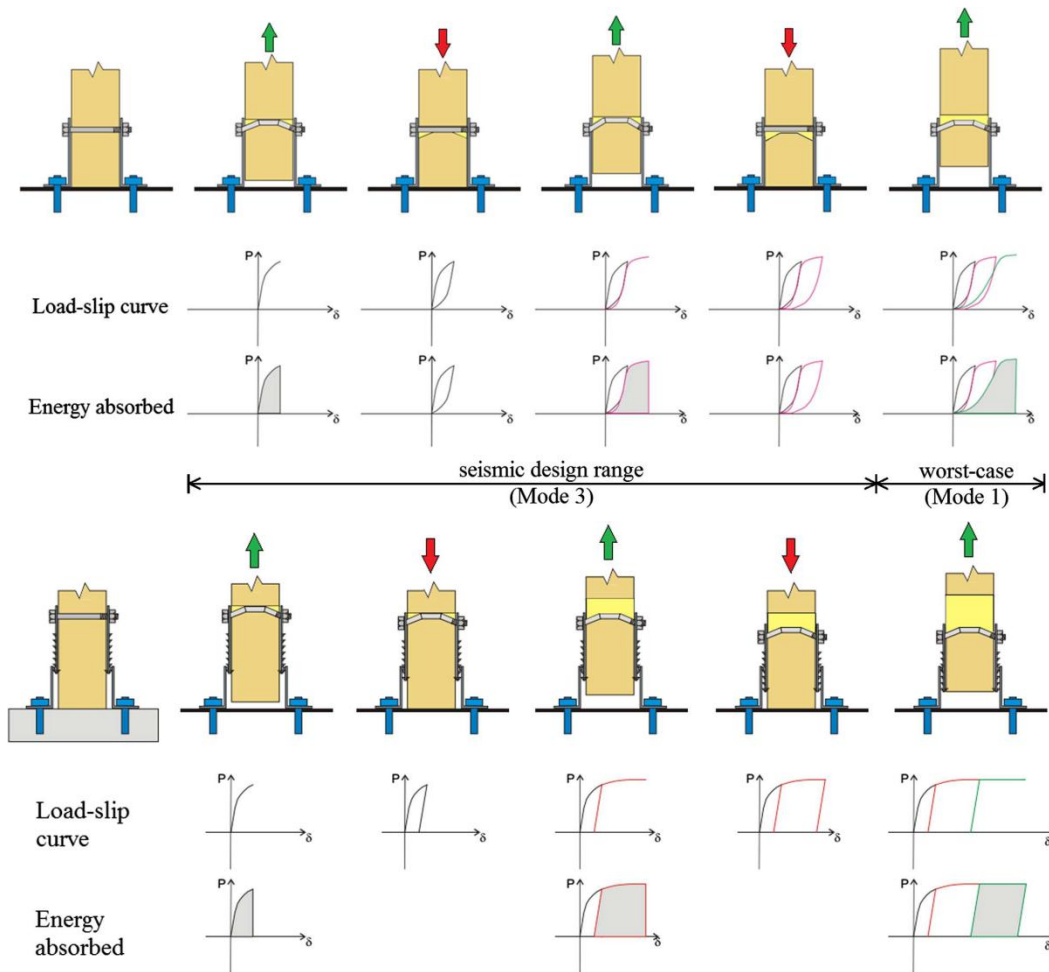


Figure 2.20. Pinching behaviour in conventional hold-downs (top) and innovative connections (bottom) with ‘strong fasteners-weak metal connector’ behaviours [2.57]

2.6.3 Constructability

In addition to the mechanical performance, construction requirements should also be carefully considered in the connector design stage, as they determine the ease, speed and quality of CLT construction. The ideal CLT connections for efficient construction should be compact, easy to install with reduced manual efforts, capable of accommodating tolerance requirements, and demountable to facilitate disassembly and future reuse.

Onsite assembly

When designing connectors for optimal constructional performance, certain specific factors should be taken into account. Firstly, connectors should offer straightforward on-site assembly methods for structural elements to enhance construction efficiency and lower construction costs, particularly considering the context of rapidly rising labour costs. Although most of the new connections still use on-site screw fastenings similar to

conventional steel plate connectors, CLT-C15 and 16 employ an interlocking technique that eliminates the need for on-site fastening. Interlocking is a connecting method used in ancient timber structures and is readopted in modern connection design to promote more efficient assembly in construction.

Secondly, the choice of fasteners that connect the connectors and structural elements should be carefully considered, as the process of fastening screws in conventional connectors accounts for the majority of the workload. In contrast to the labour-intensive installation of small-diameter fasteners used in conventional plate connections, novel connectors (CLT-C1, 4-7, and 13) more commonly employ big-diameter screws or bolts. Employing larger fasteners can enhance the load-bearing capacity of the timber-to-fastener connection while reducing the total number of fasteners, thereby improving construction efficiency and realising the “strong fasteners-weak metal connector” and ‘damage avoidance’ philosophy. Connectors designed with such philosophy, especially those use big-diameter bolts and dowels (CLT-C1, 4, 5, 7-11 and 13) can be repaired or replaced with minimal damage in timber, making them well-suited for supporting structure maintenance and enabling the recycling or reuse of structural materials. This is especially advantageous for connectors located on the exterior surface of CLT panels and require no panel modification for the fitting of connectors (CLT-C1, 4, 8 and 13). Some connectors (CLT-C2, 5, 7, 9, 10 and 12) require profiling (cutting, drilling) on timber for connector placement. This process can result in a reduction in the cross-sectional integrity of the structural elements, leading to elevated workload and costs, and reduced potential reusability.

In addition, in some new connectors (CLT-C9 and 14), chemical adhesive is employed alongside the conventional mechanical fastening method. Though very high stiffness can be achieved in these connectors, the adhesive formation process could be problematic for onsite installation, as it may be affected by numerous factors such as weather and site conditions. Thirdly, connectors should be able to accommodate considerable levels of construction tolerances for unexpected onsite adjustments. Connectors (CLT-C2, 10 and 15-16) that have complex profile and require accurate onsite operation may be difficult to assemble onsite when unexpected construction errors happen, while those (CLT-C1, 4, 6, 8, 13 and 14) attached at the exterior surface of CLT panels can be easily adaptable to project and construction changes.

Onsite Lifting

To enhance installation quality and efficiency while minimising onsite workload, connectors CLT-C2, 15, and 16 are specifically designed as prefabricated connectors. These connectors can be accurately pre-assembled and installed onto the timber in controlled environment, which is especially beneficial for those that require special tooling. For prefabricated connectors, it is crucial to have suitable design for transport vehicles and be able to use as temporary support system during panel lifting, such as the X-RAD connector (CLT-C2) (Figure 2.21.b). This can be regarded as an additional constructional benefit, since traditional panel lifting involves hole drilling and filling on panels for placing lift devices (Figure 2.21.a).

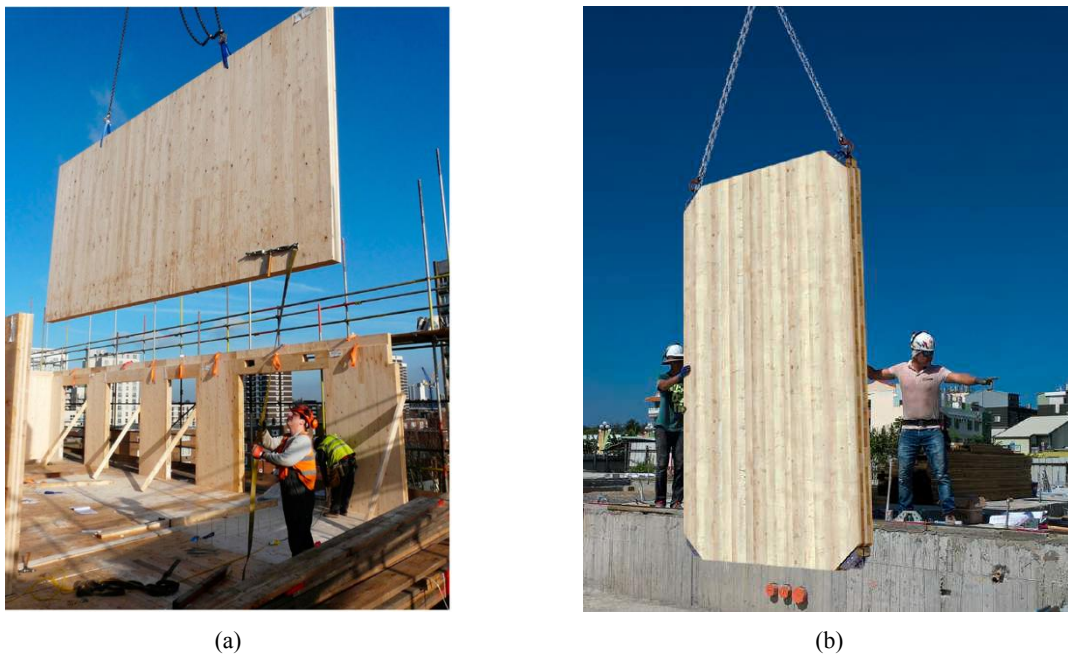


Figure 2.21. Panel lifting: (a) with conventional method [2.86] and (b) with novel connectors (CLT-C2) [2.60]

Interlocking connection

For CLT-C15-19 that adopting interlocking technique, structural elements can be self-locked onsite with the slot (groove) and ridge (tongue) connector designs that have matched shape that can fit together without additional joining operations, such as adhesive or fasteners. By adopting this approach, the requirement for accessing specific points to install fasteners is removed, effectively solving issues related to the accessibility of connections and the efficiency of installation. This method also enables disassembly without resorting to demolition, ensuring that the structures can be readily adapted to accommodate potential environmental shifts or changes in their intended function.

Interlocking systems are considered as simple and reversible mechanical connections to help simplify the assembly process in construction, as it connects elements by the interaction

instead of mechanical fasteners. This kind of connecting technique transmits load by the bearing of components which can prevent the brittle failure in materials that are sensitive to load concentration. As opposed to chemical and screwed connections, interlocking connections can also enable components to be separated more easily [2.96]. The listed recent developments enrich the importance of interlocking technique in CLT connection systems for efficient construction and upgraded structural performance. However, the listed interlocking connections for CLTVC are all bespoke connection solutions proposed for specific projects, while a universal interlocking connection solution for CLTVC has not yet been proposed. And these bespoke connections all require special modifications on CLT panels for the fitting of connections, which limit their applications in general CLT modular construction.

2.6.4 Manufacturability

The manufacturability of connectors governs the speed and quality of mass production, which can be assessed from the connector complexity (geometry, component number, material, processing procedures). Connection parts that can be easily fabricated using conventional manufacturing methods can expedite the commercialisation process and lead to substantial cost savings in construction. For those having being more geometrically complex, special manufacturing methods such as 3D printing, is required, which can significantly increase the manufacturing cost – on a positive note, the supply chain issue can be solved, especially when quick replacement is required after the damage of a connection component. All novel connections listed in Figure 2.1 can be fabricated using conventional manufacturing methods. The planar connectors such as CLT-C1, 8, 9, 12 and 14 are the most mass-producible, they can be simply cut from steel sheets. For those 3D connectors, multi-process manufacturing may be required with significantly higher cost. For example, the cap and centre plates of CLT-C5 can be sawn from merchant flat bar and then milled to achieve the tothing shape on surface. Alternatively, they can be produced from a custom rolled special section in 6m lengths, and then be sawn, drilled and slotted, which however would require minimum ordering of 100 tonnes, according to the British steel manufacturer SC4. In the case of CLT-C13, different components necessitate distinct manufacturing methods. The wall support of it can be produced from either a stock PFC or a press braked channel, while the foundation support should be produced from either a tee section or fabricated from profiled/drilled plate. The steel sleeve in the middle also requires separate manufacturing from a profiled and formed plate before being integrated with other components.

As some of the new connectors have more than two components (CLT-C4, 5, 7, 10, 11 and 13), careful assembly (installation) processes in factories or onsite is required, which also governs the cost and efficiency of production. Furthermore, certain assembly processes (e.g., welding in CLT-C10 and 13) necessitate special operations that can further diminish the production efficiency and increase cost. In addition, tolerances in the assembly processes should also be carefully considered during the connection design phase. Considering the accuracy of conventional manufacturing methods, 1-2 mm tolerance between components should be achievable to avoid fitting difficulties caused by dimensional errors.

2.7 Demolition of Timber Structure and The Reuse of Wasted Timber

2.7.1 Material reuse in timber construction

Despite the fact that UK generates over 60 million tonnes of construction and demolition waste annually, insufficient emphasis is placed on the end-of-life of buildings material among all the new advancements in the construction industry in the recent years, even though it offers significant environmental benefits [2.97]. The EU Waste Framework Directive proposed a waste hierarchy (Figure 2.22), which highlighted the importance of reuse than recycle and disposal for optimal sustainability and was adopted in the Waste (England and Wales) Regulations 2011.

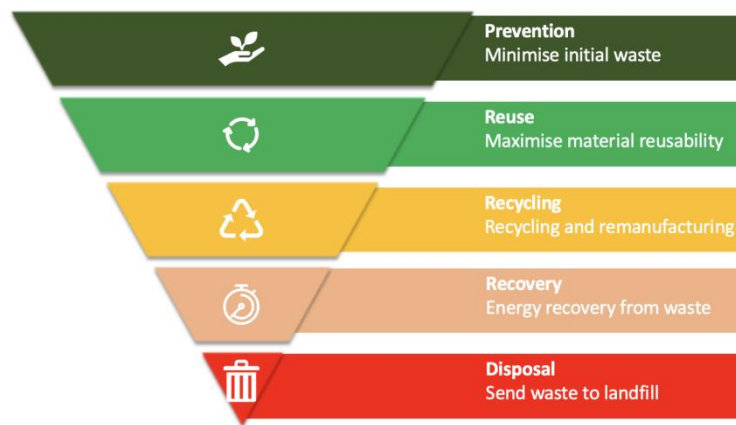


Figure 2.22. Waste hierarchy proposed by the EU Waste Framework Directive

Environmental charity Green Alliance estimated that, increasing the reuse of construction products could save 22.3 MtCO₂e of greenhouse gas emissions over 9 years [2.98], especially for timber as a biodegradable material, which is easy to modify and has greater potential of reuse over other mainstream construction such as concrete and steel. The Wood

Recycler Association (WRA) [2.99] classified the recyclability of wasted wood into 4 grades according to the source, the material type, and the included non-wood content (fixing, coatings, binders, etc.). Based on the report, the unprocessed waste wood that is free from contaminants, can serve as a viable material for animal bedding, panel board feedstock, landscaping or equestrian surfaces, as well as for biomass applications. Waste wood that has undergone treatment but poses no hazardous risk is well-suited for utilisation as feedstock in the panel board manufacturing process or for energy recovery. Conversely, hazardous waste wood must be exclusively disposed of in a licensed facility designated for the handling of such materials. However, detailed Standards that regulate the processing and properties determinations of the wasted material have not yet been published, which hinder the adoption of recycled construction material.

At present, a significant portion of wood sourced from the construction and demolition (C&D) sector can only subject to disposal methods such as incineration for energy retrieval or placement in landfills, contingent upon the specific legal, regional, and technological contexts in each country [2.98], which is the least priority in the waste hierarchy (Figure 2.22). In recent years, Europe recycles just approximately one-third of its construction and demolition (C&D) wood waste into materials suitable for board product manufacturing [2.100, 2.101], indicating the urgent need to improve systematic circularity in construction. The majority of wasted timber (~65%) was chopped into small pieces and used in producing biomass energy. Small proportion of them (~9%) that in good condition with minor amount of paint and surface coating can be used to manufacture by-products, such as landscape surface and animal bedding [2.101].

2.7.2 Reusable connection system for timber construction

Several factors currently impede the full reusability of timber in construction, with demolition methods being a primary concern. The prevalent practice involves using excavators to dismantle timber structures, a process that compromises the integrity of the materials and results in wastage. Additionally, the excessive use of nails and metal fixtures in contemporary timber construction complicates the disassembly process, often causing damage to the timber when these elements are removed. Furthermore, the concept of reusing structural materials is relatively novel and lacks comprehensive regulatory support. While there are some regulations providing general guidance on waste management, specific provisions to encourage the reuse of timber and other structural materials are limited.

As discussed above, obtaining reusable components during deconstruction is the most essential part in achieving reuse, necessitating the design of deconstruction (DfD) during the design stage. Therefore, numerous studies have been working on developing general principles to guide DfD with the growing interest in structural deconstruction. As summarised by Akinade et al., [2.102], Kanters [2.103], Tzourmakliotou [2.104], and Kim [2.105], most of the proposed DfD principles can be classified as: Building material related (e.g. avoid toxic and composite material, simplify building components and adopt lightweight, durable and separable material and joint), System Design related (e.g. employ modular, offsite and standardised construction, and accessible joint, building components, and service), Human related (e.g. provide adequate tools, training and communication, document material to ensure traceability and identifiability, and quantified information of cost and environmental impact) and Policy related factors (e.g. incorporate in building codes, set compulsory targets for deconstruction and material recycle and reuse). In addition to the general DfD principles, there are hundreds of indicators/criteria proposed for measuring the DfD performance of products/structures.

It should be noted that, the incorporation of DfD principles in building design does not directly contribute to the reusability of components. In addition to enabling deconstruction by employing DfD principles, the detached components should also pose limited damage and adequate capacity to ensure reusability [2.102, 2.106]. Therefore, two main objectives can be concluded for the design for reuse (DfR): one is the ease of separating structural components, and the other one is recovery of structural members. Since the process of deconstruction involves breaking the connection between components, the connection related factor appears one of the crucial parts among all the DfD and DfR indicators.

Table 2.3. DfR connection design Criteria and Weightings

Connection DfR Principles	Key Performance Indicators (KPIs)	Criteria	Weightings
Implementing design for deconstruction and reversible connections that allow for ease of deconstruction [2.102, 2.107-110]	Connection Type	Dry connections (e.g., click, magnetic, Velcro, self-locking connections etc.), which can be directly dismantled without damage and tools	1.00
		Connection with added elements (e.g., ferris, screw, bolt, and nut etc.), which can be dismantled by removing fasteners using hand tools	0.75
		Direct integral connection (e.g., pin, nail etc.), which can be dismantled by minor modifications with power tools	0.50
		Soft chemical connection (e.g., kit, foam etc.), which can be dismantled with moderate damage using Power or Gas/pneumatic tools	0.25
		Hard chemical connection (e.g., glue, pitch, weld, cement bond, chemical anchors etc.), which can be dismantled with significant damage using hydraulic tools	0.10
The types of structural connections in one project are minimised.	Connection Uniformity	Only one type of connection is used throughout the buildings	1.00
		Different connection types are adopted for shear and tensile connections, separately	0.50
		More than three types of connections are adopted due to the complex structural design	0.10
The cutting/modification on materials /components are minimised for connection fitting to avoid additional workload and waste generation [2.110]	Connection Complexity	Cutting on structural elements are not required for connection fitting	1.00
		Only simple cutting on material is required for fitting connections	0.50
		Complex modification on material for connections fitting (e.g. Drilling through the longitudinal direction of structural elements, multiple cutting process due to the complex connection geometry)	0.10
The level of standardisation and availability of connection [2.111]	Connection Standardisation	The connection is well standardised and widely adopted	1.00
		The connection is standardised and available on the market	0.50
		The connection is project-dependent	0.10
The level of off-site integration of connection with buildings system [2.110]	Connection Prefabrication	Connections can be accurately pre-attached to the structural element in factories and then arrive on-site already for simply assembly	1.00
		Connections need to be installed onsite	0.10
Connection-induced damage in structural elements [2.102, 106, 111]	Connection Deformation	Deformation of connection during buildings' service life would not cause damage in structural elements	1.00
		Connection and structural elements work together to process deformation, and the damaged part can be removed by cutting for reuse	0.50
		Structural elements are the primary ductility source and can experience significant deformation	0.10
Access to structural	Connection	Freely accessible from all sides without	1.00

connections for maintainability and longevity for structural components [2.102, 2.107, 2.108, 2.111]	Accessibility	damaging finishing layers	
		Accessibility with additional actions that do not cause damage (e.g. removing wall finish)	0.67
		Accessibility with additional actions with repairable damage (e.g. demolishing part of wall finish)	0.33
		Not accessible irreparable damage to objects	0.10
The tools and labour required to move components after deconstruction [2.105, 2.109, 2.111]	Ease of Transportation	One person: <20kg	1
		Two people: <42kg	0.75
		Hand trolley: <50 kg	0.5
		Forklift: <2,000kg	0.25
		Crane: >2,000kg	0.1

As summarised in Table 2.3, the connection design can impact the deconstructability of buildings from different aspects. The type of connection has the most direct impact to deconstruction, as their complexity (number of components and connecting structural elements, assembly and disassembling methods), uniformity, standardisation and prefabrication decide the ways that the structural components are separated, which impact the time, cost and labour requirements of deconstruction. All other factors in the list relate mostly to the reuse process. Connections that require no cutting and introduces no damage on structural elements ensure the integrity and the potential of being used in the next project. However, components that are dismantled integrally means that they will require heavy machine to lift and transport, which can directly increase the cost of reusing them in the next project.

According to Table 2.3, the conventional timber connections (angle bracket and hold downs) have poor DfR performance. Although they can technically be disassembled, it involves laborious de-nailing/unscrewing process or cutting timber members due to the usage of substantial amount of fasteners, leading to increased cost and unstandardised timber dimension that limits the reuse of timber. The complexity and strength of conventional permanent connections make it challenging to separate components without causing substantial damage to the connected components, leading to significant material waste during demolition. The removal of conventional permanent connections often leads to the complete destruction of interconnected elements, rendering them unsuitable for reuse, but only suitable for energy recovery or making by-products. The disassembly performance of other currently available timber connection products has been comprehensively reviewed in the literatures [2.106, 2.110, 2.111]

2.8 Novel Timber Connection Design Framework

Based on the factors should be considered in the development of a novel timber connection system, as summarised in the Section 2.6 and 2.7, a methodology scheme was proposed in this study and presented in Figure 2.23. The design framework covers the considerations of different aspects of CLT modular construction, aiming to assist the achievement of efficient, high-performing and reusable CLT structures.

To develop a comprehensive connection product, an extensive review of existing literature and on-site evaluations are essential to grasp the industry's immediate requirements thoroughly. Insights regarding structural performance, production cost and obstacles, and construction equipment and labour requirements should be gathered through current research initiatives and by visiting manufacturing plants and construction sites. This approach can facilitate the establishment of well-rounded design objectives. Subsequently, the preliminary connection design must undergo rigorous assessment through both numerical simulations and empirical testing to validate its effectiveness in meeting the established design objectives.

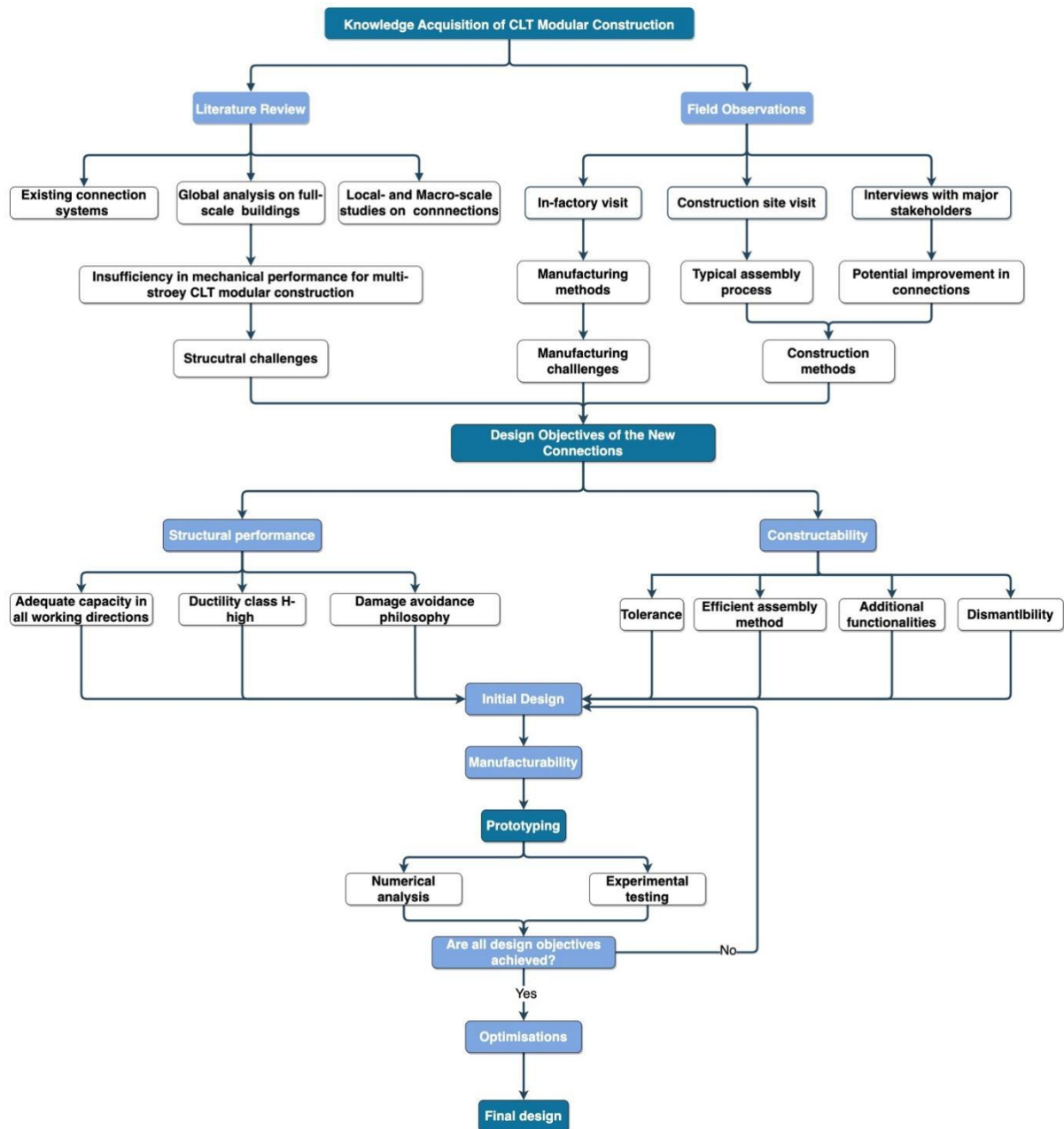


Figure 2.23. Design flowchart of novel CLT modular connections

2.9 Literature Review Findings

A comprehensive review of the CLTMC and existing connection systems was conducted, with a primary focus on the structural behaviours and the impact of connection systems. The investigations reveal several key findings:

CLT as a Sustainable Structural Material

Cross-Laminated Timber (CLT) is increasingly recognized as a sustainable structural material, notable for its advanced level of prefabrication. However, its application in multi-storey buildings remains challenging due to various structural and connection complexities.

Structural Behaviours of CLT Modular Buildings

The investigations show that CLT modular structures exhibit a significant degree of discreteness, a characteristic inherent to modular construction and compounded by the use of large-area CLT panels. This observation underscores the importance of connections between structural components and highlights the current absence of robust connection systems that are well-suited for CLTMC.

Deficiencies in Current Connection Systems

There is a notable absence of robust connection systems well-suited for CLT construction, emphasising the need for more extensive research. Current connection solutions, such as angle brackets and hold-downs, fall short in delivering the required stiffness, ductility, and construction efficiency. This gap necessitates further investigation and innovation in connection design to meet the demands of modern CLTMC.

Novel CLT Modular Connections

Various novel CLT modular connections have been reviewed, each offering unique functionalities such as limited-damage capacity, recentering capacity, interlocking, demountability, and reusability. These novel connections are designed to address the challenges and limitations associated with conventional connection techniques, providing more adaptable, efficient, and sustainable solutions for CLT construction. Their development and implementation could significantly enhance the performance and applicability of CLT in multi-storey modular buildings.

2.10 Conclusion

Despite the marked improvements in CLT structures and construction offered by the discussed innovative connections, a common limitation lies in their project-specific nature. They often lack a holistic consideration of all aspects of CLT modular construction, making standardisation a challenging prospect. Thus, a strategic design framework that

comprehensively addresses the structural, constructional, and manufacturing aspects is established in this study, to guide the development of standardised CLT connection system.

Furthermore, the growing demands for enhancing material circulation in construction necessitate a connection system that integrates the design for reuse (DfR) strategies, which is crucial in enhancing the environmental performance of CLT modular construction. Therefore, connection design criteria that emphasise the reuse potential are discussed herein, including the introduction of a weighting system to evaluate and prioritise these criteria. By adopting strategic design principles, the development, realisation, and commercialisation of innovative connection concepts can be significantly accelerated. Implementing these strategies not only responds to current environmental concerns but also aligns with future construction trends, where sustainability and efficiency are increasingly paramount.

2.11 Chapter References

- [2.1] Cherry, R., Manalo, A., Karunasena, W. and Stringer, G. *Out-of-grade sawn pine: A state-of-the-art review on challenges and new opportunities in cross laminated timber (CLT)*. Construction & building materials, 2019. **211**: p. 858-868.
- [2.2] Structural Timber Association. *Cross-laminated timber construction - an introduction*. Available from: <http://www.structuraltimber.co.uk/assets/InformationCentre/eb11.pdf>.
- [2.3] Structural Timber Association. *Engineered wood products and an introduction to timber structural systems*. Available from: <http://www.structuraltimber.co.uk/assets/InformationCentre/timberframeeb2.pdf>.
- [2.4] Davies, A. *Modern Methods of Construction: A forward-thinking solution to the housing crisis?* 2018, Royal Institution of Chartered Surveyors.
- [2.5] Pan, Y., Shahnewaz, M. and Tannert, T. *Seismic performance and collapse fragility of balloon-framed clt school building*. Journal of earthquake engineering : JEE, 2023. **27**(11): p. 3115-3135.
- [2.6] Jafari, M., Pan, Y., Shahnewaz, M. and Tannert, T. *Effects of ground motion duration on the seismic performance of a two-storey balloon-type clt building*. Buildings (Basel), 2022. **12**(7): p. 1022.
- [2.7] Li, Z., Wang, X. and He, M. *Experimental and analytical investigations into lateral performance of cross-laminated timber (CLT) shear walls with different construction methods*. Journal of earthquake engineering : JEE, 2022. **26**(7): p. 3724-3746.
- [2.8] Wang, X., He, M. and Li, Z. *Experimental testing of platform-type and balloon-type cross-laminated timber (CLT) shear walls with supplemental energy dissipators*. Journal of building engineering, 2023. **66**: p. 105943.

- [2.9] Chen, Z. and Popovski, M. *Mechanics-based analytical models for balloon-type cross-laminated timber (CLT) shear walls under lateral loads*. Engineering structures, 2020. **208**: p. 109916.
- [2.10] Yang, T.Y., Lepine-Lacroix, S., Ramos Guerrero, J.A., McFadden, J.B.W., Al-Janabi M.A.Q. *Seismic performance evaluation of innovative balloon type CLT rocking shear walls*. Resilient cities and structures, 2022. **1**(1): p. 44-52.
- [2.11] Stora Enso. *3–8 Storey Modular Element Buildings*. Available from: <https://www.storaenso.com/-/media/documents/download-center/documents/product-brochures/wood-products/design-manual-a4-modular-element-buildings20161227finalversion-40en.pdf>.
- [2.12] Lawson, R.M., Ogden, R.G. and Bergin, R. *Application of modular construction in high-rise buildings*. Journal of architectural engineering, 2012. **18**(2): p. 148-154.
- [2.13] CDC Habitat. *Supported modular housing: innovation and performance*. 2019. Available from: <https://www.adoma.cdc-habitat.fr/adoma/L-entreprise/Qui-sommes-nous-/Adoma-construit/Bien-construire-pour-bien-loger/Fiches-residence/p-552-Le-logement-accompagne-en-modulaire-innovation-et-performance.htm>.
- [2.14] Malo, K.A., Abrahamsen, R.B., and Bjertnæs M.A. *Some structural design issues of the 14-storey timber framed building “Treet” in Norway*. European journal of wood and wood products, 2016. **74**(3): p. 407-424.
- [2.15] Thomas, L. *The sky's the limit: See the world's tallest modular tower in Croydon*. 2019. Available from: <https://www.building.co.uk/buildings/the-skys-the-limit-see-the-worlds-tallest-modular-tower-in-croydon/5101741.article>
- [2.16] Karacabeyli, E. and Gagnon, S. *Canadian CLT Handbook*. 2019. Available from: <https://web.fpinnovations.ca/clt/>.
- [2.17] Green, E. and Karsh, E. *The case for tall wood buildings*. 2012. Available from: <http://www.cwc.ca/wp-content/uploads/publications-Tall-Wood.pdf>.
- [2.18] TIDE Construction. *IDE CONSTRUCTION LTD – 101 GEORGE ST, CROYDON*. Available from: <https://tideconstruction.co.uk/projects/george-street-croydon/tide-construction-ltd-101-george-st-croydon/>.
- [2.19] Ceccotti, A., Sandhaas, C., Okabe, M., Yasumura, M., Minowa, C., & Kawai, N. *SOFIE project - 3D shaking table test on a seven-storey full-scale cross-laminated timber building*. Earthquake engineering & structural dynamics, 2013. **42**(13): p. 2003-2021.
- [2.20] Ceccotti, A., *New Technologies for Construction of Medium-Rise Buildings in Seismic Regions: The XLAM Case*. Structural engineering international: journal of the International Association for Bridge and Structural Engineering (IABSE), 2008. **18**(2): p. 156-165.
- [2.21] Sandhaas, C., and Ceccotti, A. *Earthquake resistance of multi-storey massive timber buildings*. In 2nd Forum Holzbau Beaunue; FORUM HOLZBAU: Biel, Switzerland, 2012.

- [2.22] Popovski, M. and Gavric, I. *Performance of a 2-story clt house subjected to lateral loads*. Journal of structural engineering (New York, N.Y.), 2016. **142**(4).
- [2.23] Yasumura, M., Kobayashi, K., Okabe, M., Miyake, T. and Matsumoto, K. *Full-Scale Tests and Numerical Analysis of Low-Rise CLT Structures under Lateral Loading*. Journal of Structural Engineering, 2016. **142**(4).
- [2.24] Matos, F.T., Branco, J.M., Rocha, P., Mendes, N., Demschnr, T. and Lourenço, P.B. *Quasi-static tests on a two-story CLT building*. Engineering structures, 2019. **201**: p. 109806.
- [2.25] Pozza, L., Scotta, R., Trutalli, D., Pinna, M., Polastri, A. and Bertoni, P. *Experimental and numerical analyses of new massive wooden shear-wall systems*. Buildings (Basel), 2014. **4**(3): p. 355-374.
- [2.26] SOM, S. Owings, and M. LLP. (2013). Timber Tower Research Project. Available from: https://www.som.com/ideas/research/timber_tower_research_project.
- [2.27] Bezabeh, M.A., Bitsuamlak, G.T., Popovski, M. and Tesfamariam, S. *Dynamic response of tall mass-timber buildings to wind excitation*. Journal of structural engineering (New York, N.Y.), 2020. **146**(10).
- [2.28] Reynolds, Harris,T., R. and Chang, W.S. *Dynamic response of tall timber buildings to wind load*. in *IASS Annual Symposium: IABSE-IASS 2011: Taller, Longer, Lighter*. 2011. United Kingdom.
- [2.29] Foster, R.M., Reynolds, T.P.S. and Ramage, M.H. *Proposal for defining a tall timber building*. Journal of structural engineering, 2016. **142**(12): p. 2516001.
- [2.30] Connolly, T., Loss, C., Iqbal, A. and Tannert, T. *Feasibility study of mass-timber cores for the UBC tall wood building*. Buildings, 2018. **8**(8): p. 98.
- [2.31] Timmers, M. and Tsay Jacobs, A. *Concrete apartment tower in Los Angeles reimaged in mass timber*. Engineering structures, 2018. **167**: p. 716-724.
- [2.32] Bezabeh, M.A., Bitsuamlak, G.T., Popovski, M. and Tesfamariam, S. *Probabilistic serviceability-performance assessment of tall mass-timber buildings subjected to stochastic wind loads: Part I - structural design and wind tunnel testing*. Journal of wind engineering and industrial aerodynamics, 2018. **181**: p. 85-103.
- [2.33] Canadian Commission on, B. and C. Fire, *National Building Code of Canada: 2020*. 2022, National Research Council of Canada.
- [2.34] Ormarsson, S., Vessby, J., Johansson, M., and Kua, L. *Numerical and experimental study on modular-based timber structures*. Modular and offsite construction (MOC) summit proceedings, 2019: p. 471-478.
- [2.35] Chua, Y.S., Liew, J.Y.R. and Pang, S.D. *Modelling of connections and lateral behavior of high-rise modular steel buildings*. Journal of constructional steel research, 2020. **166**: p. 105901.

- [2.36] Nadeem, G., Safiee, N.A., Bakar, N.A., Karim, I.A. and Nasir, N.A.M. *Connection design in modular steel construction: A review*. Structures (Oxford), 2021. **33**: p. 3239-3256.
- [2.37] Popovski, M., Gavric, I. and Schneider, J. *Performance of two-storey clt house subjected to lateral loads*, in *World Conference on Timber Engineering*. 2014: Quebec City, Canada.
- [2.38] Gavrić, I., Fragiacomò, M. and Ceccotti, A. *Capacity seismic design of X-LAM wall systems based on connection mechanical properties*. in *46th CIB-W18 meeting*. 2013. Vancouver.
- [2.39] Gavric, I., Fragiacomò, M. and Ceccotti, A. *Cyclic behaviour of typical metal connectors for cross-laminated (CLT) structures*. Materials and structures, 2015. **48**(6): p. 1841-1857.
- [2.40] Deng, P., Pei, S., van de Lindt, J.W., Omar Amini, M. and Liu, H. *Lateral behavior of panelized CLT walls: A pushover analysis based on minimal resistance assumption*. Engineering structures, 2019. **191**: p. 469-478.
- [2.41] Soerensen, J.D., *Framework for robustness assessment of timber structures*. Engineering structures, 2011. **33**(11): p. 3087-3092.
- [2.42] Jorissen, A. and Fragiacomò, M. *General notes on ductility in timber structures*. Engineering structures, 2011. **33**(11): p. 2987-2997.
- [2.43] Fragiacomò, M., B. Dujic, and Sustersic, I. *Elastic and ductile design of multi-storey crosslam massive wooden buildings under seismic actions*. Engineering structures, 2011. **33**(11): p. 3043-3053.
- [2.44] Follesa, M., Fragiacomò, M., Casagrande, D., Tomasi, R., Piazza, M., Vassallo, D., Canetti, D. and Rossi, S. *The new provisions for the seismic design of timber buildings in Europe*. Engineering structures, 2018. **168**: p. 736-747.
- [2.45] Eurocode, *Eurocode 8: Design of structures for earthquake resistance*. 1998, European Committee for Standardization,.
- [2.46] Hristovski, V., Dujic, B., Stojmanovska, M. and Mircevska, V. *Full-scale shaking-table tests of xlam panel systems and numerical verification: specimen 1*. Journal of structural engineering, 2013. **139**.
- [2.47] Ceccotti, A. and Follesa, M. *Seismic Behaviour of Multi-Storey XLam Buildings*, in *COST E29 International Workshop on Earthquake Engineering on Timber Structures*. 2006: Coimbra, Portugal. p. 81-95.
- [2.48] Huber, J.A.J., Ekevad, M., Girhammar, U.A. and Berg, S. *Structural robustness and timber buildings - a review*. Wood material science and engineering, 2019. **14**(2): p. 107-128.
- [2.49] Branco, J.M. and Neves, L.A.C. *Robustness of timber structures in seismic areas*. Engineering structures, 2011. **33**(11): p. 3099-3105.50.

- [2.50] Gavric, I., M. Fragiaco, and Ceccotti, A. *Cyclic behavior of typical screwed connections for cross-laminated (CLT) structures*. European journal of wood and wood products, 2015. **73**(2): p. 179-191.
- [2.51] Tomasi, R. and Smith, I. *Experimental characterization of monotonic and cyclic loading responses of clt panel-to-foundation angle bracket connections*. Journal of materials in civil engineering, 2015. **27**(6).
- [2.52] Rothoblaas. *Fastening*. Available from: <https://www.rothoblaas.com/products/fastening>.
- [2.53] Rinaldin, G. and Fragiaco, M. *Non-linear simulation of shaking-table tests on 3- and 7-storey X-Lam timber buildings*. Engineering structures, 2016. **113**: p. 133-148.
- [2.54] Sandoli, A., D'Ambra, C., Ceraldi, C., Calderoni, B. and Prota, A. *Sustainable cross-laminated timber structures in a seismic area: overview and future trends*. Applied sciences, 2021. **11**(5): p. 2078.
- [2.55] Brühl, F., Kuhlmann, U. and Jorissen, A. *Consideration of plasticity within the design of timber structures due to connection ductility*. Engineering structures, 2011. **33**(11): p. 3007-3017.
- [2.56] Latour, M. and Rizzano, G. *Cyclic behavior and modeling of a dissipative connector for cross-laminated timber panel buildings*. Journal of earthquake engineering : JEE, 2015. **19**(1): p. 137-171.
- [2.57] Chan, N., Hashemi, A., Zarnani, P. and Quenneville, P. *Pinching-Free Connector for Timber Structures*. Journal of structural engineering (New York, N.Y.), 2021. **147**(5): p. 4021036.
- [2.58] Aloisio, A., Pellicciari, M., Bergami, A.V., Alaggio, R., Briseghella, B. and Fragiaco, M. *Effect of pinching on structural resilience: performance of reinforced concrete and timber structures under repeated cycles*. Structure and infrastructure engineering, 2022. **ahead-of-print**(ahead-of-print): p. 1-17.
- [2.59] O'Ceallaigh, C. and Harte, A.M. *The elastic and ductile behaviour of CLT wall-floor connections and the influence of fastener length*. Engineering structures, 2019. **189**: p. 319-331.
- [2.60] Polastri, A., Giongo, I. and Piazza, M. *An innovative connection system for cross-laminated timber structures*. Structural engineering international : journal of the International Association for Bridge and Structural Engineering (IABSE), 2017. **27**(4): p. 502-511.
- [2.61] Iacovidou, E. and Purnell, P. *Mining the physical infrastructure: Opportunities, barriers and interventions in promoting structural components reuse*. The Science of the total environment, 2016. **557–558**, pp.791–807.
- [2.62] Eurocode, *Eurocode 5: Design of timber structures*. 2004, European Committee for Standardization,.

- [2.63] Yurrita, M. and Cabrero, J.M. *On the need of distinguishing ductile and brittle failure modes in timber connections with dowel-type fasteners*. Engineering structures, 2021. **242**: p. 112496-64.
- [2.64] Izzi, M., Flatscher, G., Fragiaco, M. and Schickhofer, G. *Experimental investigations and design provisions of steel-to-timber joints with annular-ringed shank nails for Cross-Laminated Timber structures*. Construction & building materials, 2016. **122**: p. 446-457.
- [2.65] Jorissen, A.J.M., *Double shear timber connections with dowel type fasteners*. 1998.
- [2.66] Kurzinski, S., Crovella, P. and Kremer, P. *Overview of Cross-Laminated Timber (CLT) and Timber Structure Standards Across the World*. 2022. **5**: p. 1-13.
- [2.67] Trutalli, D., Marchi, L., Scotta, R. and Pozza, L. *Capacity design of traditional and innovative ductile connections for earthquake-resistant CLT structures*. Bulletin of earthquake engineering, 2019. **17 (4)**: p. 2115-2136.
- [2.68] Schickhofer, G., Brandner, R., and Bauer, H. *Introduction to CLT, Product Properties, Strength Classes*. 2016.
- [2.69] Iraola, B., Cabrero, J.M., Basterrechea-Arévalo, M. and Gracia, J. *A geometrically defined stiffness contact for finite element models of wood joints*. Engineering structures, 2021. **235**: p. 112062.
- [2.70] Hong, J.-P. and Barrett, D. *Three-dimensional finite-element modeling of nailed connections in wood*. Journal of structural engineering (New York, N.Y.), 2010. **136(6)**: p. 715-722.
- [2.71] Zhang, C., Jung, K., Harris, R. and Chang, W.-S., *'Rope effect' mechanism of self-tapping screws as reinforcement on dowel-type connections*. Proceedings of the Institution of Civil Engineers. Structures and buildings, 2021. **176(5)**: p. 380-389.
- [2.72] Gečys, T., Bader, T.K., Olsson, A. and Kajėnas, S. *Influence of the rope effect on the slip curve of laterally loaded, nailed and screwed timber-to-timber connections*. Construction and building materials, 2019. **228**: p. 116702.
- [2.73] Uibel, T. and Blaß, H.J. *Joints with dowel type fasteners in CLT structures*. , in *Focus solid timber solutions-European conference on cross laminated timber (CLT)*. 2013: Bath. p. 119-136.
- [2.74] Izzi, M., Casagrande, D., Bezzi, S., Pasca, D., Follesa, M. and Tomasi, R. *Seismic behaviour of cross-laminated timber structures: a state-of-the-art review*. Engineering structures, 2018. **170**: p. 42-52.
- [2.75] Mahlknecht, U. and Brandner, R. *Block shear failure mechanism of axially-loaded groups of screws*. Engineering structures, 2019. **183**: p. 220-242.
- [2.76] Pozza, L., Saetta, A., Savoia, M. and Talledo, D. *Angle bracket connections for CLT structures: Experimental characterization and numerical modelling*. Construction and building materials, 2018. **191**: p. 95-113.

- [2.77] Liu, J. and Lam, F. *Experimental test of coupling effect on CLT angle bracket connections*. Engineering structures, 2018. **171**: p. 862-873.
- [2.78] Marchi, L., *Innovative connection systems for timber structures*, in *Dipartimento di Ingegneria Civile, Edile ed Ambientale*. 2018, Università degli Studi di Padova.
- [2.79] Schneider, J., Karacabeyli, E., Popovski, M., Stiemer, S.F. and Tesfamariam, S. *Damage assessment of connections used in cross-laminated timber subject to cyclic loads*. Journal of performance of constructed facilities, 2014. **28**(6).
- [2.80] Izzi, M., Polastri, A. and Fragiaco, M. *Modelling the mechanical behaviour of typical wall-to-floor connection systems for cross-laminated timber structures*. Engineering structures, 2018. **162**: p. 270-282.
- [2.81] Polastri, A.n. and Pozza, L. *Proposal For A Standardized Design And Modeling Procedure Of Tall Clt Buildings*. International journal for quality research, 2016. **10**(3): p. 607-624.
- [2.82] Yurrita, M. and Cabrero, J.M. *New design model for brittle failure in the parallel-to-grain direction of timber connections with large diameter fasteners*. Engineering structures, 2020. **217**: p. 110557.
- [2.83] Zarnani, P. and Quenneville, P. *New design approach for controlling brittle failure modes of small-dowel-type connections in Cross-laminated Timber (CLT)*. Construction & building materials, 2015. **100**: p. 172-182.
- [2.84] Hanhijärvi, A. and Kevarinmäki, A. *Design method against timber failure mechanisms of dowelled steel-to-timber connections*. 2007, CIB-W18 Timber Structures: Slovenia. p. 40-7-3.
- [2.85] Yurrita, M., Cabrero, J.M. and Quenneville, P. *Brittle failure in the parallel-to-grain direction of multiple shear softwood timber connections with slotted-in steel plates and dowel-type fasteners*. Construction & building materials, 2019. **216**: p. 296-313.
- [2.86] Knapp. *Construction Manual*. 2015. Available from: <https://www.knapp-verbinder.com/en/products/prefab-walls/>
- [2.87] Karacabeyli, E. and Gagnon, S. *Canadian CLT Handbook*. 2019. Available from: <https://web.fpinnovations.ca/clt/>.
- [2.88] Younis, A. and Doodoo, A. *Cross-laminated timber for building construction: A life-cycle-assessment overview*. Journal of building engineering, 2022. **52**: p. 104482.
- [2.89] Winter, S., Jacob-Freitag, S. and Kohler, C. *Mobi-Space - a modular, reusable building system made of wood*. Die Bautechnik, 2017. **94**(3): p. 174-180.
- [2.90] Gijzen, R. *Modular cross-laminated timber buildings*, in *the faculty of Civil Engineering and Geosciences*. 2017, Delft University of Technology.
- [2.91] Carvalho, L.F., Jorge, L.F.C., and Jerónimo, R. *Plug-and-play multistory mass timber buildings: achievements and potentials*. Journal of architectural engineering, 2020. **26**(2).

- [2.92] Chao (Tom) Zhang, G.L., Lam, F. *Connections for Stackable Heavy Timber Modules in Midrise to Tall Wood Buildings*. 2019, Timber Engineering and Applied Mechanics (TEAM) Laboratory.
- [2.93] Srisangeerthan, S., Hashemi, M.J., Rajeev. P, Gad. E, Fernando. S, *Review of performance requirements for inter-module connections in multi-story modular buildings*. Journal of building engineering, 2020. **28**: p. 101087.
- [2.94] Corfar, D.-A. and Tsavdaridis, K.D. *A comprehensive review and classification of inter-module connections for hot-rolled steel modular building systems*. Journal of building engineering, 2022. **50**: p. 104006.
- [2.95] Li, Z., Tsavdaridis, K.D. and Gardner, L. *A review of optimised additively manufactured steel connections for modular building systems*. 2020: Springer International Publishing.
- [2.96] Densley Tingley, D. *Design for Deconstruction: an appraisal*. 2013, University of Sheffield.
- [2.97] Dai, X.-M., Zong, L., Ding, Y. and Li, Z.-X. *Experimental study on seismic behavior of a novel plug-in self-lock joint for modular steel construction*. Engineering structures, 2019. **181**(C): p. 143-164.
- [2.98] Vis, M.W., Mantau, U. and Allen, B. *Cascades. Study on the optimised cascading use of wood*. 2016: Brussels.
- [2.99] *WRA Grades of Waste Wood*. 2021, The Wood Recyclers' Association.
- [2.100] Risse, M., Weber-Blaschke, G. and Richter, K. *Resource efficiency of multifunctional wood cascade chains using LCA and exergy analysis, exemplified by a case study for Germany*. Resources, conservation and recycling, 2017. **126**: p. 141-152.
- [2.101] RECYCLING, C.W. *Recycling wood in the UK*. Available from: <https://communitywoodrecycling.org.uk/what-we-do/recycling-wood-in-the-uk/>.
- [2.102] Akinade, O.O., Oyedele, L.O., Ajayi, S.O., Bilal, M., Alaka, H.A., Owolabi, H.A., Bello, S.A., Jaiyeoba, B.E. and Kadiri, K.O. *Design for Deconstruction (DfD): Critical success factors for diverting end-of-life waste from landfills*. Waste management (Elmsford), 2017. **60**: p. 3-13.
- [2.103] Kanters, J. *Design for deconstruction in the design process: state of the art*. Buildings, 2018. **8**: p.150.
- [2.104] Tzourmakliotou, D., *Designing for deconstruction—The related factors*. Journal of civil engineering and architecture, 2021. **15**: p. 459-468.
- [2.105] Kim, S. and Kim, S.-A. *A design support tool based on building information modeling for design for deconstruction: A graph-based deconstructability assessment approach*. Journal of cleaner production, 2023. **383**: p. 135343.

- [2.106] Ottenhaus, L.-M., Yan, Z., Brandner, R., Leardini, P., Fink, G. and Jockwer, R. *Design for adaptability, disassembly and reuse – A review of reversible timber connection systems*. Construction & building materials, 2023. **400**: p. 132823.
- [2.107] Cottafava, D. and Ritzen, M. *Circularity indicator for residential buildings: Addressing the gap between embodied impacts and design aspects*. Resources, conservation and recycling, 2021. **164**: p. 105120.
- [2.108] Antwi-Afari, P., Ng, S.T., Chen, J. and Zheng, X.M. *Determining the impacts and recovery potentials of a modular designed residential building using the novel LCA-C2C-PBSCI method*. Journal of cleaner production, 2022. **378**: p. 134575.
- [2.109] O’Grady, T., Minunno, R., Chong, H.-Y. and Morrison, G.M. 2021. Design for disassembly, deconstruction and resilience: A circular economy index for the built environment. *Design for disassembly, deconstruction and resilience: A circular economy index for the built environment*. Resources, conservation and recycling, 2021. **175**: p. 105847.
- [2.110] Pozzi, L.E. *Design for disassembly with structural timber connections*. 2019, Delft University of Technology: Delft. p. 1-24.
- [2.111] Shamaa, A.A. and Saleh, K. *Detachable connections for circularity of timber buildings*, in *Department of Architecture and Civil Engineering*. 2021, Chalmers University Of Technology: Sweden.

Chapter 3 Conceptual Design of the Interlocking Connection System for CLT Modular Structures

Despite the emergence of new technologies and materials in the timber construction industry, standard connections continue to prevail. As the decisive elements influencing structural performance and construction efficiency, connection design poses an imminent challenge in the forefront of flexible and adaptable timber modular designs. The industry now requires intelligent connection solutions that prioritise efficiency, adaptability, and reusability in structures, departing from the conventional emphasis solely on structural performance in connection design. Therefore, driven by the motivation to optimise construction procedures and performance of medium-rise CLT modular structures, this chapter presents the development of a novel connection system for CLT modular construction, incorporating considerations from structural, manufacturing, and construction perspectives. Its purpose is to tackle the existing challenges in CLT modular construction related to current connection devices.

3.1 Overview of Interlocking Techniques in Construction

Interlocking, a versatile joining method applied in engineering, architecture, and manufacturing, offers stability and load-bearing capacity by complementary shapes such as tabs, slots, or notches. The core principle of interlocking connections is to lock structural elements through component interaction, instead of other onsite connecting methods such as fasteners, welding and glue. This approach, characterised by minimal operational requirements and immediate activation, eliminates the need for on-site manual operations involved in locating, adjusting, and fastening structural elements, thereby significantly expediting the erection process.

Common interlocking connection designs in construction include dovetail, tongue and groove, and puzzle-like connections (Figure 3.1). Historically, interlocking techniques have been integral to ancient asian architectural practices for joining structural elements. In contemporary construction, modern interlocking connections have gained popularity for their capacity to meet the demands of rapid, accurate but tool-less onsite assembly, facilitated by a wider range of modern engineered materials, including steel and advanced polymers. These

advancements are crucial in addressing the growing housing crisis and the scarcity of skilled labour.



Figure 3.1. Interlocking connection system used in (a) yingxian wooden tower in 1056 AD [3.1] and (b) modern construction (LOCK Connector from Rothoblaas Ltd.)

Some previous conceptual studies [3.2-6] have recognised the potential of the interlocking technique in promoting onsite constructability, adaptability, sustainability and dismantlability in modular structures. Similarly, utilising interlocking connections in timber modular construction can facilitate the streamline of the construction process and minimising labour requirements. In addition to enhanced efficiency, these connections also promote disassembly and reassembly of modules, allowing for easy retrofitting, relocation, or repurposing of structures.

3.2 Novel Interlocking Connection System for CLT Modular Construction

The utilisation of interlocking connections in construction, particularly in CLT modular construction, presents significant advancements. These connections are designed to interlock structural elements without the necessity for manual fixing, which liberates on-site assembly from the limitations imposed by the accessibility of connection points within structures. This is especially advantageous in the context of CLT modular construction, where large panels are a common feature. Accordingly, a new metallic connection system with interlocking features was proposed herein for CLT modular construction.

3.2.1 Overview of the interlocking joining mechanism for CLT modular structures

Unlike traditional permanent connections such as welds or cast-in-place concrete, which are fully rigid post-assembly, interlocking connections retain a degree of freedom along the installation axis. This flexibility could be beneficial during the assembly phase, allowing for minor adjustments as modules are positioned and secured, while it should be carefully

considered in the connection design when employing interlocking. Therefore, to cater to the multidirectional forces experienced by modular structures, the novel interlocking system comprises separate shear and tensile connections. The shear connections are implemented by a straightforward vertical stacking process, while the tensile connections are engaged through a horizontal sliding action.

The interlocking system integrates a two-component design featuring male and female connectors (Figure 3.2). The act of joining these components effectively locks the modules in place through a self-locking mechanism inherent to the connection design. This eliminates the need for additional tools or fastening methods, significantly expediting the assembly process and enhancing construction efficiency. In addition, this system presents a strip-like design positioned along the module edges (Figure 3.2).

Different from the conventional discrete reinforcing methods provided by the steel plate connections, the strip-like connection design provides continuous reinforcement can minimise load concentration on CLT panels as well as provide adequate planar force resistance. This feature is particularly advantageous in CLT building design, where the focus is on countering in-plane forces rather than managing bending moments, due to the inherent high in-plane stiffness of CLT panels.



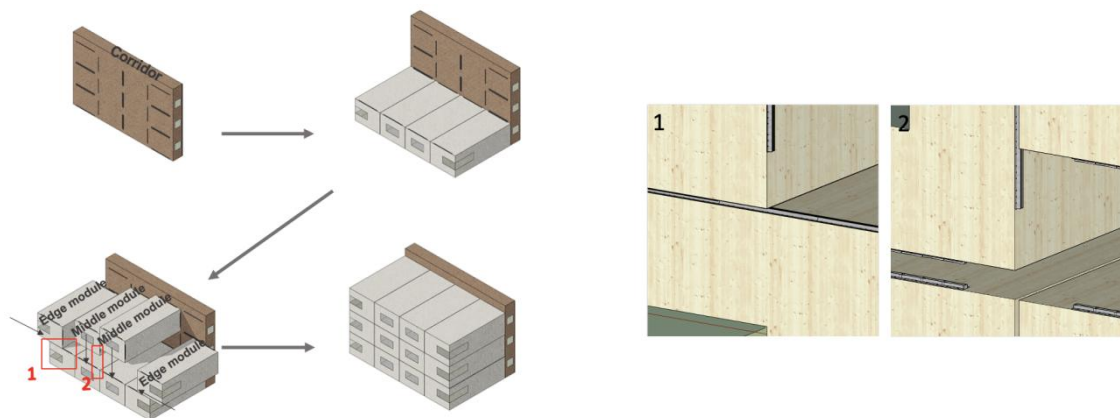
Figure 3.2. 3D renders of continuous connectors attached on the CLT panels using fasteners: (a) shear connectors, (b) tensile connectors.

Furthermore, as proved by the previous numerical analysis on similar interlocking connection [3.7], this kind of edge-supporting connection system can also help achieve enhanced integrity in volumetric structures. When damage happens in part of the connection of one of the modules, the overall structure is designed to maintain stability with minimal movement, negating the immediate need for repair or replacement. This is achieved through the formation of alternative load paths along the edges of the remaining modules, ensuring that

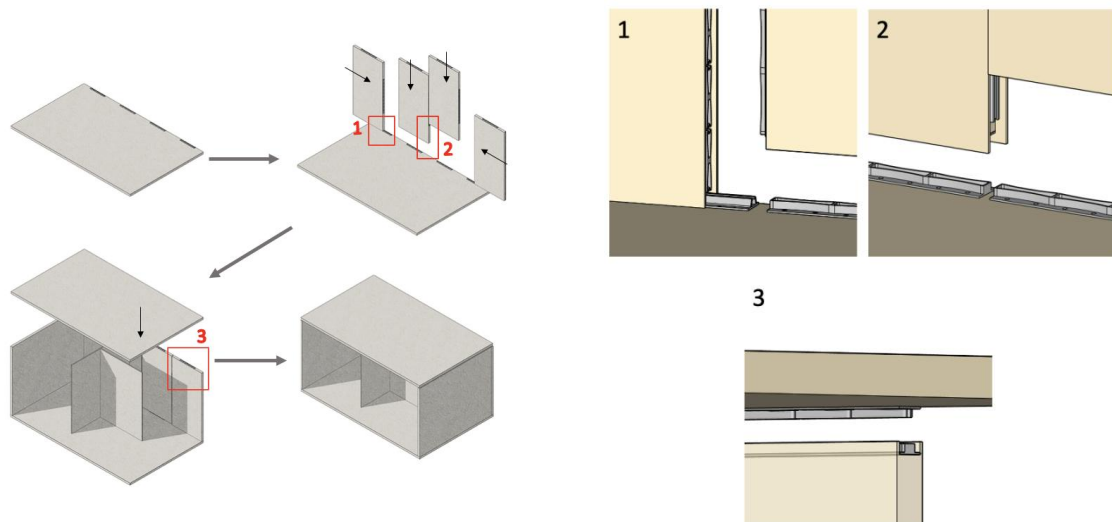
the structure's performance criteria continue to be met. This inherent redundancy within the connection design not only improves the resilience of the structure but also contributes to the safety and longevity of the building.

The new interlocking connection system offers versatile applicability across various types of CLT modular structures. For CLT Volumetric Construction (CLTVC), as depicted in Figure 3.3.a, the construction process begins by constructing the core structure, which serves as a lift shaft or staircase, incorporating pre-installed interlocking connections. Subsequently, the construction process involves the vertical stacking of middle modules and the horizontal sliding of edge room modules, adhering to the connection arrangement on the core structure.

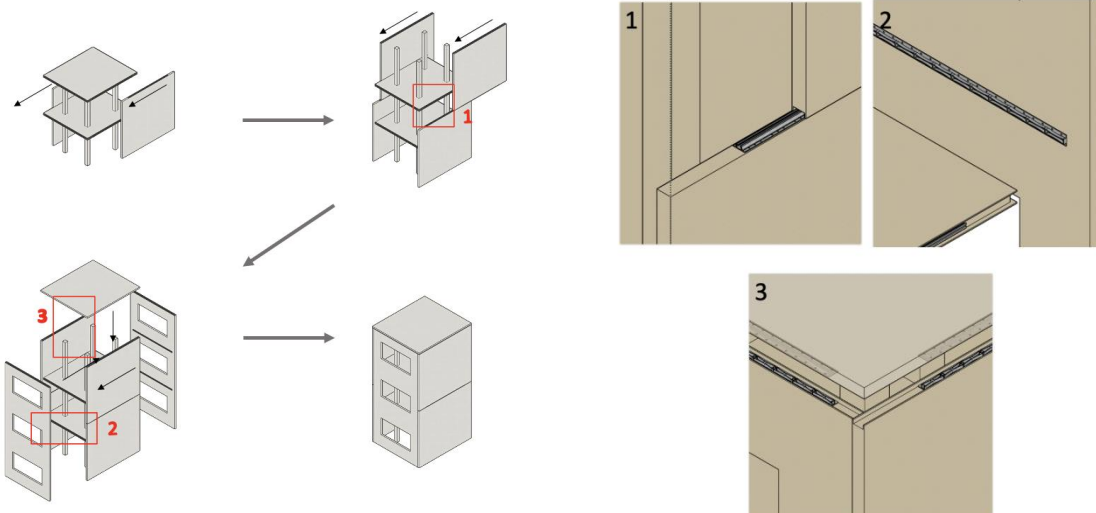
In CLT Panelised Construction (CLTPC), the interlocking connections are applicable in both platform-type and balloon-type construction methods. In platform-type CLT structures (Figure 3.3.b), the assembly is carried out in a layer-by-layer manner. Wall panels are slide or stacked on top of the initially laid floor panels. The specific wall assembly sequence is determined based on the structural requirements at different locations within the building. Once vertical wall panels are properly positioned, the upper floor panels can be directly attached to the top of the wall panels, completing the construction of the entire floor. In balloon-type CLT structures (Figure 3.3.c), the construction process begins with the erection of the flooring system. Subsequently, the continuous vertical shear walls are slide along the edges of the floor panels, utilising the sliding connections. Once the lateral load resisting system is completed, the building envelope is finalised by attaching the side wall panels and the roof onto the structure, employing stacking connections for secure and reliable integration.



(a)



(a)



(b)

Figure 3.3. Application overviews of the novel interlocking connection system for different CLT modular structures and the close-up of construction details: (a) CLT volumetric structures (b) CLT panelised platform-type structures (c) CLT panelised balloon-type structures.

Upon completing the connection assembly, the movement of connectors can be locked using straightforward end-locking systems. These systems involve extended plates with holes welded on the ends of the connectors, through which fasteners can secure two connectors together (Figure 3.4).

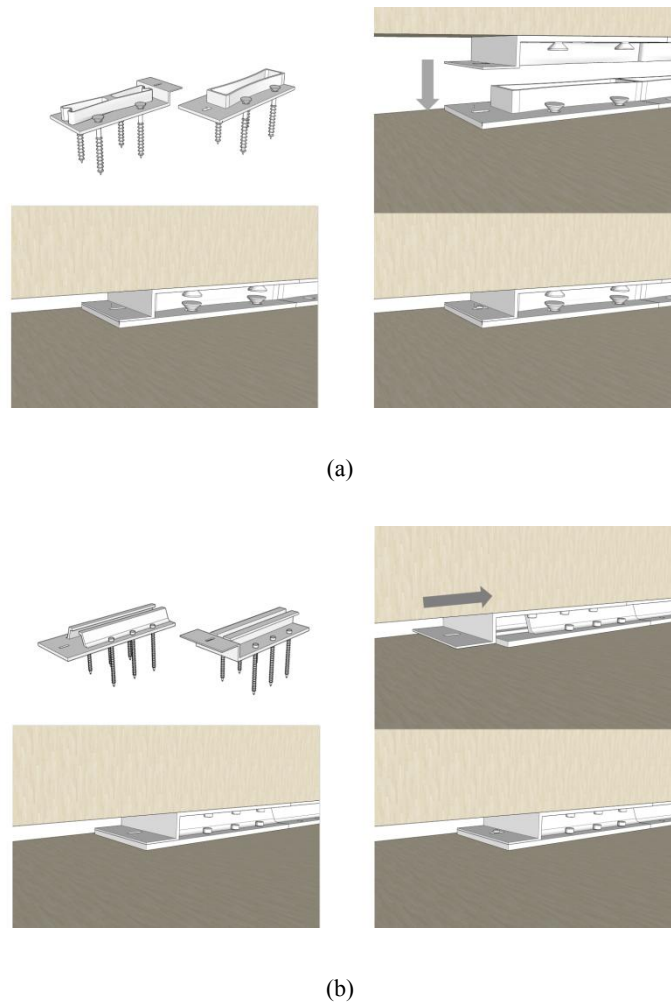


Figure 3.4. End-locking devices for (a) shear connection and (b) tensile connection.

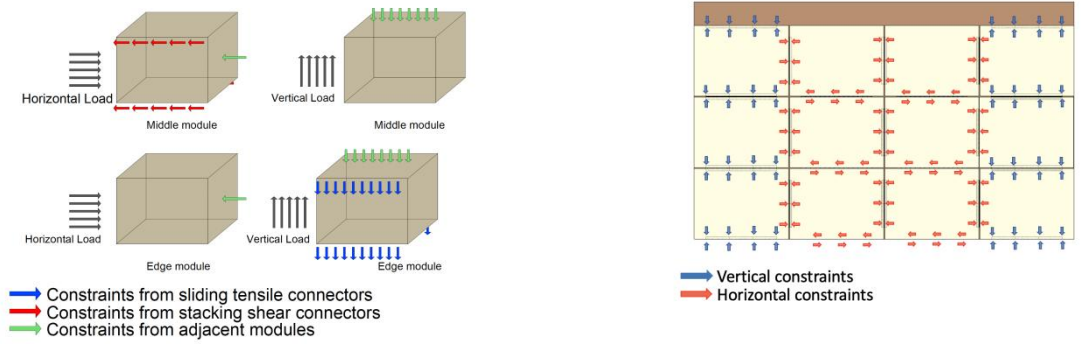
3.2.2 Reinforcing mechanism of the connection system

Since the tensile and shear reinforcement are provided by different connectors in the system, the integration of shear and tensile constraints into the structures should be achieved by strategically placing the modules. Figure 3.5 demonstrates how the interlocking connection system reinforces individual structural elements, and the continuous vertical and horizontal reinforcement on the overall CLT modular systems.

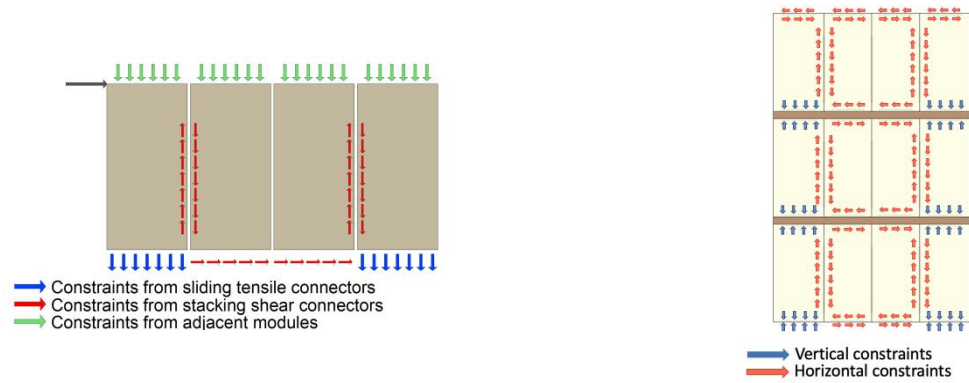
In CLT volumetric structures (Figure 3.5.a), although the edge modules feature sliding connections at the bottom that offer no shear reinforcement, their horizontal movement can be constrained by the adjacent modules, and the friction within the sliding rails, which is a result of the compression from the structure above. In the context of vertical loading, such as uplift forces, the movement of edge modules in the system is effectively constrained by a combination of factors: the modules' self-weight, the downward pressure exerted by

structures positioned above, and the sliding tensile connections located at the bottom of these modules. For a middle module which is primarily subjected to lateral movement, it is laterally restricted by the shear interlocking connections at the bottom. Meanwhile, vertical movement in these middle modules is considered minimal and can be sufficiently constrained by the weight of the structure above.

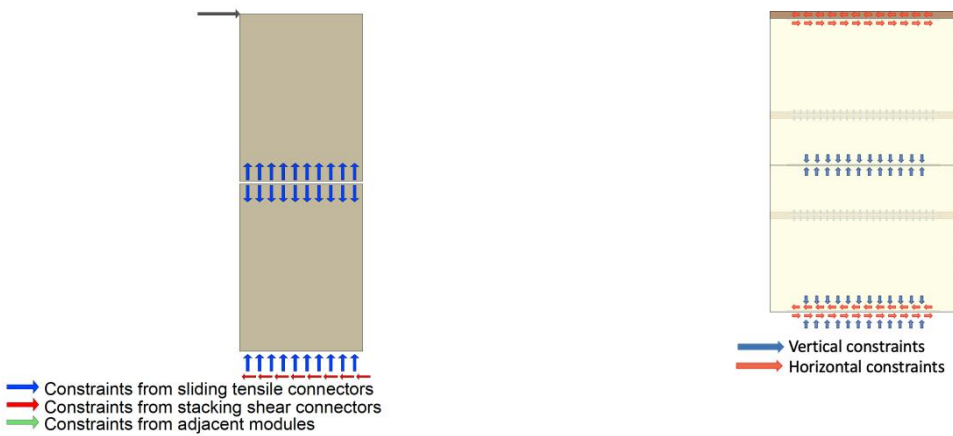
Similar reinforcing methods can be observed in CLT platform structures (Figure 3.5.b) with the proposed connection system. Here, the panels at the edges are restricted in the vertical direction primarily by the sliding (tensile) connections, and the middle panels are restricted laterally by the stacking (shear) connections. Additionally, shear connectors are strategically used between edge and middle panels to minimise panel-to-panel movement. Meanwhile, sliding connections are applied between middle panels to accommodate assembly requirements. In balloon-type CLT panelised structures (Figure 3.5.c), sliding connectors serve the dual purpose of connecting the flooring system to the shear walls and ensuring the integrity of shear walls by providing continuous vertical connections between panels.



(a)



(b)



(c)

Figure 3.5. The illustrations of the interlocking connection working mechanism in single module and the sectional elevation of the structure showing the overall constraints: (a) CLT volumetric structures; (b) CLT platform structure; (c) CLT balloon structure.

3.2.4 Interlocking connection and construction circularity

The use of interlocking connections in building construction not only improves assembly efficiency but also offers significant advantages during deconstruction and in the realms of material reuse and circulation, compared to the demolition of conventional permanent connections. Conventional permanent connections, owing to their complexity and strength,

often present challenges in component separation without causing extensive damage to the connected elements. This leads to considerable material waste during demolition processes. Furthermore, the demolition of these permanent connections typically results in the total destruction of interconnected elements, rendering them unsuitable for reuse. They are often relegated to energy recovery or the production of by-products (Figure 3.6).

In contrast, interlocking connections can facilitate easy disassembly, allowing for controlled removal of building components while preserving their integrity. This design feature encourages the transition from a linear "take-make-dispose" model to a circular economy model [3.8] (Figure 3.6), where materials are kept in use for as long as possible by enabling careful dismantling and repurposing of individual parts for new construction projects, thereby reducing waste generation and supporting sustainable resource utilisation (design for deconstruction and reuse - DfDR). Furthermore, by enabling the reuse and recycling of building components, the interlocking connections minimise the reliance on new resources. This not only decreases the demand for raw materials but also minimises the environmental impact associated with their extraction and production. Such practices are in harmony with the principles of circularity in construction, representing a sustainable and environmentally conscious approach to building design and construction.

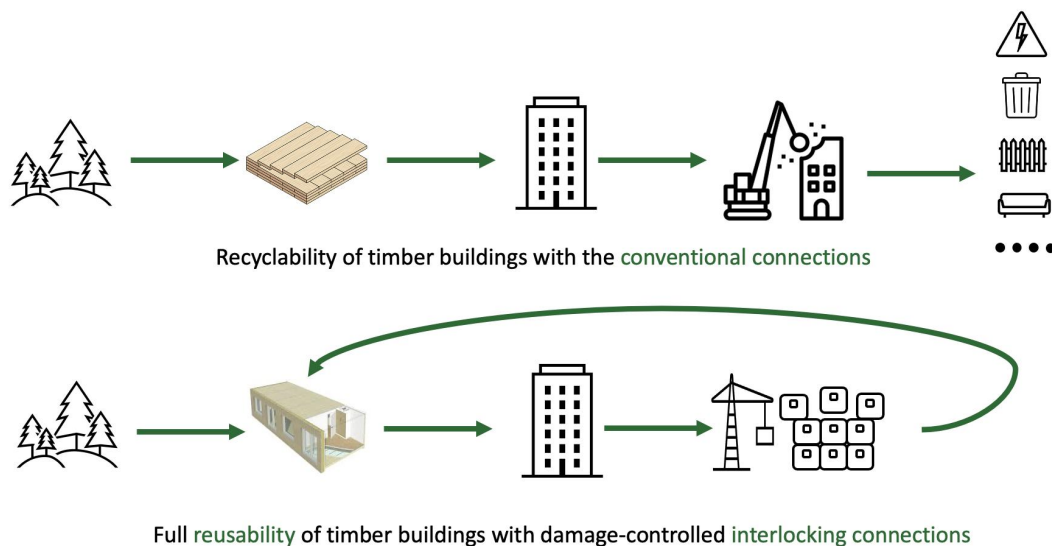


Figure 3.6. Comparison in potential building life cycles between CLT buildings using conventional connections (top) and interlocking connections (bottom).

3.3 Components Design of The Interlocking Connection System

As concluded in Chapter 2, the performance of the new connection system should be evaluated and optimised based on four standards: structural performance, novelty, constructability and manufacturability (Figure 3.7), ensuring its feasibility in construction. Regarding structural performance, the proposed connectors were anticipated to exhibit comparable or superior mechanical properties (stiffness, strength, ductility) compared to conventional connections found in today’s market. The proposed interlocking connections should also provide sufficient tolerance for onsite operation and allow for deconstruction. These connections should also possess novel functionality that offers additional advantages to timber modular construction.

Lastly, the design of these connectors has to be carefully considered to avoid unnecessary complexity in geometry, ensuring the compatibility with existing manufacturing methods and facilitating their easy adoption and enabling mass production. This approach strikes a balance between innovation and practicality, ensuring that the connectors are not only technically advanced but also feasible for widespread use in the construction industry.

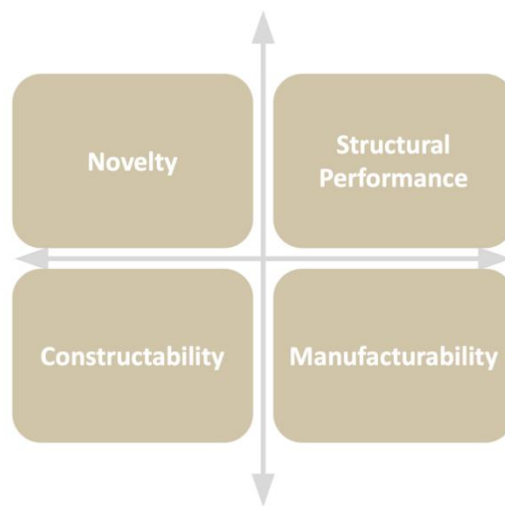


Figure 3.7. Evaluations of connection design.

3.2.1 Capacity design for damage-controlled effect

As detailed in Chapter 2, conventional connection design often relies on screw deformation to achieve ductility, a method that presents challenges due to the variable properties of timber and the complex interactions between components. These variables complicate the precise estimation of connection properties and the determination of an appropriate overstrength

factor when using existing analytical models. In response to these challenges, the proposed connection design in this research aims to redirect the source of ductility to the specially designed three-dimensional (3D) interlocking connectors. This approach ensures more reliable behaviour compared to the less predictable screw-timber interaction.

In this new design, the male connectors in both connections were regarded as the ductile elements, intended to deform and fail initially. In contrast, the female connectors, fasteners, and timber/CLT components are considered non-ductile, designed to resist significant deformation during loading. Therefore, capacity design principles were employed, incorporating appropriate overstrength factors, to enhance the capacity of timber-fastener connection ($R_{fasteners}$), fastener-to-steel plate connection (R_{plate}) and female connector (R_{female}) in the system, using the capacity of male connector (R_{male}). Consequently, the primary deformation in this connection system is the deformation of the male connectors, with the secondary deformation being the ductile deformation of the fasteners, such as one- or two-hinge yielding of screws. This aspect of the design can be aligned with the guidelines of EC5 [3.9].

By adopting this design approach, the interlocking connection system minimises the occurrence of brittle failure and damage in timber, while the male connectors bearing the majority of the deformation, achieving what can be referred to as a ‘damage-controlled capacity.’ Due to the less scattering properties of steel (in comparison to timber), timber connections with damage-controlled capacity can also contribute to more predictable behaviours. This predictability can contribute to more reliable finite element simulations, even with basic material properties like the compressive and tensile strength of timber and steel.

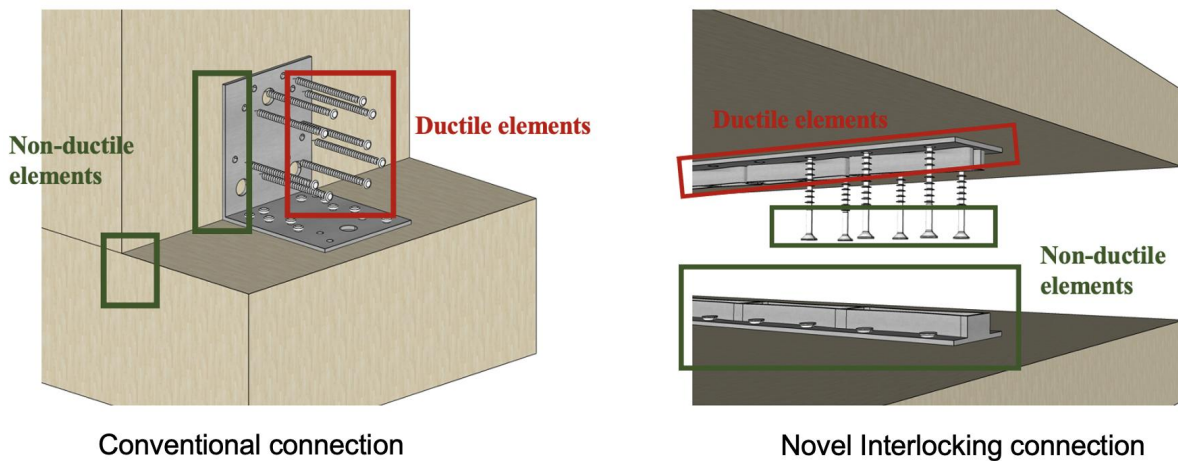


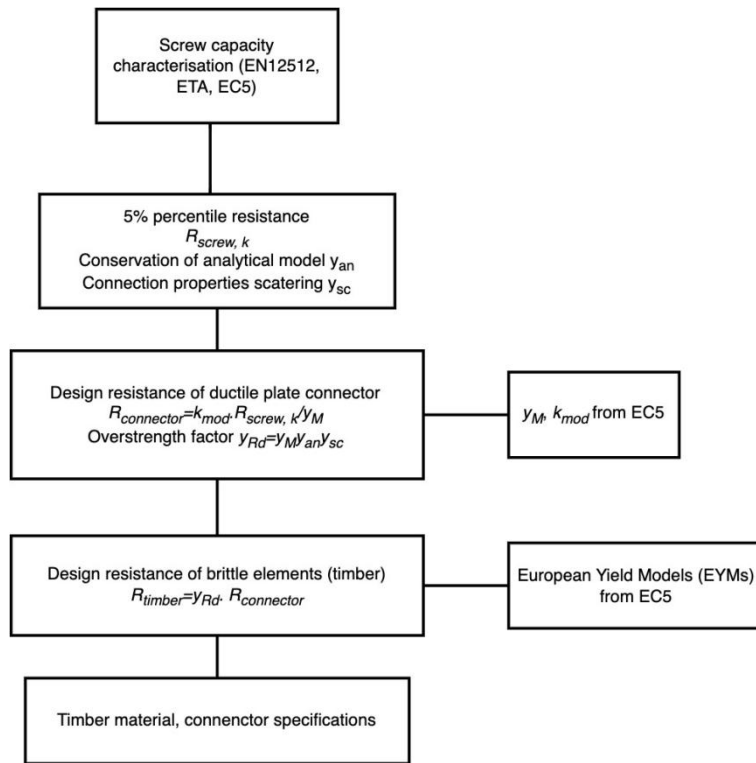
Figure 3.8. Capacity design strategies of conventional connection (left) and interlocking connection with damage-controlled capacity (right)

3.2.2 Capacity design process of interlocking connections with damage-controlled capacity

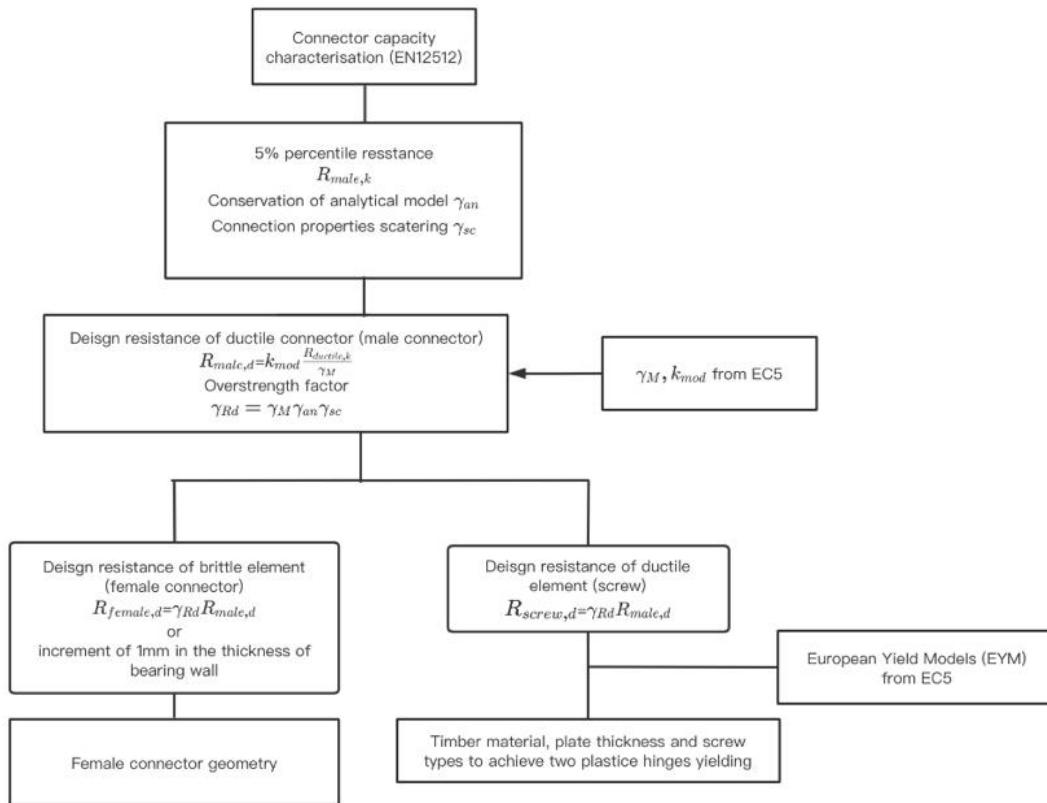
Conventional plate connections can be designed using the established analytical models in EC5, allowing for customisation of the connection configurations to meet the specific strength and ductility requirements of different projects. In these connections, screws are often employed as ductile elements and their design is guided by either experimental characterisation or calculations in accordance with EC5 guidelines. Subsequently, the dimensions of steel plate connectors and timber elements are determined based on these specifications, incorporating the use of overstrength factors (Figure 3.9.a). However, a notable challenge arises due to the absence of specific overstrength factors for timber connections within existing standards. As a result, the current practice for determining overstrength in timber connections often relies on a combination of sources: published experimental results, manufacturer recommendations, and realistic construction requirements. This approach, while practical, can lead to variations in the application of overstrength factors. Such variability underscores the need for more standardised guidelines in the design of timber connections, particularly in the context of overstrength application, to ensure consistency and reliability across different construction projects.

Contrary to the approach used in conventional systems, the connectors in the new system are designed as standardised and project-independent products. This design philosophy ensures broad applicability and consistency across various projects. The first step in the design process involves characterising the capacity of each male connector, which is conducted in accordance with EN12512. Following this characterisation, the design resistance of the male connectors becomes the basis for further design decisions. Subsequently, based on these

established design resistances and experimentally determined overstrength factors, the corresponding female connectors, screws, and timber panels are designed. This methodical approach ensures that all components are harmoniously integrated to facilitate the realisation of damage-controlled capacity (Figure 3.9.b).



(a)



(b)

Figure 3.9. Capacity design flow chart of (a) conventional plate connections and (b) novel interlocking connection

3.2.3 Geometric design of interlocking unit connectors

During the geometric design of the new connection system, the primary feature to be incorporated is the interlocking mechanism. Both tensile and shear connections in the new connection system are designed as two-components interlocking connections. These connections comprise female and male connectors, matched in shape as 3D components. The male connectors, serving as the ductile elements in both shear and tensile connections, are engineered to undergo controllable deformation, such as bending under tension. The female connectors, designed as groove-like devices, are primarily purposed to tightly accommodate the male connectors. To simplify the design process, the system is based on the concept of continuous connection achieved through the repetitive placement of unit connectors. So the connection design considerations were focused at the level of these unit connectors.

The dimensions for each unit were standardised at 100mm × 200mm, aligning with the dimensions of most currently available hold-downs and angle brackets and ensuring compatibility with existing construction practices. Additionally, the thickness of the bottom

plate in all connectors was determined based on common practices in double shear timber joints, where the steel plate thickness is typically set at half the diameter of the screws. This strategic choice not only provides sufficient strength but also aids in preventing localised steel plate deformation near the screw areas [3.36].

Version 1 – Metallic Mortise Tenon Connection

The first version of the interlocking connection design was inspired by the conventional mortise-tenon connections used in ancient timber buildings (Figure 3.10). Conventional mortise-tenon connections typically feature solid groove (Mortise) and teeth (Tenon) elements with matching shapes, enabling them to fit together seamlessly during assembly. Their design effectively transmits forces through the bearing surfaces of the connection elements, capitalising on the compressive strength of timber.

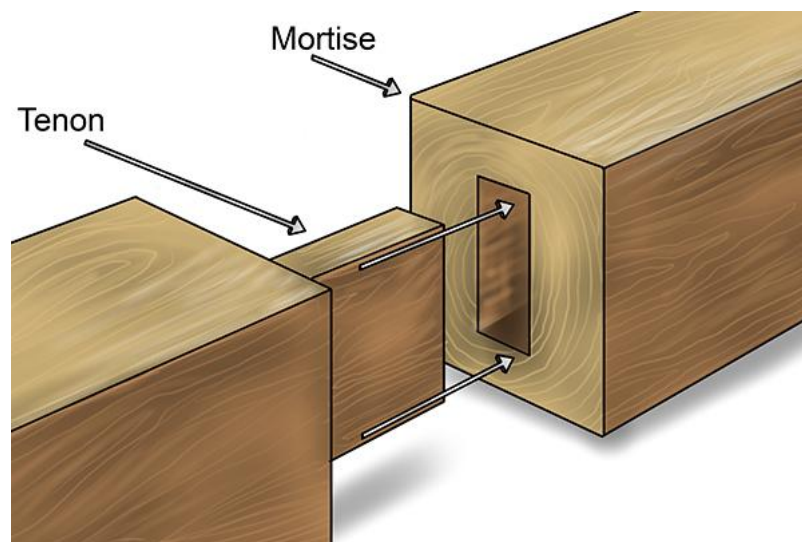


Figure 3.10. conventional mortise-tenon connections [3.10]

However, when considering the adaptation of this concept to metallic materials (Figure 3.11), certain limitations become evident. Mortise-tenon connections in metal may lead to excessive material usage due to the mode of load transmission, which occurs through the bearing of metal blocks. Consequently, 3D metal connectors demonstrate considerable strength, but this strength can impose the need for larger dimensions in CLT panels and screws. Such adjustments are necessary to achieve the intended ductile deformation and the desired damage-controlled capacity through the principles of capacity design.

Furthermore, the extensive use of metal in these connections can lead to increased overall weight and cost. These factors highlight the challenges in directly translating a design principle rooted in timber construction to metallic materials, thereby underscoring the need for careful consideration of material properties and design objectives in the development of new connection systems.

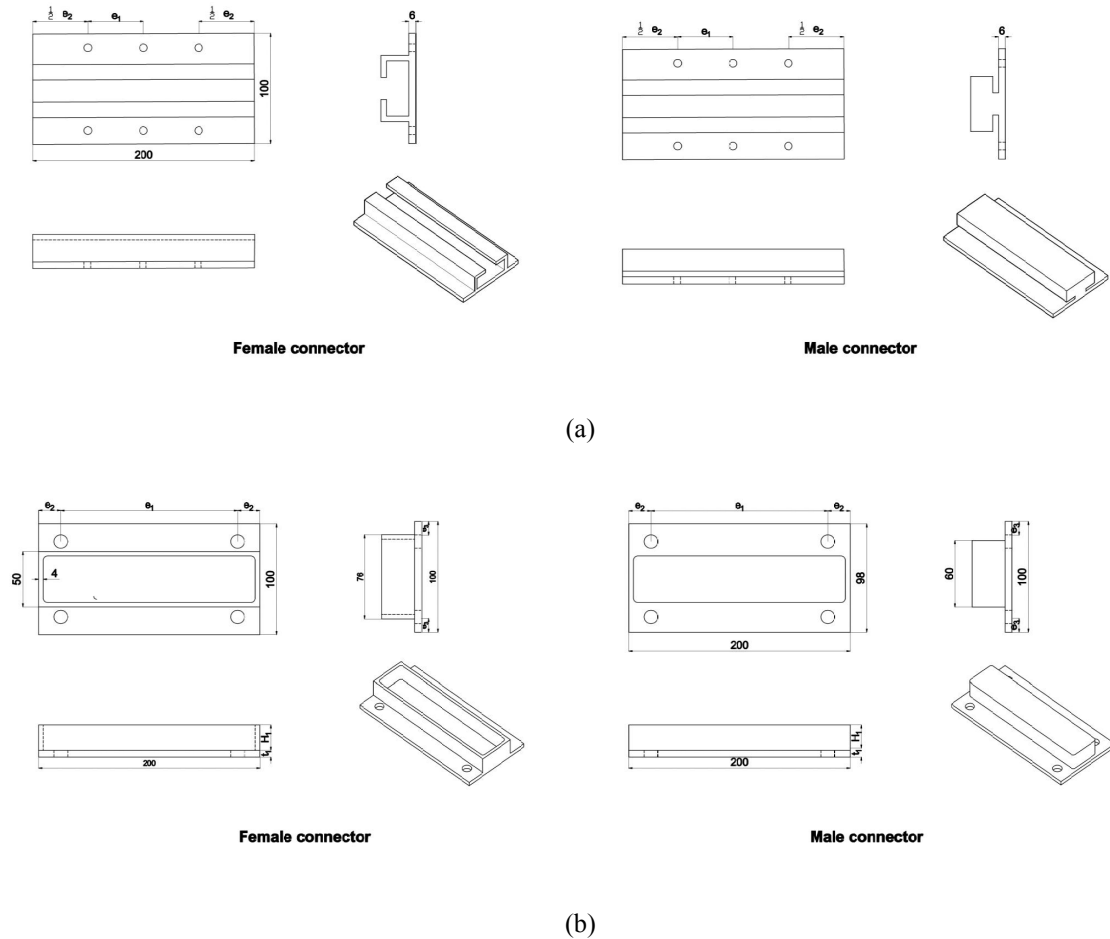


Figure 3.11. Schematisation the basic units of interlocking connection (in mm)-Version 1: (a) sliding tensile connection (b) stacking shear connection.

Version 2 – Novel Interlocking Metallic Connection

To optimise structural behaviours and material utilisation while preserving the interlocking effect, Version 1 of the interlocking shear and tensile connections underwent significant refinements. Adhering to the design strategy centred around a damage-controlled effect, the male connectors in both connection types were designated as the primary damage-controlling devices. These elements are intended to yield first, while the female connectors, timber, and fasteners are designed to remain mostly intact and perform elastically.

Therefore, a series of complex structural modifications were introduced in Version 2 connectors to shift the metal bearing in Version 1 to the more ductile metal bending. Then the female connectors were designed accordingly to accommodate the male connectors. By applying shape optimisation, significant volume reduction by 54.5% and 52% was achieved in the Version 2 of shear and tensile connections, respectively. Furthermore, in this iteration, the load transmission between connection components occurs via the bending of thin-walled steel elements, rather than compression on solid metal elements.

In the Version 2 shear connection (Figure 3.12.a), the male connector is constructed from a cantilevering, thin-walled curved steel band. This band is attached to a bottom steel plate via a cubic support located at the centre, which is specifically engineered to deform under movement. In the tensile male connector (Figure 3.12.b), two symmetrical L-shaped steel components are connected to the steel plate, separated by a 12 mm gap. This arrangement allows for their unrestricted (free to move) inward movement when sliding along the sloping walls of the female connector. The gap's width corresponds to the maximum potential horizontal movement of the L-shaped components within the female connector, ensuring effective functionality and deformation control. The design of the female connectors in both shear and tensile connections complements the shape of the male connectors, with the goal of minimising deformation. To achieve this, the female connectors are reinforced with larger thickness and rounded corners, enhancing their structural integrity.

In this way, the male connectors become the critical components that determine the strength and ductility in the interlocking connection. Moreover, as the ductility in this interlocking connection is designed to be achieved in the steel connectors instead of the fasteners, large diameter screws ($\varnothing 7\text{mm}$ - $\varnothing 14\text{mm}$) can be used in this connection system, in contrast to the common practice of using small diameter screws to ensure ductility. Previous literatures [3.8, 14] have suggested that this choice improves load distribution and helps mitigate the risk of in-service damage or brittle failure in timber.

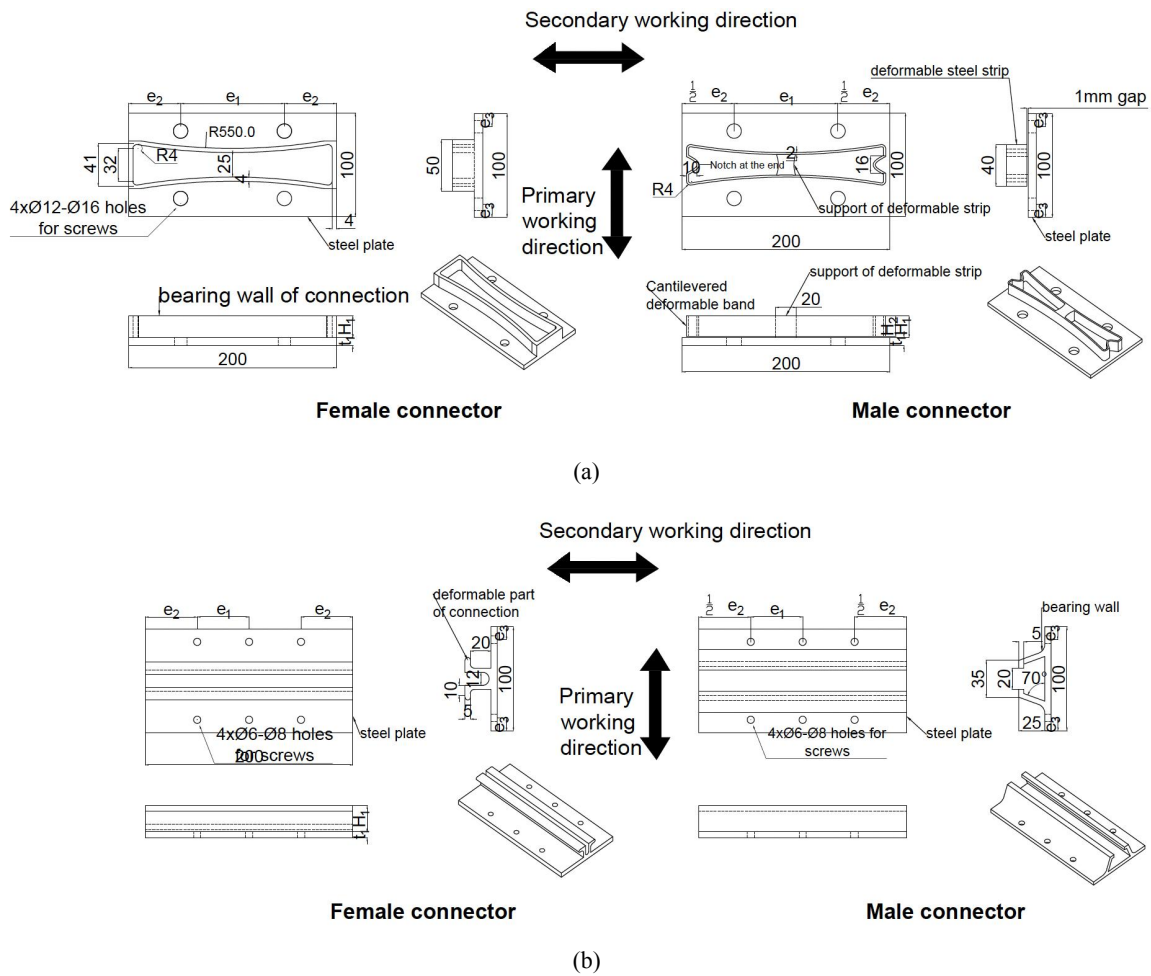


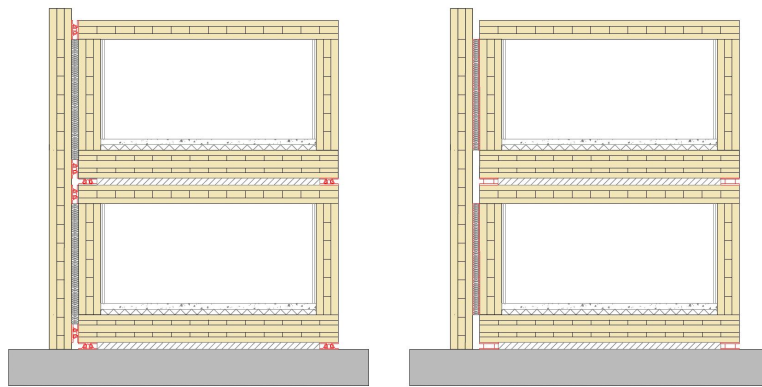
Figure 3.12. Schematisation the basic units of interlocking connection (in mm)-Version 2: (a) shear connection (b) tensile connection.

3.2.4 Prefabrication of the connection system

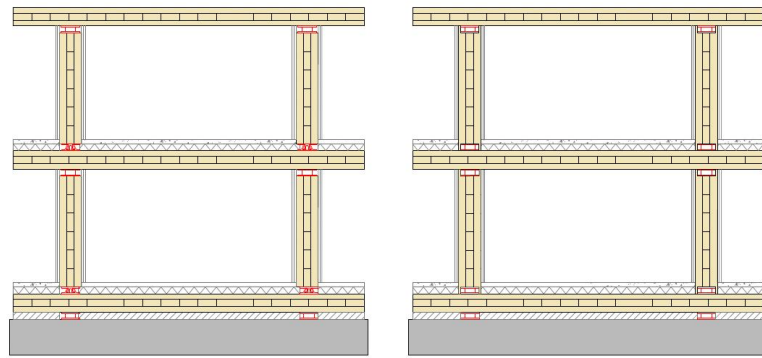
Being designed as a prefabricated connection system, the proposed system can be pre-attached to CLT panels or modules off-site, in a factory setting. This design choice prevents the need for modifications to the CLT, rendering the system compatible with a wide range of structural element specifications. This compatibility is achieved by simply adjusting the connector length, without necessitating geometrical modifications. Such a feature greatly simplifies and standardises the structural design process, transforming the system into a project-independent product with broad market applicability. Furthermore, once the project is completed, the interlocking connections are not visible from the interior of the flats and are protected from external environmental factors by the facade.

When using the interlocking connection, the reduced accessibility requirements in volumetric structure reduce the need for the gap between modules. In the case of CLTVC, the assembly of steel connection strips creates an approximate 40 mm gap between room modules. This gap can be filled by additional thermal and acoustic insulation, enhancing the living comfort within each compartment (Figure 3.13a). By filling this gap with insulation material that also possesses load-bearing capacity, a direct contact can be established between the wall and floor CLT panels and the structure beneath. This arrangement facilitates a larger area for load transmission to the underlying structure, potentially reducing the necessity for thicker floor panels. In contrast, conventional CLT volumetric structures typically require the extension of wall panels on the sides to create space for manually accessing connectors and services located in the ceiling (Figure 3.14 a), which is normally around 160 mm in current CLT volumetric structures for connection assembly. This design approach confines the floor panel to function in an edge-supported manner. Consequently, a greater thickness of the floor panel is required to provide adequate bending resistance.

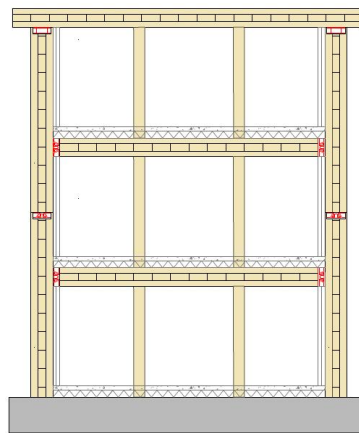
For Cross-Laminated Timber Platform Construction (CLTPC), it is essential that the connections are either sealed with insulation layers or concealed within grooves on the panel. This approach is critical to ensure fire resistance and air tightness of the structure (Figure 3.13.b and c).



(a)



(b)



(c)

Figure 3.13. Sectional views of connection within (a) CLT volumetric structure; (b) CLT panelised platform-type structure; (c) CLT panelised balloon-type structure.

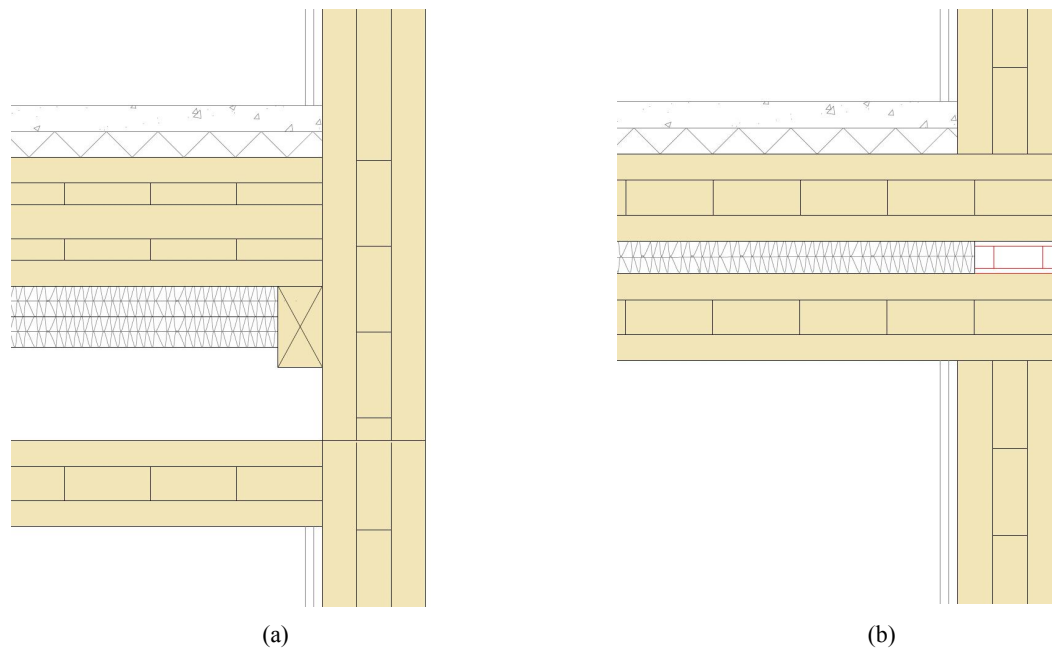


Figure 3.14. The joining details of (a) conventional CLT volumetric structures and (b) CLT volumetric structures with interlocking connections

The novel interlocking connection system and assembly technique were assessed through a scaled model, illustrated in Figure 3.15. This model utilised 3D-printed resin interlocking connectors, which were affixed to the edges of rectangular timber modules. Due to the precision of 3D printing at the employed dimensions, the scale for the connectors and modules was adjusted for clarity and precision rather than maintaining direct proportionality. The assembly initiated by precisely positioning the edge modules on either side, followed by placing the central module on top, which then interlocked with the sliding connections. The completed assembly exhibited significant stability, capable of withstanding vertical and lateral forces as a cohesive unit (Figure 3.16), with minimal movement between connections. These models demonstrated the successful integration of the interlocking connections, proving their primary feasibility for structural uses.



Figure 3.15. Illustrations of model installation and details of interlocking connections on timber modules.

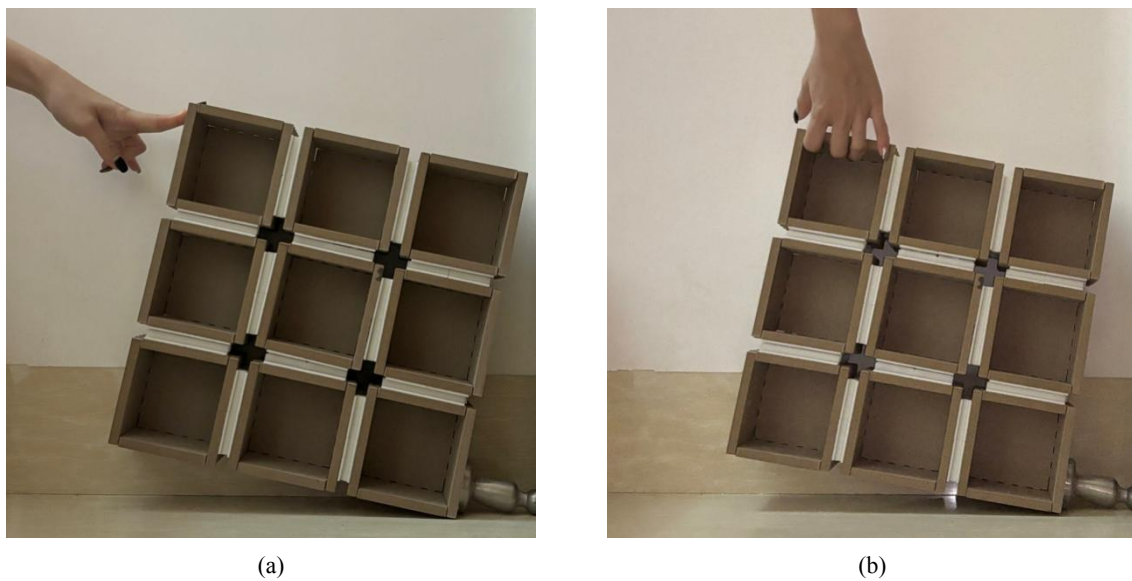


Figure 3.16. Interlocking connection-reinforced timber modules under (a) lateral and (b) vertical load.

3.4 Conclusions

The novel connection system designed herein for CLT modular construction integrate traditional interlocking techniques, featuring stacking shear and sliding tensile connections, representing a straightforward assembly approach that effectively eliminates the need for onsite fixing operations, meanwhile incorporates holistic design considerations as

summarised in Chapter 2. Therefore, this interlocking system offers multiple benefits for medium-rise CLT modular construction, as summarised in Table 3.1.

Table 3.1. Summary of design specifications of the interlocking connections

Characteristics	Corresponding solutions in the interlocking connection system
Structural Performance	
Planar capacity	Continuous shear and tensile reinforcement at structural edges for even load distribution.
Damage-controlled capacity	3D metal connectors designed for damage control, sparing screws and timber.
Constructability	
Locking mechanism	Direct connectivity achieved post-assembly without additional operations.
Module alignment	Self-aligning interlocking connections.
Access for connection installations	Interlocking technique eliminates the need for special access for installation.
Invisibility	Connectors concealed under walls or the exteriors of modules, preserving interior space.
Off-site installation	Pre-installation of connections on modules in the factory enhances accuracy and quality.
Fire resistance	Connections are less exposed to fire, protected by surrounding panels and insulation.
Maintenance, dismantlement and reuse	This impermanent connection provides easy dismantlement of modules at the end-of-service life without demolition, enabling direct reusability or recyclability.
Manufacturability	
Geometric complexity	Rather complex design that may bring difficulties in mass production
Standardisation	Standardised specifications for broad applicability without major geometry alterations on connectors.

Designed as a universal and project-independent connection system, the proposed connections offer immediate continuous reinforcement for a wide range of CLT structural element configurations in the market. At the end-of-life of buildings, structural elements can be dismantled without damaging the connections or structural materials, which reduces the waste and enables the further reuse of CLT.

In addition to the structural and construction benefits, this system can potentially contribute to better fire resistance (tests remain to prove it). The underlying principle for this potential benefit lies in the behaviours of timber when exposed to fire. As the timber surface chars, it forms a barrier that inhibits further combustion. This charring effect could play a crucial role in protecting the integrity of the steel connections, which are otherwise highly susceptible to

fire damage. Such a feature, if proven effective, would add a significant safety dimension to the system, further elevating its applicability and appeal in the construction industry.

Based on the connection DfR criteria as listed in Chapter 2, the DfR performance of the proposed connection can be summarised as in Table 3.2. It can be concluded that, the implementation of interlocking connections in building construction not only improves assembly efficiency but also offers significant benefits in terms of deconstruction, material reuse, and circulation compared to traditional demolition methods with conventional connections. Meanwhile, it fulfils some crucial criteria for developing adaptable connections, such as demountability, standardisation, individual removability and direct usability [3.7]. These characteristics facilitate individual removability and direct usability of the connections.

Table 3.2. DfR performance assessment of the interlocking connections

KPIs	Criteria	Connection performance	Weighing
Connection Type	Dry connections (e.g., click, magnetic, Velcro, self-locking connections etc.), which can be directly dismantled without damage	Building deconstruction can be executed through the direct separation of connection components, eliminating the need for working at height or onsite unscrewing/denailing	1.00
Connection Uniformity	Different connection types are adopted for shear and tensile connections, separately	The system comprises shear and tensile connections, each designed to provide reinforcement in a single direction	0.50
Connection Complexity	No modifications are needed	The connections can be directly attached to the surface of timber panels without cutting	1.00
Connection Standardisation	The connection is well standardised and widely adopted	Connections are compatible with a wide range of structural element specifications, facilitating easy standardisation and commercialisation.	1.00
Connection Prefabrication	Connections are precisely pre-attached to structural elements off-site, arriving on-site ready for assembly	Connections can be pre-screwed onto panels in the factories and be ready for direct assembly on-site	1.00
Connection Deformation	Deformation during the structure's service life does not damage the structural elements	In-service deformation is processed in the connection systems while preserving the integrity of structural components	1.00
Connection Accessibility	Accessibility with additional actions that do not cause damage (e.g., removing wall finish)	The connections are easily accessible by removing finishing	0.67
Ease of Disassembly	Crane required: >2,000kg	Complete structural components can be detached from buildings using interlocking connections, although heavy machinery may be required for their transportation	0.10

However, it is crucial to acknowledge that, the detachment of integrated components, while advantageous for deconstruction and reuse, necessitates the use of heavy machinery for lifting and transporting. This requirement can introduce additional logistical considerations and potential costs in the construction process. While promising features are presented in this conceptual connection design, it is also important to recognise that this system requires further work to validate its comprehensive applicability and efficiency in various contexts. While it offers features conducive to adaptable structures, its ability to accommodate unforeseen project changes during construction or potential functional modifications during a building's service life is subject to ongoing evaluation. Such modifications could include partial disposal or extension of buildings in response to the evolving needs of a rapidly developing society.

3.5 Chapter References

- [3.1] Wang, L. *Yingxian wooden tower comprehensive protection and research project*. 2011; Available from: <http://www.cach.org.cn/tabid/155/InfoID/514/frtid/119/Default.aspx>.
- [3.2] Karacabeyli, E. and Gagnon, S., *Canadian CLT Handbook*. Available from: <https://web.fpinnovations.ca/clt/>.
- [3.3] Sharafi, P., Mortazavi, M., Samali, B. and Ronagh, H., *Interlocking system for enhancing the integrity of multi-storey modular buildings*. *Automation in construction*, 2018. **85**: p. 263-272.
- [3.4] Di Pasquale, J., Innella, F. and Bai, Y., *Structural concept and solution for hybrid modular buildings with removable modules*. *Journal of architectural engineering*, 2020. **26**(3): p. 4020032.
- [3.5] Lacey, A.W., Chen, W., Hao, H. and Bi, K., *New interlocking inter-module connection for modular steel buildings: Experimental and numerical studies*. *Engineering structures*, 2019. **198**: p. 109465.
- [3.6] Dai, X.-M., Zong, L., Ding, Y. and Li, Z.-X., *Experimental study on seismic behavior of a novel plug-in self-lock joint for modular steel construction*. *Engineering structures*, 2019. **181**(C): p. 143-164.
- [3.7] Polastri, A., Giongo, I. and Piazza, M., *An innovative connection system for cross-laminated timber structures*. *Structural engineering international: Journal of the International Association for Bridge and Structural Engineering (IABSE)*, 2017. **27**(4): p. 502-511.
- [3.8] Benachio, G., Freitas, M.d.C. and Tavares, S., *Circular economy in the construction industry: A systematic literature review*. *Journal of cleaner production*, 2020. **260**: p. 121046.
- [3.9] Eurocode, *Eurocode 5: Design of timber structures*. 2004, European Committee for Standardization,.
- [3.10] *WOODWORKING - Joinery, what is a mortise and tenon?* 2018; Available from: <https://www.kaltimber.com/blog/joinery-what-is-a-mortise-and-tenon>.

Chapter 4 Laboratory Tests

To understand the structural behaviours of the proposed connection design and verify its feasibility, this chapter presents a comprehensive series of laboratory tests. The conducted experiments included both monotonic and cyclic tests, targeting the primary working direction of the interlocking shear and tensile connections. Additionally, this chapter introduces the supplemental testing conducted on crucial components of the connection system, aiming to assess their individual contributions to the overall connection performance. Notably, it discusses the detailed examination of screws employed in conjunction with the interlocking connections. Furthermore, the chapter addresses the evaluation of connection materials, with a specific focus on those fabricated through 3D printing technology, providing critical insights for the development of numerical connection model.

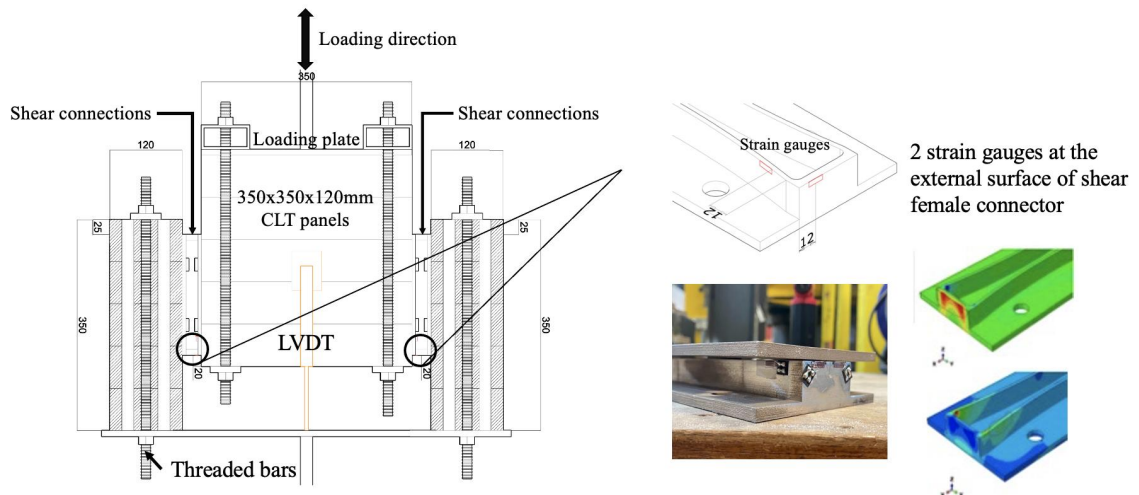
4.1 Testing Configurations and Loading Process

The experimental setups adopted in this study to test the interlocking shear and tensile connections are illustrated in Figure 4.1. Given the constraints of budget and time, the tests focused on unit connections that exhibit representative behaviours to the continuous version of the newly developed connections. The experimental campaign involved applying different loading cases to these tensile and shear connections, reflecting their operational conditions within a timber modular structure. For the shear (stacking) connection located on the bottom of middle modules in a volumetric building, typically situated at the bottom of middle modules in volumetric buildings and primarily subjected to pure shear forces, a push-out test was employed. Conversely, for the tensile (sliding) connections, which are designed to counter uplifting forces at the edges of modules, a pull-out test was conducted. This method effectively simulates the loading conditions these connections would encounter in practical applications.

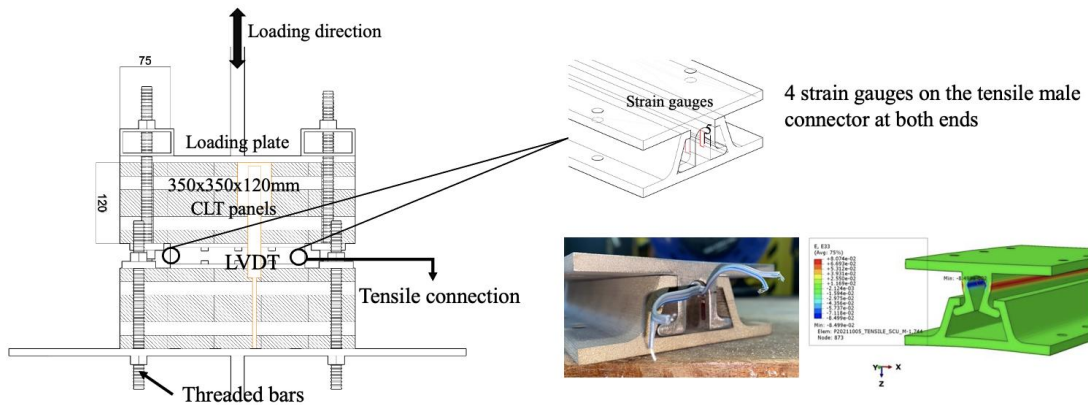
A key aspect of the shear connection testing was the adoption of a symmetrical testing arrangement (Figure 4.1. a&c) that are crucial for preventing the application of a moment to the testing apparatus, which could lead to instability. This setup requires the simultaneous testing of two shear connections using three panels. The outer panels, each featuring female connectors on their surfaces, were seated on steel plates and directly connected to the machine base by threaded steel bars and steel plates. The middle panel, equipped with male connectors on both sides, was firmly attached to the hydraulic jack through a steel plate to

evenly apply loads onto the CLT panels. As the displacement-controlled loading was applied on this panel, it was strategically positioned 150 mm away from the machine's working platform, ensuring sufficient space on loading direction to accommodate any unforeseen movement of the connections post-failure (Figure 4.6). The loading direction for the shear connectors was aligned parallel to the outer grain of the CLT panels. Each shear connector was strategically placed 25 mm from the edge of the panels, a measure taken to avoid potential failure in the unloaded side, ensuring the reliability and accuracy of the shear connection testing.

Different from the shear connections, each tensile connection was centrally positioned within the panels and tested individually, with the load direction oriented perpendicular to the outer grain direction of the panels (Figure 4.1 b&d). This configuration required only two panels for each tensile test. In this configuration, the lower panel, positioned on the machine, was equipped with the female connector and fixed to the machine via steel bars and plates. The load was then applied to the upper panel, which housed the corresponding male connector. This force was uniformly transmitted through a steel plate that was firmly attached to the hydraulic jack, ensuring a clear assessment of connection's performance under tensile stress.



(a)



(b)



(c)



(d)

Figure 4.1. Experimental set-ups for (a)&(c) interlocking shear connection and (b)&(d) tensile connection

The measurement system employed in the testing of the connections comprised Linear Variable Differential Transformers (LVDTs) and Strain gauges. LVDTs were employed to accurately gauge the relative slip between the panels and the securely affixed steel plate. Strain gauges were utilised to record the surface strain on the connections, which was important for assessing the stress distribution and deformation characteristics of the connections under various loading conditions. The strain measurements were synchronised with the analogic signals (load and displacement) from the INSTRON® load cell and LVDT. The strain responses were captured using CR3000 data logger connected to a laptop utilising a pre-installed Signal Express software. Due to the limited channel number of data logger, four strain gauges were affixed to the specimens in each test. The positioning of these gauges was strategically determined based on stress concentration points identified through preliminary numerical simulations, along with the considerations in accessibility of the measuring points on the assembled connections (Figure 4.1).

In the interlocking connection testing, a total of three monotonic tests (using three specimens) were performed on the tensile connection, while only one (using two specimens) was conducted on the shear connection, all at a rate of 0.05 mm/s. Additionally, two cyclic tests (using two specimens) were carried out on the tensile connection, and one (using two specimens) was performed on the shear connection, with a loading rate of 0.02 mm/s. The loading procedure used for both the push-out and pull-out monotonic tests is illustrated in Figure 4.2.a. Initially, the load was gradually increased from 0 to 40% of the estimated ultimate load f_u for the specimen in 120 seconds. It was then maintained at a consistent level for 30 seconds. Following this, an unloading phase was applied to reduce the load from 40% to 10% of f_u . This lower level was sustained for an additional 30 seconds, after which the secondary loading phase was initiated. The test was then conducted under a load-controlled regime, reaching up to 70% of f_u before switching to displacement control until the specimen failure. The limit of $0.4f_u$ during the first unloading/reloading cycle and the $0.7f_u$ limit for transitioning from load control to displacement control align with the serviceability limit state (SLS) and ultimate limit state (ULS) loading conditions, respectively, as specified in European standards (EN) for timber structures.

The quasi-static (cyclic) test for both connections was carried out in accordance with the EN12512 [4.1] (Figure 4.2.b). The testing involved multiple cycles, each defined by specific

loading magnitudes based on the estimated yield points V_{est} . These yield points were set at 4 mm for tensile connections and 2 mm for shear connections, based on initial findings from FE simulations. In the initial cycle for shear connection testing, each specimen was subjected to a tension displacement of 0.5 mm (25% V_{est}), unloaded, and then reloaded to 0 mm slip. This process involved loading the connection to this displacement, followed by unloading to 0 mm slip and then loading in the opposite direction up to 0.5 mm before returning to zero slip. The subsequent second cycle involved the similar loading process but with an increased displacement of 1 mm (50% V_{est}). The third to seventeenth cycles comprised sets of three cycles each, with gradually increased displacement: 1.5 mm (75% V_{est}), 2 mm (100% V_{est}), 4 mm (200% V_{est}), 8 mm (400% V_{est}), and 12 mm (600% V_{est}), followed by unloading and reloading to 0 mm slip, repeated three times per set. The tensile connections underwent a similar cyclic testing regime, while the displacement during testing was applied in only one direction.

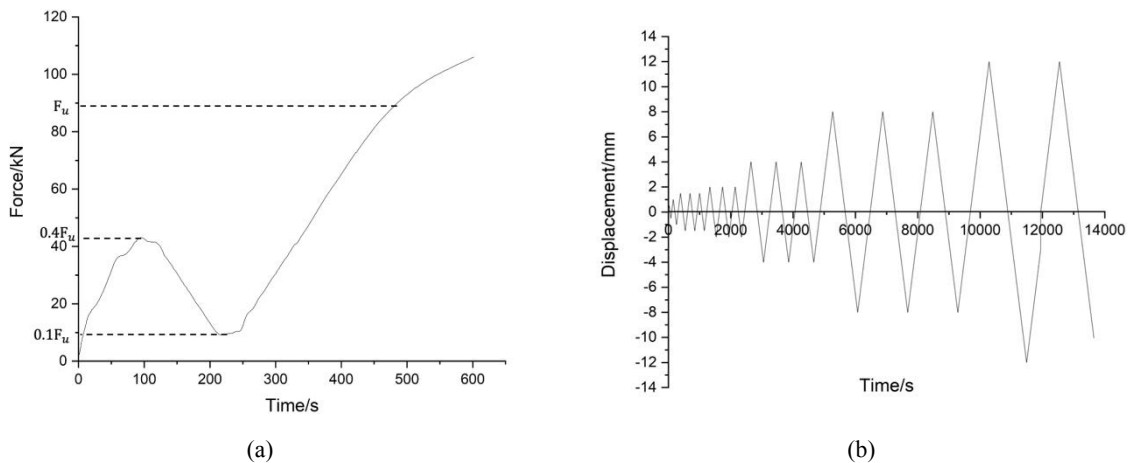


Figure 4.2. Loading profiles employed in (a) monotonic test and (b) cyclic test

4.2 Testing Material Preparation

The CLT panels adopted in the testing were 5-ply or 3-ply GL24h 350mmx350mmx120 mm CLT panels supplied by Stora Enso without any modifications (Figure 4.1). These CLT panels consist of layers with thicknesses of 20 mm, 20 mm - 40 mm - 20 mm - 20 mm for 5-ply panels and 40 mm - 40 mm - 40 mm for 3-ply panels. Therefore, 5-ply and 3-ply panels have the same cumulative thickness in the direction parallel to and perpendicular to the surface grain, which can be considered to have very similar load-carrying capacity. To comply with EN 1380, all the timber panels were conditioned in a controlled environment

using a cyclic corrosion chamber (CC ip 1000L) (Figure 4.3) at a temperature of 20°C and 65% humidity for a duration of two weeks before testing. After being conditioned, the moisture content of all panels measured as prescribed in EN 322 or EN 13183 using pin-type electronic moisture meter, which all achieved within the range of 10% to 10.8%, falling within the specified requirements of the standard (10% to 14%). According to EN 323, the density and geometric information of each connection specimen were also be recorded before testing. The tested CLT panels had density ranged from 435 to 470kg/m³ and an average density of 448.8 kg/m³.

Table 4.1. Material properties for CLT panels (spruce) [2]

Elastic modulus (MPa)			Poisson's ratio			Shear modulus (MPa)		
E_{11}	E_{22}	E_{33}	ν_{12}	ν_{13}	ν_{23}	G_{12}	G_{13}	G_{23}
11000	370	370	0.48	0.48	0.22	690	690	50
Parallel-to-grain (MPa)		Perpendicular-to-grain (MPa)			Shear strength (MPa)			
f_{c11}	f_{t11}	f_{c22}	f_{t22}	f_v	$f_{v,roll}$			
36	24	4.3	0.7	6.9	0.5			



Figure 4.3. Conditioning of CLT panels before testing



Figure 4.4. Marked position for connection and predrilling on panels

Prior to the testing, all connection specimens were affixed to the surface of panels without modifications. The initial positions of the specimens on the timber panels were clearly marked (Figure 4.4) for measurement of the relative movement between the timber and the steel connectors. The fastening screws selected were LBS7100 for tensile connections and HBSP12120 for shear connections (Figure 4.5). The quantity and types of screws were determined through capacity design, as explained in Chapter 2, to ensure deformation localisation in metal connectors during the experiment.

Both the location of connections and the spacing of screws within the connection were designed adhering to the specifications in Table 8.5 in EC5 [4.3] (Figure 4.6). The specific properties of screws detailed in the manufacturer's product brochure (Table 4.2) [4.4]. Considering the dimensions of screws used in the test, timber panels were predrilled with a diameter of 7 mm and a length of 75 mm for HBSP12120, and with a diameter of 4 mm and a length of 50 mm for LBS7100 at the locations of screws, to guide the screws into timber panels without splitting and cracking. Following the screwing process onto the CLT panels, the connection specimens were assembled by either stacking (shear connection) or sliding (tensile connection) to form the experimental set-up. No supplementary reinforcement was utilised during testing, apart from the self-locking of connectors. The mechanical and geometric characteristics of the panels and screws can be found in Figure 4.1 and Figure 4.2 respectively.

a

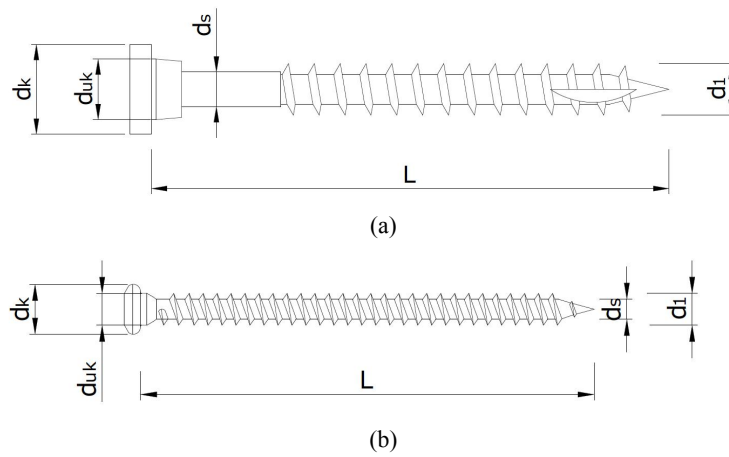


Figure 4.5. Dimensions of screws: (a) HBSP12120 (b) LBS7100

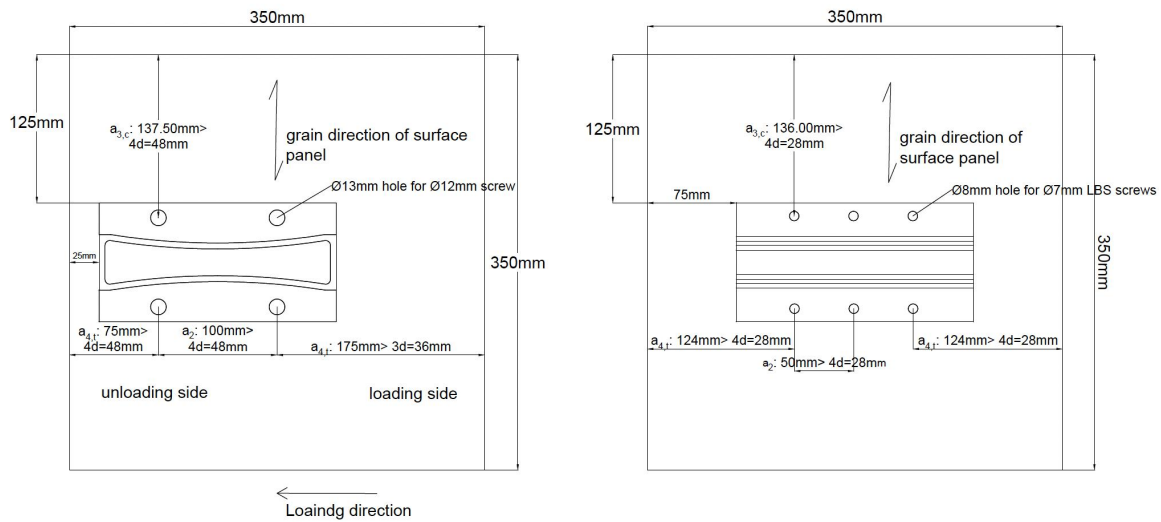


Figure 4.6. Locations of shear connectors (left) and tensile connector (right) on CLT panels.

Table 4.2. Dimensions of screws used in experiment (in mm)

	L	d_1	d_s	d_k	d_{uk}	Characteristic shear strength $R_{v,k}$ (kN)	Characteristic tensile strength $R_{ax,k}$ (kN)
HBSP12120	120	12	8	20.75	14	8.19	13.64
LBS7100	100	7	4.4	11	7	4.87	8.40

The fabrication of the proposed 3D connector using conventional manufacturing methods is potentially achievable but with diverse processes. According to the British steel manufacturer SC4 Ltd., the cantilevering curved steel band and the central support in the shear male connector can be produced separately from 3D formed strips, and subsequently weld together to the drilled base plate. For the tensile connectors, a more streamlined approach could be

employed, involving the use of specially hot-rolled sections cut to the desired length, ensuring continuous sections along their length. Consequently, the conventional manufacturing process is somewhat complicated and requires a substantial order quantity. Such requirements were not compatible with the limited time and budget constraints of the planned experiment.

Considering the high manufacturing accuracy required for connector fitting and the limited number of connection specimens required for the experimental programme, additive manufacturing (AM) was chosen to produce prototypes of the new connectors due to its versatile fabrication capabilities. AM as one of the most advanced manufacturing methods, allows new ideas to develop in terms of material and geometry while designing high-performance connections [4.5]. This technology is particularly advantageous in fabricating unique geometric features integral to the proposed connections, such as inclined and curved surfaces, and cantilevered thin-walled structures. Unlike traditional methods that often require moulding or multiple stages of assembly, AM can produce these complex forms in a single, seamless process. This capability not only ensures adherence to the required dimensional accuracy but also considerably reduces the production time for the testing specimens.

Among the available 3D printing options for the size of the specimens, Binder Jetting and Wire and Arc Additive Manufacturing (WAAM) were considered. Binder Jetting is a powder-based procedure, in which metal powder is selectively deposited layer by layer and bonded by a liquid agent to form the 3D projects. After sintering and infiltration with a secondary material such as bronze and copper, the Binder Jetted material can be considered as homogenous material [4.6]. This printing technique offers several advantages over other systems, including a larger build volume and reduced dimensional distortion related to thermal effects. WAAM, on the other hand, is the melting process involves feeding a wire electrode into a molten pool, which is used to fuse the wire onto the substrate. While WAAM has better capacity In producing large metal elements with high deposition rates, it has relatively poorer surface finish and dimensional accuracy than Binder Jetting [4.7], which might create difficulty in the fitting of connectors. Although the surface roughness could be improved by coupled processes integrating WAAM and laser polishing or high-pressure rolling [4.6, 4.8], such methods also result in increased production time and cost. In addition, the interlocking shear connector can only be printed in a hybrid manner with WAAM, as the

cantilevered elements should be printed separately and weld to the bottom plate. Therefore, Binder Jetting technology was eventually adopted for the specimen production. Considering the required strength and resistance for testing, a metallic alloy composed of 60% 420 Stainless Steel as base material and 40% Bronze for enhanced strength and resistance was selected, using Binder Jetting with layer thickness of 100 μ m provided by Sculpteo (France).

To minimise potential deformations and ensure the stability in the cantilevered parts in both connections during printing, the orientation of the printing was aligned parallel to the length of the unit connectors. However, a notable challenge with Binder Jetting, the chosen printing method, is its inherent shrinkage phenomenon during the sintering process. This shrinkage tends to be less predictable and measurable compared to other printing techniques, such as Direct Metal Laser Sintering (DMLS). Such unpredictability in dimensional changes can lead to fitting issues caused by dimensional distortions of the printed objects, then eventually cause assembly difficulty of interlocking connections studied in this project. Typically, this issue is addressed by applying pre-determined scale factors to the object dimensions before printing, thereby compensating for the anticipated shrinkage.

In this study, the potential fitting issue arising from dimensional distortion during 3D printing was mitigated by introducing a clearance gap between the male and female connectors. The specifications of male connectors remained the same as in (Figure 3.12) for both connections, while the dimensions of female connectors were adjusted before printing to allow for 0mm, 0.5 mm and 1 mm clearance between the male connectors and the female connectors. Despite the high manufacturing accuracy of 3D printing, it was found that 1 mm tolerance was the most suitable for the connection fitting in this study. Male connectors were found to be challenging to fit into female connectors designed with 0 or 0.5 mm tolerances, often necessitating milling of the female connectors, indicating the dimensional distortion occurred during printing. To minimise the impact of manufacturing tolerances on experimental results, specific measures were taken during the testing phase. In the testing of tensile connections, the remaining gap between components after assembly was eliminated using the built-in function in the loading machine, ensuring contact between the two connectors before the testing started. However, in the cyclic testing of shear connections, due to the reserve loading, complete elimination of gaps was not achievable. As a result, a small amount of initial sliding without corresponding reaction force was observed at the beginning of each loading step during the cyclic testing of shear connections.

As surface polishing was not available for the size of specimens from the manufacturer, the printed connections were left with a granular finish (Figure 4.7). To eliminate unpredictable behaviour caused by friction variations during the movement of male connections within female connections, the contact surfaces and strain gauge locations were carefully polished to achieve smooth surfaces before testing (Figure 4.8). The size of polished specimens in different areas was regularly recorded during the polishing to control size reduction, ensure dimensional consistency, and avoid creating unexpected weak spots or introducing potential asymmetrical behaviours in the connectors.

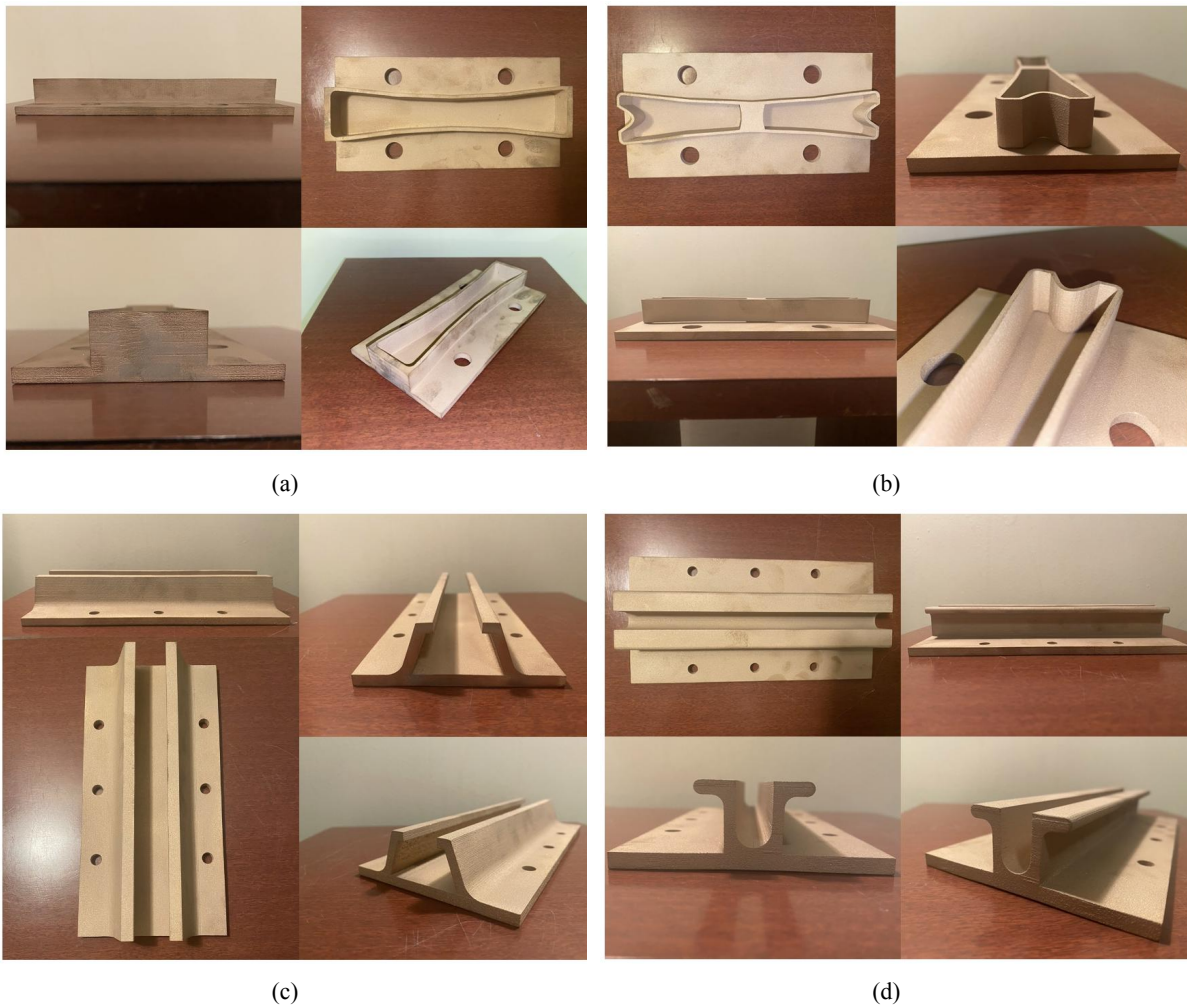


Figure 4.7. 3D printed connection specimens: (a) shear female connector; (b) shear male connector; (c) tensile female connector; (d) tensile male connector



Figure 4.8. Unpolished and polished (a) shear connector and (b) tensile connector

4.3 3D Printed Steel Material Property Characterisation - Coupon Test

To determine the tensile engineering stress-strain properties of the 3D printed SS420/BR material and support numerical validation, additional tensile coupon tests were conducted following the guidelines of EN ISO 6892-1 [4.9] (Figure 4.9). Four coupons were machined from the bottom plates of the previously tested tensile female connectors (Figure 4.10 (b)), which exhibited minimal deformation during testing. The specimens were tested in the direction parallel to the printing direction with a constant speed of 3 mm/min using an Instron testing machine. Prior to testing, the extensometer was attached to the surface of the coupons for accurately measuring the strain.

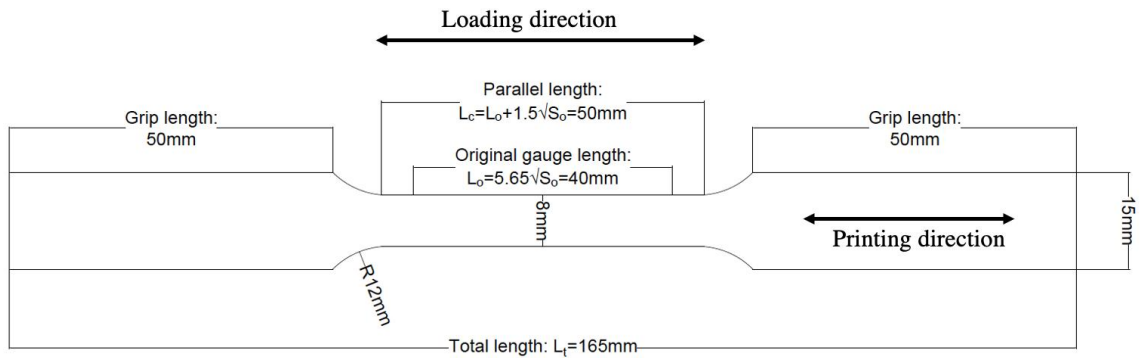


Figure 4.9. Coupon dimensions determined by EN ISO 6892-1 [9]



(a)



(b)



(c)

Figure 4.10. Coupon test of SS420/BR (a) testing set-up for coupon test (b) coupons specimens machined from the bottom plate of the tested connectors (c) tested specimens

The initial strain and stress data obtained from the coupon tests were converted into true stress and strain, followed by the calculation of the yield strength using the 0.2% offset method. The data exhibited relatively consistent values with an acceptable variation between specimens (Figure 4.11), so the averaged properties from the four coupon tests were selected for use in the subsequent numerical study. To ensure the feasibility of the test results, comparative analysis was performed between the material properties provided by the manufacturer [4.6] and the published coupon test data of SS420 [4.10] that conducted under the same printing layer thickness and printing direction. The mean values adopted for simulation showed similarities in terms of Young's modulus and ultimate strain. However, there were variations observed in the yield strength and ultimate strength. These differences can be attributed to the sensitivity of the 3D printing material to various printing parameters, such as travel speed and sintering temperature, which may vary among different manufacturers and printing machines.

Table 4.3. Material properties of SS420 3D printed coupons

Specimen No.	Elastic Modulus (GPa)	Yield Strength (MPa)	Ultimate Strength (MPa)	Elongation
1	96.3	283	606.5	7.50%
2	138.6	285	640	5.40%
3	183.6	315	680	5.54%
4	101	332	627	5.23%
Sculpteo Datasheet	147	427	496	7.00%
Published Literature	134.2	249.9	737.3	2.70%

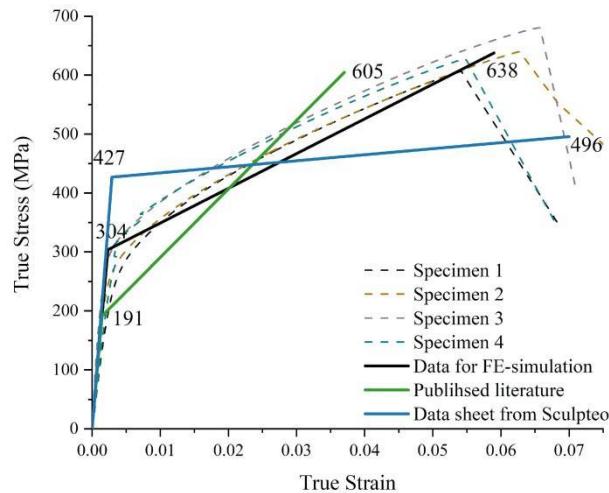


Figure 4.11. Experimental data of coupon test and the mean material properties used as input data in simulation

It is noteworthy that 3D printed materials exhibit different mechanical behaviours in the directions perpendicular to and parallel to the printing direction. However, the observed variations in these two directions are relatively small, ranging from approximately 2% to 4%. Based on the published experimental data [4.10], which corresponds to the same 3D printed material used in this research with an identical printing layer thickness, the most substantial difference in properties between the directions parallel and perpendicular to the printing direction is 2.1% in terms of ultimate strength. Therefore, it can be concluded that this disparity would have negligible impact on the results, and the material properties obtained from the coupon specimens printed in the designated direction can effectively represent the material's performance in different orientations.

4.4 Outline of Screw Testing

To gain deeper insights into the connection behaviours and contribute to capacity design, monotonic push-out and pull-out tests were also conducted on screws in the form of steel-timber composite (STC) connections for strength verification. A total of twelve tests were performed on both shear and tensile screws, with eight being new screws and four being

extracted from previously tested interlocking connector specimens. This supplementary experiment had the following objectives: (1) to determine the realistic characteristics of the screws employed with the interlocking connections and to validate the accuracy of the adopted modelling methods; (2) to compare the strength and deformation in the conventional STC connections with those in the proposed interlocking connections to illustrate the damage-controlled capacity; (3) to compare the load-carrying capacity of the used/unused screws for evaluating the potential impact of previous interlocking connector failure on the screws' mechanical performance. However, due to limitations in the availability of screws during the testing period, achieving a like-to-like configuration in STC connections matching the screw layout of unit connectors was unfeasible. Therefore, the STC connections were designed to have similar shear plane conditions to the screws in interlocking connections to ensure the feasibility of comparison.

4.4.1 Test set-up

For the push-out testing of shear screws (HBSP12120), a symmetric timber-steel-timber arrangement, as depicted in Figure 4.12, was utilised to achieve a uniform load distribution and predictable friction effects on the force-displacement results. Two LVDTs were employed on both sides of the set-up to measure the relative displacement between the steel profile and timber panels. The LVDTs were positioned on the CLT panels, with their bases attached to the steel profile. The steel profile used as the loading device in the push-out test was a hot-rolled Grade-S355JO steel universal beam with dimensions of 254×102×22, with no coating or painting. To align with the shear plane conditions of screws within the shear interlocking connectors, the flange thickness of the beam was adjusted to match the thickness of the connector's bottom plate (6mm). Four holes with diameter of 15 mm were drilled into the universal beam to provide adequate tolerance for screw installations. On each flange side, two screws were affixed, spaced at 78 mm from one another, aligning with the screw arrangement in the shear interlocking connections. So, four HBSP12120 screws were tested simultaneously in each push-out test.

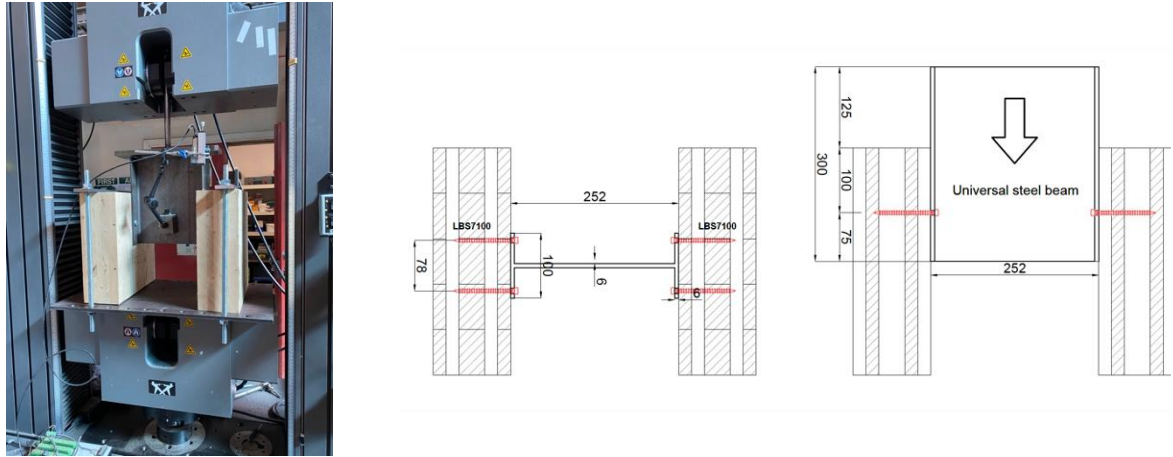


Figure 4.12. Geometry, cross-section, and details of in push-out test on HBSP12120

In the pull-out testing of tensile screws (LBS7100) (Figure 4.13), only one screw was tested in each test. The screws were connected to the middle of CLT using a steel holding device with a thickness of 6mm, corresponding to the thickness of interlocking tensile connector. The displacement of screws was recorded directly by the INSTRON® load cell.

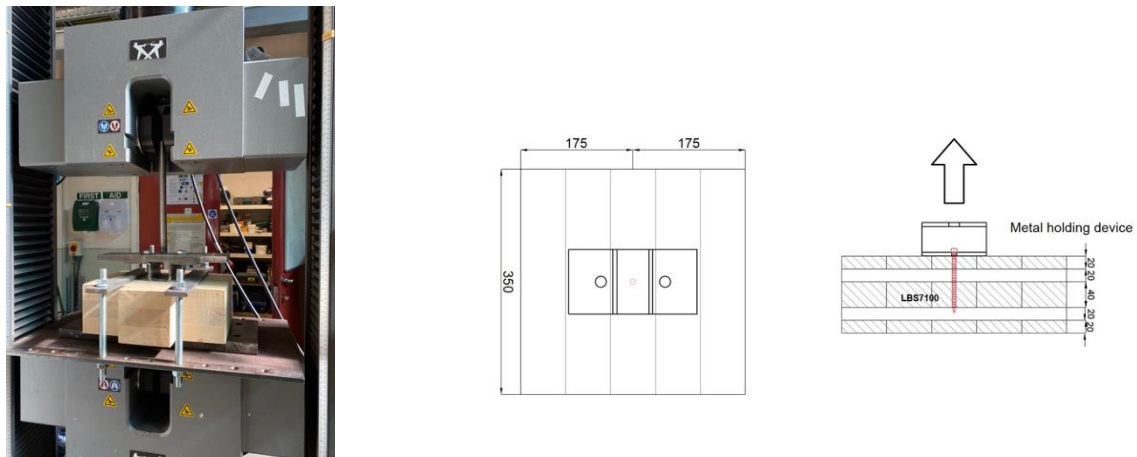


Figure 4.13. Geometry, cross-section, and details of pull-out test on LBS7100

The screw testing employed identical predrilling diameter and length as the previous tests on metal interlocking connectors. The loading scheme from EN12512 (Figure 4.2) was also applied in the screw testing. The adjustments to the estimated ultimate strength f_u of the tested screws was first made based on the calculation following EC5 [4.3]. Subsequently, the value of f_u for the subsequent test was modified in accordance with the first test result, leading to a redefinition of the loading procedure.

4.4.2 Screw testing results

The characterisation of the monotonic load-displacement responses of screws in this study was in accordance with EN 26891 [4.11] and EN 12512 [4.1] (Figure 4.14). The instantaneous elastic stiffness of the connection (K_{ser}), is defined as the slope of the line drawn through 10%-40% f_{max} . As outlined in EN 12512 [4.1] (Figure 4.14), the plastic stiffness (K_{pl}) can be defined in two ways: (1) when the load displacement curve exhibits two distinct linear segments, K_{pl} is defined as the slope of the plastic displacement; (2) in the case similar to those investigated in this study, where no clearly defined linear segment exists, K_{pl} may be defined as a tangent line to the curve with a slope calculated by $K_{ser}/6$. The intersection between lines with K_{ser} and K_{pl} represents the yield load (F_y) and yield displacement (V_y). The ultimate displacement (V_u) and the corresponding ultimate load (F_u) are determined based on earliest occurring condition: either the displacement at failure, the displacement corresponding to 80% of the maximum load, or the limiting ultimate failure displacement of 30 mm. The connection ductility factor D is defined as the ratio between the ultimate displacement and the yield displacement: $D=V_u/V_y$.

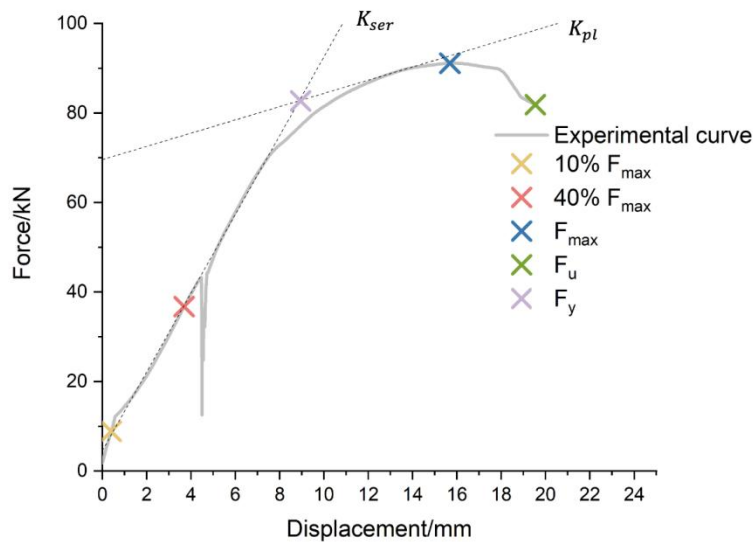


Figure 4.14. Typical connection behaviours when applying EN 26891 [4.11]

As illustrated in Figure 4.15, the force-displacement response of shear STC connections can be classified into four stages. The force-displacement curves started with a zone with non-slip when force increased, which is due to the friction between steel beam and timber. As the applied load exceeded the friction (normally at $0.1 f_{max}$) and the steel beam commenced

sliding relative to the timber, causing the screws to start bearing the load, the curve transitioned into the consolidation stage. At this stage, the stiffness of connection was lower than the elastic stiffness. This can be attributed to the damaged timber around the screw threads resulting from the predrilling and screwing process. The displacement involves with consolidation stage was measured as 3.5mm, aligns with the length of the screw threaded part (2.6mm), validating the stiffness reduction attributed to the thread insertion into the timber. While this phenomenon is particularly pronounced in dowel-type fasteners with smooth surfaces, its impact can be evaluated by various optimal surface measurement methods [4.12, 4.13]. It is commonly disregarded when evaluating the mechanical properties of screwed connection, by taking the elastic modulus from the 10%-40% load range [4.13]. When the screws continued to deform and reached the undamaged timber, the resistance of STC increased notably and reached the elastic stage. After a certain level of plasticisation, the majority of the test was terminated by the shear-offs of the screw head (Figure 4.15). Additional deformation modes such as bending in screws and ductile crushing in timber with the width equals to screw diameter and the length equals to displacement applied in test, were also identified. These deformation modes did not result in any cutting-through in timber fibre, attributed to the usage of large screws.

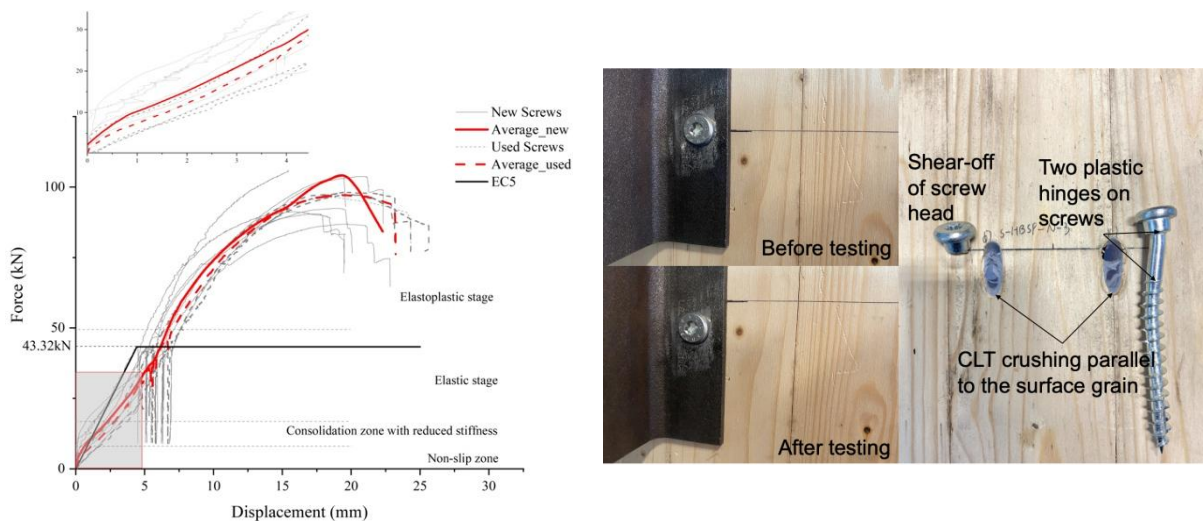


Figure 4.15. Force-displacement (left) and deformation response (right) of the new and the used HBSP12120

As seen in Figure 4.16, the load-displacement behaviour of tensile screws in pulling-out test was rather straightforward, which was mostly linear elastic until the yield load was reached. After achieving the maximum load, sudden decrease was observed in load until ultimate failure, which was due to the debonding between screws and timber.

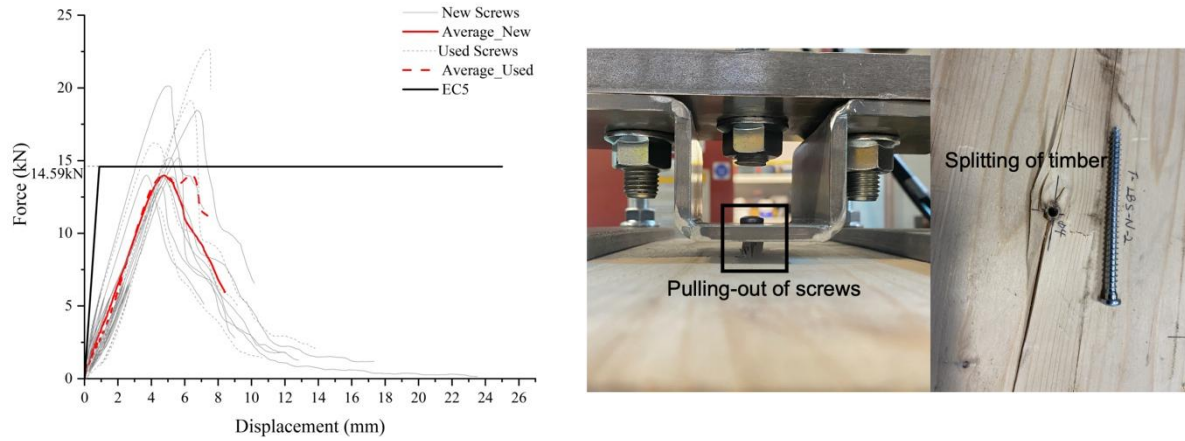


Figure 4.16. Force-displacement (left) and deformation response (right) of the new and the used LBS7100

Table 4.4. Key test results (mean values) obtained for both shear and tensile testing (EN26891)

	S-HBSP12120 new, n=8	S-HBSP12120 used, n=4	T-LBS7100 -new, n=8	T-LBS710 used, n=4
f_{max} (kN)	96.39 (8.2%)	97.31 (0.8%)	15.50 (16.1%)	17.58 (25.1%)
f_u (kN)	81.09 (15.6%)	81.01 (8.0%)	12.40 (16.1%)	14.50 (29.3%)
V_u (mm)	19.62 (15.5%)	24.84 (2.8%)	5.69 (15.0%)	6.10 (20.6%)
f_y (kN)	88.47 (8.7%)	90.79 (1.6%)	15.35 (15.9%)	17.25 (24.9%)
$f_{y,EC5/ETA}$ (kN)	43.32(51.0%)	43.32 (52.3%)	14.59 (5.0%)	14.59 (15.4%)
V_y (mm)	11.20 (19.0%)	13.04 (13.8%)	4.81 (18.0%)	4.98 (30.5%)
K_{ser} (kN/mm)	7.47 (17.9%)	6.82 (8.6%)	3.34 (14.0%)	3.70 (6.9%)
$K_{ser,EC5/ETA}$ (kN/mm)	9.80(31.2%)	9.80 (43.7%)	16.45 (392.5%)	16.45 (344.6%)
K_{pl} (kN/mm)	1.25 (17.9%)	1.14 (8.6%)	0.56 (14.0%)	0.62 (6.9%)
D	1.93 (11.1%)	1.93 (11.1%)	1.18 (7.5%)	1.25 (10.5%)

Note: The experimental results for HBSP12120 are for 4 screws that were tested simultaneously in shear, while the result of LBS7100 is for single screw tested in tension; All presented results denote the mean value of all specimens; Whitin parentheses, the values denote the coefficient of variation, in those of analytical data denote the errors between experimental results and analytical results

The calculation of analytical values was conducted in accordance with both EC5 [4.3] and ETA-11/0030 [4.14] for Rothoblaas screws. $\rho_m = 448.8 \text{kg/m}^3$ and $\rho_k = 385 \text{kg/m}^3$ were taken based on the CLT measurement in experiment and the product brochure of Rothoblaas screws. As prescribed in ETA-11/0030, the outer thread diameters of screws were used in the calculation in this study, although EC5 requires effective diameter (shank diameter) to be used in determining the $M_{y,Rd}$ and $f_{h,k}$ to account for the threaded part. The axial slip modulus K_{ser} it not defined in EC5, therefore the formulas were taken from ETA-11/0030

as $K_{ser} = 25 \cdot d \cdot l_{ef}$ for soft wood, where l_{ef} is the penetration length of screws in timber members.

As summarised in Table 4.4, tensile screws have higher stiffness over shear screws but with less ductility, which contributes to a larger variation in test outputs of tensile screws. Based on the observed behaviours, the ductility classification for all connections falls within the low-ductility range. The analytical model overestimated the stiffness of shear connections by 31.2% and 43.7%, but significantly underestimated the strength by around 50%. The observed deformation modes, significant disparities in testing outcomes, and the overestimated stiffness and underestimated strength of screws in analytical calculations, are consistent with findings reported in the published research [4.15-18] and can be considered reliable. By comparing the mean experimental curves for the new and used screws in both Figure 4.15 and Figure 4.16, along with the statistical data derived from test results in Table 4.4, it can be concluded that there is negligible differences in the average mechanical properties of used screws compared to new ones in both shear and tensile tests. This finding indicates that the performance of the screws remained largely unaffected by the failure of interlocking connectors in tests.

4.5 Test Results of Interlocking Connections

4.5.1 Interlocking shear connection

In the cyclic testing of shear connections (Figure 4.17.a), buckling was the primary deformation that associated with the sudden force reduction in the force-displacement curve. The first buckling occurred when the displacement reached 4 mm (marked as point 1 in Figure 4.18.a), followed by another buckling at a displacement of 6.5 mm (point 2 in Figure 4.18.a), both occurring under a similar force of approximately 16kN. This pattern suggested simultaneous buckling in the shear connections on both sides of the panels, thereby inducing instability in the experimental setup. In the reverse loading direction, buckling was also noted on the opposite side of the male connector (point 3 in Figure 4.18.a), occurring at a force level similar to the initial buckling events, around 16kN. However, the connection stiffness at the reversed loading direction was lower than the stiffness at the previous direction, indicating that both parts of male connection contribute simultaneous to the connection behaviours, so the buckled part leads to reduced stiffness when the loading reverse.

After the buckling, the connection strength continued to develop in the deformed steel band and the end sunken (Figure 4.17.b), contributing to the plumper hysteresis loop at large displacement. When reaching 10 mm at the reversed loading direction, breakage happened at one of the buckled male connectors (point 4 in Figure 4.18.a) due to the excessive deformation and terminated the test.

Therefore, in the testing of shear connections, different types of deformations (buckling, bending and breakage) can be identified in two primary areas (Figure 4.17.b); the middle of deformable band and the end sunken of deformable band. The buckling locations were relatively consistent among all the specimens. The buckling and cumulative deformation in the shear connection specimens caused unsymmetric behaviours in two loading directions (Figure 4.17.a), which are unfavourable considering the stability of structures and limit the connection's capacity in dissipating energy. It is worth noting that, according to Figure 4.17.a, the maximum strength and stiffness of the proposal shear connection is much lower than the yield strength of STC connections formed by the bottom plate of interlocking connectors and timber. Therefore, the STC connections were still in their elastic stage even after the failure of interlocking connectors, ensuring the attainment of damage-controlled design.

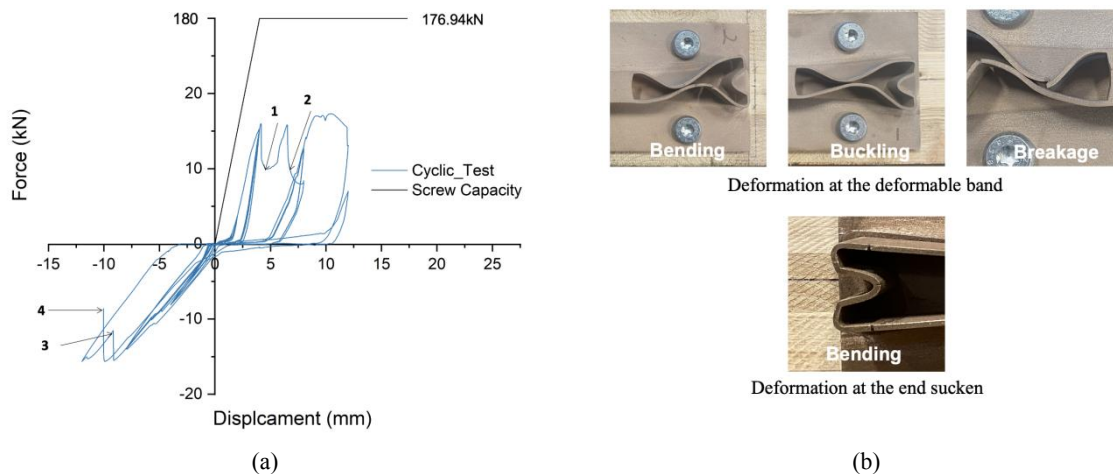


Figure 4.17. The hysteresis loops (a) and (b) the primary deformation modes in shear connection specimens

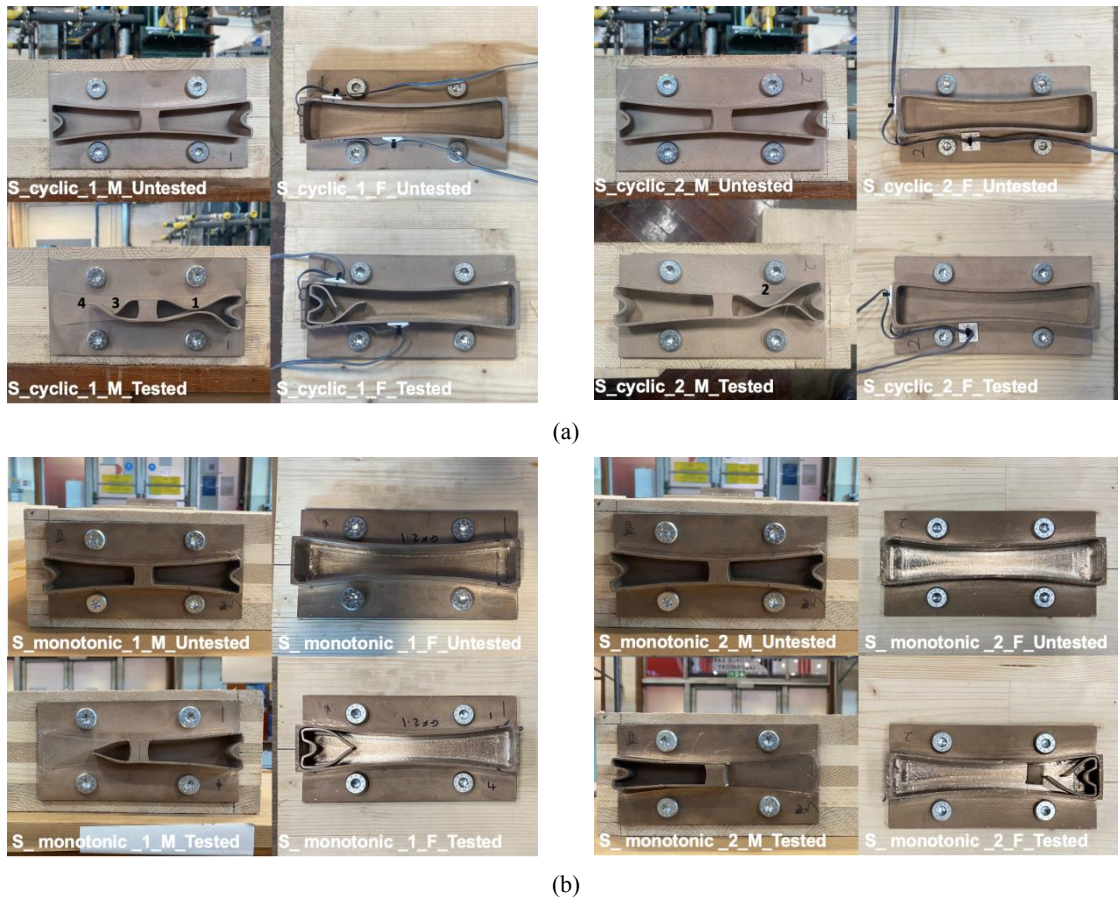


Figure 4.18. Deformation of shear connection specimens: (a) cyclic testing and (b) monotonic testing

4.5.2 Interlocking tensile connection

Figure 4.19.a depicts the hysteresis loops for the proposed tensile connections. Different from the cyclic behaviours of conventional timber connections, the connection performance in the first cycle of each loading step in cyclic test showed good consistency with the monotonic test, as stiffness and maximum strength in monotonic loading at each step can be reached in cyclic loading with no strength degradation, indicating the plastic deformation in the male connector does not affect the maximum capacity in the subsequent loading. However, the plastic deformation caused gaps between the two connectors, leading to the sliding of the male connector within the female connector with no reaction force. With the increase of the applied displacement, the bearing walls of the female connector started to open-up and close elastically, along with the upward and downward movement of the male connector, due to the moment at the wall base applied by the reaction force of male connectors. This indicated that the bearing walls also contributed to the connection stiffness under large displacement, which

led to the degraded stiffness degradation of each repeated circle, alike the pinching effect in the conventional timber connections.

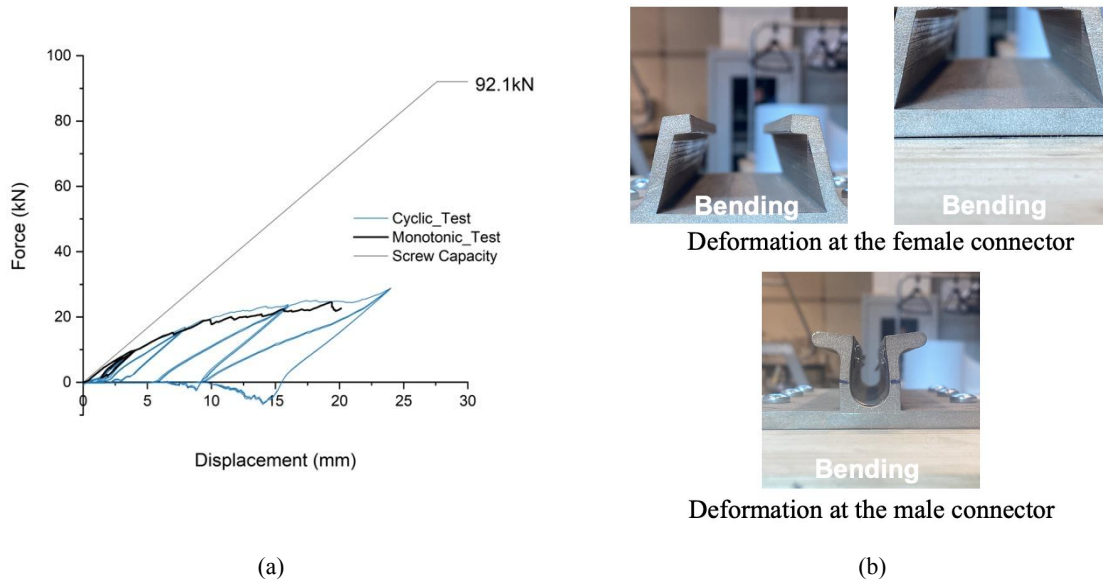


Figure 4.19. The hysteresis loops (a) and (b) the primary deformation modes in tensile connection specimens

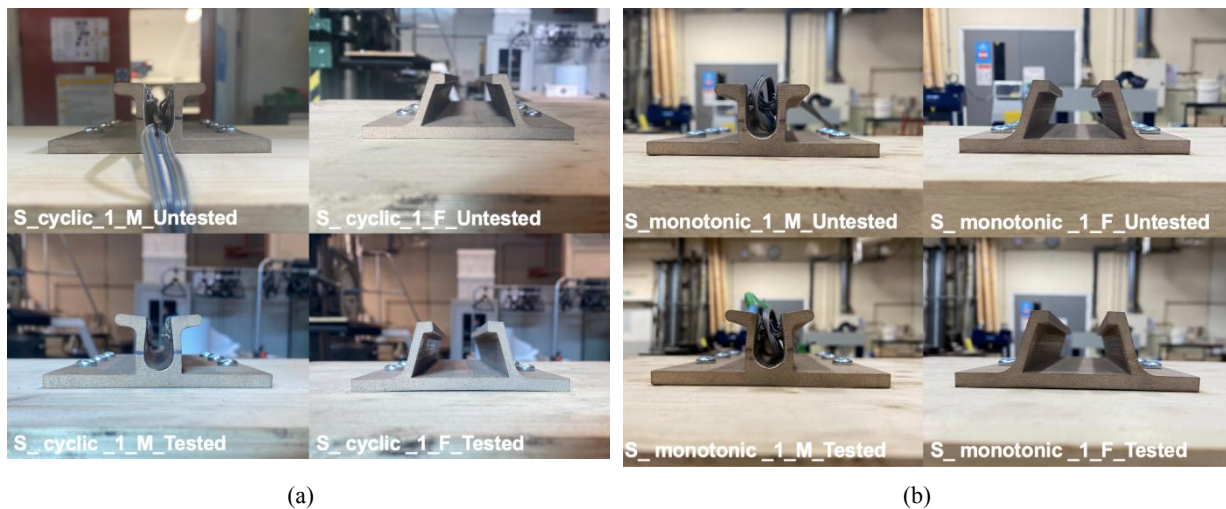


Figure 4.20. Deformation of shear connection specimens in (a) cyclic testing and (b) monotonic testing

The deformation mode in all tensile connection specimens was relatively consistent (Figure 4.19.b). The primary deformation mode in the tensile connection was the bending of the L-shaped elements in the male connector as designed (Figure 4.20). Bending of the L-shape elements started at the marked locations for strain gauge installation, corresponding to the estimated areas where largest strain appears. The female connector and screws remained mostly undeformed at the end of testing (Figure 4.20), and only very slight open-up in the bearing walls and slight bending in the bottom plate (Figure 4.19.b) were visible, indicating that most of the deformation was successfully controlled within the male connector.

Therefore, the deformed male connector can be easily slid out and detached from the female connector after the end of testing. In the case of interlocking tensile connections, the STC connections were still in their elastic stage even after the failure of interlocking connectors, ensuring the attainment of damage-controlled design.

Table 4.5. Key test results (mean values) obtained for both interlocking shear and tensile connection testing (EN26891)

	Interlocking Shear Connection	Interlocking Tensile Connection
f_{max} (kN)	17.3	27.22
f_u (kN)	13.84	27.22
V_u (mm)	11.96	24.0
f_y (kN)	15.7	20.55
V_y (mm)	3.73	8.34
K_{ser} (kN/mm)	6.9	2.56
K_{pl} (kN/mm)	0.27	0.43
D	3.2	2.88

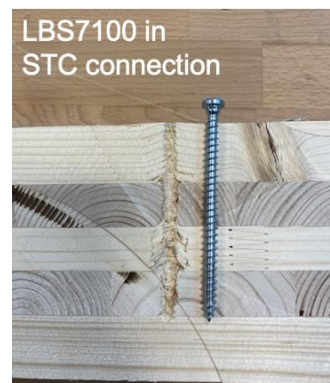
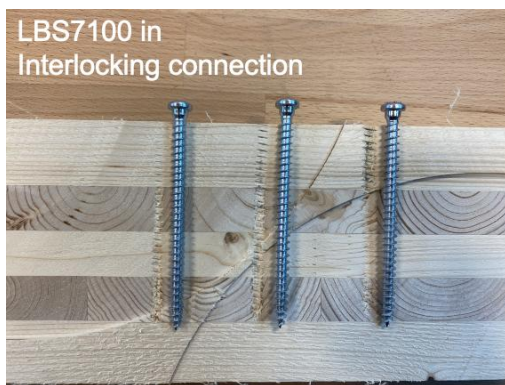
Note: The results were taken from the cyclic test of both connections; The K_{pl} , F_u , F_{max} and V_u were determined from the post-buckling behaviours of interlocking shear connections.

Although the characteristic properties of the proposed connections was not available due to the insufficient statistical data, both connection systems demonstrated adequate mechanical properties, and the results from the monotonic and cyclic tests (Table 4.5) on both shear and tensile connections revealed distinct differences in their deformation performance. The tensile connection exhibited lower stiffness, higher maximum strength, and enhanced ductility, showcasing a ductile failure mode due to bending. In the contrary, the shear connection displayed higher stiffness, but lower maximum strength and ductility, characterised by a brittle failure mode resulting from buckling in the cantilevered elements of the male connector. The male connectors in both connections yielded before reaching the full capacity of the surrounding fasteners when working in the primary direction, corresponding to the capacity design strategy.

4.6 Verification of Damage-Controlled Effect of the Innovative Interlocking Timber Connection

To verify the effectiveness of the damage-controlled effect in the proposed interlocking connections, timber panels were separated at the screw locations after the screws were removed from the tested specimens. According to the cross-sections illustrated in Figure 4.21,

little deformation can be identified on either the CLT panel, nor the tensile or shear screws, after the failure of interlocking tensile and shear connection specimens. In contrast, the conventional STC shear connection (Figure 4.21.b), deformation with two plastic hinges can be seen on HBSP12120 screws. This deformation resulted in crushing of the first layer of the CLT panels along the grain direction. Observing the STC tensile connection (Figure 4.21.b), the LBS7200 remained mostly intact. A combined shear/tension failure perpendicular to grain can be seen around the threaded part of screw, which was produced during the pulling out of the screws and is similar to the observations in published tensile testing on screws [4.19]. The difference in damage patterns between the conventional STC connections and the proposed interlocking connections underscore the latter's capacity to control damage effectively. The proposed interlocking shear and tensile connections, as opposed to the conventional STC connections, demonstrate superior performance in preserving the integrity of both the timber panels and the connecting screws.



(a)



(b)

Figure 4.21. Comparison of screw deformation in interlocking connection and STC connection: (a) tensile screws; (b) shear screws (Note: the curvy mark on the cross section of timber was created by table saw that used to slide panels)

4.7 Conclusions

This chapter outlines laboratory tests conducted on innovative interlocking unit connections, focusing on their mechanical properties and deformation behaviours. Monotonic and cyclic testing were carried out on both shear and tensile connections, with experimental setups reflecting their real-world working conditions. A cutting-edge manufacturing technology, 3D printing, was adopted in this study to manufacturing this novel and rather complex specimens, taking advantage of its flexibility and high-level accuracy. The quality/strength of the 3D printed material were validated through coupon testing, ensuring a thorough assessment of this technique's impact on the experimental results.

The testing reveals the adequate mechanical properties of the interlocking of both connections in working conditions, even without additional reinforcement. Notably, no evidence of screw pull-out or significant movement between connectors and timber was observed post-testing, and the female connectors exhibited only minimal deformation upon reaching peak strength. This meant that most of the connection components, apart from the male connectors, remained intact following connection failure, indicating successful plastic deformation localisation within the designated areas (male connectors). This outcome highlights the effectiveness of strategically localising plastic deformation within the male connectors, confirming the success of the controlled damage strategy in managing deformations.

4.5 Chapter References

- [4.1] Eurocode, *Timber structures- test methods- cyclic testing of joints made with mechanical fasteners* 2005, European Committee for Standardisation.
- [4.2] Sandhaas, C. *Mechanical behaviour of timber joints with slotted-in steel plates*. 2012, Delft University of Technology: Netherlands.
- [4.3] Eurocode, *Eurocode 5: Design of timber structures*. 2004, European Committee for Standardisation,.
- [4.4] Rothoblaas. *Screws and Connectors for Wood*. Available from: <https://www.rothoblaas.com/products/fastening/screws/screws-structures>
- [4.5] Li, Z., Tsavdaridis, K.D. and Gardner, L. *A review of optimised additively manufactured steel connections for modular building systems*. 2020: Springer International Publishing.

- [4.6] Sculpteo. *Steel/ Bronze 420SS/BR Material Guide*. Available from: <https://www.sculpteo.com/en/materials/binder-jetting-material/binder-jetting-stainless-steel-material/>.
- [4.7] Jafari, D., Vaneker, T.H.J., and Gibson, I. *Wire and arc additive manufacturing: Opportunities and challenges to control the quality and accuracy of manufactured parts*. *Materials & design*, 2021. **202**: p. 109471.
- [4.8] Lu, S.L., Meenashisundaram, G.K., Wang, P., Nai, S.M.L. and Wei, J. *The combined influence of elevated pre-sintering and subsequent bronze infiltration on the microstructures and mechanical properties of 420 stainless steel additively manufactured via binder jet printing*. *Additive manufacturing*, 2020. 34, pp.101266-.
- [4.9] BS EN ISO 6892-1:2016, *Metallic materials. Tensile testing. Method of test at room temperature*. 2016, British Standards Institute.
- [4.10] Doyle, M., Agarwal, K., Sealy, W. and Schull, K., *Effect of layer thickness and orientation on mechanical behavior of binder jet stainless steel 420 + bronze parts*. *Procedia manufacturing*, 2015. **1**: p. 251-262.
- [4.11] Eurocode, *Timber structures. Joints made with mechanical fasteners. General principles for the determination of strength and deformation characteristics*. 1991, European Committee for Standardisation,.
- [4.12] Dorn, M., *Investigations on the serviceability limit state of dowel-type timber connections = Untersuchungen zum Gebrauchstauglichkeitszustand von Dübelverbindungen im Holzbau, in Untersuchungen zum Gebrauchstauglichkeitszustand von Dübelverbindungen im Holzbau*. 2012, 2012. p. III, 187 S., Ill., graph. Darst.
- [4.13] Iraola, B., Cabrero, J.M., Basterrechea-Arévalo, M. and Gracia, J., *A geometrically defined stiffness contact for finite element models of wood joints*. *Engineering structures*, 2021. **235**: p. 112062.
- [4.14] Rotho Blaas s.r.l, *European Technical Assessment ETA-11/0030 of 2019/10/08*, in Technical Assessment Body issuing the ETA and designated according to Article 29 of the Regulation (EU) No 305/2011: ETA-Danmark A/S. 2019.
- [4.15] O'Ceallaigh, C. and Harte, A.M. *The elastic and ductile behaviour of CLT wall-floor connections and the influence of fastener length*. *Engineering structures*, 2019. **189**: p. 319-331.
- [4.16] Hassanieh, A., Valipour, H.R., Bradford, M.A. and Sandhaas, C. *Modelling of steel-timber composite connections: Validation of finite element model and parametric study*. *Engineering structures*, 2017. **138**: p. 35-49.
- [4.17] Yang, R., Li, H., Lorenzo, R., Ashraf, M., Sun, Y. and Yuan, Q. *Mechanical behaviour of steel timber composite shear connections*. *Construction & building materials*, 2020. **258**: p. 119605.
- [4.18] Hassanieh, A., Valipour, H.R. and Bradford, M.A. *Load-slip behaviour of steel-cross laminated timber (CLT) composite connections*. *Journal of constructional steel research*, 2016. **122**: p. 110-121.

- [4.19] Ringhofer, A., Augustin, M. and Schickhofer, G. *Basic steel properties of self-tapping timber screws exposed to cyclic axial loading*. Construction & building materials, 2019. **211**: p. 207-216.

Chapter 5 Numerical Simulations and Analytical Studies

Based on experimental findings, this chapter further advances the understanding of the proposed connection system by presenting a series of numerical and analytical studies at the local scale. To construct accurate numerical models that effectively capture the behaviours of the connections, comprehensive 3D fully discretised continuum models were first created using the finite element analysis (FEA) software ABAQUS/Standard and validated against experimental results. Furthermore, a series of parametric study was undertaken using these connection models to thoroughly examine the influence of geometric design on connection behaviours. Complementing these numerical studies, an analytical investigation was also conducted, drawing on the insights gained from the parametric analysis. This combined approach aims to enhance the practical design and understanding of interlocking connections, providing a robust foundation for their application and optimisation.

5.1 Validation of Numerical Connection Model

5.1.1 Materials

To ensure the accuracy of FEA, models for shear and tensile connections were constructed with full geometric details in the unit steel connectors, fasteners, fixing structures and timber. In the models of both connections, the 5-ply CLT panels were modelled using an orthotropic elastoplastic material model with the properties as listed in Table 4.1. This model considered each layer separately, accounting for loading parallel and perpendicular to the grain for respective layers. Specifically, the first (20mm), third (40mm), and fifth (20mm) layers were modelled under loading parallel to the grain, while the second (20mm) and fourth (20mm) layers were under loading perpendicular to the grain, corresponding to experiment.

For all steel fixtures and screws, a modulus of elasticity 200GPa and a Poisson's ratio of 0.3 were assumed. Grade-300PLUS steel with a yield strength of 320MPa and an ultimate strength of 440MPa was used in all steel fixture devices. The Grade 10.9 carbon steel with a yield strength of 940.3MPa and an ultimate strength of 940.3MPa at 0.5% ultimate strain, was adopted for HBSP12120 and LBS7100, which were validated by Tomasi et al. [5.1]. For the modelling of the 3D printed connectors, a modulus of elasticity of 130GPa, a yield strength of 304MPa, an ultimate strength of 638MPa and an ultimate strain of 5.9 % that extracted from the coupon test as explained in Section 4.3, were taken. Throughout the model,

8-node linear brick elements with reduced integration (C3D8R) were used for the mesh, ensuring detailed and accurate representation of all components.

5.1.2 Modelling of shear connection

To achieve a more precise replication of the experimental conditions, the FE shear connection model was built closely adhered to the experimental setup, with full dimensional details of steel fixtures and connections on both sides as explained in Section 4.1 (Figure 5.1). Incorporating a detailed model of the fixing device within the simulation is crucial for identifying potential discrepancies in experimental results. These discrepancies often stem from minimal deformation and relative movement of components within the fixing system. For the boundary conditions of the model, three directional movement constraints were imposed on the steel foundations and the grip bar, representing the support and fixture of loading machine. The loading exerted by the testing machine was applied directly onto the top surface of the CLT panel. This application was executed in a displacement-controlled manner, ensuring a precise replication of the loading conditions observed in the actual testing setup.

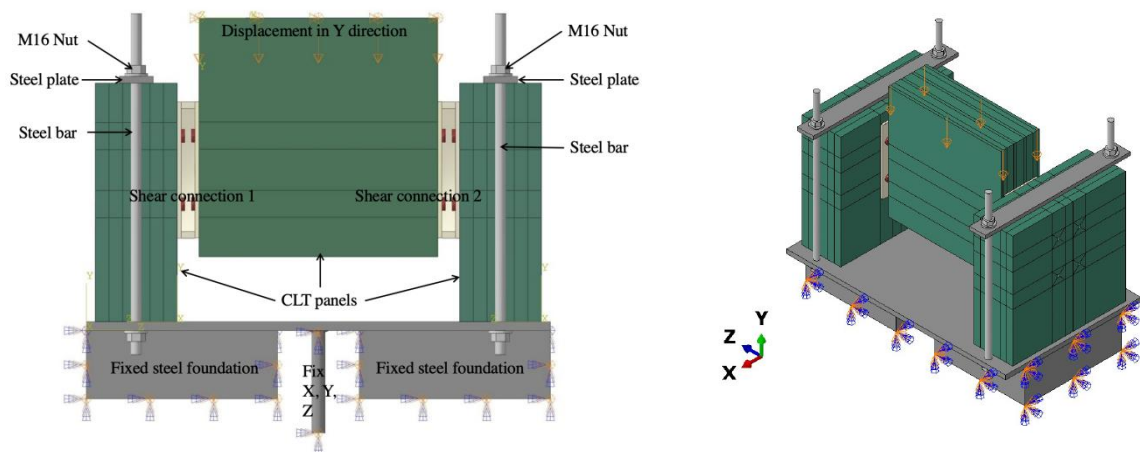


Figure 5.1. The outline and boundary conditions of FE model of the shear connection

Given the working mechanism of conventional steel-to-timber composite connections (STCs) as introduced in Chapter 2, the modelling of interaction between timber and steel fasteners is imperative to the model accuracy. In shear loading scenarios, the screws within STCs predominantly endure compressive forces from the surrounding timber and the steel plate, which is primarily transmitted through the screw's shank. Accordingly, screws in the

interlocking shear connection were modelled as cylindrical elements with a diameter corresponding to d_s of HBSP12120, as listed in Table 4.2.

For contact modelling at all interfaces within the simulation, the surface-to-surface discretisation method was employed. The interaction properties were defined with the “Hard Contact” option in the normal direction and the “penalty friction formulation” in the tangential direction. The coefficient of friction was set at 0.4 for all steel-steel contacts [5.2], and 0.25 for all steel-CLT contacts [5.3]. To simulate the tightening effect between the nuts and threaded bars in the fixing system, which was rigid and stable with no relative movement during the experimental tests, tie constraints were incorporated at all interfaces between these components.

In modelling the interactions between screws and timber along the tangential direction, a non-linear relationship between contact pressure and displacement, as detailed in Equation 5.1, was adopted. This non-linear relationship was implemented in the normal direction using the "Tabular" option available in ABAQUS. This approach was specifically selected to account for the lower timber strength in the vicinity of the screw surfaces, which is particularly crucial given the use of big-diameter screws in the shear connections, where the pre-drilling effect is more pronounced. In the curve fitting process for the test results of HBSP12120, the LAME function was carefully implemented with the contact deformation u_0 being set at 0.35mm, and, σ_0 , representing the maximum compressive strength of timber, being assumed to be 30 MPa [5.2]. Therefore, the control factors n_u and n_σ of LAME function were determined to be 1.23 and 1.09, respectively. These specific values contrast with those previously determined values of $n_u=3.9$ and $n_\sigma = 7.7$, derived from Dorn's testing on $\emptyset 12$ dowels [5.4]. The higher values of n_u and n_σ obtained in the dowel testing can be attributed to the smoother surface of dowel connections, which does not exacerbate timber damage during insertions, thereby facilitating a more rapid recovery in connection strength at the onset of screws' bending.

$$\left(\frac{u_{inter}}{u_0}\right)^{n_u} + \left(\frac{\sigma_0 - \sigma_L}{\sigma_0}\right)^{n_\sigma} = 1$$

Equation 5.1

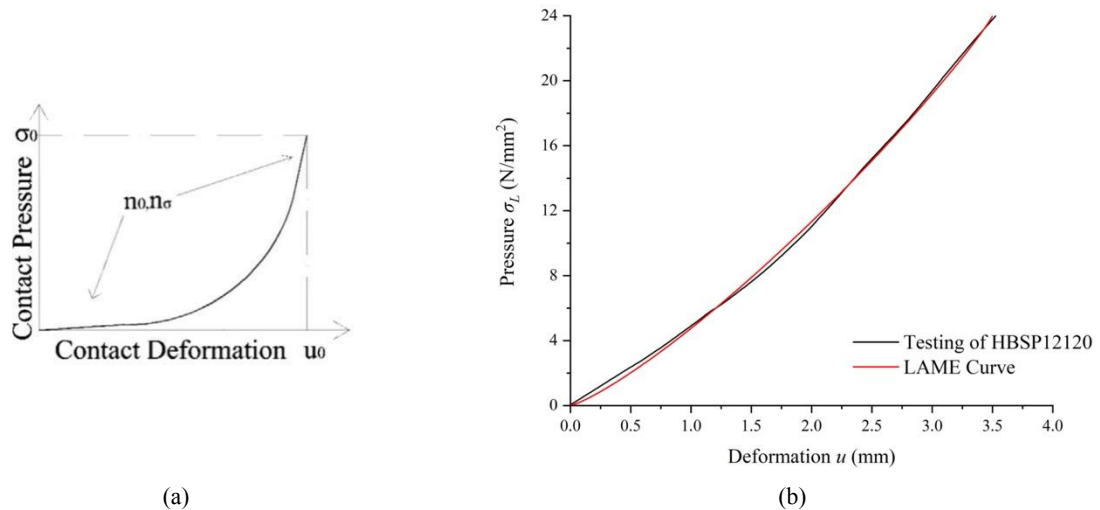


Figure 5.2. Non-linear contact relationship employed in shear screws-timber contact modelling: (a) the LAME function [2] and (b) the curve fitting results

The occurrence of buckling in the shear connection necessitated the use of geometrically and materially nonlinear analysis with imperfections (GMNIA) in the validation model, a method that incorporates imperfections. Due to the inherently perfect nature of the initial FE model, it tended to exhibit bending behaviours rather than buckling. To address this, the linear Eigenbuckling analysis, which is a common method for predicting the buckling strength and generating ‘imperfection’ on the model to trigger nonlinear buckling analysis, was first conducted. In the Eigen buckling analysis, a unit pressure was applied at the top of the middle panel in the original shear connection model to predict the critical load of buckling and the buckling mode shapes of the ideal structure based on the ‘Block Lanczos’ method. As shown in Figure 5.3, the generated four buckling modes in the male connectors on both sides agreed qualitatively with the test results, so they were extracted and imported into the nonlinear analysis as ‘imperfection’ with a factor of 0.2. Furthermore, to accurately simulate the observed sliding during the initial loading stage in the connection model, a crucial adjustment was made by including a 1 mm gap between the male and female connectors. This modification enhances the model's capacity to realistically portray the early-stage interaction dynamics of the connection under loading.

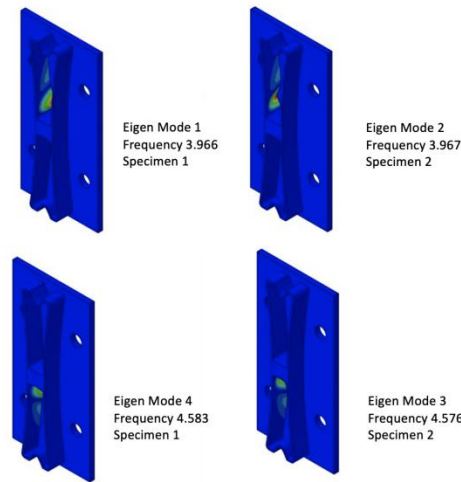


Figure 5.3. Four Buckling Modes Extracted by ‘Block Lanczos’ Method

5.1.3 Modelling of tensile connection

Similar to the shear connection model, the boundary conditions in the tensile connection model were set according to the experiment set-up. A simplified steel fixture, as illustrated in Figure 5.4, was modelled to apply the necessary movement restrictions. Displacement-controlled loading in the Y-direction was implemented on the steel fixture attached to the panel with the male connector.

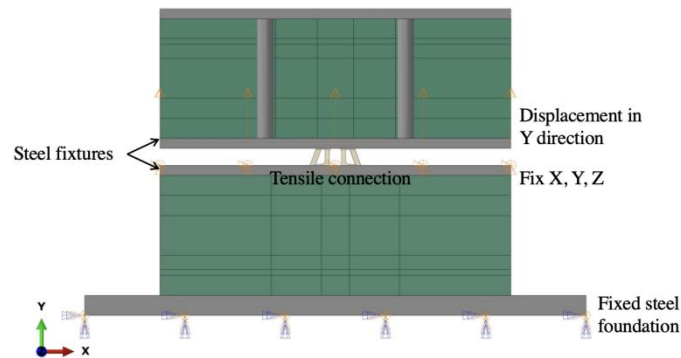


Figure 5.4. The outline of boundary conditions of FE tensile connection model

When simulating timber screwed connections loaded in tension, two modelling methods are commonly adopted. The first approach involves constructing a comprehensive model of the screws, inclusive of detailed threading [5.5]. In this method, the performance of the screws is entirely determined by their geometric characteristics, preventing the need for assumptions about screw properties. The second one is a simplified method proposed and validated by Avez et al. [5.6] and Bedon et al. [5.7], which introduces a fictitious ‘soft material’ (Figure

5.5) to represent the threaded part with the diameter equals to d_7 of LBS7100 in Table 4.1. The 'soft material' is assumed to be perfectly elastic and has the same capacity as the wood, except for the radial modules that is reduced to 50MPa to eliminate its contribution in the compressive direction, representing the weakening effect of threads on the timber. Wrapped by 'soft material' is the 'core' that simulates the shank of screws, the dimensional value of which is taken as d_s of LBS7100 (Table 4.1). Compared to the complete modelling approach, this simplified method offers enhanced computational efficiency by eliminating the details of the screw threads and reducing the extensive contact area between the threads and timber, thus it has been adopted in this study.

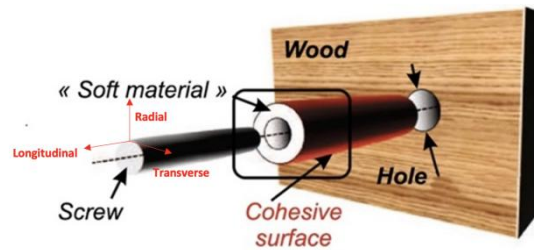


Figure 5.5. Simplified FE model for screws in tension [5.6]

The withdrawal capacity of screws in the timber panel was simulated by defining a cohesive surface. This surface was modelled between the internal surface of the pre-drilled holes in the timber panel and the external surface of the 'soft material'. An assumed rigidity of 40N/mm³ was set in the longitudinal direction, while a rigidity of 0N/mm³ was maintained in both the tangential and radial directions (Figure 5.5) [5.6]. To simulate the initiation of interaction failure, the 'damage initiation criterion' option within the model utilised the maximum nominal stress (MAXS) approach at this cohesive surface:

$$\max\left\{\frac{t_n}{t_n^0}, \frac{t_s}{t_s^0}, \frac{t_t}{t_t^0}\right\} = 1 \quad \text{Equation 5.2}$$

where the t_n^0 , t_s^0 and t_t^0 are the peak allowable stresses in the normal (n), first (s) and second (t) shear direction of the bonding interface, the values of which were taken as 36MPa, 6.9MPa and 6.9MPa, equalling to the compressive and shear strength of timber as listed in Table 4.1.

Once the cohesive resistance limit is reached in the model, the simulation transitions to represent the strength degradation of the bond. This is achieved through the implementation of a 'linear damage evolution' law. This law assumes that the cohesive surface attains its full residual stiffness upon reaching a deformation of 4mm. Consequently, the contact behaviours of the connection become elastic-brittle, effectively simulating the brittle failure typical of dowel-type timber connections under tension. To further enhance the realism of the model, the cohesive interaction approach was strategically paired with specific contact settings. In the normal direction, the 'Hard Contact' setting was employed to effectively prevent the penetration of screws into the timber during the post-failure stage. Additionally, in the tangential direction, the 'Penalty Friction Formulation' was utilised, accompanied by a coefficient of friction set at 0.4.

5.1.4 Mesh sensitivity

To evaluate the influence of mesh size on the accuracy of the proposed FE connection models, a comprehensive mesh sensitivity analysis was conducted. This analysis aimed to ensure the optimal selection of mesh size for the simulation. It was assumed that certain components are mesh size-independent in the analysis, such as the timber panels, fasteners, metal fixtures, and the female connectors, since these elements exhibited minimal deformation in the experimental tests. Therefore, increasingly smaller mesh size was only applied in the interested areas of both connection models (Figure 5.6), while the mesh size in other parts of the testing set-up remained consistent. The male connectors of both connections, which are designed to govern connection properties, were first studied with 3 mm mesh size. Then the mesh size was refined to 1.5 mm and 1mm. It can be observed in Figure 5.7.a that, the changes in mesh size have little impacts on the numerical predictions of shear connector model. In the model of tensile male connector (Figure 5.7.b), the initial stiffness is independent to the mesh size, while yielding strength is slightly sensitive. Ultimately, a mesh size of 1.5 mm was identified as an effective balance between result accuracy and computational efficiency for both models. Therefore, this mesh size was selected for use in subsequent studies.

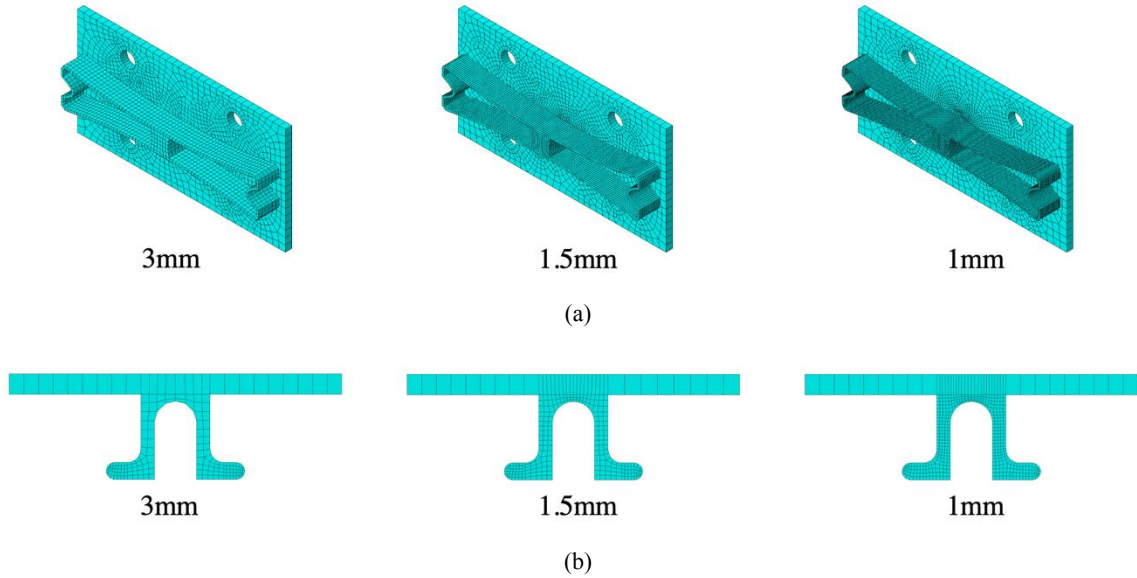


Figure 5.6. Mesh size considered in the mesh sensitivity study of (a) shear male connector (b) tensile male connector

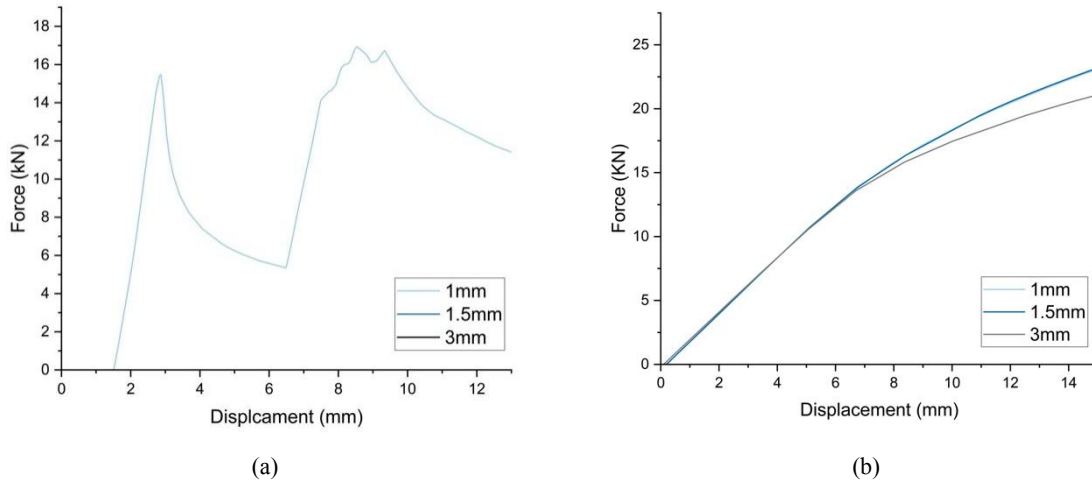


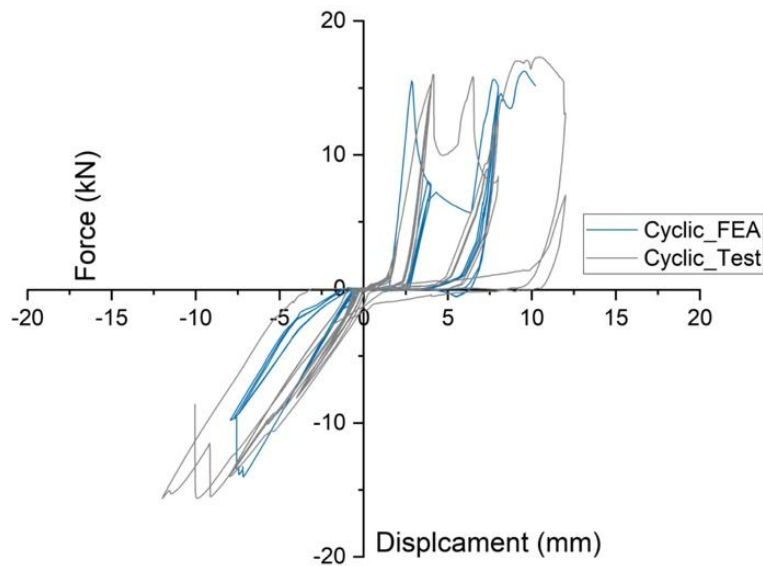
Figure 5.7. Force-displacement response obtained from different mesh size in (a) shear male connector model and (b) tensile male connector model

5.1.5 Numerical validation of shear connection

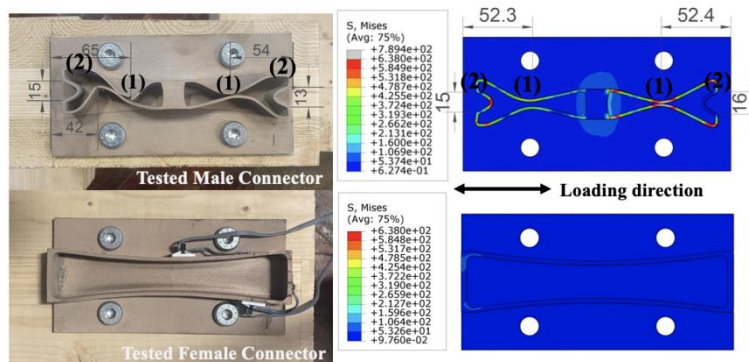
Figure 5.8 presents the validation of the proposed shear connection model against testing results. By comparing the experimentally and numerically generated connection properties and deformation, it can be concluded that the FE shear connection model closely matches the experimental test outcomes, accurately capturing asymmetric behaviours observed in the two loading directions. This alignment underscores the model's efficacy in replicating real-world connection behaviours.

A critical aspect of the model is the incorporation of a 1 mm gap, which is instrumental in simulating the initial sliding observed at the onset of each loading step. In the pre-buckling

phase during positive loading, the FE model displays a similar critical load to the experimental data, but with marginally higher stiffness. These discrepancies are likely to occur due to errors arising from the implementation of the imported buckling modes into the model. After the buckling, the numerical model successfully replicated the unloading stiffness and the reduced energy dissipations, evidenced by narrower hysteresis loops. Furthermore, with the incorporated initial imperfections, the numerical model successfully replicated the negative stiffness associated with buckling in the negative loading direction. In terms of connection deformation, the simulation accurately captured the buckling shapes on both sides and the bending at the sunken ends. This precision, in terms of both location and size, is clearly illustrated at points 1 and 2 in Figure 5.8.b. This level of detail confirms the validation model's accuracy.



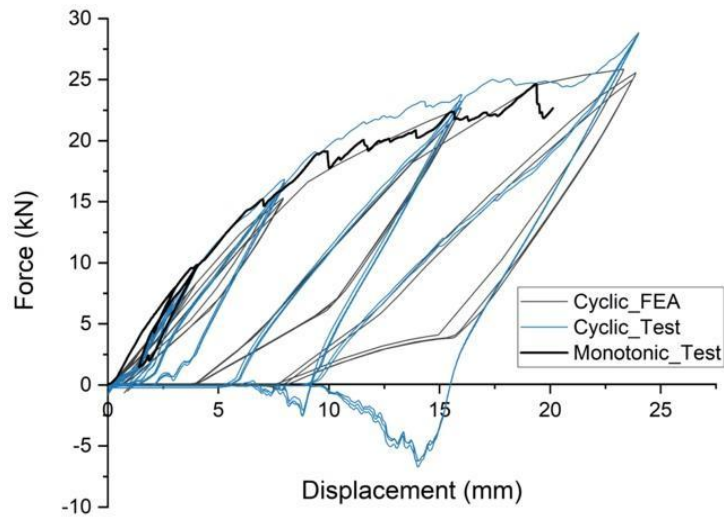
(a)



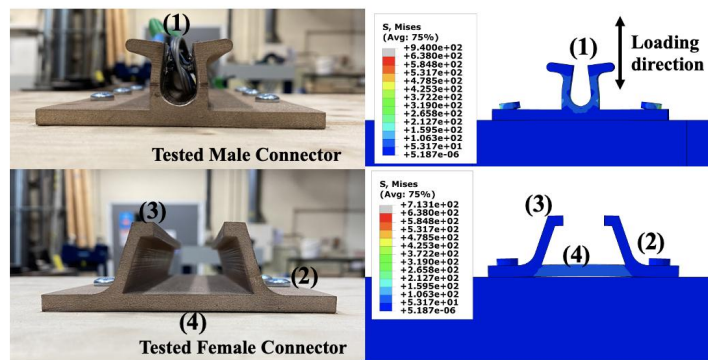
(b)

Figure 5.8. Comparisons between experimental results and FEA output in (a) hysteresis loops and (b) the deformation modes in shear connection specimens (in mm)

5.1.6 Numerical validation of tensile connection



(a)



(b)

Figure 5.9. Comparisons between experimental result and FEA in (a) hysteresis loops and (b) the deformation modes in tensile connection specimens (in mm)

The FE model of the tensile connection demonstrated a high level of agreement with the experimental output. This alignment was evident in the accurate replication of key aspects such as the maximum strength of each loading cycle, as well as the initial and reduced stiffness values (Figure 5.9.a). Additionally, the four deformation modes identified in the tensile connection were successfully reproduced in the model, both in terms of their shapes and dimensions (Figure 5.9.b). This achievement highlights the effectiveness of the proposed modelling method for interlocking tensile connections. Despite the slight pulling out of screws observed in the male connector within the model, the continuous force-displacement curve suggested that the interfaces between the screws and timber remained elastic. This observation was corroborated by the fact that the 'linear damage evolution' feature in the FE

model was not triggered. Therefore, the model effectively captured the elastic behaviours at the screws-timber interfaces, further validating the accuracy of the simulation.

5.2 Translational Behaviours of the Interlocking Connections with S235

5.2.1 Shear connection

After being successfully validated for predicting the structural performance of connections, the validated methods were applied to subsequent analyses. Given that the original testing utilised specimens made from a special grade of 3D printed steel, a monotonic analysis was carried out on the validated models using the material properties of a more common and ductile steel grade (S235), characterised by a modulus of elasticity of 210 GPa, a yield strength of 235 MPa, and an ultimate strength of 360 MPa. This analysis was conducted along the primary and secondary working directions of both connections, to further understand the translational behaviours of the proposed shear and tensile connections and to explore their performance potential using S235 steel material. The numerical model provided additional insights into the deformation trends within the shear connections, offering an understanding of connection behaviours that was not accessible during physical testing due to the concealed nature of the shear connection design.

The force-displacement responses of the interlocking shear connection FE model in the primary and secondary directions are reported in Figure 5.10. Similar to the tested specimens, the shear connection with S235 first buckled at the cantilevered steel band, resulting in negative stiffness in the FE model. With the continuous loading, the buckled steel band continued to bend, and the deformation started to develop in the end sucken on the other side. Corresponding to the experiments, most of the plasticity was observed in the designated deformable band (Figure 5.12.a) in the male connector after a 30 mm displacement in the primary direction, while little plastic strain was developed in the female connector and fasteners, which also resulted in very small damage on timber panels.

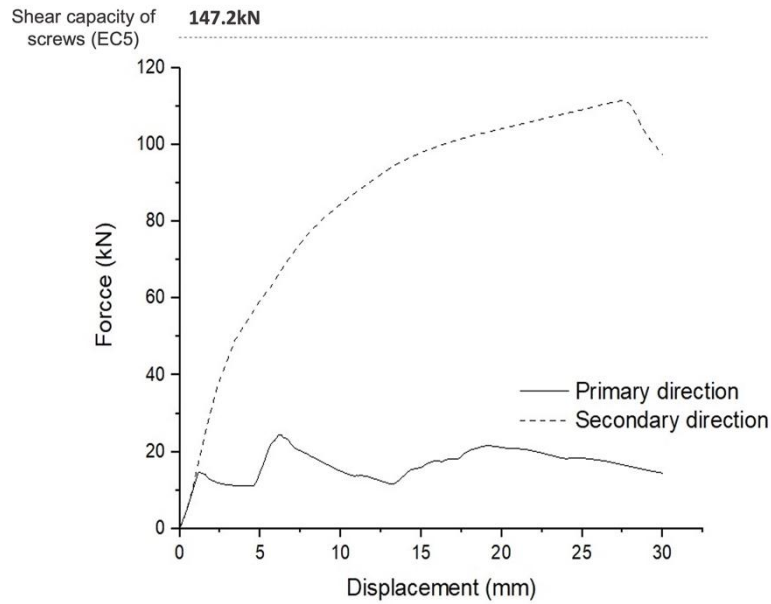


Figure 5.10. Force and displacement curve of interlocking shear connection

According to the connection deformation observed in the FE models, the interlocking shear connection's behaviours in the primary direction can be characterised as in Figure 5.11. The initial portion of the curve, which is known as the primary path, is often steeper and represents the elastic behaviour of the connection before reaching the bifurcation point. The first bifurcation point marks the end of the primary path where the material or connection experiences buckling, a form of instability leading to sudden changes in deformation patterns and reduced force in the connection. Beyond this point, the behaviour is no longer purely elastic, and the structure or material may not recover back to the original shape if the load is removed, which normally happens in thin-walled structures with a low width to thickness ratio. The path it follows post-buckling is less steep, indicating a change in stiffness and energy absorption characteristics of the connection. At this stage, the buckled steel bands on both sides begin to bend inward. This inward bending continues until the bands make contact, closing the gap between them. Upon this contact, stability within the connection is re-established, resulting in an increase in resistance. These buckled steel bands collectively assume a new form of cantilevered structure, which is continuously compressed by the female connector, then buckles again when reaching the second bifurcation point. The second buckling led to an asymmetric shape in the steel band, which then starts to bend under compression with low resistance. As the load progresses, the connection reaches a second bifurcation point, leading to another buckling event. This second buckling event imparts an asymmetric shape to the steel bands, which subsequently begin to bend under the

compressive force but with markedly reduced resistance. This dynamic sequence of buckling, contact, and re-buckling summarises the complex mechanical behaviours of this connection.

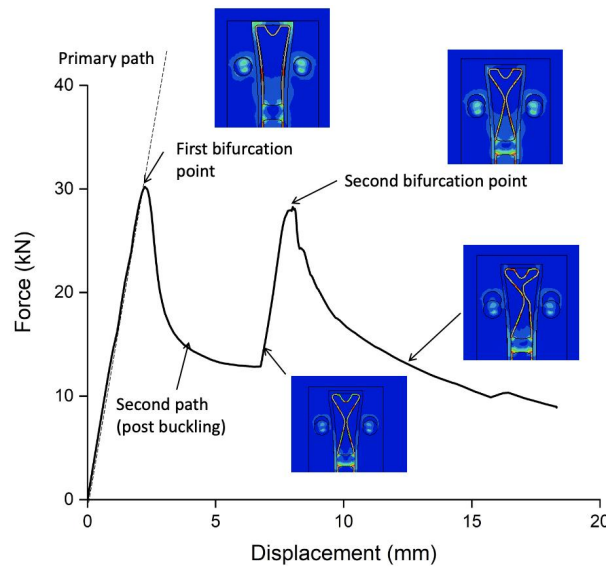


Figure 5.11. Shear connection buckling behaviours analysis on primary working direction

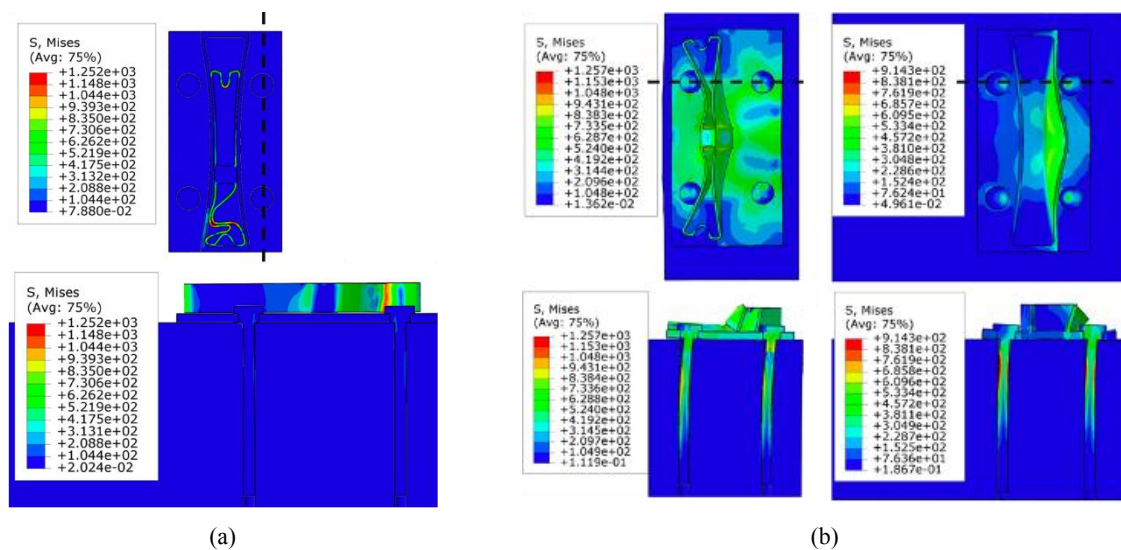


Figure 5.12. Stress distribution on shear connections and screws under the displacement of 30 mm in (a) the primary direction and (b) the secondary direction

Under loading in the secondary direction (Figure 5.12.b), the interlocking shear connection demonstrated considerably higher strength and ductility compared to its performance in the primary direction. The plastic deformation process involved a composite action: bending of the middle cubic support in the male connector, bending of the wall in the female connector on the load-bearing side, and bending of the screws. In this orientation, the shear connectors function similarly to conventional steel-to-timber composite connections, characterised by substantial timber deformation and increased plastic strain in the screws. This behaviour

confirms that the fasteners play a significant role in contributing to the strength of the connection when it is loaded in the secondary direction.

5.2.2 Tensile connection

Figure 5.13 illustrates the mechanical response of the interlocking tensile connection with S235 steel, which can be delineated into three distinct stages: the elastic stage, the yield plateau stage, and the densification stage. Initially, under loading, the male connector begins to slide within the female connector, causing the sloping walls to exert compressive forces on the L-shaped elements, prompting them to bend inward. As the male connector continues its vertical displacement, the L-shaped elements reach their yield point, and the walls of the female connector gradually start to open-up due to the increasing moment at their bases. This action results in a slight reduction in the connection's reaction force, characterising the yield plateau stage.

The transition to the densification stage occurs when the male connector makes contact with the top of the female connector, constraining its upward movement. This leads to significant increase in the connection stiffness. In this final stage, the connection becomes exceedingly rigid, effectively inhibiting any further displacement or opening. Consequently, the force-displacement ($F-\delta$) curve for the tensile connection in the primary working direction can be conceptualised using three key parameters: initial stiffness, yielding strength, and the displacement at the onset of densification.

Figure 5.14 shows that, at the displacement of 15 mm in the primary working direction, the L-shaped elements in the male connection processed most of the plastic deformation, while the other components of the connection show minimal deformation. Though the stress of the screws under tension cannot be reflected directly from the stress contour due to the employment of fictitious elastic 'soft material', the force-displacement curve does not exhibit any reduction in strength. This suggests that, even at a slip of 20mm, brittle failure has not occurred in the screws, and they remain within the elastic phase of deformation.

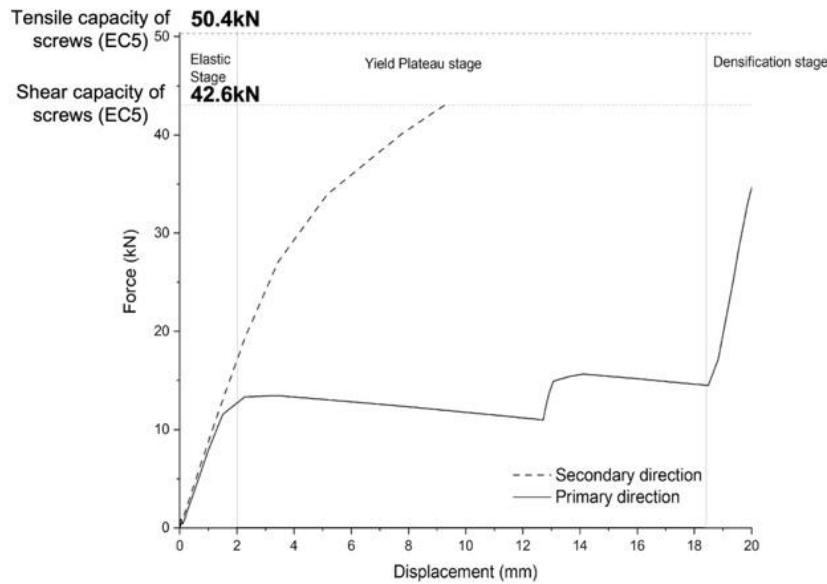


Figure 5.13. Force and displacement curve of interlocking tensile connection

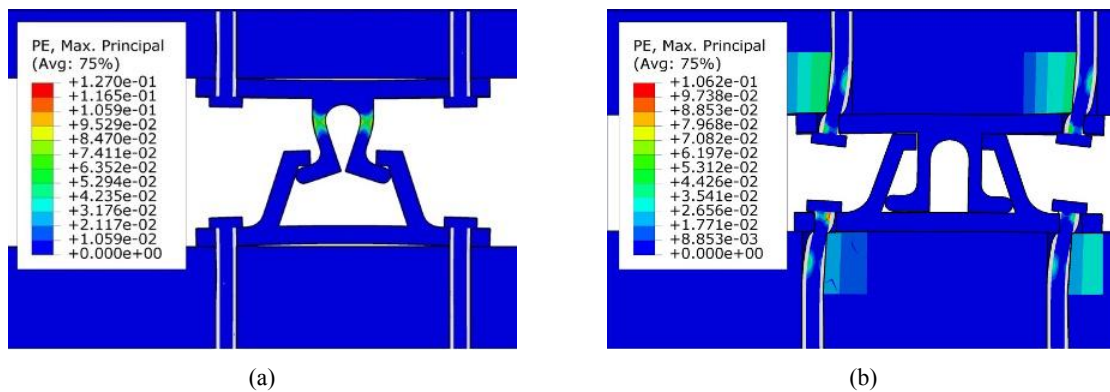


Figure 5.14. Von Mises Stress contour in the interlocking tensile connections under the displacement of 15 mm in (a) the primary direction and (b) the secondary direction

Under loads in the secondary working direction, the plastic strain contour plot reveals that the interlocking tensile connection exhibits a working mechanism similar to that of conventional steel plate connections. In this mode, screw bending and timber crushing emerge as the primary deformation modes. Consequently, the embedment strength of the timber and the bending strength of the screws become the principal contributors to the connection's overall strength, while the interlocking steel connectors maintain their rigidity.

5.2.3 Conclusion

The FE models of both interlocking shear and tensile connections made of S235 steel have shown that the proposed designs are capable of providing sufficient strength and ductility under translational loadings. The primary working mechanisms of these connections demonstrate a strong correlation with the behaviours observed during testing, indicating a

highly effective damage-controlled capacity. This is exemplified by the notably reduced deformation in screws under primary directional loading compared to the secondary direction, reflecting the effectiveness of the proposed connector design in timber damage control. When considering the secondary working direction, the connection's deformation is characterised by reduced ductility, predominantly influenced by the composite action between the fasteners and the steel connector. This pattern of deformation is similar to the well-established conventional steel plate connections, known for their high stiffness but relatively lower ductility.

5.3 Parametric Study

To enhance the design and detailing of the proposed interlocking connections, and to validate the accuracy of the proposed analytical models, a thorough parametric study is essential. The parametric study detailed in this section examines the impact of varying key design factors, on the fundamental mechanical properties of connection, such as stiffness, strength, and failure modes. Utilising the validated FE models of the interlocking connections, the study focuses on key geometric parameters of the interlocking connectors in addition to stainless steel grade, both were selected for their significant influence on performance. To ensure uniformity and comparability in the assessment, the standard configurations for the connections as examined in Chapter 4 was established as the benchmark, with a consistent unit connector size of 200mm×100 mm being adopting across all models.

The parametric study was performed in a two-stage manner, with five and six parameters being chosen in the study for tensile and shear connections, separately. The initial phase of the study involved the analysis of five distinct models for each parameter. In each case, a single parameter was varied while maintaining constant values for the others to isolate the effects on connection properties. The parameters that have pronoun impact on properties were then selected for more in-depth investigation in the detailed phase of the study. This two-stage approach ensures a balance between simplicity in analysis and the comprehensiveness of results. Consequently, a total of 60 models for shear connections and 55 for tensile connections were executed, providing a robust dataset for evaluating the efficacy and behaviours of the interlocking connections under varied design conditions.

5.3.1 Parametric model information

Based on previous numerical and experimental investigations on the proposed shear connections, the deformation modes of tensile connections present a higher level of complexity, including three primary modes: 1) the bending of the L-shaped element in the male connector, 2) the opening-up of the female connector, and 3) the bending of the bottom plate of the male connector. Therefore, in addition to connection material, the related form factors to these specific deformation areas are considered in the parametric study. These factors encompass the angle of the sloping wall, the thickness and separation of the L-shaped elements, and the overall height of the connection (Table 5.1).

Table 5.1. Geometries and material parameters of tensile connection models in the parametric study

Label	1 Angle of sloping wall	2 Thickness of the L-shaped elements	3 Gap between L-shaped elements	4 Height of connection	5 Connection material
Tensile connection					
Benchmark	70	4	14	25	SS235
T1-60	60	-	-	-	-
T1-65	65	-	-	-	-
T1-75	75	-	-	-	-
T1-80	80	-	-	-	-
T2-3	-	3	-	-	-
T2-3.5	-	3.5	-	-	-
T2-4.5	-	4.5	-	-	-
T2-5	-	5	-	-	-
T3-10	-	-	10	-	-
T3-12	-	-	12	-	-
T3-16	-	-	16	-	-
T3-18	-	-	18	-	-
T4-15	-	-	-	15	-
T4-20	-	-	-	20	-
T4-30	-	-	-	30	-
T4-35	-	-	-	35	-
T5-Aluminium	-	-	-	-	Aluminium
T5-S275	-	-	-	-	S275
T5-S375	-	-	-	-	S375
T5-S420	-	-	-	-	S420

In contrast to tensile connections, notable phenomena such as buckling and slight bending at the ends of the male connectors were constantly identified. These observations guided the focus of the parametric study on shear connections, which concentrated on form factors

linked to these critical areas. Variables studied included the curvature and thickness of the deformable steel plate, the depth of the end sunken, the height of the connection, and the width of the middle support in the male connector. Comprehensive details of each model are summarised in Table 5.2.

Table 5.2. Geometries and material parameters of shear connection models in the parametric study

Label	1 Curvature of the cantilevered steel band	2 Thickness of the cantilevered steel band	3 Height of connection	4 Depth of the end suck	5 Connection material	6 Width of middle support
Shear Connection						
Benchmark	550	2	25	10	SS235	20
S1-450	450	-	-	-	-	-
S1-500	500	-	-	-	-	-
S1-650	650	-	-	-	-	-
S1-700	700	-	-	-	-	-
S2-1	-	1	-	-	-	-
S2-1.5	-	1.5	-	-	-	-
S2-2.5	-	2.5	-	-	-	-
S2-3	-	3	-	-	-	-
S3-15	-	-	15	-	-	-
S3-20	-	-	20	-	-	-
S3-30	-	-	30	-	-	-
S3-35	-	-	35	-	-	-
S4-8	-	-	-	8	-	-
S4-9	-	-	-	9	-	-
S4-11	-	-	-	11	-	-
S4-12	-	-	-	12	-	-
S5-Aluminum	-	-	-	-	Aluminum	-
S5-S275	-	-	-	-	S275	-
S5-S375	-	-	-	-	S375	-
S5-S420	-	-	-	-	S420	-
S6-10	-	-	-	-	-	10
S6-15	-	-	-	-	-	15
S6-25	-	-	-	-	-	25
S6-30	-	-	-	-	-	30

5.3.2 Parametric study outcome

5.3.2.1 Tensile connection – Initial study

To facilitate the quantification of the three-stage performance of tensile connections, the force-displacement curves derived from these connection models were linearised for

simplicity. As depicted in Figure 5.15, the tensile connection's response can be characterised by four key parameters as follows: elastic stiffness (k_{el}), yield strength (F_y), plateau stiffness (k_{pl}), and densification stiffness (k_d). In some specimens, a slight increase in resistance was observed during the plateau stages, attributed to the locking effect caused by friction at the contact point between the end of the L-shaped element and the surface of the female sloping wall. This locking effect, while beneficial to mechanical performance, is dependent on the length of the L-shaped element's bottom part and was not factored into the parametric study's analysis. Consequently, a linearised and simplified model of these responses was employed in the subsequent study to enable a more straightforward demonstration and comparison (Figure 5.15).

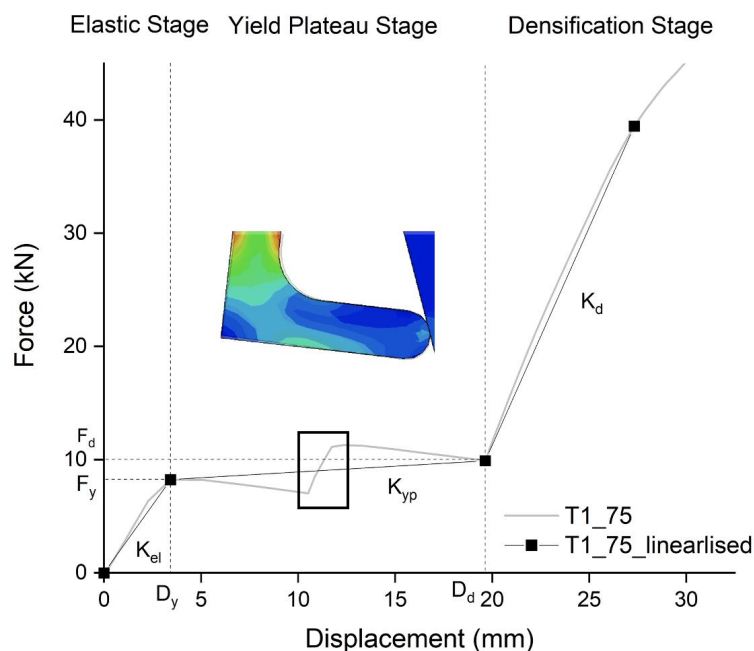


Figure 5.15. Linearisation of tensile connection response.

The outputs of the initial parametric study of tensile connection are shown in Figure 5.16. The investigation revealed that the various parameters examined exert differing degrees of influence on the elastic stiffness (k_{el}) and strength of connections (f_y), while the stiffness in both the plateau stage (k_{pl}) and the densification stage (k_d) remained relatively uniform across most models. An exception was observed in parameter T5, which employed aluminium with a different modulus of elasticity and led to significantly different connection behaviours. This uniformity can be attributed to the fact that, in the plateau and densification stages, the deformation behaviours of the connections are consistent among all

models. This involves the yielded male connectors with progressive plastic deformation and sliding within the female connector during the plateau stage, followed by bottom plate bending in the densification stage of the male connectors. These two deformation modes are primarily influenced by geometric and material factors in the female connectors and bottom plates, which were not the central focus of this parametric study.

Among the parameters analysed, T1 (Angle of sloping wall) predominantly influences the k_{el} and the f_y of connectors. These properties were observed to increase as the wall slope decreased. The angle of the wall modifies the geometric interaction between the L-shaped element and the wall, thereby affecting load distribution and transfer to the L-shaped element. This slope decides both the direction of force exerted on the L-shaped element by the female connector and the sliding extent of the male connector within the female connector, influencing the overall connection properties. A steeper slope enhances the reaction force's perpendicular component against the L-shaped element, increasing the structure's capacity to withstand vertical loads and increasing frictional resistance. However, it is crucial to note that with a wall slope exceeding 80 degrees (Figure 5.17.a), approximating vertical alignment, there is a reduction in moment resistance at the base of the wall. Consequently, the load-bearing component shifts from the L-shaped element in the male connector to the wall in the female connector (Figure 5.17.a). Thus, a steeper wall slope creates a more supportive and restrictive environment for the L-shaped element, significantly affecting the connector's performance.

The thickness of the L-shaped element (T2) in the male connector is notably the most influential factor in determining connection performance (Figure 5.17.b), as it directly determines the element's cross-sectional area responsible for undergoing deformation. Conversely, the gap between L-shaped elements (T3) demonstrates a negligible impact on connection properties, suggesting that this gap primarily serves to accommodate the horizontal displacement of the L-shaped element (Figure 5.17.c). The height of connection (T4) is proved to have considerable impacts on not only the elastic stage, but also the plateau stage. Connectors with an increased T4 value, featuring taller L-shaped elements, have a higher tendency to bend under compression from the female connector, resulting in reduced yield strength. In addition, taller female connectors provide greater vertical space for male connector movement, thus delaying the densification stage (Figure 5.17.d). However, an excessively reduced connector height results in a shorter L-shaped element in the male

connector, potentially becoming too rigid and limiting the achievement of a damage-controlled effect. In the cases of minimum height (T4-15) (Figure 5.17.d), most deformation occurred at the steel plate, and the model was halted due to excessive deformation. While different materials were also identified to have significant impact on the overall connection properties, the deformation modes remained largely consistent, as indicated in Figure 5.17.e. This suggests that deformation modes are predominantly governed by the geometric design of the connection.

Given these observations, parameters T1 and T4 were chosen for in-depth analysis in the detailed parametric study. Despite the evident impact of T2, its influence is relatively linear and minor adjustments, such as around 0.1mm, are unrealistic to practical manufacturing, leading to its exclusion from further study.

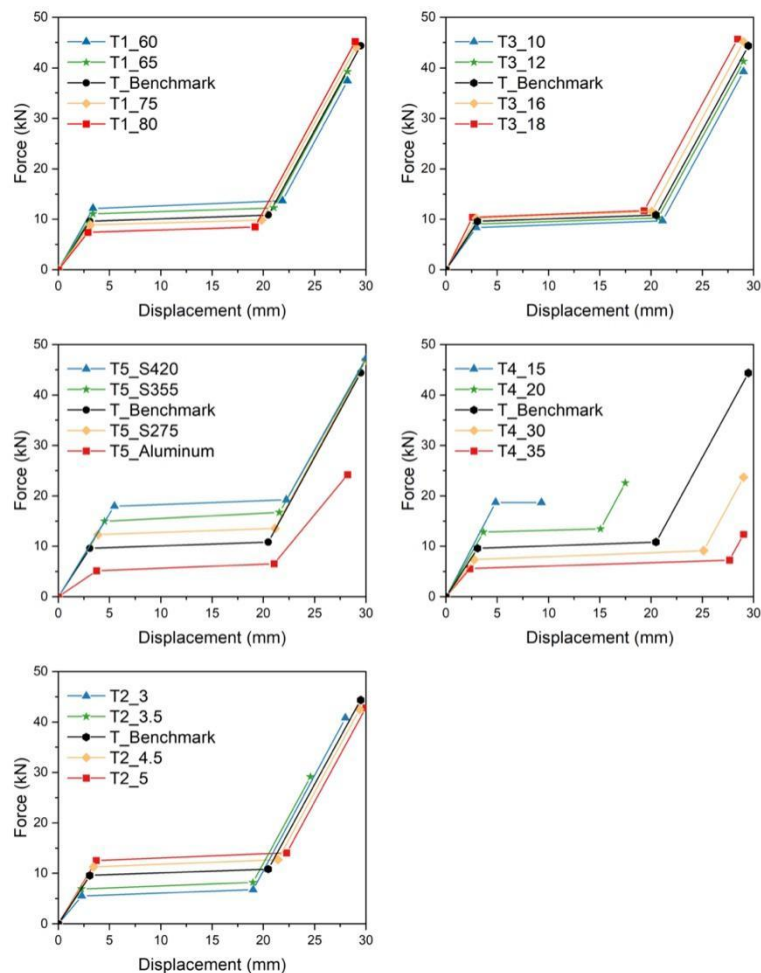
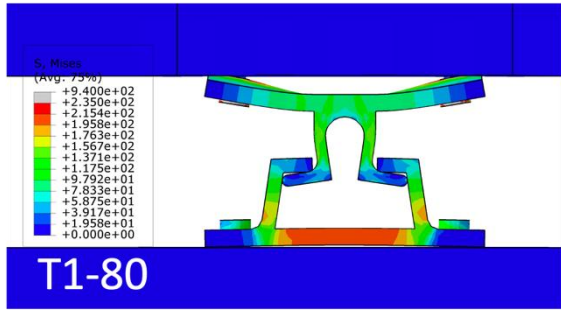
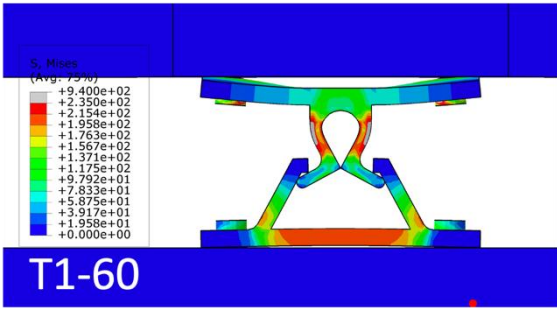
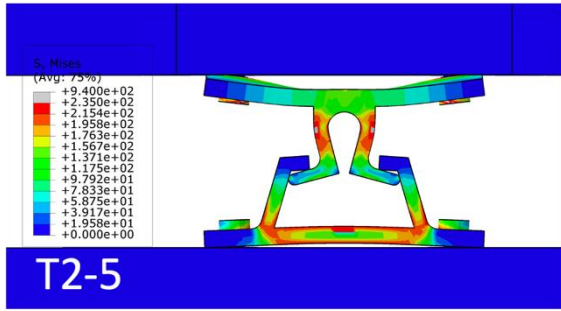
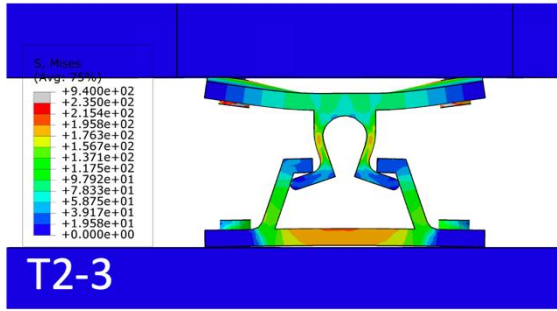


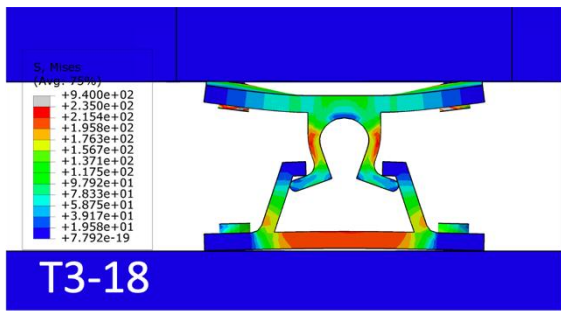
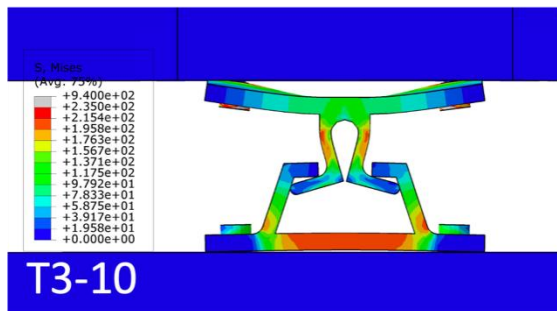
Figure 5.16. Initial parametric study on tensile connections for parameter T1-T5



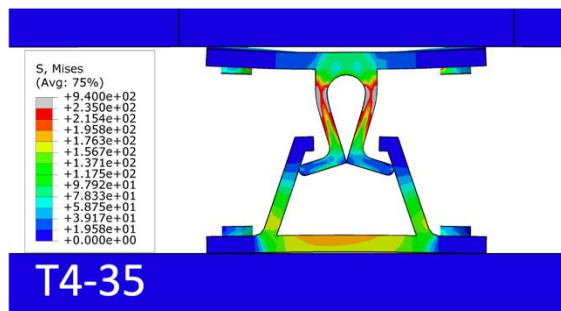
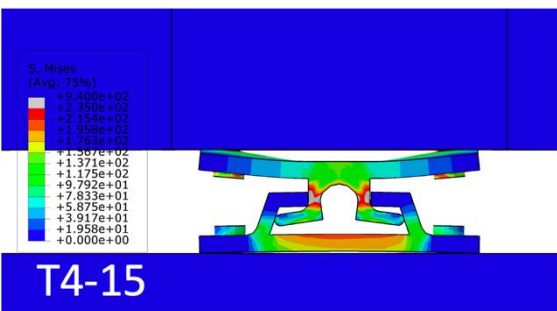
(a)



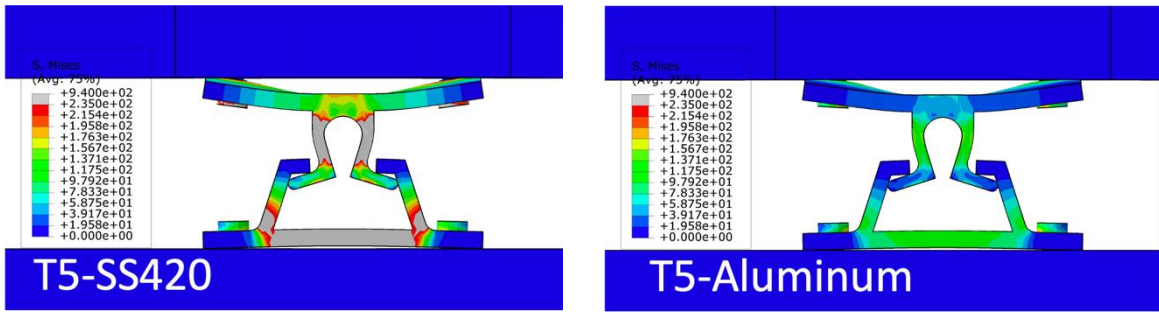
(b)



(c)



(d)



(e)

Figure 5.17. Deformed shapes of tensile connection at 25 mm vertical displacement with the minimum and maximum values in parameter (a) T1, (b) T2, (c) T3, (d) T4, (e) T5

5.3.2.2 Tensile connection – Detailed study

Figure 5.18 demonstrates the relationship between parameters T1 and T4 and their impact on connection strength. The data clearly indicate a negative correlation for both parameters. A comparison of the results from T1 and T4 models reveals that an increase in connection height (T4) significantly diminishes the numerical yield strength of the connection. In contrast, the influence of T1, while still impactful, is comparatively less pronounced. This differential impact highlights the more substantial role that connection height plays in determining the mechanical behaviours of the connection.

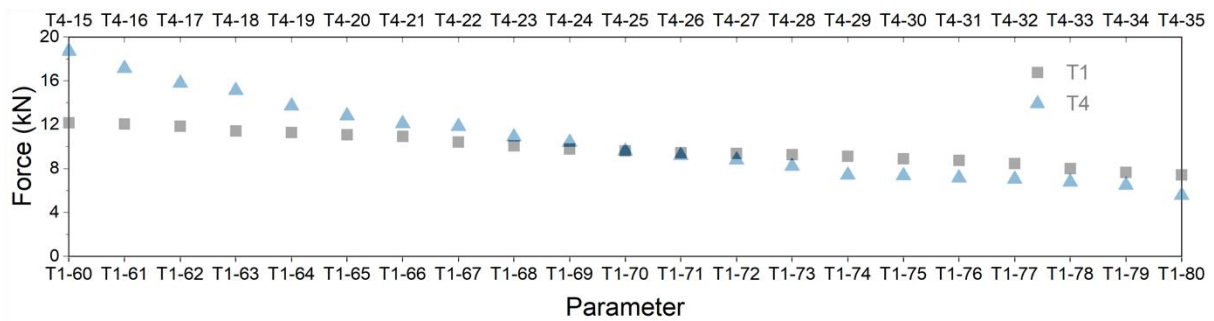


Figure 5.18. Output of detailed parametric on tensile connection

Figure 5.19 provides a comprehensive summary of how connection stiffness varies in response to changes in parameter T1 and T4. A key observation from the analysis is that the stiffness values during the plateau and densification stages remain constant across all models, indicating that these stiffness stages are not influenced by the geometric factors of the examined parts of the connections. In all model, the stiffness during the densification stage, which corresponds to the bending stiffness of the bottom plate, consistently registers as the highest. Conversely, the plateau stage, characterised by the sliding of the yielded male

connector within the female connector, exhibits the lowest stiffness, approaching an approximate value of zero. Furthermore, it is observed that only the elastic stiffness of the connections is affected by changes in parameters T1 and T4. Increases in the values of both T1 and T4 are correlated with a more pronounced reduction in the connection's elastic stiffness. This relationship highlights the sensitivity of the connection's initial load-bearing capacity to these specific geometric parameters.

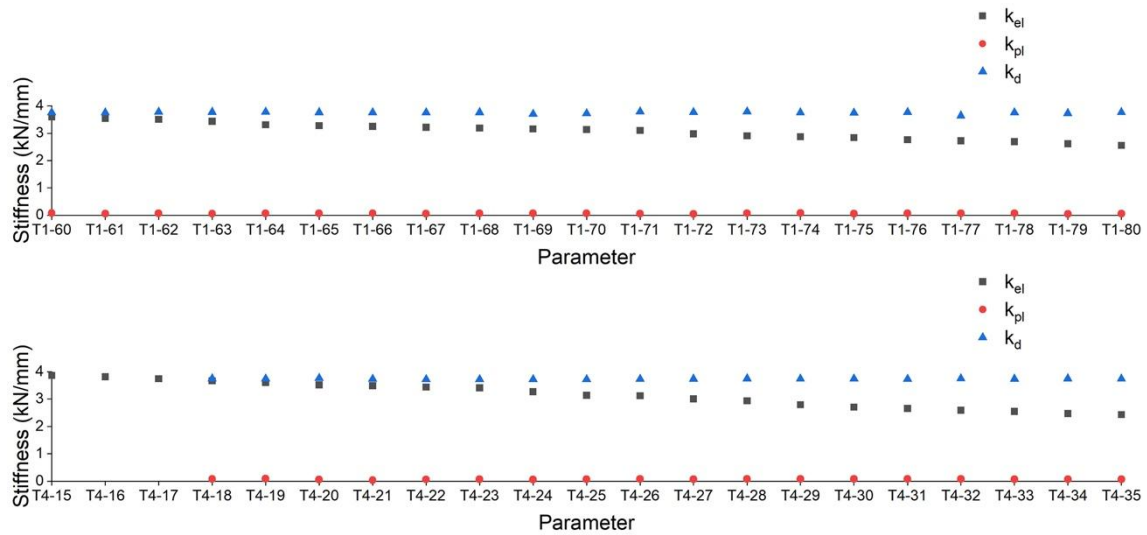


Figure 5.19. The changes in connection stiffness at different stages with the changes in parameters T1 and T4

5.3.2.3 Shear connection - Initial study

As buckling is often associated with brittle failure, only the strength at the initial bifurcation point was considered in this parametric study for shear connection (Figure 5.20). The initial analysis of shear connections revealed failure modes that aligned consistently with experimental findings: buckling of the cantilevered steel band occurred without any deformation in the female connectors, screws, or timber.

Figure 5.20 illustrates that, the curvature of the cantilevered steel band (S1) exhibited minimal influence on the mechanical properties of the shear connections. Its influence is more pronounced in determining the spacing between the symmetric steel bands (Figure 5.21.a). The connector with bigger curvature has larger gap between steel bands, which can extend the second path at post-buckling stage and therefore delay the attainment of the second bifurcation point.

The thickness of the steel band (S2) was found to have a substantial impact onto both the buckling and post-buckling behaviours of the connections (Figure 5.21.b). Notably, the critical load demonstrated a linear relationship between the thickness of the steel band. The model with the thinnest steel band, labelled as S2-1, exhibited the lowest critical load and stiffness among the models of S2 series. Additionally, this model also records the lowest second critical load, exhibiting only minimal buckling effects with reduced level of strength reduction after both bifurcation points.

Initial modifications to parameter S3 (connection height) were positively associated with an increased yield strength; however, this positive correlation diminished and became negative with the modification development. This inverse relationship became apparent when exceeding a connection height of 30mm, as seen in models S3-30 and S3-35, where a subsequent decline in yield strength was observed. This is because that, an increased connection height contributes to the slenderness of the central cubic support, precipitating bending in this structure along with steel band buckling (Figure 5.21.c).

In contrast, parameter S4 demonstrated a negligible impact on the mechanical performance of the connectors with similar stress distribution across all models (Figure 5.21.d), suggesting that the end of the connector does not significantly contribute to its deformation. Regarding the material composition (S5), a positive correlation was observed between the connector's yield strength and its material properties. Connectors fabricated from different steel grades maintained similar stiffness levels, attributable to consistent Young's modulus values, whereas aluminium connectors exhibited a marked reduction in stiffness, which can be attributed to a lower Young's modulus (Figure 5.21.e). The parameter S6 represents the overall changes in cantilevered steel band length by changing the size of cubic middle support. Figure 5.21.f indicates that, this parameter significantly affected the critical load, stiffness and displacement at the second loading path, as well as the second bifurcation point, in a non-linear manner. Owing to these insights, parameters S3 and S6 were specifically chosen for the detailed parametric study, while other parameters were neglected given the focus on practical applications, such as the use of common metal materials and avoidance of extremely fine thicknesses.

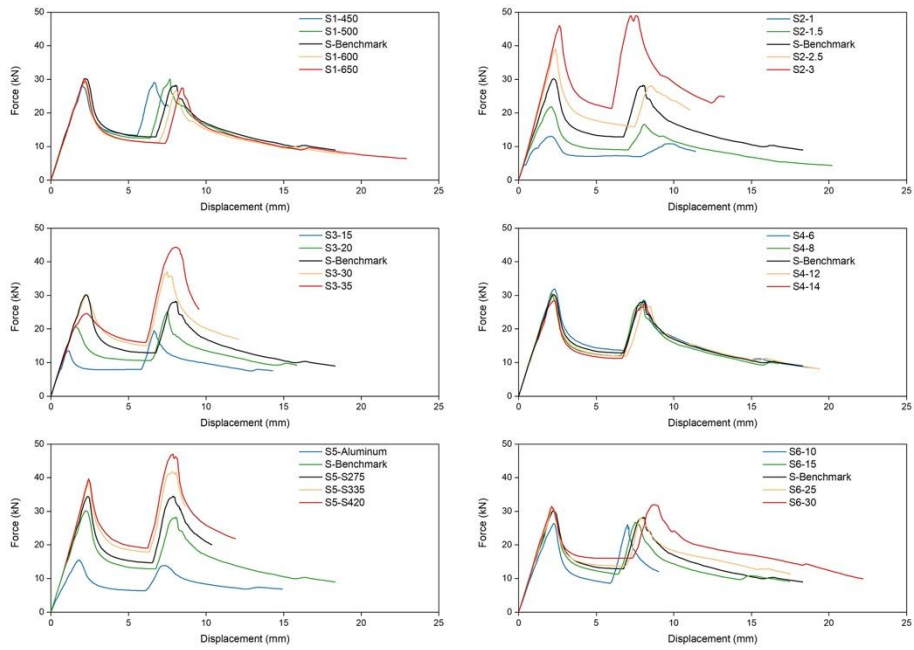


Figure 5.20. Initial parametric study on shear connections for parameter S1-S6

It was also noted that variations in the geometric parameters within the buckling zone influenced the system's damage-control capabilities (Figure 5.21). Specifically, models equipped with a stronger cantilevered steel band, such as S2-3, S5-SS420, and S6-30, exhibited higher stress in the bottom plate around the screw holes during buckling events. Conversely, models with a less robust cantilevered steel band, including S2-1, S3-15, and S5-Aluminum, revealed a superior damage-control capacity, maintaining a stress-free state in the bottom plate.

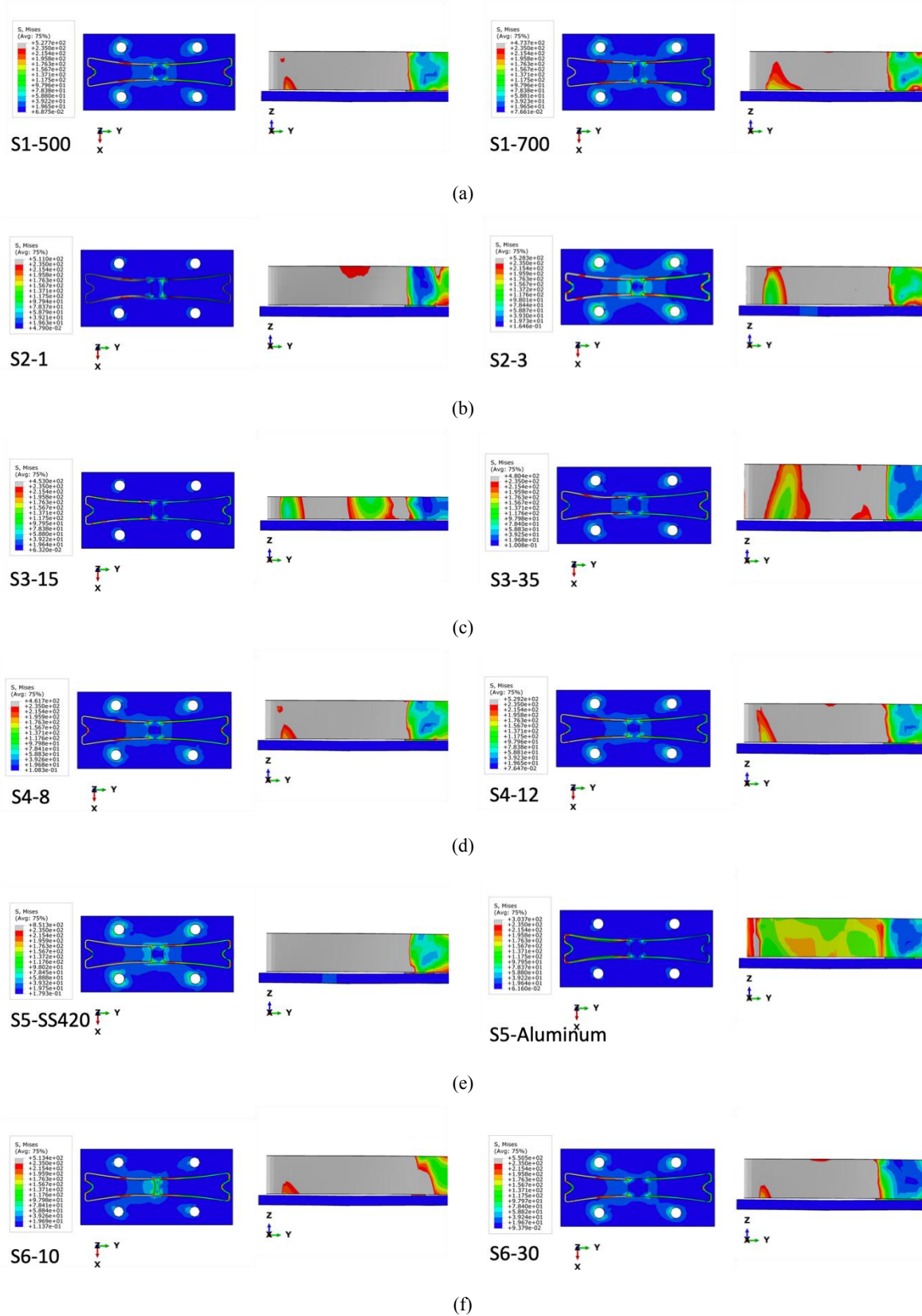


Figure 5.21. The buckled shape of shear connection at the first buckling point with the minimum and maximum values in parameter (a) S1, (b) S2, (c) S3, (d) S4, (e) S5, (f) S6

5.3.3.4 Shear connection - Detailed study

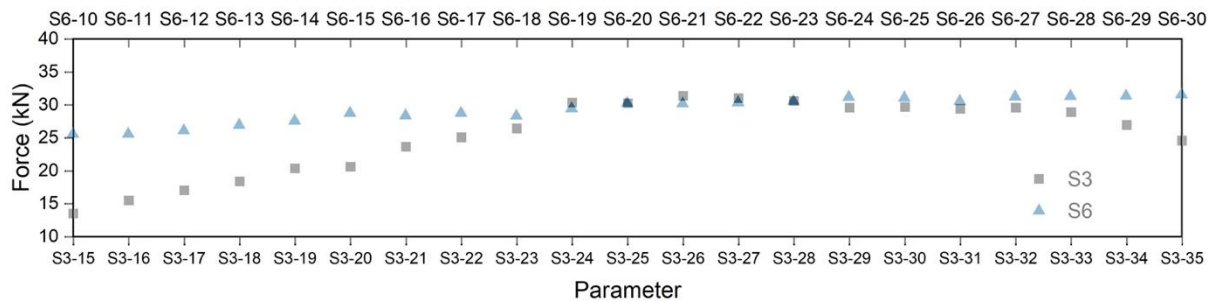


Figure 5.22. Output of detailed parametric on shear connection

Figure 5.22 plots the relationship between the buckling force in shear connections and the variations in parameters S3 (ranging from S3-15 to S3-35) and S6 (from S6-10 to S6-30) generated in the detailed parametric study. The results indicate that models with changes in S6 consistently registered higher buckling force values compared to those with variations in S3. However, the sensitivity of the connection strength to changes in S6 was less pronounced than that in S3. An increase in S6 demonstrated a positive but relatively modest correlation with the critical load. Conversely, parameter S3 initially showed a positive correlation with the critical load, which plateaued at models S3-26, S3-27, and S3-28, and subsequently inverted to a negative correlation once the connection height exceeded 29 mm (S3-29).

5.3.4 Conclusion

The extensive initial and detailed parametric studies conducted on the proposed interlocking shear and tensile connections have significantly enhanced the understanding of how various geometric and material parameters interact to determine the mechanical performance of these interlocking systems. The initial studies accurately evaluated the impacts of different parameters, offering valuable insights into the critical aspects influencing connection behaviours. The detailed parametric study provided further insights into the selected parameters for both tensile and shear connections. By constructing a more detailed dataset of how these parameter influences connection performance, the detailed parametric studies allow for the development of more sophisticated analytical models.

5.4 Analytical Work

To facilitate the capacity design of connections for achieving a damage-controlled effect, an analytical study was conducted with the objective of developing equations to predict

connection properties accurately. This study strategically incorporated critical parameters identified from the parametric study into the analytical models, while factors assessed as having minimal influence on the connection properties were considered to have a minor impact on the accuracy of analytical models and were excluded for the sake of simplification in the analytical modelling process.

5.4.1 Tensile connection

In the development of analytical models for the interlocking tensile connection, three deformation modes were considered (Figure 5.23): (i) the inward bending of the L-shape element in the male connector (deformation 1), (ii) the outward bending of bearing walls in the female connectors (deformation 2), and (iii) the bending of bottom plate (deformation 3). These deformation modes are associated with the cross-sectional properties of different parts in the interlocking tensile connection (Figure 5.23). For the purpose of simplification in the analytical modelling, these three deformation modes were treated as independent phenomena.

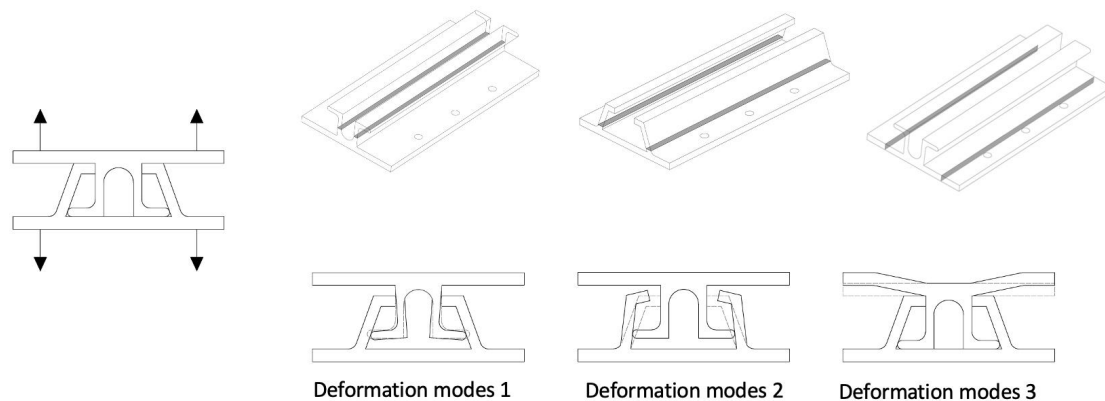


Figure 5.23. Different deformation modes considered in the interlocking tensile connector

Deformation mode 1:

In the deformation mode 1 (Figure 5.24), which is considered as the favourable deformation mode of tensile connection, only in-plane bending of cantilevered L-shaped elements around the bottom of connector (M_{male}) was considered. The L-shaped element, inclusive of its extended foot, was assumed to remain undeformed, given that torsional and axial deformations are considered negligible. Therefore, the connection capacity is governed by the bending capacity of the straight section of the L-shape element in

male connector (Figure 5.24.b). Taking into account the interaction with the female connector and the fillet between the L-shaped element and the bottom plate, the L-shaped element was simplified as a fixed-end beam at one end, while being subjected to loading at the opposite end in the analytical model (Figure 5.24.c).

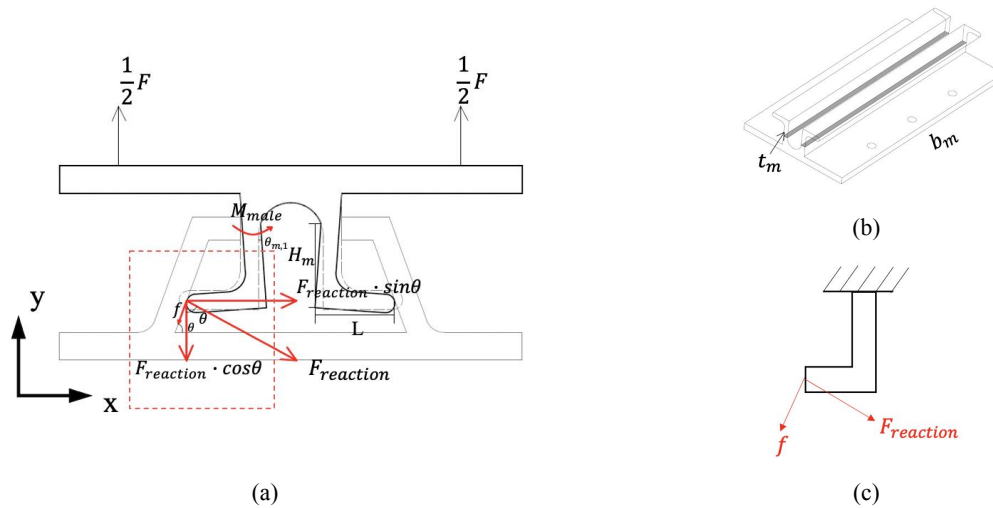


Figure 5.24. Force analysis of tensile connection under tension for deformation 1: (a) force analysis; (b) illustration of yielding plane; (c) simplified analytical model

According to the force analysis illustrated in Figure 5.24, the reaction force on the tensile male connector can be calculated as:

$$f \cdot \sin\theta + F_{reaction} \cdot \cos\theta = \frac{1}{2}F \quad \text{Equation 5.3}$$

where F is the applied load on the tensile connection, $F_{reaction}$ is the reaction force between the male and female connector, the term θ represents the angle of female connector.

f is the frictional force that can be determined as:

$$f = F_{reaction} \cdot \mu$$

where μ is the coefficient of friction, taken as 0.4 in this study, corresponding to the FE models.

Therefore $F_{reaction}$ can be calculated as:

$$F_{reaction} = \frac{F}{2(\mu \cdot \sin\theta + \cos\theta)}$$

The moment on ‘L-shaped’ element (M_{male}) introduced by the applied external load can be calculated as:

$$\begin{aligned}
M_{male} &= F_{reaction} \cdot \cos\theta \cdot L + F_{reaction} \cdot \sin\theta \cdot H_m + f \cdot \sin\theta \cdot L - f \cdot \cos\theta \cdot H_m \\
&= \frac{F \cdot \cos\theta \cdot L}{2(\mu \cdot \sin\theta + \cos\theta)} + \frac{F \cdot \sin\theta \cdot H_m}{2(\mu \cdot \sin\theta + \cos\theta)} + \frac{F \cdot \mu \cdot \sin\theta \cdot L}{2(\mu \cdot \sin\theta + \cos\theta)} - \frac{F \cdot \mu \cdot \cos\theta \cdot H_m}{2(\mu \cdot \sin\theta + \cos\theta)} \\
&= \frac{F \cdot (\cos\theta \cdot L + \sin\theta \cdot H_m + \mu \cdot \sin\theta \cdot L - \mu \cdot \cos\theta \cdot H_m)}{2(\mu \cdot \sin\theta + \cos\theta)}
\end{aligned} \tag{Equation 5.4}$$

L and H_m are the length and the height of L-shaped element in the male connector, as illustrated in Figure 5.24.

$$M_{yield,1} = S_{yield} \cdot \sigma_y = \frac{b_m t_m^2}{6} \cdot \sigma_y$$

where $M_{yield,1}$ is the yielding moment of the cross section when the yielding strength of connection $F_{yield,1}$ is reached; $S_{yield} = \frac{bh^2}{6}$ is the elastic section modulus of a rectangular section; b_m and t_m are the breadth and thickness of the L-shaped element; and σ_y is the yield stress of the connector material.

At the connection yielding point, $M_{male} = M_{yield,1}$, therefore the yield strength of deformation mode 1 ($F_{yield,1}$) can be calculated as:

$$F_{yield,1} = \frac{b_m t_m^2 \cdot \sigma_y \cdot (\mu \cdot \sin\theta + \cos\theta)}{3 \cdot (\cos\theta \cdot L + \sin\theta \cdot H_m + \mu \cdot \sin\theta \cdot L - \mu \cdot \cos\theta \cdot H_m)} \tag{Equation 5.5}$$

Deformation mode 2:

The deformation mode 2, as illustrated in Figure 5.25.a, is featured by the opening-up of the female connector. This movement is initiated by the reaction load from the male connector, causing the sloping wall of the female connector to rotate outward around its connection point with the bottom plate (M_{female}). In modelling this deformation, the inclined wall was represented as a fixed, L-shaped structure (Figure 5.25.c), with the load applied

perpendicular to its vertical section. Similar to the analytical model of deformation mode 1, inherent deformation of the inclined wall itself was considered negligible and thus excluded from the analytical model.

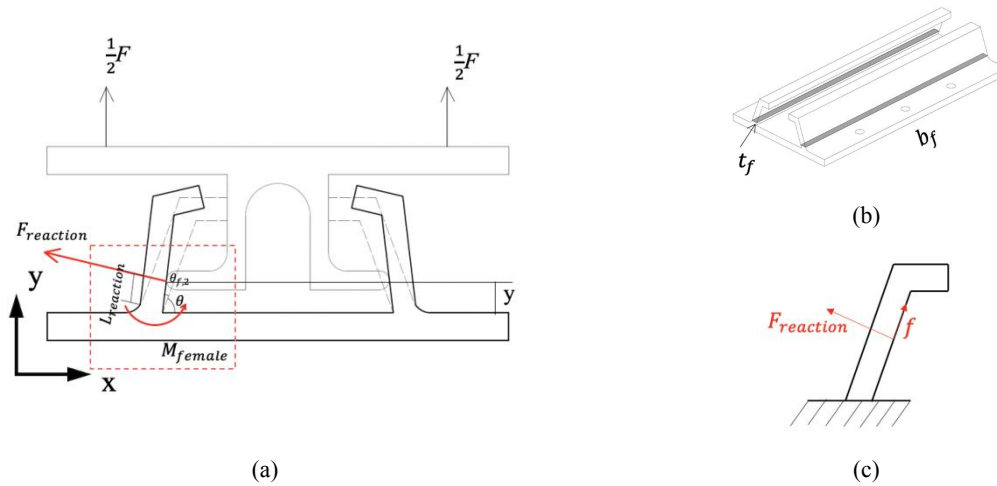


Figure 5.25. Force analysis of vertical connection under tension for deformation 2: (a) force analysis; (b) illustration of yielding plane; (c) simplified analytical model

According to Figure 5.25, Where the reaction force $F_{reaction}$ from male connector can be calculated as:

$$F_{reaction} = \frac{F}{2(\mu \cdot \sin\theta + \cos\theta)}$$

As the point of load application shifts along with the vertical displacement of the male connector, the moment exerted at the base of the sloping wall becomes a function of the male connector's vertical movement, denoted as y . So M_{female} can be calculated as:

$$M_{female} = F_{reaction} \cdot \frac{y}{\sin\theta}$$

$$= \frac{F \cdot y}{2 \sin\theta (\mu \cdot \sin\theta + \cos\theta)}$$

$$M_{yield,2} = S \cdot \sigma = \frac{b_f t_f^2}{6} \cdot \sigma_y$$

Where $M_{yield,2}$ is the yielding moment of the cross section when the yielding strength of deformation mode 2 ($F_{yield,2}$) is reached. S is the elastic section modulus of a rectangular

section; b_f and t_f are the breadth and thickness of the sloping wall. Therefore, the yielding strength $F_{yield,2}$ can be calculated as:

$$F_{yield,2} = \frac{b_f t_f^2 \cdot \sigma_y \cdot \sin\theta}{3y} \cdot (\mu \cdot \sin\theta + \cos\theta)$$

As the deformation 2 is considered as an unfavourable mode in the connection design, in capacity design, consideration is given to both the maximum and minimum yield strengths of the female connector, with particular emphasis on the minimum yield strength:

$$F_{yield,2,max/min} = \frac{b_f t_f^2 \cdot \sigma_y \cdot \sin\theta \cdot (\mu \cdot \sin\theta + \cos\theta)}{3 \cdot y_{max/min}} \quad \text{Equation 5.6}$$

Where y_{min} is the minimum distance between the load application point and the bottom of the female connectors (at connection bottom); y_{max} denotes the maximum distance, occurring at the top of sloping wall when the male connector reaches the top of female connector.

Deformation mode 3:

The deformation mode 3, as illustrated in Figure 5.26.a, considers the bending of the bottom plate of the tensile male connector. This particular mode of deformation typically occurs in two scenarios: first, when the connector becomes excessively rigid during the elastic stage, and second, during the densification stage, where the male connector reaches the top of the female connector stop sliding. To simplify the analytical model, this deformation is represented as a cantilevered beam with a fixed end, experiencing a centrally applied moment (Figure 5.26.c).

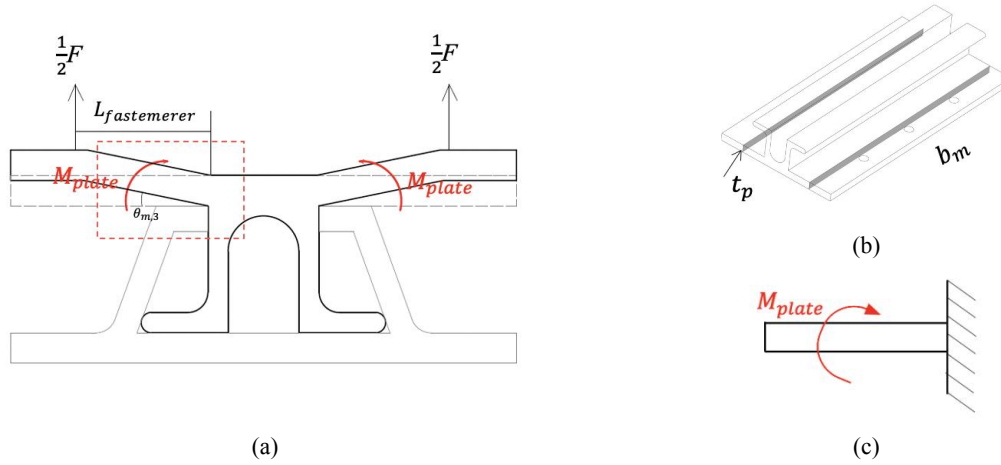


Figure 5.26. Force analysis of vertical connection under tension for deformation 3: (a) force analysis; (b) illustration of yielding plane; (c) simplified analytical model.

$$M_{plate} = \frac{F}{2} \cdot L_{fastener}$$

Where F is the applied load, $L_{fastener}$ is the distance from the fixed end to the fastener's location, where the load is applied. Therefore, yielding strength of bottom plate ($F_{yield,3}$) can be calculated as:

$$M_{yield,3} = S \cdot \sigma = \frac{b_m t_p^2}{6} \cdot \sigma_y$$

$$F_{yield,3} = \frac{b_m t_p^2 \cdot \sigma_y}{3 \cdot L_{fastener}}$$

Equation 5.7

5.4.3 Analytical model validation

Figure 5.27 presents a comprehensive overview of the validation process for the analytical models of the interlocking tensile connection, employing FEA data, which focused on the models related to parameter T1 and T4. In these models, the analytically estimated strength for the mode 3 (bottom plate bending, $F_{yield,3}$), was consistently the highest. This was followed by the estimated strength for mode 2 (sloping wall opening, $F_{yield,2}$). Notably, the strengths for these two modes exceeded those calculated for deformation mode 1 ($F_{yield,1}$), both in analytical and numerical assessments. This trend aligns with the damage localisation phenomena observed in the FE models, proving the effective application of capacity design principles in the connectors. Figure 5.27 further reveals that the analytical models, though tending to provide conservative estimates of strength for interlocking tensile connections,

successfully capture the negative correlations associated with both parameters T1 and T4. Furthermore, these analytical models exhibit higher sensitivity to variations in parameter T4 as opposed to T1, which is in alignment with the behavioural patterns in the FE models.

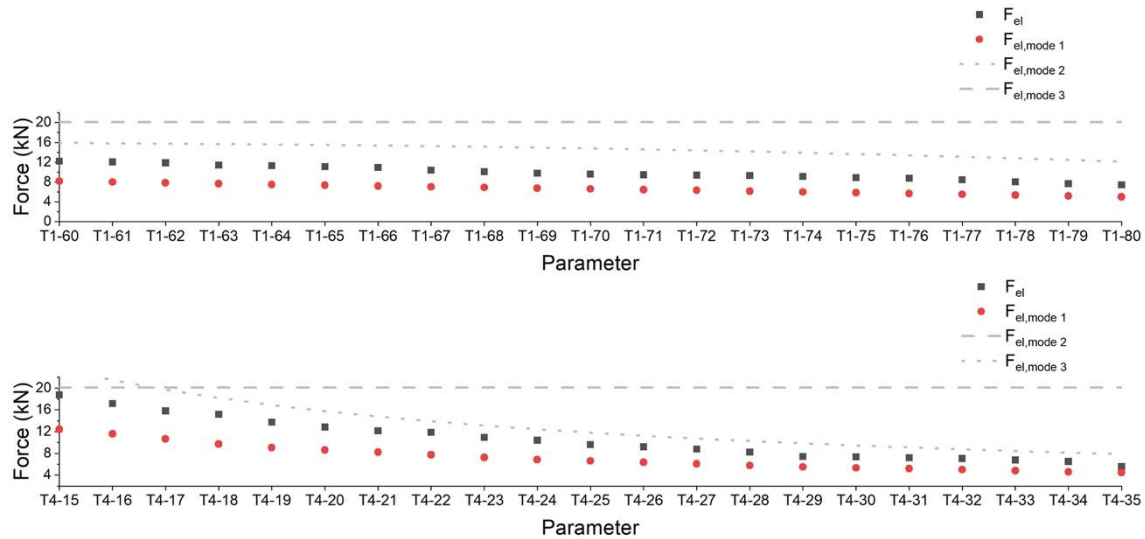


Figure 5.27. Comparison between analytical and FEM results of parameters T1 (top) and T4 (bottom)

Figure 5.28 shows an evaluation of the accuracy of the analytical model in calculating the yield strength of tensile connections. The data presented in the Figure 5.29 indicate that the simplified techniques employed in the model tend to result in the underestimation of the connection properties, with an average error in the detailed parametric study of around 48%. The extent of this error varied, with the maximum deviation not exceeding 56% and a minimum error around 34%. Such underestimation is largely attributable to the complexities of interactions and the nonlinear material response inherent in the studied connection type.

Furthermore, it is observed that the analytical models demonstrate increased accuracy in their predictions when corresponding to numerical models exhibiting more pronounced damage localisation, as seen in examples like T4- 29-35. This enhanced accuracy highlights the effectiveness of the analytical models in scenarios where deformation localisation is clearly defined, and interactions within other connection components are avoided. However, this trend tends to diminish when the strength of components in deformation mode 1 is comparable to that of modes 2 and 3. In such instances, as observed in models T4- 15-20, other elements of the connection, notably the female connectors and the bottom plates, also experience significant deformation. This results in a notable disparity between the predicted and actual behaviours. The primary cause for these discrepancies can be traced back to the underlying assumption in the analytical models that treats the three deformation modes as

independent entities. This assumption, while simplifying the analytical process, can lead to a misrepresentation of the interaction between different connection components under various loading conditions, thus contributing to the noted discrepancies in yield strength estimation.

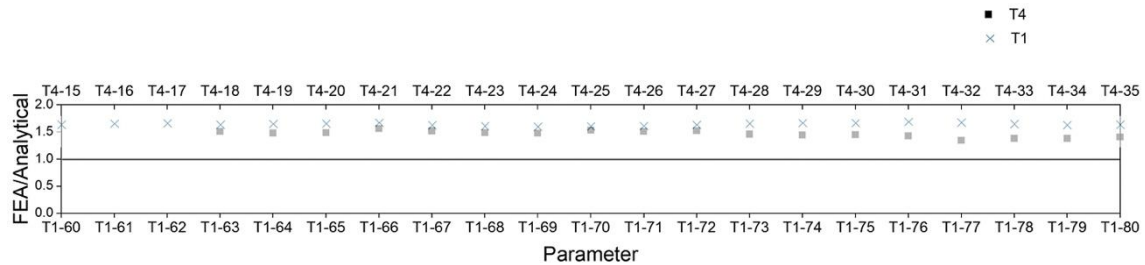


Figure 5.28. Comparison of FE and analytical connection detailed key parameter for the tensile connection

5.4.4 Shear connection

The parametric study of the shear connection identified key parameters - S2 (thickness of the cantilevered steel band), S3 (height of connection), S5 (steel material), and S6 (length of middle support) — as having a significant impact on connection behaviours. These parameters were thus selected for inclusion in the analytical model of the shear connection. Given the symmetric configuration of the cantilevered steel beam, the model simplifies one quarter of the curved steel band in the shear connection as a loaded cantilevered thin-walled plate. This plate is modelled with one end pinned and the other fixed, as depicted in Figure 5.29. The boundary conditions for this simplification incorporate the fillet at the joint between the cantilevered thin-walled plate and the middle support. Additionally, consideration is given to the compressive loading applied on top of the plate and the pinned support at the side, exerted by the female connector.

As illustrated in Figure 5.29, the specific curvature of the shear connection creates a distance between the direction of the applied load and the centroid of the cross-section in the male connector. This spatial arrangement guides the direction of buckling, fostering predictable buckling behaviours. The analytical model thus aims to accurately capture the buckling of the shear connection system, considering the critical parameters identified in the study.

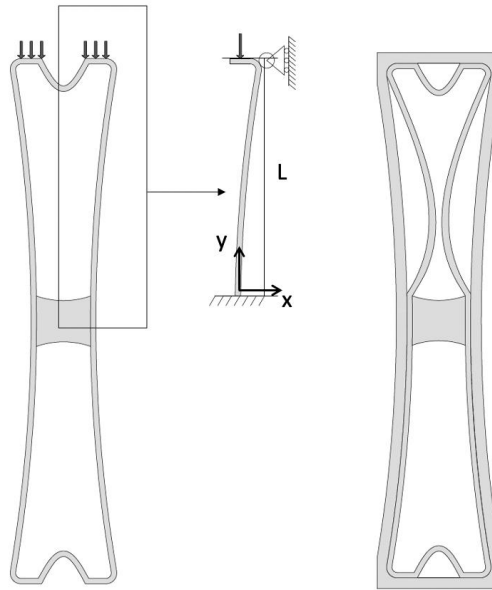


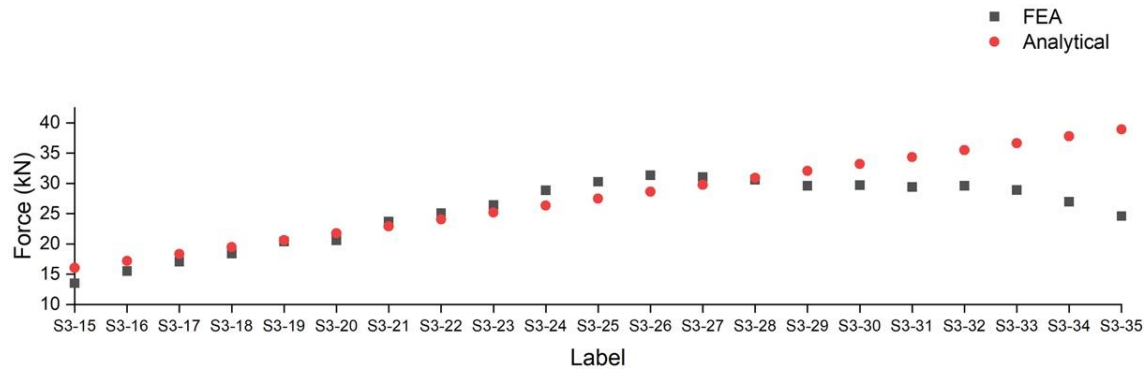
Figure 5.29. Force analysis of shear connection under lateral load

In the analytical models developed, the critical load $F_{cr, s}$, is calculated using established buckling formulas, which take into account the specific boundary conditions outlined in these models. The formula for determining the critical load at the first bifurcation point is given by:

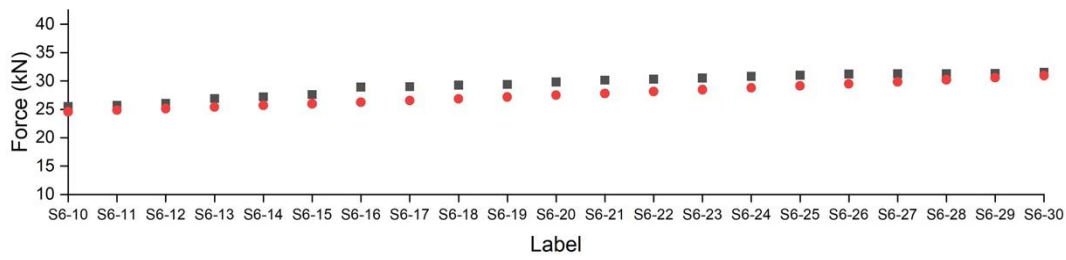
$$F_{cr, s} = \frac{\pi^2 EI}{L_e^2} \quad \text{Equation 5.8}$$

$$L_e = 0.8 \cdot L$$

Where EI represents the product of the modulus of elasticity and the moment of inertia of the cross-section, and L_e , the effective length factor, is defined as $0.8 \cdot L$ for the influence of the simplified boundary conditions on the effective length; L represents the original length of the proposed buckling model.



(a)



(b)

Figure 5.30. Comparison between analytical results and FEM in (a) parameter S3 and (b) parameter S6

Figure 5.29 presents the results of a comparative analysis conducted between numerical models and the proposed analytical models for shear connections. This analysis reveals that the analytical model is capable of accurately predicting the critical load for these connections. Moreover, the model successfully captures the relationship between the critical load and the changes in design parameters, along with a degree of conservatism. Specifically, in the S6 series of models, there was a noticeable increase in the estimated strength corresponding to increments in the parameter. This trend is consistent with observations from the numerical models, suggesting a reliable alignment between the two approaches. The enhancement in critical load can be attributed to the increase in the length of the middle support (S6), which results in a shorter span for the cantilevered thin-walled element. Consequently, this structural change leads to an increase in the critical load, as effectively demonstrated by the analytical equation.

For connections involving parameter S3 (height of connections), the strength initially exhibits an upward trend with increasing height. However, upon reaching a connection height of 26mm, equivalent to a slenderness ratio of 1.33, the estimated resistance of the connection begins to decrease as the height continues to increase. This decline in resistance is attributed to the increased slenderness ratio of the middle cubic elements, which leads to their bending

in conjunction with the buckling of the thin-walled structures. Consequently, this results in a reduction in both the stiffness and strength of the connection.

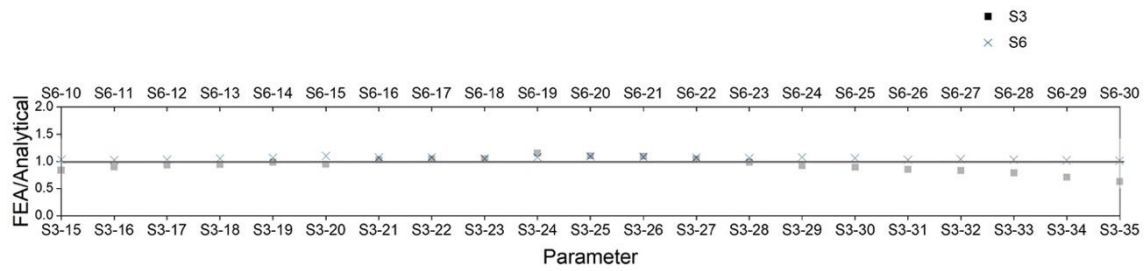


Figure 5.31. Performance of the analytical methods in predicting the yield strength of shear connection

Figure 5.31 shows an evaluation of the analytical model’s ability to calculate the critical strength for the shear connections. The data from the Figure 5.32 reveals that the simplified buckling model employed tends to result in underestimations when determining the connection properties. On average, the error in estimating the critical load was found to be approximately 6%, with the maximum deviation not exceeding 10%. This relatively low margin of error indicates a reasonable level of accuracy in the model's predictions, proving the model’s effectiveness in approximating critical load values despite the simplifications, highlighting its utility in practical applications.

5.5 Capacity design for damage-controlled in interlocking connection

As previously discussed in Section 3.2.1, capacity design employed in the proposed interlocking connection focuses on redirecting the source of ductility to the additional 3D interlocking connectors, particularly the male connectors, to facilitate a damage-controlled effect. This objective is achievable by calibrating the yield strength of the male connectors to be lower than that of their corresponding female connectors and self-tapping screws, using appropriate overstrength factor.

In the tensile connections, capacity design is applied at two levels: first, between the connection bottom plate and the surrounding screws (Steel-to-timber composite connections, STCs), and between the female and male connectors. The primary level of capacity design is crucial to ensure failure is confined to the interlocking connection rather than occurring in the screws or timber. This is guided by the overstrength factor $R_{t,p}$, and is expressed as:

$$F_{inter,t} \cdot R_{t,1} < F_{STCs, EC5} \tag{Equation 5.9}$$

The secondary level of capacity design aims to localise deformation within the male connector, adhering to a preferred deformation mode. This is achieved by leveraging another overstrength factor, $R_{t,2}$, ensuring the yield strength of the preferred deformation mode ($F_{yield,1}$) is lower than that of the female connector ($F_{yield,2}$) the strength associated with the bending of the bottom plate ($F_{yield,3}$):

$$F_{inter,t} = F_{yield,1}$$

$$F_{yield,1} \cdot R_{t,2} < F_{yield,2/3} \quad \text{Equation 5.10}$$

In the context of shear connections, similar capacity design principles are employed to ensure that buckling is initiated in the male connector:

$$F_{inter,s} = F_{cr,s}$$

$$F_{inter,s} \cdot R_s < F_{STCs, EC5} \quad \text{Equation 5.11}$$

Where $F_{cr,s}$ represents the estimated critical load of the shear connections, and R_s is the overstrength factor for shear connection.

5.5 Conclusion

In depth understanding of connection behaviours is vital for safe and economic design, thus this study presented a comprehensive numerical and analytical study on the proposed interlocking connections. Numerical modelling protocols were first constructed for both shear and tensile connections and validated against experimental results, proving the efficiency of the proposed models in accurately predicting connections' strength and deformation. These models were specifically tailored for the proposed interlocking shear and tensile connections, incorporating modelling methods from published literature and using either nominal or experimentally tested material properties. Thus, they emerge as vital tools that are applicable in the design of the proposed connections with reliable estimations.

Utilising the validated models, an extensive parametric analysis was performed for both shear and tensile interlocking connections with overall 115 models. This analysis revealed that parameters such as thickness, height, and material composition play a pivotal role in dictating

the connections' properties. It was also concluded that the failure modes were consistent throughout the study, yet the predominance of specific deformation modes was influenced by the connectors' geometric designs.

Exploiting the numerically generated results in the parametric analysis, simplified analytical methods for predicting the yield strength of connections across diverse failure modes were proposed. These methods included a series of analytical equations, rooted in the basic geometric and material properties of the connections. By validating the analytical results against the FE models, it is evident that the analytical model is capable of providing accurate estimations, particularly for the connection yield strength. The accuracy of shear connection analytical model was satisfactory with minimum errors, suggesting the uniform and independent nature of the shear connection's deformation mode, which can strongly promote its utilisation in future research as well as in practical structural applications. However, the analytical model for tensile connections, while accurately reflecting the trends in connection properties in relation to geometric factors, presented conservative predictions with notable discrepancies of approximately 50%. While such conservative estimates are beneficial for structural design from a safety standpoint, they could potentially lead to material overutilisation and increased construction costs, necessitating further refinement for practical implementation.

The conducted parametric and analytical study was pivotal in shaping the capacity design in the interlocking connections. It highlights the importance of applying sufficient overstrength in designing connection geometries related to different deformation modes, to achieve an optimal damage-controlled effect. Nonetheless, the identification of suitable overstrength factors for the proposed system requires extensive experimental validation; an aspect limited by the project's constrained timeframe.

The parametric study conducted in this research, while enhancing the understanding of this connection's behaviours, remained limited to the initial unit plate size proposed. The overall length and width of the connection can significantly affect the moment of inertia; a key geometric property influencing a beam's resistance to bending. Future study will extend the parametric to include a variety of connection sizes that meet diverse structural demands. Expanding the scope of the models to predict connection behaviour under varied conditions promises to advance construction practices towards enhanced safety, efficiency, and cost-effectiveness.

5.6 Chapter References

- [5.1] Tomasi, R., Crosatti, A., and Piazza, M., *Theoretical and experimental analysis of timber-to-timber joints connected with inclined screws*. Construction & building materials, 2010. **24**(9): p. 1560-1571.
- [5.2] Hassanieh, A., Valipour, H.R., and Bradford, M.A., Sandhaas, C., *Modelling of steel-timber composite connections: Validation of finite element model and parametric study*. Engineering structures, 2017. **138**: p. 35-49.
- [5.3] Liu, X., Bradford M.A., and Lee M.S.S., *Behavior of high-strength friction-grip bolted shear connectors in sustainable composite beams*. Journal of structural engineering (New York, N.Y.), 2015. **141**(6): p. 4014149.
- [5.4] Dorn, M., *Investigations on the serviceability limit state of dowel-type timber connections*, in *Untersuchungen zum Gebrauchstauglichkeitszustand von Dübelverbindungen im Holzbau*. 2012, 2012. p. III, 187 S., Ill., graph. Darst.
- [5.5] Nassiri, S., Chen, Z., Lamanna, A., Cofer, W. *Numerical simulation of failure mechanism in screw anchors under static tension*. Advances in structural engineering, 2020. **23**(16): p. 3385-3400.
- [5.6] Avez, C, Descamps, T., Serrano, E., Léoskool, L., *Finite element modelling of inclined screwed timber to timber connections with a large gap between the elements*. European journal of wood and wood Products, 2016. **74**(3): p. 467-471.
- [5.7] Xu, B.H., Taazount, M., Bouchaïr, A., Racher, P., *Numerical 3D finite element modelling and experimental tests for dowel-type timber joints*. Construction & building materials, 2009. **23**(9): p. 3043-3052.

Chapter 6 Push Over Analysis – CLT Shear Wall Behaviours Comparative Study

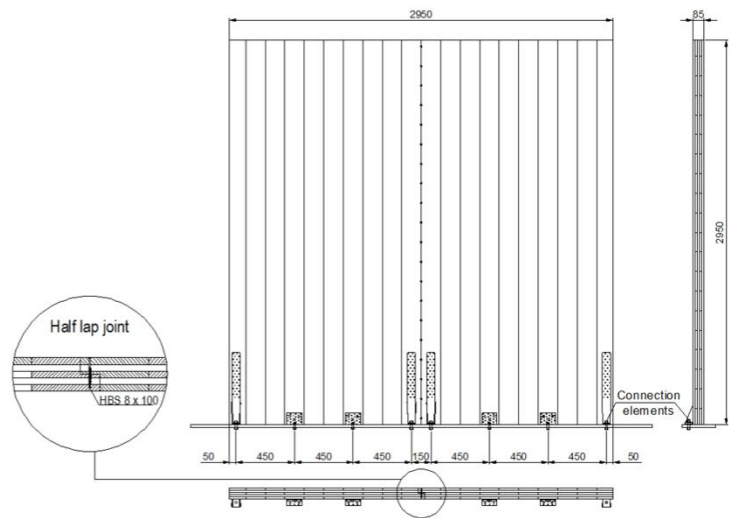
As discussed in Chapter 2 - Literature Review, the lateral behaviours of CLT shear walls have significant impact on structural performance under seismic and wind load. The optimal lateral mode for timber shear wall systems is often characterised by rocking with a self-centring capability, for optimal energy-dissipating performance, which is highly dependent on the connection configurations and properties. With CLT shear wall systems that employ conventional connectors, lateral behaviour is typically a mix of sliding and rocking motions, where the degree of each is contingent upon the design and properties of the plate connectors. However, for shear walls with the proposed interlocking connections, despite the proven mechanical properties, interlocking effect and damage-controlled capacity of connectors through experimental studies, the interaction between shear and tension connections on the shear wall setting has not been thoroughly understood. The comparative mechanical benefits of these novel interlocking connections over traditional ones also remain ambiguous, largely due to the complexities of comparing connections that operate on different principles at a local scale. Therefore, this chapter presents a macro-scale numerical analysis on full-scale shear wall assemblies with varying kinds and arrangements in connections, aiming to determine suitable modelling approaches and investigate the mechanical behaviour and deformation characteristics of these shear wall structures.

6.1 CLT Shear Wall Modelling and Validation

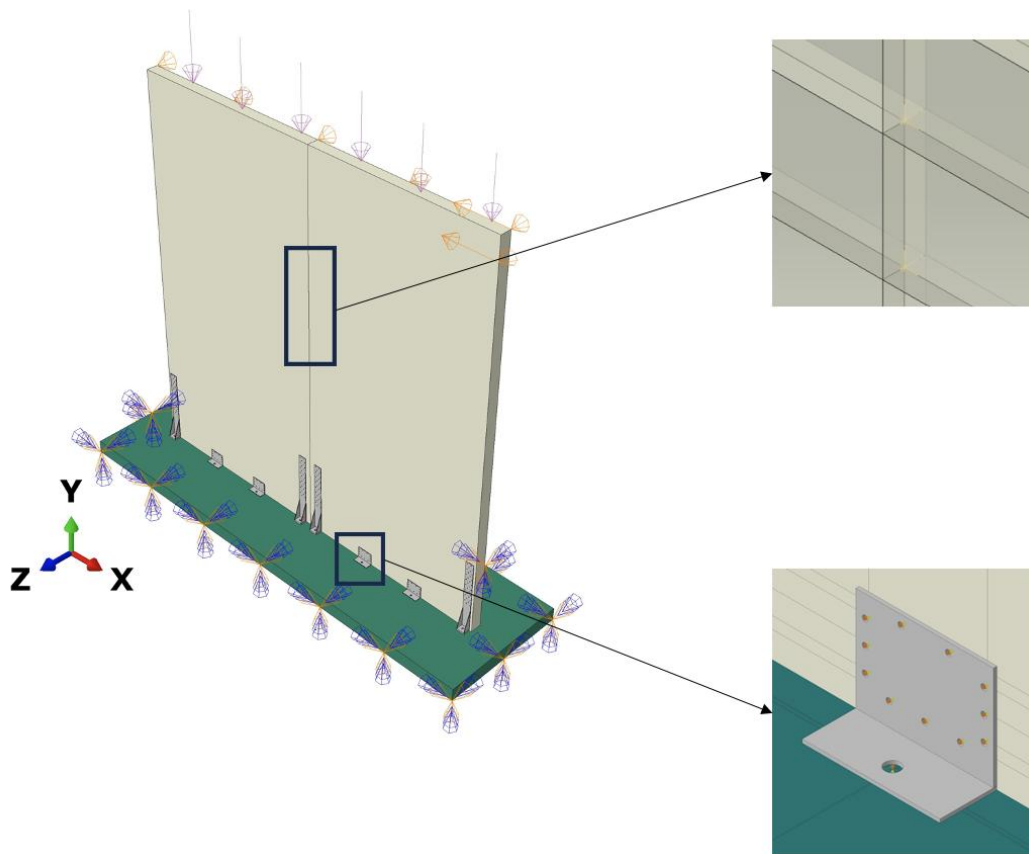
6.1.1 Modelling methods of CLT shear wall

To construct an accurate CLT shear wall model capable of capturing its precise behaviour, initial validation was conducted referencing the experimental work of Pozza et al. [6.1]. The referenced experiment involved a shear wall system consisted of two CLT panels (each 2.95 m×1.50 m and 85 mm thick), which are connected by a half-lap joint fastened with 10 Ø8 × 100 mm self-tapping screws. The panels were anchored to the floor with two HTT22 hold-downs (12 Ø4 × 60) and four BMFs105 angle brackets (11 Ø4 × 60), arranged as depicted in Figure 6.1.a. This arrangement mirrors the standard design employed in a full-scale CLT building examined within the SOFIE project [6.2].

The shear wall specimens underwent quasi-static cyclic loading as prescribed in EN 12512 [6.3], with a reference yielding displacement (V_y) of 20 mm based on previous tests at IVALSA during the SOFIE project. The maximum horizontal displacement in the test was 80 mm, equating to 4 V_y and an inter-storey drift of 2.5%. The load was applied onto the top corner of one panel using a steel bracket linked to the hydraulic jack, with a constant vertical load of 18.5 kN/m on the top of the walls to simulate the load from upper structures in real-world scenarios, like floors and walls. The boundary conditions in model simulating experiment are illustrated in Figure 6.1.b. In the model, the CLT panels and connectors were situated on the fixed foundation. The vertical loading was simulated by compression applied to the top surfaces of the panels. Displacement was introduced through an area measuring 125 mm by 85 mm at the top corner of one panel, representing the action from the metal bracket.



(a)



(b)

Figure 6.1. Validation model (a) experimental set-up [6.1] (b) FE model

The model's validity was confirmed through the comparison with published experimental results. The modelling techniques employed were derived from the validated methodologies of Izzi et al. [6.4]. 3D solid bodies using 8-node linear brick elements with reduced

integration (C3D8R) were utilised to represent both the CLT panels and the metal plate connectors as well as the steel foundation. The foundation was modelled with an elastic isotropic material with Young's modulus equal to 210 GPa and Poisson's ratio set to 0.3. Angle brackets and hold-downs were simulated using steel grades S250 and S355, respectively, both with a modulus of elasticity of 210 GPa. The respective yield strengths were set at 250 MPa and 355 MPa, with ultimate strengths of 330 MPa and 430 MPa. The CLT panels were modelled as orthotropic elastic materials as outlined in Table 6.1, without considering the layered properties. This simplified approach was selected because the experiments indicated that deformation in the panels was not significant.

Table 6.1. Material parameters for CLT panels [6.5]

ER [MPa]	ET [MPa]	EL [MPa]	RT [-]	TL [-]	RL	GRT [MPa]	GRL [MPa]	GTL [MPa]
600	600	12,000	0.558	0.038	0.015	40	700	700

To manage the complexity due to the multitude of screws in the shear walls, a simplified modelling technique was employed. The screws were represented as bilinear elasto-plastic springs with three degrees of freedom (DoF) (Figure 6.1.b) to simulate behaviours in the transverse direction (Figure 6.2.a). For axial behaviours, linear springs (Figure 6.2.b) were implemented due to the brittle behaviours of screws in tension. The connector properties were calculated in accordance with EC5, as detailed in Chapter 5 (Table 6.2). To account for the interaction effect among screws in connectors such as angle brackets and hold-downs, where multiple screws are closely spaced within one connector, EC5 introduces the concept of the 'effective number of nails in a row' in calculating the overall connection capacity. This concept involves an effective factor k_{eff} , as defined in Equation 6.1.

$$k_{eff} = \frac{n^{0.9}}{n} = n^{-0.1} \quad \text{Equation 6.1}$$

In the model, the number of nails in each metal plate connection was kept unchanged. The adjustment on connection capacity involved reducing F_{lat} and F_{ax} of connector element by the effective factor k_{eff} . For HSB $\emptyset 8 \times 100$ nails that used in panel-to-panel connections, the coupling effect was not considered due to the large distance in between, therefore the effective factor was not applied. Regarding the interaction among all components, the 'Hard Contact' in ABAQUS was set for normal direction interactions and the 'penalty friction

formulation' was for tangential responses. The friction coefficients were designated as follows: 0.4 for all Steel-Steel interfaces [6.6], 0.25 for Steel-CLT interfaces [6.7] and 0.4 for CLT-CLT interfaces.

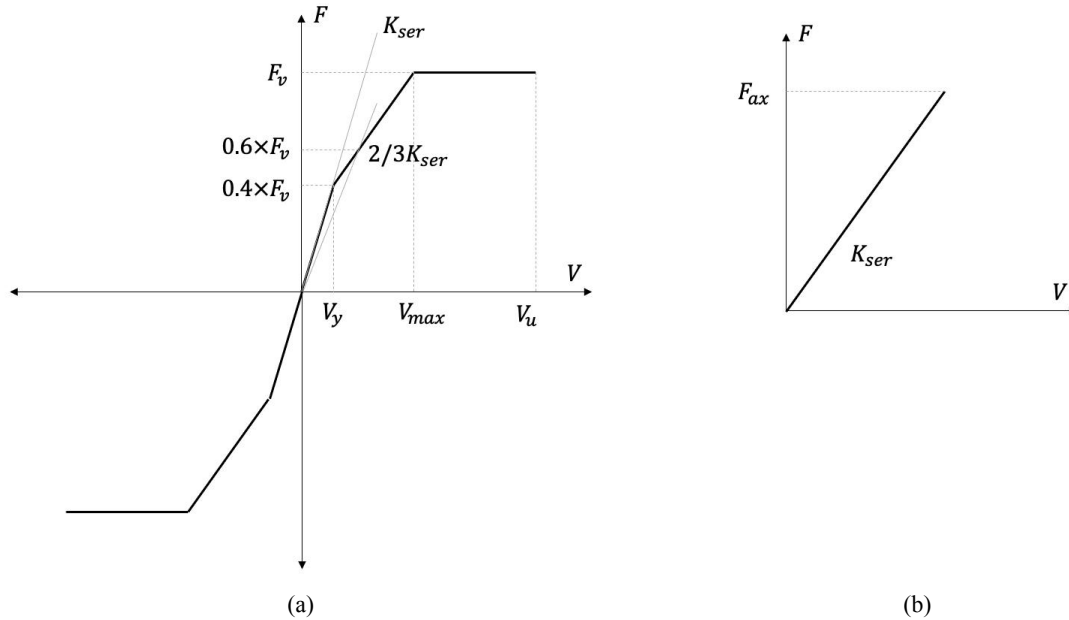


Figure 6.2. Load-displacement relationship for fasteners in (a) Transverse direction and (b) Axial direction

Table 6.2. The screw properties calculated from EC5 and adopted in the models

	Ringed Anker nails 4x60 mm ¹	HSB Ø8x100 nails	LBS7100	HBSP12120
Transverse direction				
f_v	3.04	10.37	9.00	17.23
V_y	0.47	1.12	1.19	3.70
V_{max}	2.2	6.72	5.09	7.05
V_u	20	20	20	20
Axial direction				
f_{ax}	2.28	7.54	6.07	9.08
$K_{ser,ax}$	5000	18000	16625	27000

Note 1: k_{eff} of 0.79 and 0.78 were applied to the connector properties of the hold-down and angle bracket in the model

Note 2: Axial stiffnesses were calculated from ETA-11/0030 of Rotho Blaas

6.1.2 Validation results

Figure 6.3 and Figure 6.4 depict the comparison between the test and the FE model. The connection deformation, and wall movements observed in the original test, are also presented in the FE model. The load-displacement behaviour of the FEM closely aligns with the

experimental hysteresis loop's skeleton curve during the elastic stage, reflected by similar stiffness and yield strength. However, during the plastic stage, the FE model slightly overestimated the resistance of the shear walls. This discrepancy is likely to have happened due to the elastic connector model adopted for panel-to-panel screws, inherent analytical model errors, and the omission of shear wall deformation at larger displacements. Observations from both the test and FEM indicate that plastic deformation is predominantly localised in the angle brackets with only marginal bending in the hold-downs, and the CLT panels remain largely undeformed. Furthermore, the model exhibited rocking of the panel as the dominant behaviour with minor relative in-plane and out-of-plane sliding, similar to the tested system. These findings suggest that the simplifications made in the FE shear wall model do not markedly detract from its predictive accuracy, thus supporting its application in further studies.

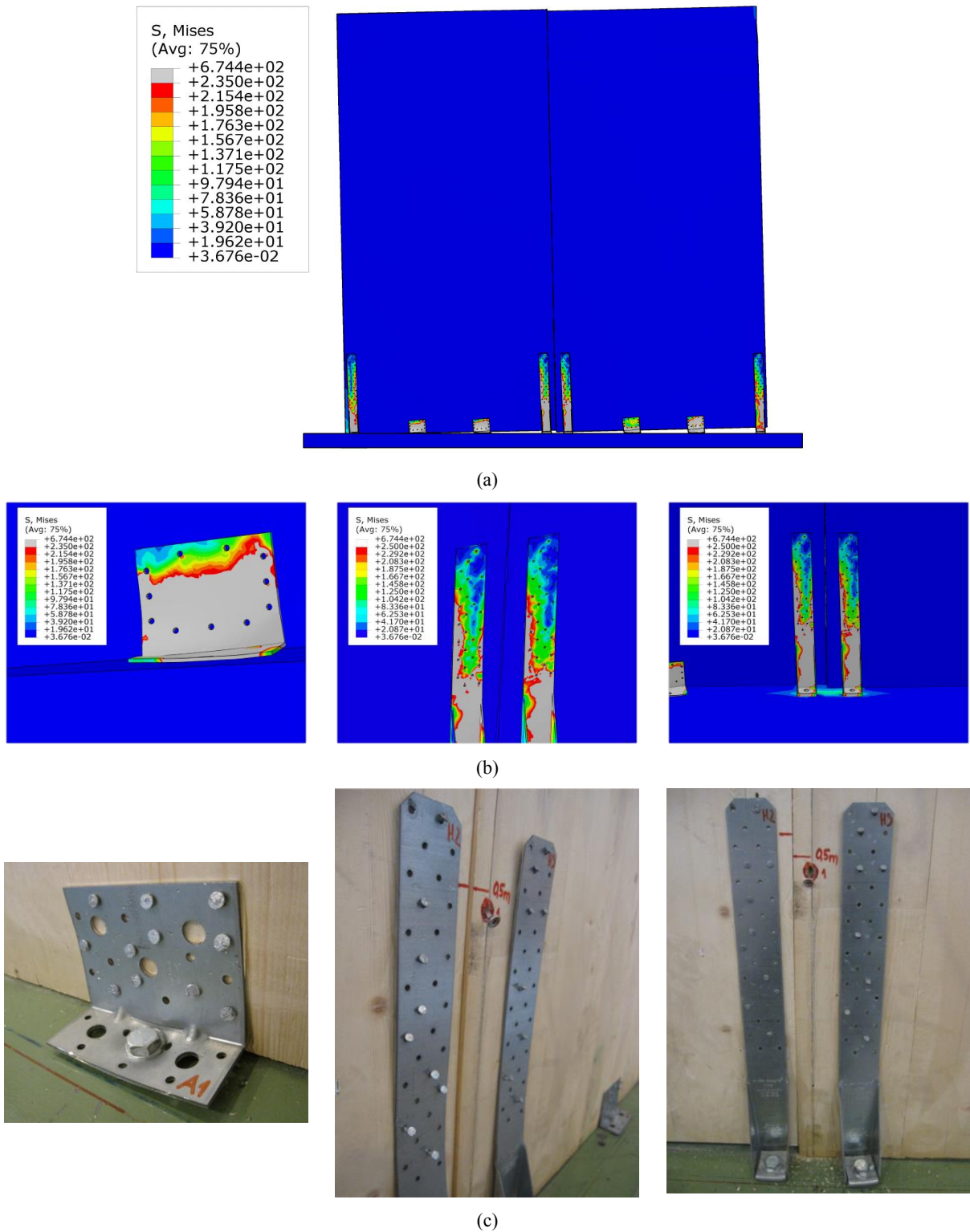


Figure 6.3. CLT shear wall modelling validation (a) Overview of FE model of CLT shear wall (b) FEM results (c) experimental results [6.1]

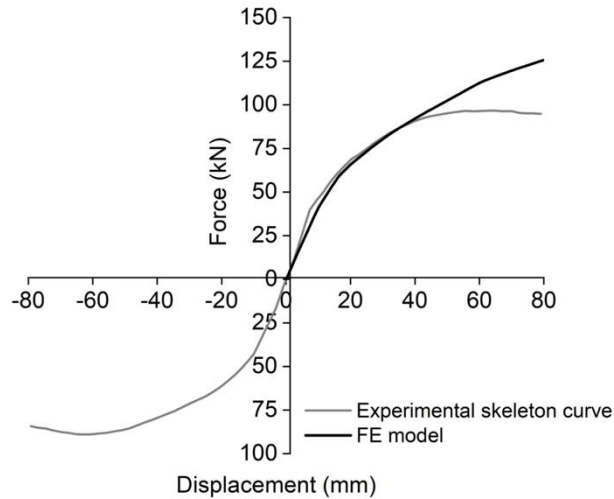


Figure 6.4. Force-displacement curves of experiment and FEM of conventionally reinforced CLT shear walls.

6.2 Set-Up of Shear Wall Comparative Study

6.2.1 Shear wall configurations

To evaluate the lateral behaviours of shear walls reinforced by conventional and interlocking systems, and to understand the reinforcing effects and interaction mechanisms of interlocking shear and tensile connections, a numerical comparative study was conducted on full-scale CLT shear walls with different connection arrangement. As detailed in Figure 6.5, the study encompasses two series. The first series labelled ‘Wall-P,’ consists of walls with conventional plate connections. In ‘Wall-P-1,’ the layout mirrors that of the validation model, while ‘Wall-P-2’ reduces the connector count to two hold-downs and two angle brackets. The second series, ‘Wall-I,’ consists of panels anchored with the proposed interlocking connections. Within this series, ‘Wall-I-1’ and ‘Wall-I-2’ incorporate full-length continuous tensile and shear connections, with ‘Wall-I-1’ preserving a half-lap joint and ‘Wall-I-2’ implementing a 2m connection strip acting as a sliding rail to guide panel movement. Systems ‘Wall-I-3’ and ‘Wall-I-4’ employ 200 mm unit connectors, as detailed in Chapter 3, maintaining the inter-panel connections seen in ‘Wall-I-1’ and ‘Wall-I-2’, correspondingly.

In this study, a like-to-like comparison between the two systems was not the primary objective, hence the number and distance of connections were not consistent between the two series of shear walls. The number and locations of interlocking connectors were determined based on prior experimental studies and potential arrangement solutions. Since the primary interest lies in the shear-tension interaction at this stage, only monotonic testing was

conducted. This method is particularly effective for examining the deformation modes of these configurations under consistent load application.

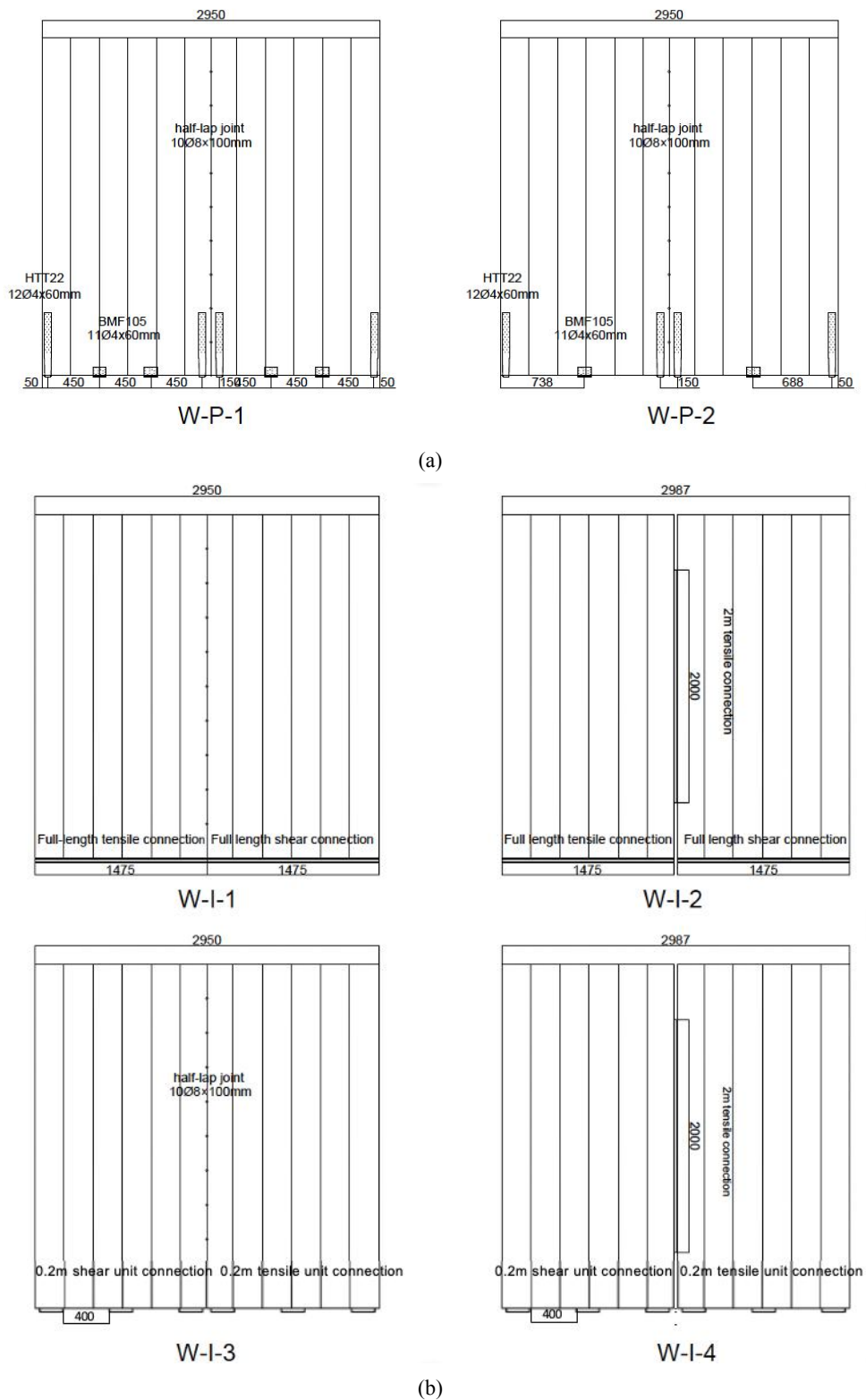


Figure 6.5. Geometries and connection arrangements of the investigated walls: (a) walls with conventional plate connectors, (b) walls with the proposed interlocking connectors

6.2.2 Modelling of interlocking connection in shear wall system

The validated modelling methods and boundary conditions were employed in all shear wall models in this comparative study. The interlocking connectors were simulated using S235 material and 3D models including all the geometric details, as introduced and validated in the Chapter 5. For Wall-I-1 and Wall-I-2, which feature continuous connections, the tensile connection was modelled as a continuous element, acknowledging its potential to be extruded as part of the connection design. Conversely, for practicality in manufacturing and modelling efficiency, the continuous shear connection was represented by a series of repeated unit connectors. In the models of Wall-I-3 and 4, the size of unit connector was chosen to be consistent with the benchmark unit connector as adopted in the parametric study. Corresponding to the validation model, the screws were also modelled as non-linear connector elements. This approach was based on the assumption that screws would minimally impact the performance of the interlocking connections. However, the concept of the 'effective number of screws', typically applied in conventional connections, was not used for the interlocking connections. Due to considerably larger diameter and increased spacing of screws in the interlocking connections, the screws on the same connectors were assumed to have negligible interactions.

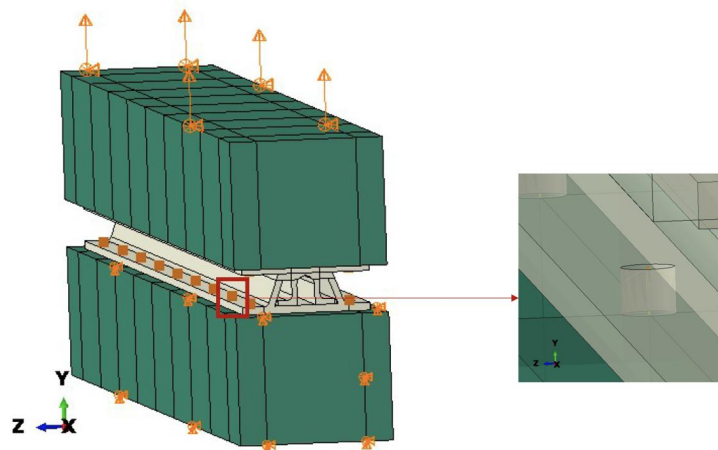


Figure 6.6. Model of continuous tensile connection with simplified screws elements

As introduced in Chapter 5, tests have revealed excessive redundant strength in steel-to-timber connections even after the failure of interlocking connectors. Capacity design was therefore applied to obtain the appropriate number of screws for use with the interlocking connections. Previous studies have demonstrated that connections designed with damage-controlled capacity can potentially require lower overstrength factors compared to conventional metal connections [6.8]. As summarised in Table 6.3, conventional metal

connectors and fastened connections, which largely depend on the deformation of fasteners and timber, tend to exhibit higher material variability and larger errors in analytical models. On the other hand, those new connection designs that rely more on metal components deformation can contribute to less scattering and more predictable behaviours, which means smaller values of γ_{sc} and γ_{an} . Therefore, the proposed connection system theoretically has reduced requirements on overstrength factors, leading to reduced usage of screws, which however should be verified by additional experimental data.

Table 6.3. Comparison of overstrength factors for different connection systems

Connector/Fastener	γ_{sc}	γ_{an}	γ_{Rd}
Novel metal connectors			
X-bracket in tension [6.8]	1.04	1.68	1.76
X-bracket in shear [6.8]	1.04	1.11	1.15
Pinching-Free Connector in tension [6.9]	1.37	1.01	1.45
Metal dovetail connection in shear [6.10]	1.20	1.28	1.54
Metal dovetail connection in pushing-down [6.10]	1.13	1.65	1.86
Conventional metal connectors			
Hold-down in tension [6.11]	1.30	2.60	3.38
Hold-down in shear [6.11]	1.38	-	-
Angle bracket in tension [6.11]	1.23	2.80	3.44
Angle bracket in shear [6.11]	1.16	1.70	1.97
Conventional fasteners			
Nails loaded parallel to face lamination [6.12]	1.27	1.11	1.41
Nails loaded perpendicular to face lamination [6.12]	1.53	1.69	2.59
Self-tapping screws in tension	1.61	1.64	2.65
Self-tapping screws loaded perpendicular to face lamination [6.13]	1.60	1.67	2.67
Self-tapping screws loaded parallel to face lamination [6.13]	1.39	1.80	2.50
Dowel [6.14]	1.59	1.06	1.68

However, the limited availability of experimental data posed a challenge in accurately establishing the overstrength factor for these interlocking connections. Consequently, in this study, the overstrength factors for both tensile and shear connectors were estimated based on the secondary deformation mode in the interlocking connection (specifically, screw bending in steel-to-timber composite connections). Therefore, the overstrength factors taken in this study were 2.65 (equivalent to Self-tapping screws in tension) for the tensile connection and 1.68 for the shear connection (equivalent to Doweled connections). In the model, the number

of LBS7100 (n_t) for interlocking tensile connections and HBSP12120 (n_s) for shear connections were redesigned using Equation 6.2:

$$n_{s/t} = \frac{\gamma_{Rd} \cdot F_{interlocking, continuous}}{F_v} \quad \text{Equation 6.2}$$

As a result, for the 1.4m continuous shear and tensile connections in Wall-I-1 and Wall-I-2, it was determined that 12 and 18 screws, respectively, should be used in each connector with the adopted overstrength factors. This is a significant reduction from the original design, which specified 28 and 42 screws, respectively. The model with continuous version tensile connection and simplified connectors were validated with the connection model with full details in screws as introduced in Chapter 5. Figure 6.7 illustrates that the screw simplifications and optimisations do not markedly impact the connection behaviours, even when using the analytical screw capacity values from EC5 rather than experimental data. This outcome can be attributed to the damage-controlled capacity featured in the proposed connections, which effectively reduces the reliance on screws for overall connection strength. The applied overstrength factor proved adequate for achieving the desired damage-controlled effect, despite the decrease in the number of screws. Consequently, this reduction in screws led to a lowered ultimate strength (168.3kN) of the continuous connection at the densification stage, corresponding to the combined capacity of 18 LBS7100 screws employed in the tensile connection.

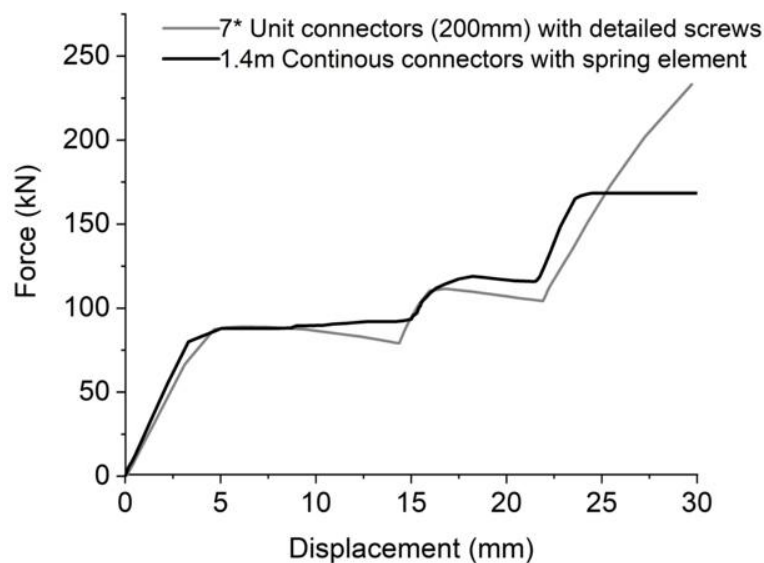


Figure 6.7. The strength comparison between the detailed and the simplified tensile model

6.3 Results of CLT Shear Wall Comparative Study

6.3.1 Connection deformation

The Figure 6.8-13 demonstrate the deformation modes in different shear wall models. According to Figure 6.8Figure 6.9, the overall deformation patterns in shear walls reinforced by conventional connections were consistent. Deformation was predominantly localised in the plate connectors, while the panels themselves exhibited minimal deformation. Although the models, due to their simplifications, did not directly depict the deformation in screws, the significant deformation in the metal plate implies the deformation in screws and the timber around the connectors, aligning with the working mechanism of plate connectors as discussed in the previous chapter. In the conventionally reinforced shear walls, the angle brackets and hold-downs nearest to the point of load application experienced the most considerable deformation. Notably, Wall-P-2, which utilised a reduced number of connectors, displayed a slightly higher maximum stress value compared to Wall-P-1, indicating more pronounced deformation in its connectors. Additionally, Wall-P-2 exhibited more noticeable separation between panels, indicating a weaker single-wall effect between panels compared to Wall-P-1.

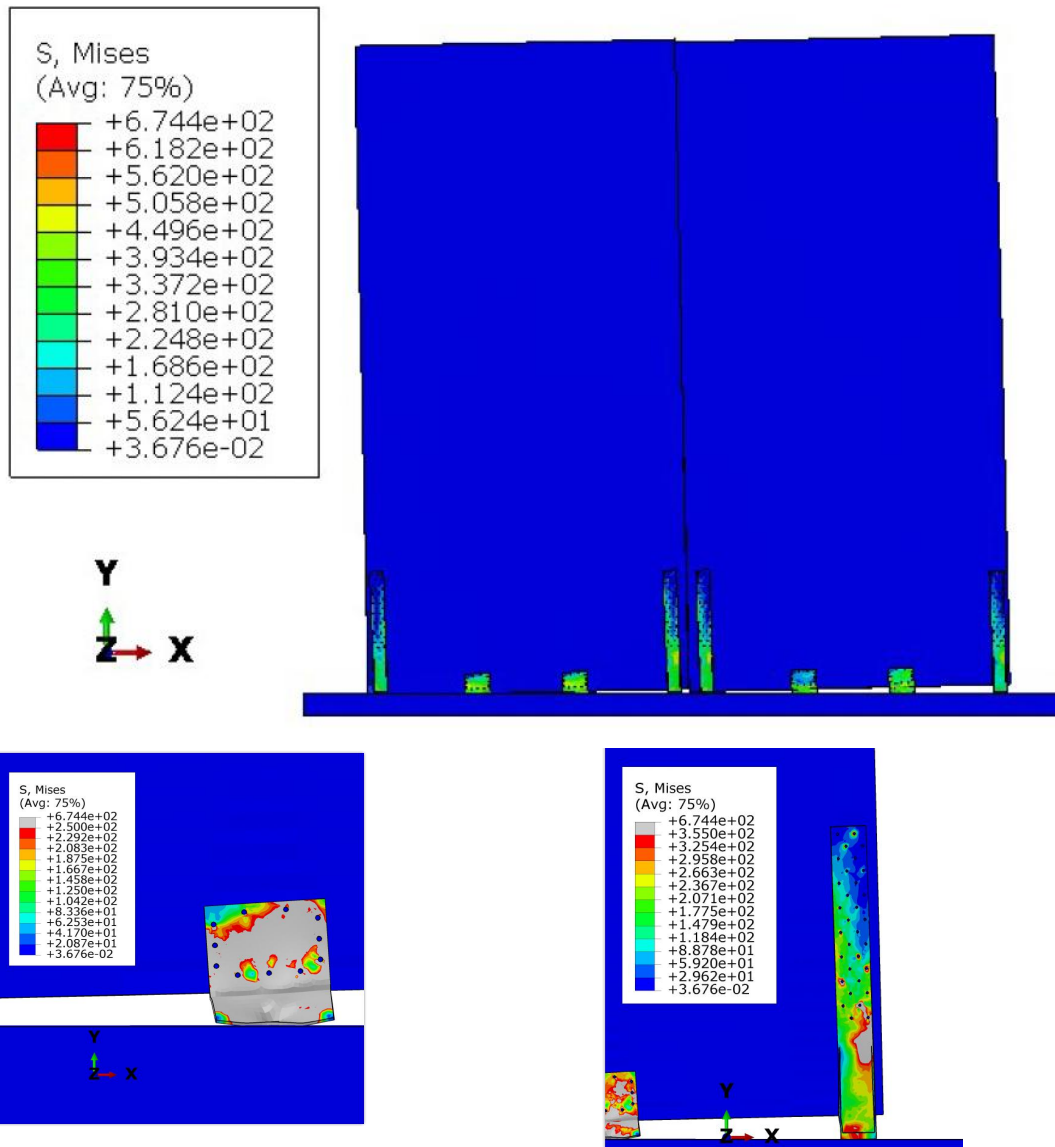


Figure 6.8. Deformation in Wall-P-1 at 80 mm displacement

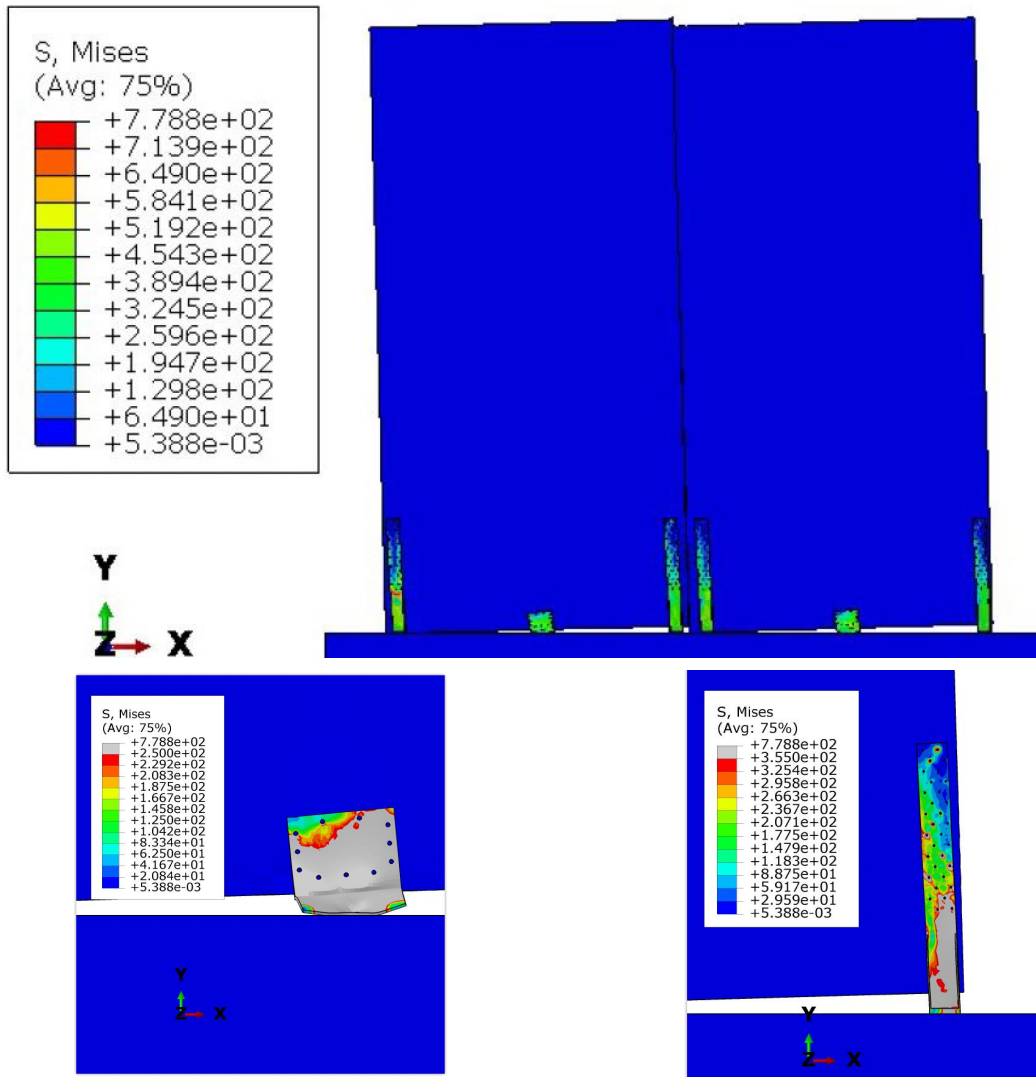


Figure 6.9. Deformation in Wall-P-2 at 80 mm displacement

Figures 6.10-12 demonstrate the deformation behaviours of shear walls reinforced with proposed interlocking connections in the 'Wall-I' series, observed at a displacement of 65 mm. Notably, rocking is the dominant lateral behaviours in all shear wall models. In addition, plastic deformation was consistently localised in the male connectors across all types of connections, indicating the successful implementation of a damage-controlled effect achieved through capacity design, applicable to both continuous and discontinuous connections. Specifically, in Wall-I-1, even at the applied displacement of 65 mm, the shear connections did not reach critical load levels, resulting in only minimal sliding movement and effectively preventing buckling.

The presence of screwed inter-panel connections enabled the two CLT panels to exhibit a strong single wall effect, leading them to rotate as a single unit around the bottom left corner, without any noticeable relative movement between them. Accompanying the panel rotation, a slight separation was noticeable in the shear connections at the farthest side from the rotation centre. The rocking behaviours can also be proved by the minimal horizontal movement in the tensile connection near the rotation centre of the right panel, as the male connector remained within the female connector without significant sliding. In response to the shear wall system's sliding tendency, the shear female connector at the rotation centre experienced considerable compression by the male connector, yet the deformation remained within the elastic range.

In the section of the tensile connection nearest to the applied load, which experienced the most substantial vertical displacement, the material transitioned into the plastic stage. In contrast, the end closer to the shear connection showed little to no change, remaining largely unaffected. This behaviour suggests that the tensile connector underwent bending not just in the Y-Z plane but also in the Y-X plane, highlighting the complex interactions within these systems. Notably, during the later stages of loading, minimal stress concentration was observed in the bottom plate of both shear and tensile connections, which are fastened to the timber. This observation indicates that the shear wall system, utilising a continuous version of the connection, is capable of enduring significant deformation without inflicting damage on the timber components.

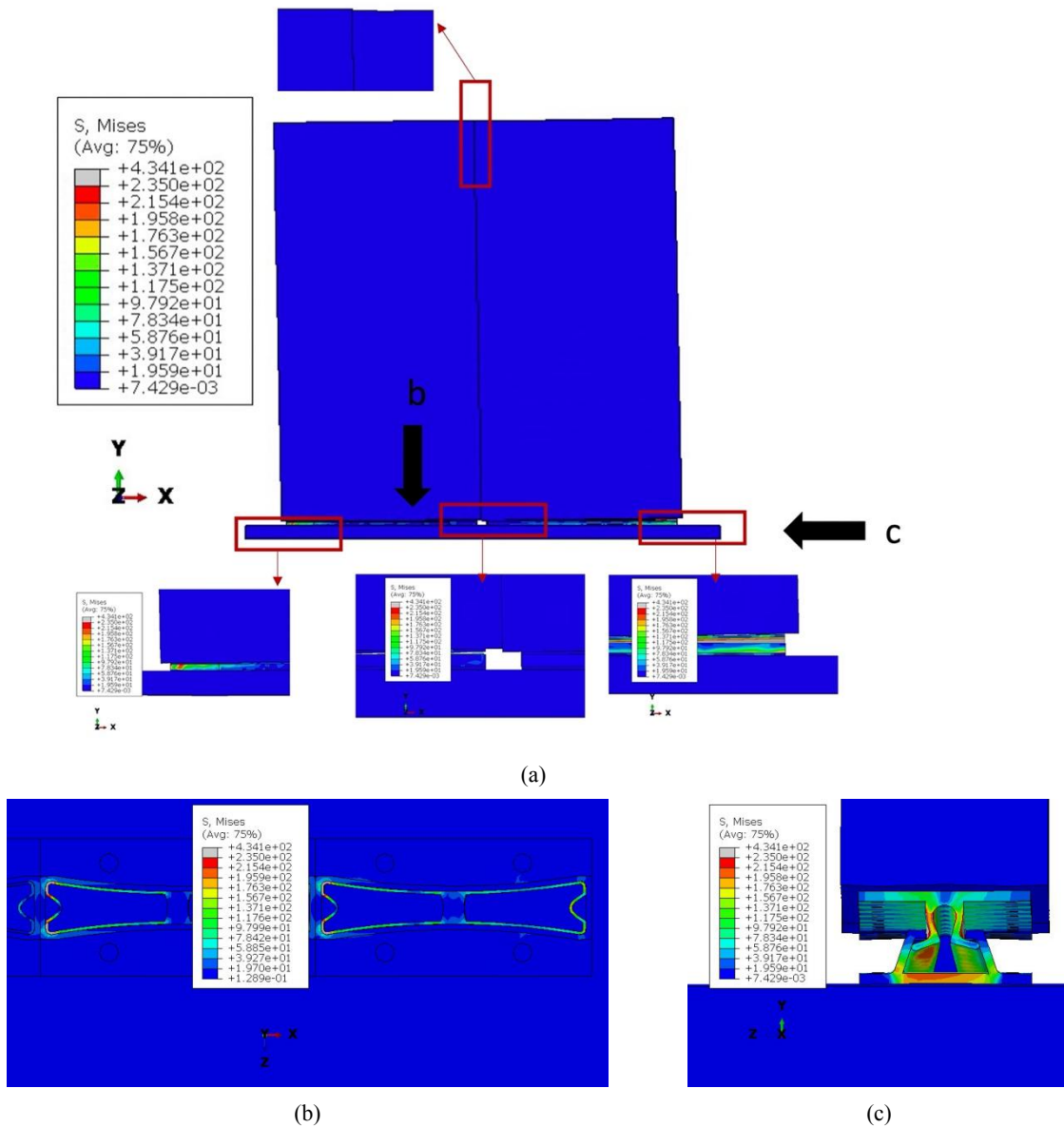


Figure 6.10. Deformation in Wall-I-1 at 65 mm displacement

In Wall-I-2, where a sliding rail was used instead of screwed inter-panel connections, increasing coupling effect can be observed between panels. Similar to Wall-I-1, bending in tensile male connector was the primary deformation in Wall-I-2, while buckling of shear connection was not evident. The sliding rail, running along the height of the panels, allowed for more freedom of movement, facilitating the independent rocking of each panel. It should be noted that the separation at the midpoint of the inter-panel sliding rail led to compression between the connectors.

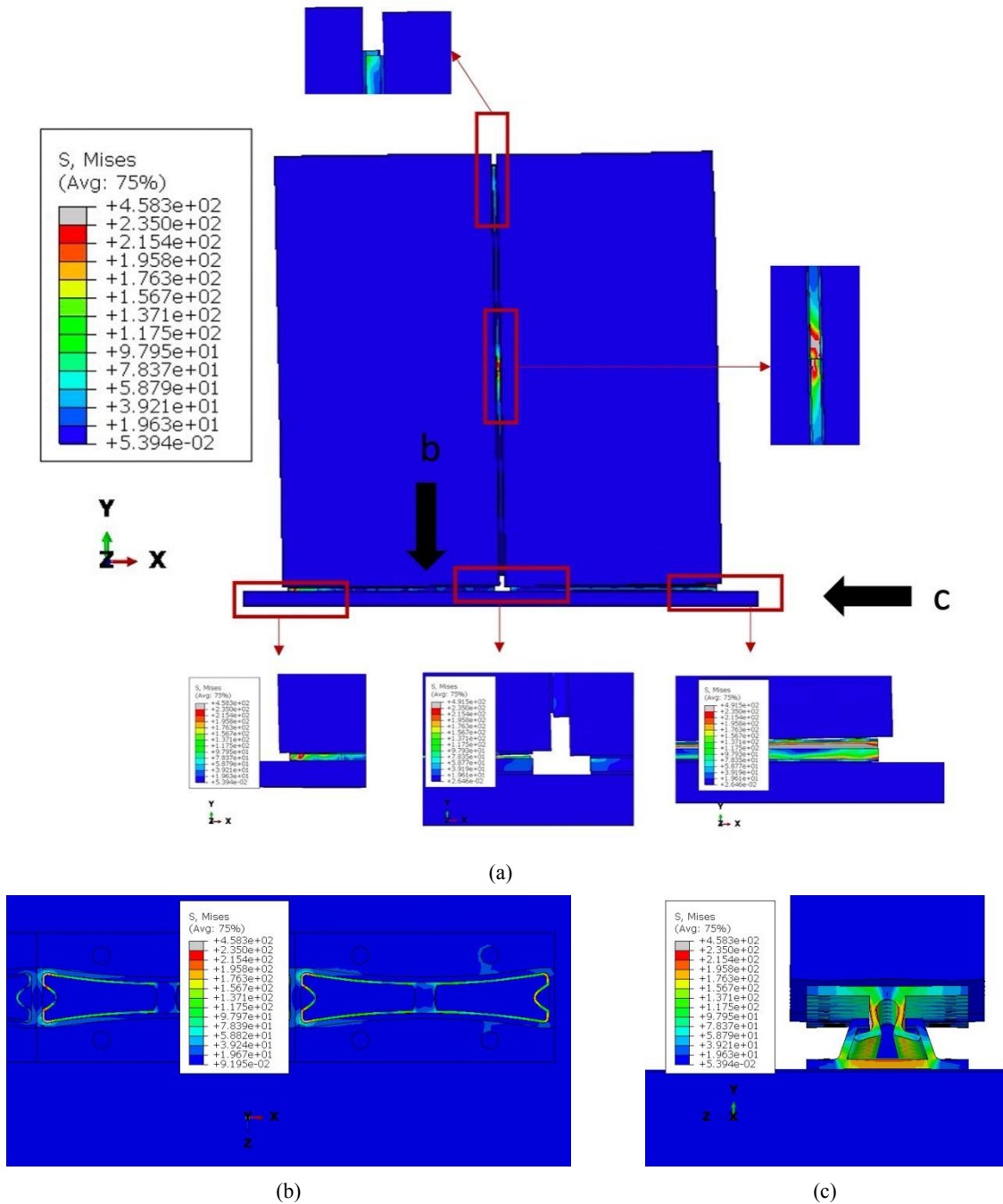


Figure 6.11. Deformation in Wall-I-2 at 65 mm displacement

For Wall-I-3 and 4 that employed the discontinuous version of connection at the bottom of panels, a higher level of stress concentration can be observed compared to the walls with continuous connections. At a displacement of 65 mm, the tensile male connector near the loading side underwent considerable vertical displacement. This was accompanied by bending in the bottom plate of the female connector, indicative of potential tension experienced by the screws. The walls in both systems exhibited more pronounced sliding due to their reduced shear resistance, leading to buckling in two of the shear connections (Figure

6.12&13). In Wall-I-3 and Wall-I-4, the effects of varying inter-panel connections were observed to be akin to those discussed for Wall-I-1 and Wall-I-2.

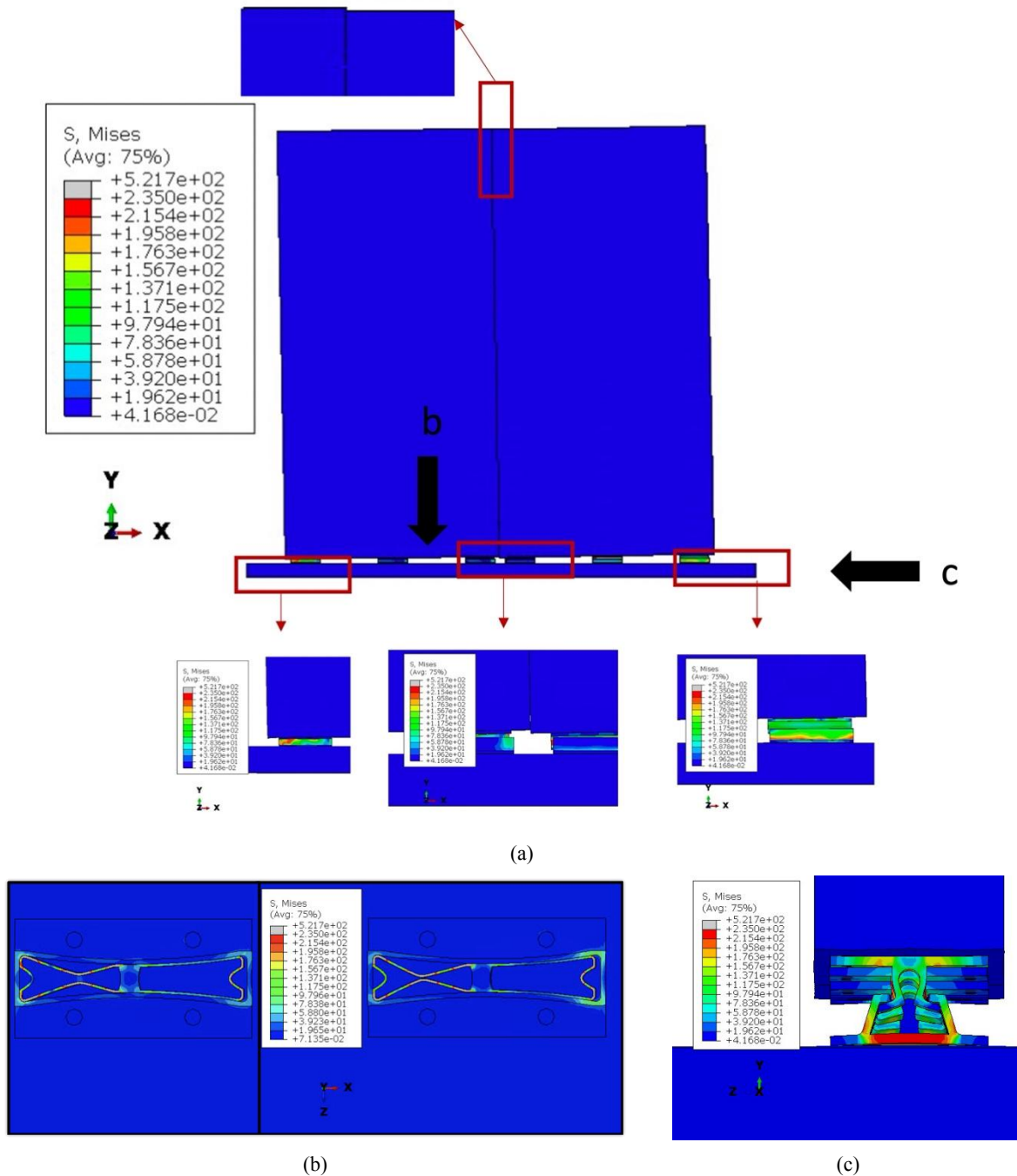


Figure 6.12. Deformation in Wall-I-3 at 65 mm displacement

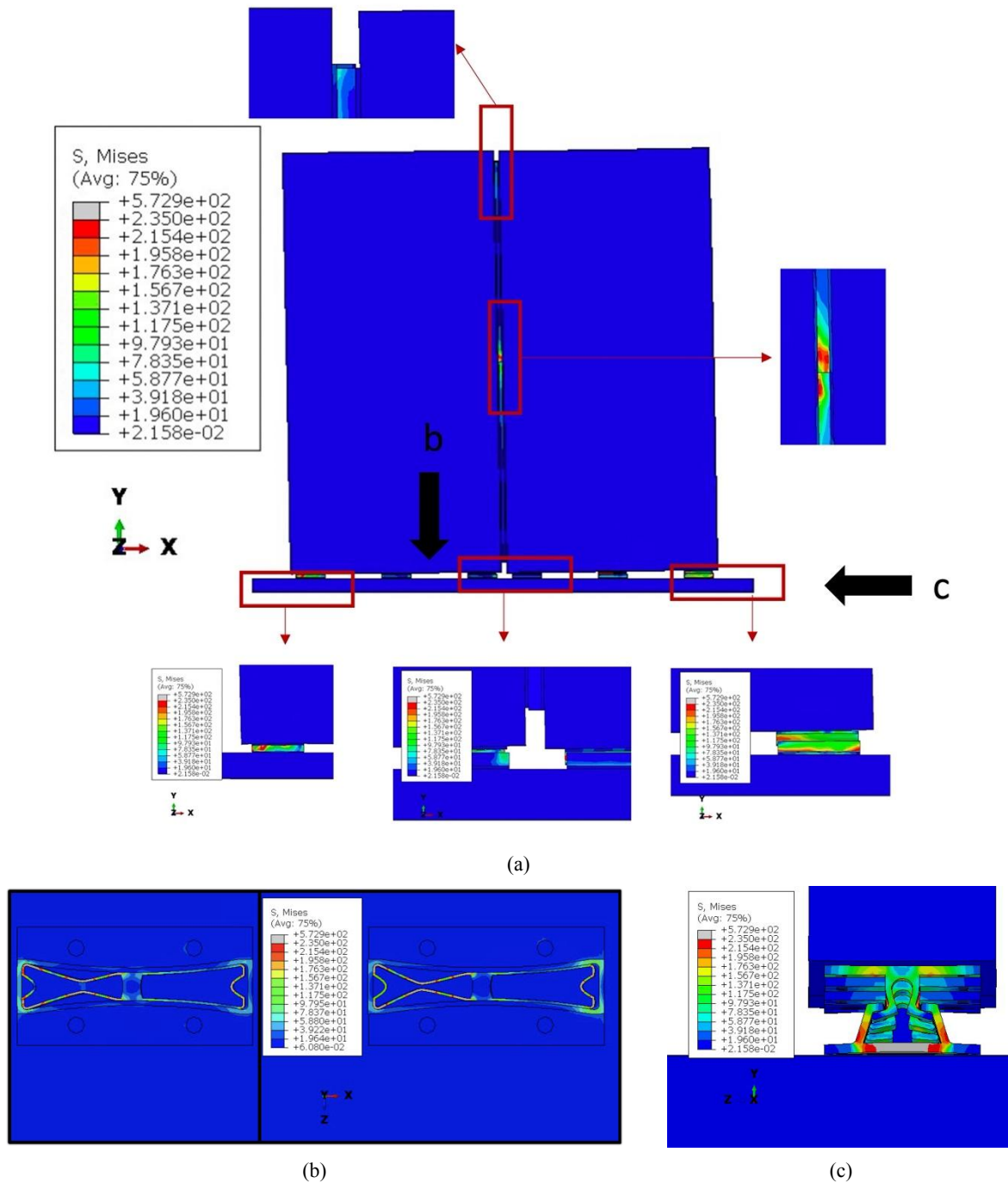


Figure 6.13. Deformation in Wall-I-4 at 65 mm displacement

6.3.2 Structural performance

The structural performance of each shear wall is summarised in Table 6.4 and Figure 6.14. The data presented suggest that the walls with conventional plate connections (Wall-P) exhibit higher stiffness, ultimate strength, and ductility ratios compared to those with interlocking connections (Wall-I). On the other hand, the Wall-I series provided lower initial resistance due to the increased degree of freedom inherent in the interlocking connections.

Among all models, Wall-P-1 has the highest stiffness and ultimate resistance. With reduced number of angle brackets, Wall-P-2 demonstrates a similar structural performance but with slightly lower stiffness and strength, which is consistent with the published testing results [6.15]. In terms of shear walls with continuous interlocking connections (Wall-I-1 and 2), their force-displacement curves exhibit gradual increase in resistance under loading, lacking a distinct yield plateau typically indicative of a plastic stage. Such behaviour suggests a complex interaction within the shear wall system, possibly indicating that the connections are yielding progressively (in tensile connection) rather than simultaneously entering a clear plastic stage. This gradual yielding also suggests a distribution of forces along the connection strip, leading to a progressive engagement of various connections within the system. Additionally, these findings indicate that the majority of connections in the shear wall have not yet reached the plastic stage, as corroborated by observations in Figure 6.10 and 11. On the contrary, the curves of Wall-I-3 and 4 both have two slight fluctuations, corresponding to the buckling in two shear connections respectively (Figure 6.12 and 13). The smooth strength reduction due to buckling, compared to the more abrupt changes seen in local-scale testing of individual connectors, indicates the support from other connections in the system that contributes to the subsequent resistance increment.

Table 6.4. Interpretation of FEA results according to EN 12512 [6.3]

Identification of Parameters	Wall-P-1	Wall-P-2	Wall-I-1	Wall-I-2	Wall-I-3	Wall-I-4
Elastic stiffness [kN/mm]	4.09	3.99	1.74	2.14	1.64	1.86
Hardening stiffness [kN/mm]	1.02	0.87	1.21	1.12	0.95	1.08
Yielding displacement V_y [mm]	16.62	14.42	30.84	23.87	15.94	10.62
Yielding force f_y [kN]	68.42	62.64	53.69	51.31	26.35	19.95
Ultimate force f_u [kN]	125.66	131.15	112.43	112.60	78.29	84.17
Ductility ratio $\mu = V_u/V_y$	4.82	5.55	2.59	3.35	4.08	6.59

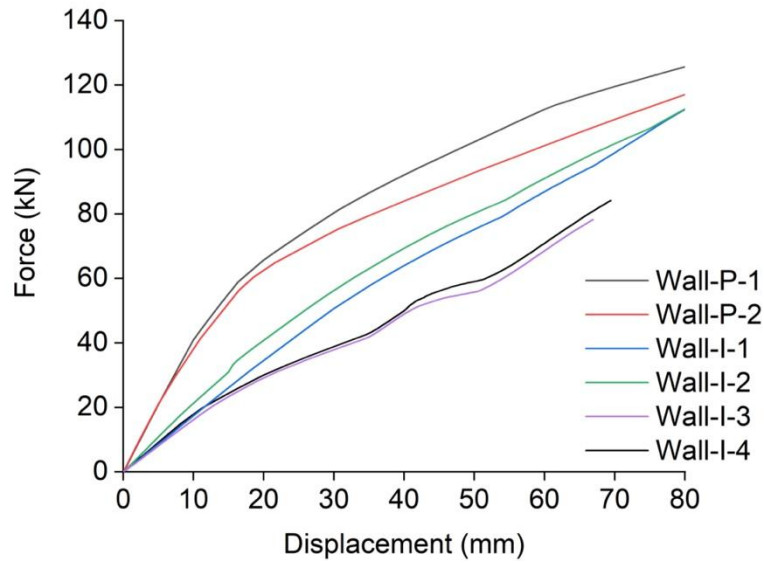


Figure 6.14. Push-over results summary

6.3.3 Lateral behaviours

Based on previous experimental studies [6.16, 6.17] on CLT shear walls, the overall lateral movement of CLT shear wall consists of four components, which are rocking, sliding, shear, and in-plane panel bending. The dominant deformation mode of CLT shear wall is defined by the contribution of these components. Observing the FE results of the current study, the shear and in-plane panel bending in panels were found to be negligible. Consequently, the focus was placed on rocking and sliding, which were quantified using methods outlined in a previous study [6.18]. The incremental applied displacement at the top of panel is denoted as δ , with the sliding component being defined as δ_s , and both of which can be measured directly from the model. The portion of rocking motion δ_r can then be calculated as $\delta_r = \delta - \delta_s$ (Figure 6.15). In addition, the coupling effect in shear wall system can be quantified using the coupled wall behaviour parameter $\kappa = \frac{u_2}{u_1 + u_3}$, where u_1 , u_2 , and u_3 respectively represent the uplift of first wall panel, the relative vertical displacement between two wall panels, and the vertical displacement of the rotation centre in the second panels (Figure 6.15). When the wall behaves as a single wall, both u_2 and κ approach 0. Conversely, when the wall behaves as a coupled wall, κ approaches 1.

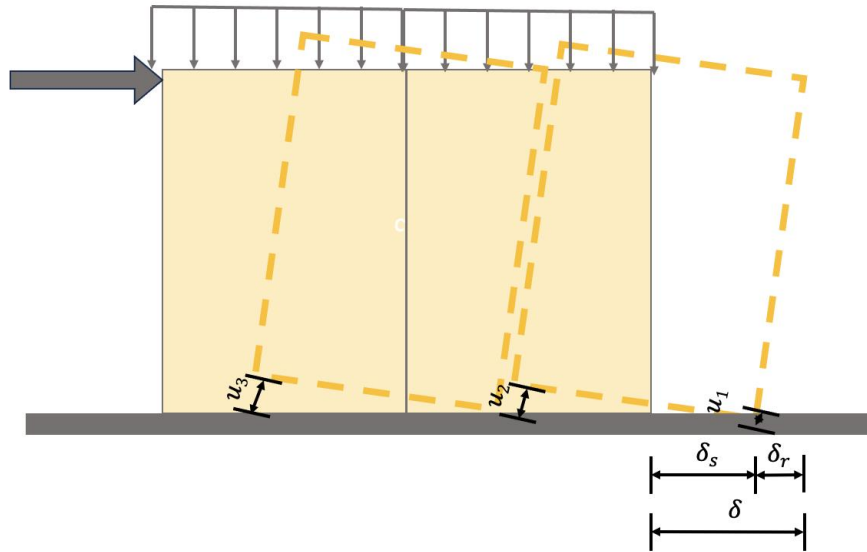


Figure 6.15. Calculation of sliding and rocking contribution

The results, as summarised in Figure 6.16, delineate the contributions of rocking and sliding to the overall drift in different shear wall systems. Under the applied condition boundary, both sliding and rocking contributed to the wall drift, with rocking emerging as the dominant deformation mode in all systems. Notably, Wall-P-2 exhibits the highest sliding contribution among all models. However, this contribution diminishes in Wall-P-1 due to the increased lateral resistance afforded by a greater number of angle brackets.

In the shear wall reinforced by the proposed interlocking connections, the contribution of sliding is significantly reduced. This is attributed to the higher stiffness of the interlocking shear connections compared to the tensile connections, prompting the panels to move more vertically and thus increasing the contribution from rocking. The shear walls employing a sling rail between panels (Wall-I-2 and Wall-I-4) exhibit increased rocking behaviours relative to their counterparts (Wall-I-1 and Wall-I-3). This is due to the decreased coupling effect between panels, allowing for more independent rotation. Conversely, in Wall-I-3 and Wall-I-4, which feature separated connection units, a higher proportion of sliding behaviors is observed, likely resulting from the reduced shear resistance. At larger wall drifts (beyond 1.5%), when the tensile connections in these two shear walls reaches the consolidation stage, a sudden increase in stiffness restricts the vertical movement of the panels, leading to the increased horizontal movement (sliding).

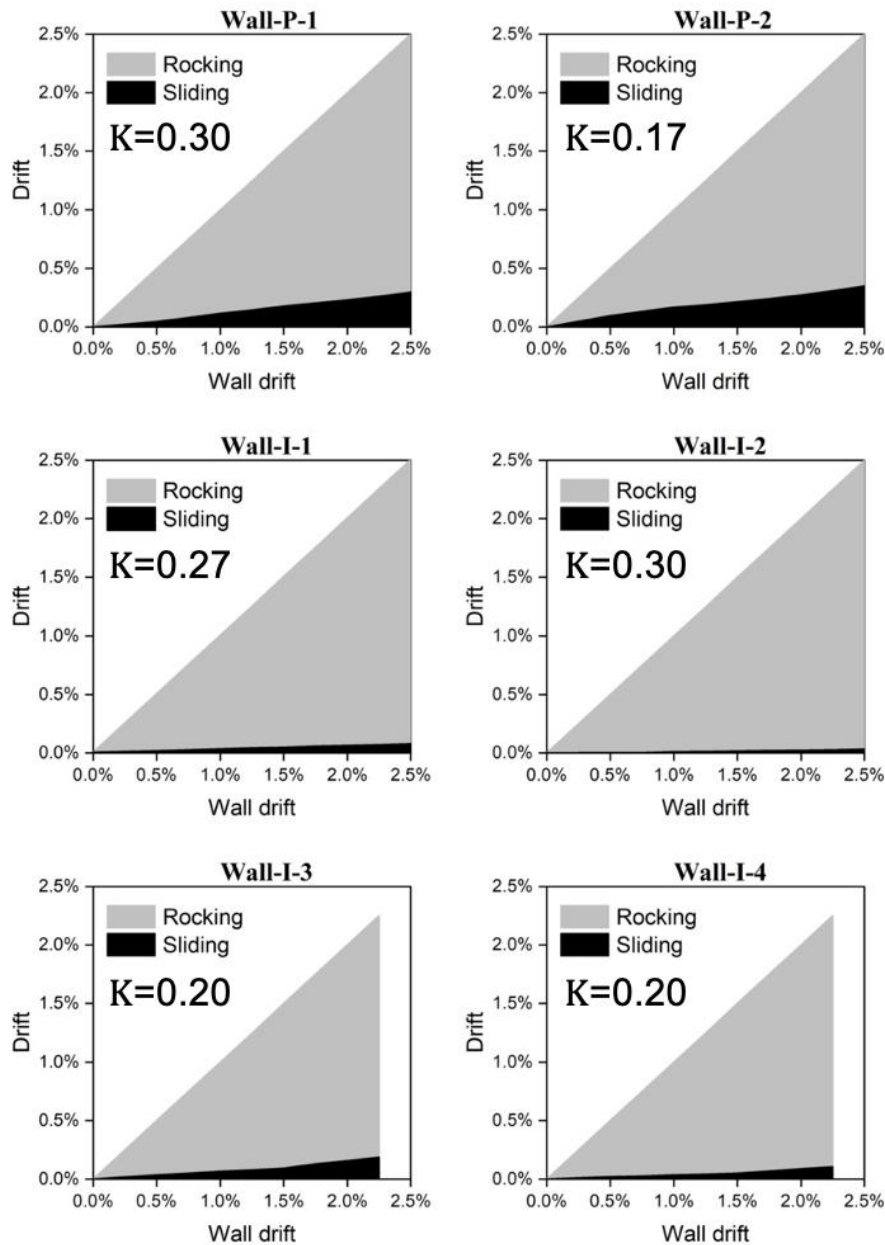


Figure 6.16. Sliding and rocking drift in shear walls with different connection configurations

6.4 Conclusions

The FE shear wall analysis reveals the different deformation mechanisms between conventional connections and interlocking connections (Figure 6.17), showcasing the effective interaction between interlocking shear and tensile connections, and their damage-controlled capacity. The inherent degree of freedom provided by interlocking techniques leads to a reduction in stiffness compared to conventionally reinforced shear walls. However, the damage-controlled capacity allows the shear wall to sustain significant deformation without timber damages, ultimately achieving an ultimate strength comparable to conventional shear walls. In addition, the unique combination of weak shear and strong

tensile connections in the interlocking system, coupled with the innovative use of an inter-panel sliding rail, effectively fosters rocking behaviours in the shear wall system. This design allows each timber panel to rotate around its own axis. Nonetheless, the precise behaviours and energy dissipation of this panel system merit further experimental investigation.

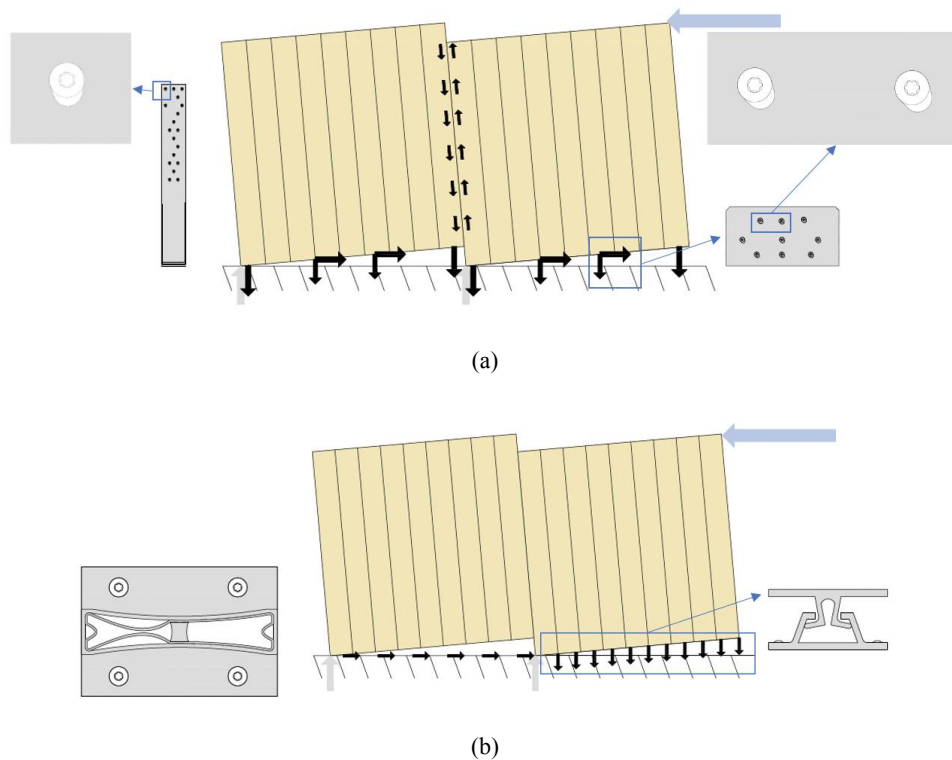


Figure 6.17. Deformation mechanisms of CLT shear wall with (a) conventional connections and (b) interlocking connections

The study also demonstrates that the continuous design of connection can effectively improve the overall mechanical properties, while the distance between screws should be carefully designed to avoid excessive bending in the bottom plate. In configurations using unit connectors to form the connection strip, the bottom plate bending is neglectable due to the limited distance between screws, while the resultant compression between connectors should be considered. The sliding rail, when functioning as inter-panel connections, allows the relative movement to occur in a controlled, predefined manner, meanwhile effectively mitigates out-of-plane and in-plane panel separation. Such rocking behaviours is advantageous in seismic design, facilitating energy dissipation through controlled movement and allowing for natural recovery under gravitational loads, whereas sliding movements typically necessitate external forces for correction. The incorporation of a damage-controlled philosophy in the design further enhances the structural performance. Moreover, the creation of a cavity between panels and foundations by the connections serves an additional purpose.

It prevents compression transfer from the wall panel to the floor panel during rocking, thus further safeguarding against damage in structural components.

6.5 Chapter References

- [6.1] Pozza, L., Scotta, R., Trutalli, D., Pinna, M., Polastri, A. and Bertoni, P. *Experimental and numerical analyses of new massive wooden shear-wall systems*. Buildings (Basel), 2014. **4**(3): p. 355-374.
- [6.2] Ceccotti, A., Sandhaas, C., Okabe, M., Yasumura, M., Minowa, C. and Kawai, N. *SOFIE project - 3D shaking table test on a seven-storey full-scale cross-laminated timber building*. Earthquake engineering & structural dynamics, 2013. **42**(13): p. 2003-2021.
- [6.3] Eurocode, *Timber structures- test methods- cyclic testing of joints made with mechanical fasteners* 2005, European Committee for Standardization,.
- [6.4] Izzi, M., Polastri, A. and Fragiaco, M. *Modelling the mechanical behaviour of typical wall-to-floor connection systems for cross-laminated timber structures*. Engineering structures, 2018. **162**: p. 270-282.
- [6.5] Fortino, S., Mirianon, F. and Toratti, T. *A 3D moisture-stress FEM analysis for time dependent problems in timber structures*. Mechanics of time-dependent materials, 2009. **13**(4): p. 333-356.
- [6.6] Hassanieh, A., Valipour, H.R., Bradford, M.A. and Sandhaas, C. *Modelling of steel-timber composite connections: Validation of finite element model and parametric study*. Engineering structures, 2017. **138**: p. 35-49.
- [6.7] Liu, X., Bradford, M.A., and Lee, M.S.S. *Behavior of high-strength friction-grip bolted shear connectors in sustainable composite beams*. Journal of structural engineering (New York, N.Y.), 2015. **141**(6): p. 4014149.
- [6.8] Marchi, L. *Innovative connection systems for timber structures*, in *Dipartimento di Ingegneria Civile, Edile ed Ambientale*. 2018, Università degli Studi di Padova.
- [6.9] Chan, N., Hashemi, A., Zarnani, P. and Quenneville, P. *Pinching-Free Connector for Timber Structures*. Journal of structural engineering (New York, N.Y.), 2021. **147**(5): p. 4021036.
- [6.10] Li, Z., Wang, X., He, M., Shu, Z., Huang, Y., Wu, A. and Ma, Z. *Mechanical performance of pre-fabricated metal dovetail connections for Cross-Laminated Timber (CLT) structures*. Construction & building materials, 2021. **303**: p. 124468.
- [6.11] Gavric, I., Fragiaco, M. and Ceccotti, A. *Cyclic behaviour of typical metal connectors for cross-laminated (CLT) structures*. Materials and structures, 2015. **48**(6): p. 1841-1857.
- [6.12] Izzi, M., Flatscher, G., Fragiaco, M. and Schickhofer, G. *Experimental investigations and design provisions of steel-to-timber joints with annular-ringed shank nails for Cross-Laminated Timber structures*. Construction & building materials, 2016. **122**: p. 446-457.
- [6.13] O'Ceallaigh, C. and Harte, A.M. *The elastic and ductile behaviour of CLT wall-floor connections and the influence of fastener length*. Engineering structures, 2019. **189**: p. 319-331.
- [6.14] Ottenhaus, L.-M., Li, M., Smith, T. and Quenneville, P. *Overstrength of dowelled CLT connections under monotonic and cyclic loading*. Bulletin of earthquake engineering, 2018. **16**(2): p. 753-773.

- [6.15] Zhang, X., Isoda, H., Sumida, K., Araki, Y., Nakashima, S., Nakagawa, T. and Akiyama, N. *Seismic performance of three-story cross-laminated timber structures in japan*. Journal of structural engineering (New York, N.Y.), 2021. **147**(2): p.04020319.
- [6.16] Li, Z., Wang, X. and He, M. *Experimental and analytical investigations into lateral performance of cross-laminated timber (CLT) shear walls with different construction methods*. Journal of earthquake engineering : JEE, 2022. **26**(7): p. 3724-3746.
- [6.17] Wang, X., He, M. and Li, Z. *Experimental testing of platform-type and balloon-type cross-laminated timber (CLT) shear walls with supplemental energy dissipators*. Journal of Building Engineering, 2023. **66**: p. 105943.
- [6.18] Deng, P., Pei, S., Van De Lindt, J.W., Omar Amini, M. and Liu, H. *Lateral behavior of panelized CLT walls: A pushover analysis based on minimal resistance assumption*. Engineering structures, 2019. **191**: p. 469-478.

Chapter 7 Conclusion

Intending to explore more efficient CLT modular construction method and to bridge the theoretical gaps in connection design of it, this study demonstrates the design practice of novel connection with thorough considerations of CLT modular construction.

7.1 Limitations in Existing CLT Connections

Through comprehensive review of existing research on CLT modular structures, conventional connections, and recent innovative connections, the limitations of current conventional connection systems, such as complex assembly processes, inconsistent mechanical behaviours, and inadequate sustainability performance, were highlighted. These limitations hinder the advancement of CLT construction methods with insufficient assembly process and inadequate structural performance. Some recent connection systems have introduced novel properties and functionalities that benefit CLT construction in three fundamental aspects: structural performance, construction efficiency, and manufacturing efficiency. However, the market still lacks standardised products with comprehensive capabilities, primarily due to insufficient holistic considerations and standardised guidelines for connection development. To address this, the study establishes a strategic design framework that encompasses structural, constructional, and manufacturing dimensions, with a particular focus on connections for CLT modular construction. The literature review also discusses the significant reuse potential of CLT structures, summarising the design indicator that can contribute to detachable and reusable connection designs.

7.2 Novel Interlocking Connection Development

Guided by the developed design framework, the study introduced a novel, universal, and project-independent connection system for CLT panelised (platform- and balloon-type) and volumetric structures. Drawing inspiration from traditional interlocking methods, this system is different from most of the existing products on the market, offering efficient assembly method with direct onsite usability, eliminate the needs of onsite adjustment and connection installations. Revolutionising the conventional point-to-point reinforcing method to continuous reinforcing method, this system is more suitable for panelised structure where comprise large, flat panels.

7.3 Feasibility Evaluation of The Novel Connection

To assess the proposed connection system's feasibility, a series of experimental investigations were conducted, comparing the 3D printed new connections prototypes with conventional screwed steel-to-timber composite connections. These investigations extended beyond basic mechanical properties to examine the unique features of the new connection, such as interlocking and damage-controlled capacity. Subsequent to the development and validation of numerical connection models against experimental findings, an in-depth investigation into the behaviours of connections was undertaken, focusing on various planar forces using common steel grades. Parametric studies were then conducted using the validated models to evaluate the impact of various geometric factors, which also confirmed that damage localisation leads to more accurate analytical models by isolating deformation. The numerical study further expanded to macro scale, examining the proposed connections in a shear wall environment, which proved that continuous connection could ensure better structural integrity, enhanced deformation resistance, and more adequately distribute loads.

In conclusion, this research contributes to the development of design strategies for CLT modular connections, aiming for comprehensive performance in structure, construction, manufacturing, and sustainability, thus proposing a product with significant novelty and practical potential. The proposed novel connection employs a 'fuse system,' where the energy-dissipating elements are part of the steel connection itself, rather than the steel fasteners. This design allows for predictable energy absorption, minimising plastic deformation of fasteners and preventing timber damage, thereby reducing the risk of brittle failure and enhancing structural resilience under extraordinary loads, such as seismic events. Importantly, the timber panels can be fully reused post-structure lifecycle, as the novel connection system prevents fastener failure, promoting a more flexible, demountable, and fully reusable modular construction approach.

Chapter 8 Limitations and Recommendations

Despite the promising results, further studies are needed to standardise and commercialise the proposed connection system. The initial test scope was limited to the connector scale due to budget constraints, and broader testing on macro and global scales is necessary to establish a comprehensive understanding of the system's performance. Additionally, the current research did not fully explore various sizes of unit connectors, the practicality of the interlocking assembly process in real-world settings, or the long-term sustainability and reusability of the connections. The following areas need additional work to enhance the understanding and implementation of this system:

- **Additional Experimental Tests:** Conduct more experimental tests to thoroughly characterise the connection behaviours and determine the overstrength factor. This broader testing is essential to establish a comprehensive understanding of the system's performance beyond the initial limited scope.
- **Expanded Parametric Study:** Expand the parametric study to include various sizes of unit connectors. This will help confirm the broader applicability of the proposed design and ensure it can be effectively used in different contexts and configurations.
- **Practical Evaluation of Interlocking Assembly:** Evaluate the practicality of the interlocking assembly process with full-scale structural components. This includes assessing the labour, space, and machinery requirements to determine the feasibility and efficiency of the assembly process in real-world construction settings.
- **Full-Scale Numerical Modelling:** Develop a full-scale CLT modular building numerical model that incorporates the validated connection model. This will allow for the assessment of the connection system's impact on the overall structural performance of modular buildings and confirm its feasibility for use in medium-rise CLT modular construction.
- **Sustainability and Reusability:** Investigate the detachment of connections and the reuse of structural elements. This will further study the sustainability benefits of integrated CLT panels, emphasising the potential for reducing waste and promoting circular economy practices in construction.

- **Cost-Benefit Analysis:** Perform a comprehensive cost-benefit analysis comparing the novel interlocking connection system with conventional methods. This will provide insights into the economic feasibility and potential cost savings associated with the new system.

By addressing these limitations and pursuing the recommended areas of study, the proposed connection system can be further developed and optimised for widespread use in CLT modular construction, ultimately contributing to more efficient, sustainable, and resilient building practices.

Appendix A Numerical and Analytical Results of Parametric Study

Parameter	$k_{el,FEA}$	$F_{yeild,FEA}$ (kN)	$k_{plateau,FEA}$ (kN/mm)	$F_{plateau,FEA}$ (kN)	$k_{solidation,FEA}$ (kN/mm)	FEA/Analytical	$F_{1,yeild,analytic}$ (kN)	$F_{2,yeild,analytic}$ (kN)	$F_{3,yeild,analytic}$ (kN)
Tensile connection									
T1-60	3.60	12.18	0.08	13.67	3.75	1.49	8.17	15.90	20.10
T1-61	3.54	12.06	0.06	13.13	3.75	1.51	7.99	15.81	20.10
T1-62	3.51	11.85	0.07	13.10	3.78	1.52	7.82	15.75	20.10
T1-63	3.43	11.42	0.06	12.52	3.77	1.49	7.65	15.68	20.10
T1-64	3.31	11.27	0.07	12.56	3.78	1.51	7.49	15.59	20.10
T1-65	3.27	11.08	0.07	12.30	3.76	1.51	7.33	15.49	20.10
T1-66	3.25	10.95	0.08	12.32	3.75	1.53	7.18	15.37	20.10
T1-67	3.22	10.41	0.07	11.56	3.75	1.48	7.03	15.24	20.10
T1-68	3.19	10.07	0.07	11.26	3.76	1.46	6.88	15.10	20.10
T1-69	3.16	9.79	0.07	10.97	3.70	1.45	6.74	14.94	20.10
T1-70	3.13	9.62	0.07	10.86	3.72	1.46	6.59	14.77	20.10

T1-71	3.10	9.45	0.06	10.56	3.79	1.47	6.45	14.58	20.10
T1-72	2.98	9.38	0.06	10.32	3.76	1.49	6.30	14.37	20.10
T1-73	2.91	9.28	0.08	10.62	3.78	1.51	6.15	14.15	20.10
T1-74	2.87	9.12	0.08	10.46	3.75	1.52	6.00	13.91	20.10
T1-75	2.84	8.89	0.06	9.86	3.74	1.52	5.84	13.65	20.10
T1-76	2.76	8.75	0.07	9.98	3.76	1.54	5.68	13.38	20.10
T1-77	2.72	8.44	0.07	9.61	3.64	1.53	5.51	13.09	20.10
T1-78	2.69	8.01	0.08	9.24	3.75	1.50	5.34	12.78	20.10
T1-79	2.61	7.65	0.05	8.48	3.73	1.48	5.16	12.45	20.10
T1-80	2.55	7.42	0.07	8.48	3.76	1.49	4.97	12.11	20.10
T4-15	3.87	18.74	-0.01	-	-	-	12.43	23.62	20.10
T4-16	3.81	17.15	-0.01	-	-	-	11.59	21.48	20.10
T4-17	3.74	15.82	-0.01	-	-	-	10.63	19.69	20.10
T4-18	3.67	15.16	0.08	15.93	3.74	1.51	9.72	18.17	20.10
T4-19	3.60	13.75	0.08	14.60	3.74	1.48	9.06	16.87	20.10

T4-20	3.52	12.83	0.06	13.48	3.76	1.49	8.61	15.75	20.10
T4-21	3.49	12.13	0.04	12.61	3.73	1.56	8.21	14.77	20.10
T4-22	3.43	11.86	0.06	12.76	3.72	1.52	7.74	13.90	20.10
T4-23	3.41	10.93	0.07	12.05	3.72	1.49	7.24	13.12	20.10
T4-24	3.27	10.42	0.06	11.33	3.72	1.48	6.86	12.43	20.10
T4-25	3.13	9.62	0.07	10.86	3.72	1.53	6.59	11.81	20.10
T4-26	3.12	9.20	0.08	10.60	3.73	1.51	6.36	11.25	20.10
T4-27	3.00	8.81	0.07	10.16	3.73	1.52	6.08	10.74	20.10
T4-28	2.94	8.24	0.08	9.76	3.74	1.46	5.77	10.27	20.10
T4-29	2.79	7.43	0.08	9.02	3.74	1.45	5.52	9.84	20.10
T4-30	2.70	7.37	0.08	9.15	3.74	1.45	5.34	9.45	20.10
T4-31	2.66	7.17	0.08	9.02	3.72	1.43	5.19	9.09	20.10
T4-32	2.59	7.05	0.08	8.93	3.75	1.35	5.01	8.75	20.10
T4-33	2.54	6.80	0.07	8.52	3.74	1.38	4.80	8.44	20.10
T4-34	2.47	6.50	0.07	8.24	3.74	1.38	4.62	8.15	20.10

Parameter	$F_{cr,analytical}$ (kN)	$F_{cr,FEA}$ (kN)	FEA/Analytical
S3-15	13.50	16.03	1.19
S3-16	15.50	17.18	1.11
S3-17	17.04	18.32	1.08
S3-18	18.40	19.47	1.06
S3-19	20.38	20.61	1.01
S3-20	20.60	21.76	1.06
S3-21	23.66	22.90	0.97
S3-22	25.08	24.05	0.96
S3-23	26.43	25.19	0.95
S3-24	30.36	26.34	0.87
S3-25	30.28	27.48	0.91
S3-26	31.36	28.63	0.91
S3-27	31.06	29.77	0.96
S3-28	30.60	30.92	1.01
S3-29	29.60	32.06	1.08
S3-30	29.70	33.21	1.12
S3-31	29.40	34.35	1.17
S3-32	29.60	35.50	1.20
S3-33	28.90	36.64	1.27
S3-34	26.96	37.79	1.40
S3-35	24.60	38.93	1.58
S6-10	24.57	25.50	1.04
S6-11	24.84	25.50	1.03
S6-12	25.11	26.04	1.04
S6-13	25.39	26.89	1.06

S6-14	25.68	27.50	1.07
S6-15	25.96	28.70	1.11
S6-16	26.26	28.33	1.08
S6-17	26.56	28.70	1.08
S6-18	26.86	28.26	1.05
S6-19	27.17	29.39	1.08
S6-20	27.48	30.20	1.10
S6-21	27.80	30.13	1.08
S6-22	28.13	30.30	1.08
S6-23	28.46	30.50	1.07
S6-24	28.79	31.13	1.08
S6-25	29.14	31.02	1.06
S6-26	29.48	30.50	1.03
S6-27	29.84	31.17	1.04
S6-28	30.20	31.28	1.04
S6-29	30.57	31.30	1.02
S6-30	30.94	31.5	1.02

Appendix B Planned Publications

Li, Z., Tsavdaridis, K. D., Katenbayeva, A. (2024). Timber Modular Buildings and Material Circularity and Automation: The Role of Inter-Locking Connections. *Journal of Building Engineering*. (Under review)

Parametric and Analytical Studies of A Novel Self-locking Connection System for Modular Cross Laminated Timber (CLT) Structures. (Planned)

Comparative Study Of The Conventional Connections And The Novel Interlocking Connections For CLT Modular Structures. (Planned)